TABLE OF CONTENTS

LIST OF FIGURES

LIST OF ABBREVIATIONS AND ACRONYMS

AAA+	ATPases associated with diverse cellular activities
AIDS	acquired immunodeficiency syndrome
ADP	adenosine diphosphate
ATP	adenosine triphosphate
AP-1	activator protein-1
APOBEC	apolipoprotein B mRNA editing enzyme, catalytic polypeptide-like
B-MLV	B-tropic murine leukemia virus
BSL	biosafety level
CA	capsid protein, p24
Cas9	CRISPR-associated protein 9
CB	cytoplasmic body
CARDs	caspase activation and recruitment domains
CCR5	C-C chemokine receptor type 5
CD4	cluster of differentiation 4
CD4+	cell bearing the CD4 receptor
CDC	United States Centers for Disease Control and Prevention
cDNA	complementary DNA
cGAS	cyclic GMP-AMP synthase
co-IP	co-immunoprecipitation
CPSF6	cleavage and polyadenylation specific factor 6
CRISPR	clustered regularly interspaced short palindromic repeat
CROI	Conference on Retroviruses and Opportunistic Infections
CTD	C-terminal domain

CXCR4	chemokine receptor type 4
CypA	cyclophilin A
DHC	dynein heavy chain
DIC	dynein intermediate chain
DLIC	dynein light intermediate chain
DNA	deoxyribonucleic acid
dNTP	deoxyribonucleotide triphosphate
dsRNA	double-stranded RNA
EB	end-binding
EHNA	erythro-9-(2-hydroxy-3-nonyl)adenine
EIAV	equine infectious anemia virus
Env	envelope
ESCRT	endosomal sorting complexes required for transport
FIV	feline immunodeficiency virus
FN3	fibronectin type III domain
FRET	fluorescence resonance energy transfer
GTP	guanosine triphosphate
GDP	guanosine diphosphate
HAART	highly active antiretroviral therapy
HC	heavy chain
HIV-1	human immunodeficiency virus type 1
HIV-2	human immunodeficiency virus type 2
IF	immunofluorescence
IFN	interferon
IKK *i*	IκB kinase *i*
IN	integrase

IPS1	interferon-beta promoter stimulator 1
IRF-3	IFN-regulatory factor 3
ISG	IFN-stimulated genes
JAK	Janus kinase
KIF17	kinesin family member 17
LIS1	lissencephaly
LTR	long terminal repeat
L1	linker1
L2	linker2
MA	matrix protein
MAP	microtubule-associated protein
MDA-5	melanoma differentiation-associated protein 5
MDM	monocyte-derived macrophages
MID1	midline 1
MID2	midline 2
MIM	microtubule-interacting motif
MLV	murine leukemia virus
MTOC	microtubule-organizing center
Mx2/ MxB	myxovirus resistance 2/ B
N-MLV	N-tropic murine leukemia virus
NC	nucleocapsid protein
Nef	negative factor
NF-κB	nuclear factor κ-light-chain-enhancer of activated B cells
NMDA	N-methyl-D-aspartate
NNRTI	non-nucleoside reverse transcriptase inhibitors
NPC	nuclear pore complex

NRTI	nucleoside/nucleotide reverse transcriptase inhibitors
NTD	N-terminal domain
NUDE	nuclear distribution protein E
PAMP	pathogen-associated molecular pattern
PDZD8	PDZ domain containing 8
PEP	post-exposure prophylaxis
PF74	Pfizer-3450074
PML	promyelocytic leukemia protein
PMIM	putative microtubule-interacting motif
PI	protease inhibitor
PIC	pre-initiation complex
PrEP	pre-exposure prophylaxis
PRR	pattern-recognition receptor
PR	protease
p.i.	post infection
RBCC	RING finger, B-box, and coiled-coil
Rev	regulator of expression of virion
RIG-I	retinoic acid-inducible gene 1
RILP	Rab-interacting lysosomal protein
RING	really interesting new gene
RIP1	Receptor-interacting protein 1
RNA	ribonucleic acid
RT	reverse transcriptase
RTC	reverse transcription complex
SAMHD1	SAM domain and HD domain-containing protein 1
SCID	severe combined immunodeficiency

SIV	simian immunodeficiency virus
siRNA	small interfering RNA
ssRNA	single-stranded RNA
STAT	signal transducer and activator of transcription
SU	surface protein, gp120
TALEN	transcription activator-like effector nucleases
Tat	trans-activator of transcription
TasP	treatment as prevention
TcTex-1	T-complex testis-specific protein 1
TLR	Toll-like receptor
TM	transmembrane protein, gp41
TRAF6	TNF receptor associated factor 6
TRIF	TIR-domain-containing adapter-inducing interferon-β
TRIM	tripartite motif
TRIM5α	tripartite motif-containing protein 5α
UNAIDS	United Nation program on HIV/AIDS
VCC	virus-containing compartments
Vif	viral infectivity factor
Vpu	viral protein unique
Vpr	viral protein R
Vpx	viral protein X
vRNA	viral RNA
ZFN	zinc-finger nucleases
+TIP	plus-end tracking proteins

CHAPTER I

INTRODUCTION

1.1 HIV-1 as the causative agent of AIDS

In the early 1980s a mysterious immune disorder epidemic emerged, initially within the homosexual population, intravenous drug users and immigrants from Haiti, which gradually spread into the general population. The starting point of the epidemic is dated June 5th 1981, when the Centers for Disease Control and Prevention (CDC) reported several outbreaks of opportunistic diseases in previously healthy patients. (CDC, 1981). At that time, the disorder was referred to as gay-related immunodeficiency due to reported incidence of the disease among this group. In 1982, it was renamed acquired immunodeficiency syndrome (AIDS)(CDC, 1982). Its causative agent was discovered by two independent groups in 1983-4 and the virus was called human immunodeficiency virus (HIV). (Barre-Sinoussi *et al*, 1983; Gallo *et al*, 1984; Popovic *et al*, 1984). Shortly after the identification of HIV, later referred to as HIV-1, a second virus causing AIDS was discovered, named HIV-2 (Clavel *et al*, 1986). The two viruses differ substantially, resulting in differences in serological detection (Clavel *et al*, 1987). Although HIV-1 and HIV-2 cause the same disease, individuals infected with HIV-2 usually have a longer life span than those infected with HIV-1, as it takes more time to develop into full-blown AIDS (Reeves & Doms, 2002).

Both HIV-1 and HIV-2 originate from closely related simian immunodeficiency virus (SIV) found in many African primate species. The genetic sequence of HIV-1 resembles SIV from chimpanzees (*Pan troglodytes*), while HIV-2 is similar to SIV infecting sooty mangabeys (*Cercocebus atys*) (Sharp *et al*, 2001; Sharp *et al*, 2005). The transfers of SIV from primates to humans happened multiple times. Interestingly, the oldest documented case of HIV-1 infection dates to 1959; the virus was detected in a specimen collected in Kinshasa, the capital of Congo (Zhu *et al*, 1998). Although the

virus was present in the human population likely as early the 1920s, it did not reach an epidemic threshold until 1980s, as a result of colonialism-related trade in Cameroon (Sharp & Hahn, 2011).

HIV-1 can be divided into four genetically diverse groups M, N, O and P that reflect separate transfers of SIV from chimpanzees to humans (Sharp *et al*, 2005). The most widespread is HIV-1 from the M group, while the N, O and P groups, as well as HIV-2, are limited to Africa (De Cock *et al*, 1993; Sharp & Hahn, 2011). The M group can be further divided into at least nine genetically distinct subtypes (or clades); subtypes A, B, C, D, F, G, H, J and K. This thesis focuses on the aspects of infection caused by HIV-1 belonging to M group, as this virus is the major cause of the present AIDS epidemic.

1.1.1 The AIDS epidemic

In 2012, the United Nations program on HIV/AIDS (UNAIDS) reported that 35.3 million people were estimated to be living with HIV-1 or HIV-2 (UNAIDS, 2013). That year, the number of newly infected individuals reached 2.3 million people and approximately 2 million deaths resulting from AIDS-related diseases were reported (UNAIDS, 2013). Thanks to pharmacological treatments, education and interventions of various organizations, these numbers reached stable levels, however there is still no perspective to eradicate the disease. The most dramatic situation is in sub-Saharan Africa, where in some countries more than 25% of population is infected (Fig. 1.1).

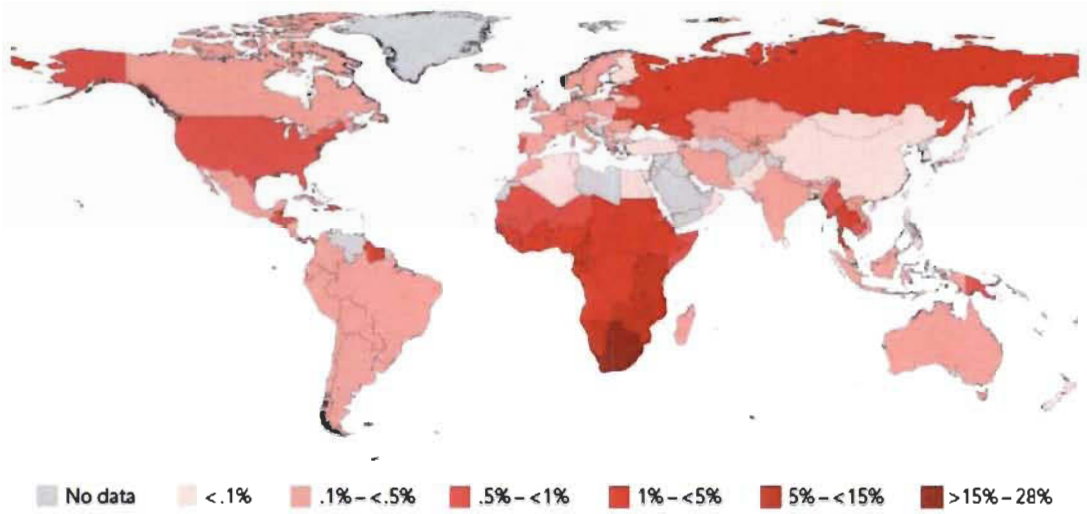

Figure 1.1 Global prevalence of HIV-1.
Image source: (UNAIDS, 2010).

Following HIV-1 contraction a patient may experience an acute phase of infection with flu-like symptoms which gradually transforms into an asymptomatic chronic infection. The latter usually lasts several years during which T lymphocytes bearing clusters of differentiation 4 receptor ($CD4^+$ T-cells) are slowly eradicated (Organization., 2007). The $CD4^+$ T-cell count in healthy individuals ranges from 500 cells/μl to 1,500 cells/μl. AIDS is defined by low $CD4^+$ T-cell count (less than 200 cells/μl) and/or occurrence of opportunistic diseases, such as pneumonia caused by *Pneumocystis carinii* (Gottlieb, 2006) or Kaposi's sarcoma (Friedman-Kien, 1981; Hymes *et al*, 1981). People with AIDS usually die as a result of opportunistic diseases.

1.1.2 Treatment and prevention HIV-1 infection

To this date, neither a cure nor a vaccine effective against HIV-1 have been developed. There are multiple obstacles in developing safe, effective and durable vaccines, including the fast mutation rate of the virus and high glycosylation of its spike proteins, which unables immune system detection of viral epitopes. Only one trial, RV144, consisting of two vaccines that individually shown no efficacy, resulted in a moderate, ~30%, protection (Rerks-Ngarm *et al*, 2009). This study suggests that developing an effective vaccine could be feasible in the future.

The first drug effective against HIV-1 azidothymidine (AZT) was introduced in 1987. (Yarchoan & Broder, 1987). This drug is now classified as nucleoside/nucleotide reverse transcriptase inhibitor (NRTI). NRTIs are nucleoside analogues that resemble naturally occurring nucleosides and are incorporated into nascent DNA by viral reverse transcriptase but not human polymerases. AZT, which was initially used as monotherapy, quickly resulted in the emergence of drug-resistant viruses and subsequent failure of the treatment. Between 1991 and 1995, four additional NRTIs were developed. A breakthrough came in 1995 when a new protease inhibitor (PI, saquinavir) was introduced, which led to the current approach of combining multiple antiretroviral drugs targeting various steps of the viral replication cycle, known as highly active antiretroviral therapy (HAART) (Flepp *et al*, 2001). In 1996 nevirapine, a drug belonging to a new class of pharmaceuticals, was introduced, along with two additional PIs. Nevirapine is a non-nucleoside reverse transcriptase inhibitors (NNRTI) and acts directly on the reverse transcriptase. In 2003, the first fusion inhibitor was introduced (enfuvirtide), and in 2007 inhibitors of entry (maraviroc) and integrase (raltegravir) were approved (Palmisano & Vella, 2011), increasing therapy options for infected patients. Currently, there are over twenty pharmaceuticals available. Despite increased life expectancy and overall health improvement of patients, HAART has serious drawbacks, *e.g.* it has to be taken for the whole of the patient's life and administered daily; viral targets might acquire drug resistance; finally, side effects such as anemia, hepatotoxicity, hyperglycemia, hyperlipidemia and lipodystrophy are common (Flepp *et al*, 2001).

A very important aspect of fighting HIV-1 epidemics is education about its transmissibility and the prevention of new infections. In general, three approved protocols employing antiretroviral pharmaceuticals to prevent HIV-1 infection/transmission are commonly used. Treatment as prevention (TasP) is an approach, in which infected patients receive antiretroviral drugs in order to lower the chances of infecting others, and can be as effective as in 96% of cases; this approach is commonly used in HIV-discordant couples and to prevent mother-to-child transmission (De Cock *et al*, 2000). Also, healthy individuals can decrease the odds of becoming

infected by taking prophylactic antiretroviral drugs. This approach is known as pre-exposure prophylaxis (PrEP) and is commonly practiced in HIV-discordant couples and sex workers; it has been shown to be effective in 70% of cases (Anglemyer *et al*, 2011; Liu & Chibwesha, 2013; Vaid *et al*, 2013). In the case of a healthy individual that has been exposed to HIV-1 a post-exposure prophylaxis (PEP) can be employed to reduce the chances of becoming infected. This is approach is commonly used in health workers after accidental exposure to the virus, for example a needlestick injury (Cardo *et al*, 1997; Smith *et al*, 2005). Interestingly, male circumcision has been found to decrease HIV-1 transmission by at least 60% in males that have been circumcised (Auvert *et al*, 2005). Additionally, it is estimated that male circumcision might prevent male-to-female transmission by 46% (Hallett *et al*, 2011).

In conclusion, while the past years have seen a tremendous development in antiretroviral therapy, mitigating adverse effects and simplifying treatments, finding either a cure or a vaccine has proven elusive.

1.1.3 Perspectives for a cure

The ultimate aim of HIV-1 research is a complete eradication of the virus from the infected organism, which is known as a 'sterilizing cure'. Up to this date, only one case of this kind of cure has been described, known as the 'Berlin patient'. Timothy Brown as a therapy for acute myeloid leukemia underwent myeloablative treatment and then received a bone marrow transplant from a donor whose cells were resistant to HIV-1 infection; this intervention resulted in a complete elimination of the virus (Hutter *et al*, 2009; Hutter & Thiel, 2011). The donor had a homozygotic deletion in the HIV-1co-receptor *C-C chemokine receptor 5 (CCR5)* gene (Alkhatib *et al*, 1996; Deng *et al*, 1996; Dragic *et al*, 1996); lack of which prevents infection with this virus (Liu *et al*, 1996). Until this date this remains the only case of a 'sterilizing cure'. The other famous cases turned out to be prematurely optimistic. For example, the famous 'Mississippi' infant was an infant reported to be cured as a result of an aggressive antiretroviral

treatment prior to, it was thought, the virus being able to establish its reservoir (Cohen, 2013). Unfortunately, in July 2014 the virus re-emerged in the baby's blood.

While the sterilizing cure is still beyond our reach a more feasible goal may be obtained, known as a 'functional cure'. The functional cure is defined as spontaneous drug-free control of the viral replication. For example, the members of the ANRS VISCONTI study in which up to ~15% of early treated individuals wereshown to display spontaneous control of viremia (Saez-Cirion *et al*, 2013). The reasons for this viral control are still not fully understood, but it could be that early treatment, while limiting the viral load, enables the immune system to produce a specific response against the virus.

1.1.4 The HIV-1 genome and its structure

Taxonomically HIV-1 belongs to the viral Group VI, family *Retroviridae*, subfamily *Lentivirus*. The genome of retroviruses exists in the form of a single-stranded RNA (ssRNA) which upon infection is reverse transcribed into a double-stranded complementary DNA (cDNA) by the viral enzyme reverse transcriptase. This DNA is later inserted into the host's genome by the viral enzyme integrase. The hallmark of lentiviruses is their ability to actively import their cDNA into the nucleus through the nuclear pore complex (NPC), which allows for infection of non-dividing cells.

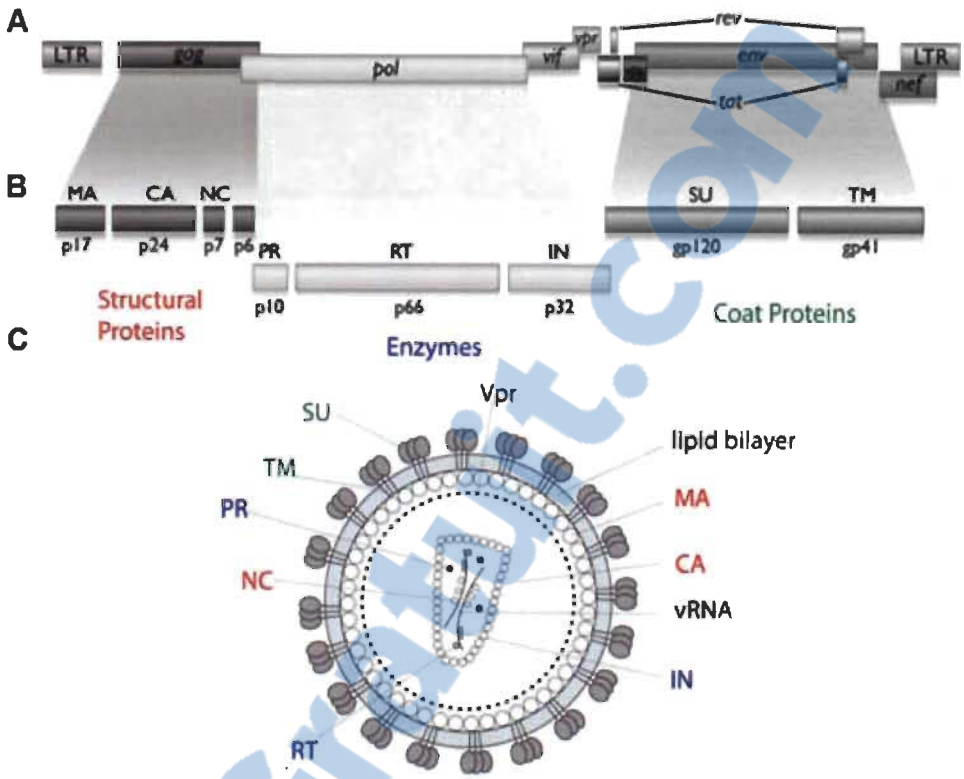

Figure 1.2 **Organization of HIV-1 genome and the structure of the virus.**
(A) A schematic representation of the organization of HIV-1 genome. LTR - long terminal repeat. (B) A schematic representation of cleavage products of HIV-1 polyproteins. Gag is cleaved to MA (matrix, p17), CA (capsid, p24), NC (nucleocapsid, p7) and p6; Pol to PR (protease), RT (reverse transcriptase) and IN (integrase); Env to SU (surface protein, gp120) and TM (transmembrane protein, gp41). (C) A schematic representation of HIV-1 virion. vRNA - viral RNA.
Image source: (Krogan, 2011).

The HIV-1 genome consists of two positive-sense ssRNAs, ~10 kb in length (Ratner *et al*, 1985; Wain-Hobson *et al*, 1985) that contain nine genes (Fig. 1.2A). Three encode the polyproteins Gag, Pol and Env, while the others encode regulatory and accessory proteins, some of which are the result of post-transcriptional splicing. The regulatory proteins regulator of expression of virion proteins (Rev), trans-activator of transcription (Tat) and negative factor (Nef) are expressed during the viral replication. The accessory proteins viral infectivity factor (Vif), viral protein R (Vpr) and viral protein unique (Vpu) are usually packed into the virion and play roles during the early

steps of infection. Interestingly. the related HIV-2 does not encode Vpu, but in its place encodes viral protein X (Vpx) (Coffin *et al*, 1997).

HIV-1 is an enveloped virus whose size is estimated to be approximately 120 nm (Kuznetsov *et al*, 2003). The structural proteins matrix (MA, p17), capsid (CA, p24), nucleocapsid (NC, p7) and p6 are the result of cleavages of the Gag precursor (p55) (Fig. 1.2). The CA protein forms a conical-shaped core that encases the viral RNA (vRNA) associated with NC. The CA core also contains three viral enzymes, products of the Pol precursor: reverse transcriptase (RT, p66), integrase (IN, p32) and protease (PR, p10). The virions also enclose accessory proteins Vif, Vpr, Vpu (or Vpx). MA forms an inner shell below the lipid envelope originating from a producer cell. The envelope, shielding the CA core, mediates viral entry. This lipid membrane is spanned with transmembrane (TM, gp41) viral protein, one of the products of the Env precursor. Associated with gp41 is the surface protein (SU, gp120), which is responsible for receptor recognition and its binding (Coffin *et al*, 1997).

1.1.5 HIV-1 replication cycle

The replication cycle of lentiviruses can be clearly divided into two phases, early and late, whereby the first consists of the steps leading to the integration of the viral genome into the host's genome. The late phase consists of all subsequent events.

1.1.5.1 Early phase

The primary targets for HIV-1 are cells of the immune system bearing the CD4 receptor, mainly macrophages, dendritic cells and helper T-cells (Dalgleish *et al*, 1984; Klatzmann *et al*, 1984a; Klatzmann *et al*, 1984b). Initially, the gp120 (SU) triplet, protruding from the viral envelope, attaches to the CD4 receptor and one of the two co-receptors; either CCR5 (Alkhatib *et al*, 1996; Deng *et al*, 1996; Dragic *et al*, 1996) or C-X-C chemokine receptor type 4 (CXCR4) (Deng *et al*, 1996; Feng *et al*, 1996) (Fig. 1.3). Receptor binding results in a conformational change of gp120, allowing for

penetration of the cellular membrane by gp41 (TM). This event brings the two membranes together which causes their fusion (Melikyan, 2014). Next, the HIV-1 CA core is released into the cytoplasm and this is followed by two processes: reverse transcription and core disassembly (uncoating), which are likely inter-dependent (Hulme *et al*, 2011; Roa *et al*, 2012). Interestingly, RT has no proofreading properties and its fidelity is considerably low (1.4×10^{-5} errors per base pair (Abram *et al*, 2010)), thus the reverse transcription process is extremely error-prone. This results in an enormous HIV-1 mutation rate which allows the virus to quickly adapt to a changing environment, such as the presence of an antiretroviral drug. Transcribed double-stranded cDNA together with IN and other remaining viral proteins form the pre-integration complex (PIC) which associates with the NPC. The distinctive feature of lentiviruses is their ability to actively pass through the NPC and infect non-dividing cells (Lewis & Emerman, 1994; Roe *et al*, 1993). This process is not fully understood, but it is likely supported by the viral protein Vpr (Kogan & Rappaport, 2011). Once in the nucleus, the viral cDNA is inserted into the host's genome, with a preference towards actively transcribed regions (Schroder *et al*, 2002).

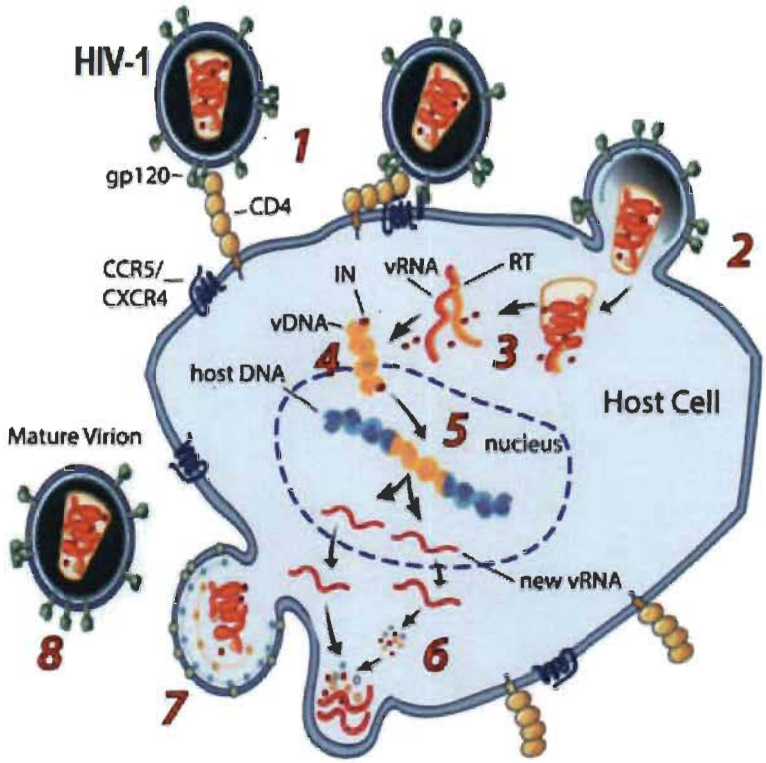

Figure 1.3 **HIV-1 replication cycle.**
(1) Recognition of the cellular receptors. (2) Fusion of the viral and cellular membranes. (3) Core uncoating and reverse transcription. (4) Formation of the pre-integration complex (PIC). (5) Import and integration of vDNA (cDNA) into the host genome. (6) Synthesis of vRNAs and viral proteins. (7) Viral budding from the cellular membrane. (8) Maturation of released virions.
Image source : (NIH, 2012).

1.1.5.2 Late phase

Once integrated, the viral genetic material is called a provirus and is actively transcribed by cellular RNA polymerase II. The transcription is mediated by a single promoter in the 5' LTR of the provirus and requires cellular transcription factors, of which the most crucial is NF-κB (Nabel & Baltimore, 1987). Notably, long-living cells carrying proviruses can be deactivated, during which the virus can remain transcriptionally dormant for many years while retaining the ability to be reactivated with full pathogenic capacity upon the cell's activation (Chun *et al*, 1998). This state is called latency and is the reason why HIV-1 infection remains incurable.

Post integration, the first transcripts are spliced and regulatory proteins Tat, Rev and Nef are expressed (Greene & Peterlin, 2002; Jordan *et al*, 2003). Tat and Rev proteins shuttle back to the nucleus. Tat activates the production of full length transcripts and in *trans* stimulates the expression of all HIV-1 genes (Kao *et al*, 1987). Rev binds to newly transcribed unspliced vRNA and allows it to leave the nucleus (Pollard & Malim, 1998). In the cytoplasm, unspliced vRNA either serves as a template for the production of the polyproteins Gag, Pol and Env, or is to be incorporated in newly produced virions. Nef is a virulence factor that significantly increases viral titers and is crucial for the development of AIDS (Kimpton & Emerman, 1992). Nef has many functions, of which the best described is its down-regulation of CD4 receptors (Aiken *et al*, 1994). When Env precursor (gp160) is synthesized it remains attached to endoplasmic reticulum and then transported to Golgi where it is cleaved by cellular enzymes furin or other, related subtilisin-like proteases to gp120 and gp41(Decroly *et al*, 1994; Decroly *et al*, 1996). gp41 is embedded in the membrane and anchors gp120, which protrudes into the Golgi lumen. Then the vesicles are transported to the cellular membrane at which in case of T-cells the viral assembly takes place (Finzi *et al*, 2007). Alternatively, in the case of macrophages, newly synthesized virions bud inside so-called viral containing compartments (VCCs) (Nguyen *et al*, 2003; Pelchen-Matthews *et al*, 2003), which then frequently connect with the plasma membrane to release the virions into extracellular environment (Tan & Sattentau, 2013). gp41 associates with Gag and Gag-Pol precursors (Wyma *et al*, 2000), while the NC region of Gag interacts with vRNA (Sandefur *et al*, 1998). Gag has been reported to interact with the KIF4 kinesin motor (Martinez *et al*, 2008; Tang *et al*, 1999), Staufen 1 (Milev *et al*, 2010) and with components of intracellular vesicle trafficking pathways (Batonick *et al*, 2005; Camus *et al*, 2007; Dong *et al*, 2005). Viral budding is mediated by cellular endosomal sorting complexes required for transport (ESCRT) machinery, whose members are recruited by the p6 region of Gag (Martin-Serrano *et al*, 2003). Once virions detach, PR is activated and undergoes auto-cleavage releasing the other viral enzymes IN and RT, and then cleaves Gag precursor into MA, CA, NC and p6 (Freed, 1998; Fu & Rein, 1993). Subsequently, these proteins assemble into the CA core, which encapsulates NC together with vRNA. This process is called maturation and is necessary for HIV-1 infectivity. Mature virions

also enclose accessory proteins and cellular molecules, such as $tRNA^{Lys3}$ that serves as a primer for reverse transcription (Ott, 2008; Sundquist & Krausslich, 2012).

1.1.6 The capsid core and its uncoating

The mature HIV-1 CA core is a ~60 nm x 120 nm (Briggs *et al*, 2003) cone-shaped, protein lattice and is composed of 1,500 CA monomers arranged in ~250 hexamers and 12 pentamers (Briggs *et al*, 2004; Pornillos *et al*, 2009) through interactions involving their N-terminal domains (NTD) (Pornillos *et al*, 2009), while CA C-terminal domains (CTD) are important for homodimerization and connecting the rings into a lattice (Gamble *et al*, 1997) (Fig. 1.4).

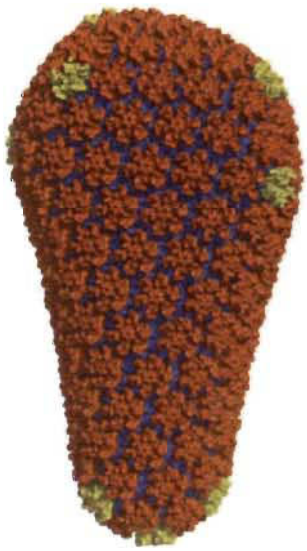

Figure 1.4 Model of HIV-1 capsid core.
Fullerene cone model composed of 1,056 CA subunits. NTD driven CA hexamers are coloured in orange, pentamers in yellow, while CTD driven homodimers in blue. NTD – N-terminal domain, CTD – C-terminal domain.
Image source: (Pornillos *et al*, 2011).

For many years it was thought that the HIV-1 CA core disassembled immediately after its entry to the cytoplasm, which would then be followed by reverse transcription. This reasoning stemmed from the difficulties of isolating particulate cores from infected cells, as this structure is very fragile (Bukrinsky *et al*, 1993; Farnet & Haseltine, 1991;

Karageorgos *et al*, 1993). However, more recently we have gained critical insight into the importance of the HIV-1 CA core and its proper disassembly, referred to as uncoating.

1.1.6.1 Evidence supporting regulated HIV-1 uncoating

The first line of evidence suggesting that uncoating is an important step in HIV-1 replication was provided by mutagenesis. CA mutants resulting in either hypostable or hyperstable cores are not infectious (Forshey *et al*, 2002; Tipper & Sodroski, 2013).

The retroviral restriction factors TRIM5α and TRIMCyp inhibit viral infection (Sayah *et al*, 2004; Stremlau *et al*, 2004) through binding to incoming CA cores and destabilizing them (Bérubé *et al*, 2007; Stremlau *et al*, 2006). TRIM5 proteins will be discussed in the next section. Nevertheless, their action provides functional evidence of the significance of the 'intact' HIV-1 capsid core during the first few hours post infection (p.i.). Additionally, the HIV-1 small-molecule inhibitor PF-3450074 (PF74) is known to inhibit HIV-1 infectivity specifically by destabilizing the CA core (Shi *et al*, 2011).

Interesting evidence on the importance of uncoating was provided by linking uncoating with reverse transcription, since an inhibition of the latter led to a slower CA core disassembly (Hulme *et al*, 2011; Roa *et al*, 2012; Yang *et al*, 2013). The initiation of reverse transcription likely depends on an initial destabilization or increased permeability of the CA core after entry into the cytoplasm (Hulme *et al*, 2011; Zhang *et al*, 2000; Zhang *et al*, 1998). However, it has been suggested that the completion of reverse transcription takes place inside the CA core (Arhel *et al*, 2007; Schaller *et al*, 2011) which at that time would likely be at the NPC. It is most likely that uncoating takes place in several well-orchestrated steps instead of being a rapid single-step process; one report suggested it might happen in at least two phases (Xu *et al*, 2013).

Additionally, a recent study reported that cellular factors are recruited to the incoming CA core thus shielding actively transcribing viral genetic material from detection by pattern-recognition receptors (PRRs) (Rasaiyaah *et al*, 2013). The same study showed that HIV-1 viruses bearing mutations in the CA protein, which unable CA interaction with certain cellular partners, fail to replicate in macrophages due to activation of innate immune response.

Finally, CA mutagenesis also suggested that this protein has a role in nuclear entry (Dismuke & Aiken, 2006) and in the ability to transduce non-dividing cells (Yamashita & Emerman, 2004; Yamashita *et al*, 2007). It was also suggested that CA is linked with specificity to integration sites of proviral DNA (Schaller *et al*, 2011). Altogether, these reports demonstrate that the full uncoating does not happen immediately after the release of the CA core into the cytoplasm.

1.1.6.2 HIV-1 uncoating

The knowledge regarding HIV-1 uncoating is very limited. This process is thought to be initiated soon after the exposure to the cellular environment, within the first hours from infection (Hulme *et al*, 2011). Large amounts of CA cores can still be observed in infected cells 6 hours post infection and longer (Li *et al*, 2009; Pawlica *et al*, 2014; Stremlau *et al*, 2006). Where uncoating takes place is still under debate: some reports proposed that it occurs in the cytoplasm (Hulme *et al*, 2011; McDonald *et al*, 2002), while others suggested that uncoating takes place at the NPC (Arhel *et al*, 2007; Rasaiyaah *et al*, 2013; Schaller *et al*, 2011). The latter is supported by microscopic observations in which HIV-1 CA cores reach the proximity of the nucleus 1-2 h p.i. (Arhel, 2010; Arhel *et al*, 2007; McDonald *et al*, 2002). Additionally, CA was also observed at the NPC and was proposed to be responsible for the docking of the virus at the nuclear membrane (Arhel *et al*, 2007; Di Nunzio *et al*, 2012). Interestingly, the NPC members Nup358 and Nup153 were shown to directly bind to CA protein, as demonstrated by immunoprecipitation (Matreyek *et al*, 2013; Schaller *et al*, 2011). Additionally, both CA-binding domains of Nup153 and Nup538 when fused to the

effector domain of the rhesus TRIM5α restricted HIV-1, providing an intracellular readout for the direct interaction during retroviral infection. One study reported that a small fraction of CA proteins might be transported inside the nucleus (Zhou *et al*, 2011).

1.1.6.3 Cellular proteins regulating uncoating

Following its entry, the HIV-1 CA core interacts with various cellular factors (Ambrose & Aiken, 2014). So far a handful of cellular partners have been shown to directly bind CA core after its entry to the cytoplasm: Cyclophilin A (CypA) (Fricke *et al*, 2013; Li *et al*, 2009; Shah *et al*, 2013), cleavage and polyadenylation specific factor 6 (CPSF6) (De Iaco *et al*, 2013; Shah *et al*, 2013), peptidyl-prolyl isomerase Pin1(Misumi *et al*, 2010) and PDZ domain-containing protein 8 (PDZD8) (Guth & Sodroski, 2014). It was proposed that CypA and CPFS6 are recruited to the CA core to conceal the viral genetic material from detection by innate immunity sensors (Lahaye *et al*, 2013; Rasaiyaah *et al*, 2013).

Another protein playing a definite yet unclear role in HIV-1 replication is transportin TNPO3 (Ambrose & Aiken, 2014), and its importance for HIV-1 was genetically mapped to CA protein (Krishnan *et al*, 2010). It has been suggested that the function of TNPO3 is indirect and that it acts positively on HIV-1 replication by sequestering CPSF6 (De Iaco *et al*, 2013; Shah *et al*, 2013). At the later early stage of HIV-1 infection the CA core associates with nucleoporins Nup358 and Nup153 (Schaller *et al*, 2011; Shah *et al*, 2013), which mediate nuclear import of viral PIC. These two NPC members also directly bind to CA proteins (Matreyek *et al*, 2013; Schaller *et al*, 2011).

Interestingly, two recent studies have validated the existence of cellular proteins responsible for modulation of CA core stability, as evidenced by incubation with cellular lysates which increased the stability of CA cores (Fricke *et al*, 2013; Guth & Sodroski, 2014). These also support the hypothesis that following entry the CA core is initially shielded from the cellular environment and uncoats later in a well-orchestrated manner.

However, the knowledge about the uncoating process and its cellular partners remains very poor and additional studies are needed for its better understanding.

Some steps of the viral replication, such as intracellular transport, rely on the host's cytoskeleton. The eukaryotic cytoskeleton is a good target to be intercepted by viruses, as it is essential for cellular life and is involved in many cellular processes.

1.2 The cytoskeleton

The eukaryotic cytoskeleton is an abundant, complex and dynamic network of various filaments and regulatory proteins associated with them. They are divided into three groups: actin filaments (also known as microfilaments), intermediate filaments and microtubules. These filaments have distinct roles, structure and organization (Fig. 1.5).

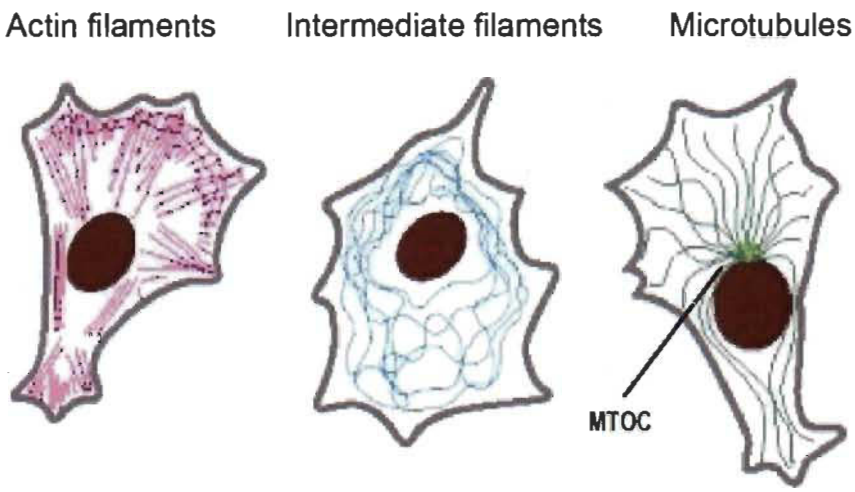

Figure 1.5 Schematic representation of cytoskeletal filaments.
MTOC – microtubule-organizing centre.
Image source: (Alberts, 2002).

Actin filaments are the smallest, 5-9 nm in diameter, and are dispersed throughout the cytosol with the greatest concentration below the plasma membrane, known as the actin cortex. Microfilaments play major functions in cytokinesis, maintaining cellular shape and cell migration; they are the main components of lamellipodia and filopodia.

Intermediate filaments belong to a large heterogeneous family of rod-like filaments ~10 nm in diameter. Most of them, such as vimentins, cytokeratins, desmins neurofilaments, are found in the cytosol, while others, such as lamins, are in the nucleus. They are stress-resistant, conferring great mechanical strength, and are responsible for maintaining the cell's integrity, organelle positioning and contributing to cellular adhesion *e.g.* as a component of desmosomes (Alberts, 2002; Lodish, 2004).

1.2.1 The microtubule network

Measuring 25 nm in diameter, microtubules are the longest, most rigid and thickest components of the cytoskeleton. These filaments are important in many cellular processes. They are responsible for organelle positioning, intracellular transport, cell division and migration. Additionally, they serve as an internal scaffolding of cilia and flagella.

The basic components of microtubules are heterodimers of α- and β-tubulin which are tightly associated with each other by a noncovalent bond. Tubulin heterodimers assemble head-to-tail, forming polar protofilaments. Usually 13 protofilaments interact laterally to form a hollow tube known as a microtubule. These fibres assemble towards their plus-end, usually orientated towards the cell periphery, while the minus-end is usually focused in microtubule-organizing centres (MTOC) (Fig. 1.5). The MTOC, which is often localized in the perinuclear region (except during the cell division), consists of a pair of centrioles, built of nine microtubule triplets surrounded by a number of proteins, including γ-tubulin. Microtubule growth is initiated on the γ-tubulin complex (Alberts, 2002; Lodish, 2004).

Microtubules are highly dynamic structures constantly switching between being assembled and disassembled. This property is called 'dynamic instability' (Mitchison & Kirschner, 1984). It allows the plus-end of microtubules to explore the cellular environment in the process called 'search and capture' and adapt rapidly to changing conditions, *e.g.* during cell division (Kirschner & Mitchison, 1986). Once in the right

place, the filaments are bound by a specialized family of proteins and undergo post-translational modifications modulating their stability (Alberts, 2002; Kueh & Mitchison, 2009; Lodish, 2004).

1.2.1.1 Regulation of microtubule dynamics

Dynamic instability provides the basis for microtubule plasticity, which is highly regulated by cellular factors such as microtubule-associated proteins (MAPs), molecular motors and others proteins, such as kinases (Mandelkow & Mandelkow, 1995). MAPs specifically bind to microtubules and either stabilize (*e.g.* Tau, MAP2 or MAP4) or destabilize them (*e.g.* katanin, stathmin). An important group of MAPs are the plus-end tracking proteins (+TIPs) that usually prevent depolymeization of microtubules. Additionally, +TIPs serve in connecting microtubules to actin filaments and organelles (Gouveia & Akhmanova, 2010). The most well-known members of this group are end-binding (EB) proteins that promote growth of microtubules (Komarova *et al*, 2009). Other important regulators of microtubule dynamics are kinesin motors, especially the kinesin-8 family, members of which are known to destabilize microtubules (Su *et al*, 2012). Interestingly, the cortex-associated dynein motor complex was also proposed to play a role in binding the plus-end of microtubules and stabilizing them (Hendricks *et al*, 2012).

Additional mechanisms regulating microtubule dynamics are post-translational modifications, usually carried out on polymerized microtubules. It was proposed that these modifications generate a specific 'code' readable by MAPs and molecular motors that allows carrying divergent functions on microtubules (Verhey & Gaertig, 2007). For example, acetylation increases binding of molecular motors (Friedman *et al*, 2010) while detyrosination decreases binding affinity of destabilizing MAPs and promotes formation of a stable sub-population of microtubules (de Forges *et al*, 2012). Additionally, tubulin subunits have different isoforms, which contribute to the extreme diversity of microtubules (Luduena, 1998). In conclusion, microtubule dynamics is highly regulated by many cellular factors.

1.2.1.2 Treatments targeting microtubules

Drugs targeting microtubules can be divided into two groups: those preventing microtubule assembly and others preventing their disassembly. Some of the drugs preventing assembly bind to α/β-tubulin heterodimers, such as colchicine (Ravelli *et al*, 2004) and nocodazole (Xu *et al*, 2002), while others bind between the dimers, *e.g.* vinblastine (Gigant *et al*, 2005). The second group of drugs (such as paclitaxel, originally named taxol (Schiff & Horwitz, 1981)), binds to and stabilizes tubulin polymers, also resulting in a loss of their dynamics (Derry *et al*, 1995). An alternative way to study microtubule dynamics is to target various MAPs that regulate it: for instance a depletion of EB1 results in a dramatic loss of microtubule dynamics (Rogers *et al*, 2002).

1.2.2 Molecular motors and their role in cellular transport

The cytoplasm is a crowded and viscous environment where only small molecules and proteins can freely diffuse. Movement of larger components, 20 nm of size and more, requires active transport (Ellis, 2001; Luby-Phelps, 2000). This transport, usually ATP-driven, is mediated by three classes of molecular motors: actin-based myosins and microtubule-based kinesins and dyneins. The myosin motor superfamily consists of 22 groups of proteins (Foth *et al*, 2006). Myosins are involved in various cellular processes, such as cytokinesis, actin-dependent transport, membrane trafficking and signal transduction. Interestingly, different types of myosin motors are responsible for movements in opposite directions; most of the myosins move towards the plus-end of microfilaments, while the members of group VI move towards the minus-end (Buss & Kendrick-Jones, 2008).

There are 45 known members of the kinesin motors superfamily, grouped into 14 families. Kinesin motors are responsible for microtubule-dependent anterograde transport, towards the plus-end of microtubules (Hirokawa *et al*, 2009; Verhey & Hammond, 2009), with an exception of the kinesin-14 family that moves towards the

minus-end (Ambrose *et al*, 2005). In addition to the transport, kinesin motors play roles in cell division, exocytosis and organelle positioning.

Dynein motors are the least diverse; there are only two members that are responsible for retrograde transport towards the minus-end of microtubules: the cytoplasmic dynein motor complex (known as dynein 1) and the intraflagellar transport dynein motor (known as dynein 1B or dynein 2). In most cells, all retrograde transport is carried out by dynein 1, thereafter referred to as the dynein motor complex. There are, additionally, 13 axonemal dyneins that are a part of axoneme and are responsible for cilia beating and are not involved in molecular transport. The dynein motor complex has multiple functions in the cell: transporting cargos towards the minus-end of microtubules; positioning organelles, such as Golgi, nucleus and lysosomes, and, during cell division, forming the mitotic spindle, attaching kinetochores and pulling astral microtubules (Gennerich & Vale, 2009; Roberts *et al*, 2013; Vale, 2003).

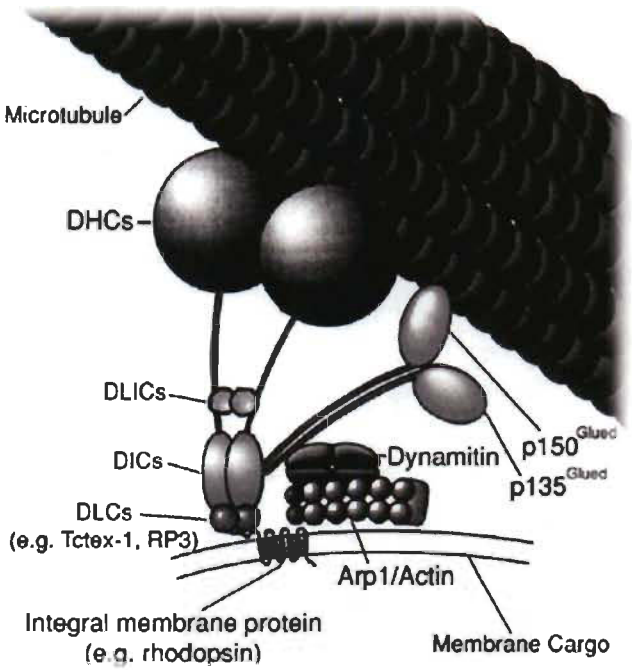

Figure 1.6 **The dynein motor complex.**
DHC - dynein heavy chain, DLIC - dynein light-intermediate chains, DLC - dynein light chain, RP3 - dynein light chain Tctex-type 3, Arp1 - actin-related protein 1.
Image source: (Sung, 2006).

1.2.2.1 The dynein motor complex

The dynein motor complex, belongs to the AAA+ superfamily (ATPases associated with diverse activities) (Neuwald *et al*, 1999). This motor is a large protein complex consisting of two heavy chains (DHC, for dynein heavy chain) and several pairs of lighter chains (Fig. 1.6). DHC is a large protein (~520 kDa) and consists of a head - made of six AAA+ domains arranged into a ring -, a stalk with a microtubule-binding site, and a tail. The tail of DHC associates with five pairs of homodimers of intermediate, light-intermediate and three light chains. There are three classes of light chains: LC8 and Roadblock (also known as LC7) and T-complex testis-specific protein 1 (Tctex-1) (Pfister *et al*, 2005). 'Lighter' subunits of the dynein motor complex are responsible for determining cargo specificity and thus the function of the whole complex (Pfister *et al*, 2005). Additionally, the dynein motor complex interacts with regulatory and adaptor protein complexes, including the dynactin complex, lissencephaly (LIS1), nuclear distribution protein E (NUDE) and others. The dynactin complex is composed of eleven different subunits, such as $p150^{Glued}$, p50 (also known as dynamitin) and actin-related protein 1 (Arp1), and seems to be essential for most of the functions performed by the dynein motor complex (Fig. 1.6). The dynactin complex enables *inter alia* an association of dynein motor complexes with cargos *via* Apr1 and $p150^{Glued}$. Additionally, this complex seems to be required for the processivity of the dynein motor complex (McKenney *et al*, 2014). Regulators, such as LIS1 and NUDE, mediate targeting the dynein motor complex to the plus-end of microtubules and thus are essential for mitotic spindle formation and in kinetochore activity, as well as in intracellular transport (Kardon & Vale, 2009).

The ATP-driven movement is carried out by DHCs that most likely associate and disassociate with microtubules in an alternating manner, which could be said to resemble 'walking'. The binding of ATP to the head of dynein DHC results in the disassociation of the stalk from microtubules (Imamula *et al*, 2007). Then DHC undergoes ATP-driven remodelling and the 'free' stalk can reach in search for a new binding site on microtubules. Initially, the binding is weak, but gets very strong as a result of the phosphate released through ATP hydrolysis (Roberts *et al*, 2013).

1.2.2.2 Inhibitors of the dynein motor complex function

Until recently, dynein-specific pharmacological agents were not available. The drug erythro-9-(2-hydroxy-3-nonyl)adenine (EHNA), used in this study, is a potent adenosine deaminase inhibitor and was also shown to inhibit ATPase activity associated with the DHC of axonemal dyneins (Bouchard *et al*, 1981; Penningroth *et al*, 1982). EHNA was sometimes used to study cytoplasmic dynein (Pawlica *et al*, 2014; Zhang *et al*, 2012), however this drug might result in other changes in the cytoskeleton, such as the disruption of F-actin (Schliwa *et al*, 1984).

More specific approaches to inhibit dynein-mediated transport consist of disrupting adaptor complexes. The best example is over-expression of p50/dynamitin, which causes disassociation of the dynactin complex and thus inhibition of dynein-dependent transport (Burkhardt *et al*, 1997). Rab7-interacting lysosomal protein (RILP), which is a Rab7 effector found in late endosomes, is another interesting example. RILP interacts with $p150^{Glued}$-C and this interaction promotes the localization of the dyncatin complex (and thus the dynein motor complex) to Rab7-containing late endosomes. As a result of RILP over-expression, the dynein motor complex is employed in transporting the late endosomes to MTOC and thus dynein-mediated transport towards the cell periphery is impaired (Cantalupo *et al*, 2001).

A common approach to inhibiting dynein function is the use of small interfering RNA (siRNA) to target one of the chains of the dynein motor complex; siRNA is often utilized against the DHC of dynein (He *et al*, 2005; Lehmann *et al*, 2009; Pawlica *et al*, 2014).

1.2.2.3 Coordination of bidirectional transport

In vivo observations revealed that transported on microtubules cargos exhibit saltatory bidirectional movements reversing the direction every few seconds (Welte, 2004). This led to understanding that most likely multiple kinesin and dynein motors are simultaneously attached to the transported cargo (Gross, 2004). Each of the motors has

different cargo-binding adaptors, but some adaptors, like the dynactin complex, can be important for the attachment of both the kinesin and dynein motor complexes (Deacon *et al*, 2003). How the bidirectional transport is coordinated remains to be elucidated. 'Tug-of-war' is the leading theory (Hendricks *et al*, 2010; Muller *et al*, 2008) and suggests that both motors are active at the same time and undergo competition. When the force coming from one type of motors prevails, it pulls the cargo in its direction causing transient detachment of the opposite motors (Hendricks *et al*, 2010; Muller *et al*, 2008).

1.2.3 Hijacking of the host cytoskeleton by viruses

Many, if not all, viruses evolved to hijack cellular transport machinery during their replication cycle (Cohen *et al*, 2011; Dodding & Way, 2011; Radtke *et al*, 2006). Multiple viruses subvert the microtubule network and microtubule-associated molecular motors; examples of such viruses are adenoviruses (Leopold *et al*, 2000; Suomalainen *et al*, 1999), parvoviruses (Xiao & Samulski, 2012), herpes simplex virus (Radtke *et al*, 2010; Wolfstein *et al*, 2006) and, finally, retroviruses (Arhel *et al*, 2006; McDonald *et al*, 2002; Petit *et al*, 2003). Also, the actin filaments are broadly subverted for viral trafficking, as evidenced by herpes simplex virus (van Leeuwen *et al*, 2002), influenza virus (Sun & Whittaker, 2007) and retroviruses (Arhel *et al*, 2006; Lehmann *et al*, 2005). The knowledge on this subject is quickly expanding, providing more and more insight on the importance of the cytoskeleton in viral replication.

1.2.3.1 HIV-1 trafficking towards the nucleus

The first step in which HIV-1 seems to require the cytoskeleton is receptor-mediated entry to the cytoplasm; actin filaments were proposed to be necessary for clustering of the receptors used by HIV-1 (Iyengar *et al*, 1998; Viard *et al*, 2002). Post fusion of viral and cellular membranes HIV-1 might temporarily associate with actin filaments (Fig. 1.7) (McDonald *et al*, 2002). This is supported by studies reporting that actin inhibitors inhibit HIV-1 infectivity (Bukrinskaya *et al*, 1998; Yoder *et al*, 2011).

Additionally, as observed by immunofluorescence (IF) microscopy, a treatment with an actin inhibitor prior to HIV-1 infection caused an accumulation of viral CA *foci* in the cell periphery (Arhel *et al*, 2006). Such CA foci detected in infected cells are thought to be individual viruses (Arhel *et al*, 2006; Arhel *et al*, 2007; Campbell *et al*, 2007b; McDonald *et al*, 2002). These observations confirmed that actin cytoskeleton is important in the early steps of viral movement towards the nucleus.

After this initial phase, HIV-1 most likely uses the microtubule network for its transport towards the nucleus, specifically towards the MTOC (Fig. 1.7) (McDonald *et al*, 2002). The transfer between microfilaments and microtubules could be mediated by cellular microtubule-associated proteins or motors having the ability to bind both microtubule and actin filaments (Rodriguez *et al*, 2003). As observed by IF, HIV-1 particles associated with microtubules and exhibited saltatory movements with a velocity of approximately ~1 μm/s (Arhel *et al*, 2006; McDonald *et al*, 2002). Next, HIV-1 RTCs were found to accumulate in the proximity of the MTOC (Arhel *et al*, 2006; McDonald *et al*, 2002; Zamborlini *et al*, 2007). Additionally, upon treatment with nocodazole an accumulation of viral complexes in the vicinity of the nucleus was observed (Arhel *et al*, 2006; Arhel *et al*, 2007). Recently, one team reported that HIV-1 induces the formation of a stable sub-population of microtubules and uses them for its transport to the nucleus (Sabo *et al*, 2013). Preventing the formation of these stable microtubules abolished HIV-1 infectivity (Sabo *et al*, 2013).

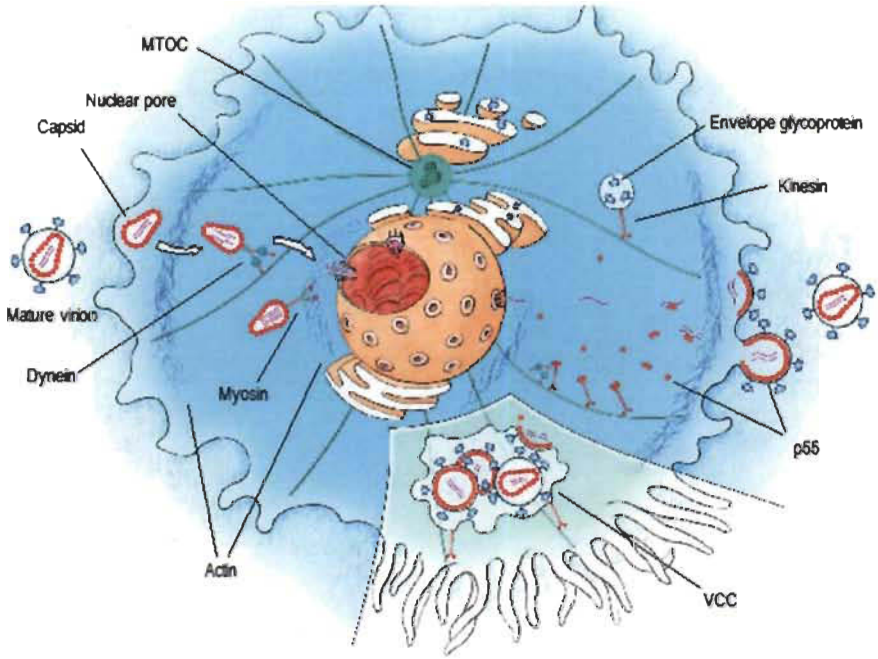

Figure 1.7 Schematic representation of HIV-1 trafficking inside the cell.
Following entry, HIV-1 briefly associates with the actin cortex, after which it is transferred to microtubules, along which it is transported towards the nucleus. This transport is carried out by the dynein motor complex. In the proximity of the nucleus HIV-1 is likely transferred to microfilaments, which would enable association with the nuclear pore complex. Newly produced viral proteins are transported towards the plasma membrane either in endosomes or directly on microtubules, likely employing kinesin-mediated transport. In the case of macrophages, virions bud inside virus-containing compartments (VCC).
Image source: (Gaudin *et al*, 2013).

To complete the picture, this transport is likely mediated by the dynein motor complex, as evidenced by an accumulation of HIV-1 virions in the cell periphery following microinjection of anti-dynein antibodies (McDonald *et al*, 2002). It remains uncertain which of the HIV-1 proteins would interact with the dynein motor complex, and with which of its chains.

Once in the vicinity of the nucleus, HIV-1 is likely transferred to perinuclear actin filaments, as evidenced by an observation of a slow velocity actin-like movement before docking at the NPC (Arhel *et al*, 2006). Furthermore, an actin inhibitor added 1 h p.i. resulted in an accumulation of HIV-1 foci in the proximity of the nucleus, but not at the nuclear membrane (Arhel *et al*, 2006).

Post the entry into the cell, viruses encounter not only proteins that enable their replication, but also specific mechanisms that have evolved to counteract the infection. These cellular protective systems are part of the host's immune system and are discussed in the next section.

1.3 Innate immunity and TRIM5α

Most organisms have developed protective systems against pathogens known as immune systems. Starting with a relatively simple clustered regularly interspaced short palindromic repeat (CRISPR)/CRISPR-associated protein 9 (Cas9) system in Archaea and Bacteria (Marraffini & Sontheimer, 2010), continuing with an innate immune system in all *Eukaryota*; including plants, with various effector mechanisms (Jones & Dangl, 2006), and finishing with a composed immune system in vertebrates. Vertebrates, in addition to the innate immune system, evolved an adaptive immune system (Janeway, 2001). The adaptive immune system provides target-specific, long-lasting response, and its hallmark is the production of antigen-specific antibodies. Patients infected with HIV-1 also produce specific antibodies, but the virus quickly mutates recognized epitopes and escapes antibody-mediated neutralization.

While it takes a few days for the adaptive immune system to be protective, the innate immune system is active within minutes of infection. It is the first line of defence; fast, but nonspecific. When a pathogen enters the cell, specific sensors called pattern-recognition receptors (PRRs) can detect conserved pathogen-specific motifs called pathogen-associated molecular patterns (PAMPs). Various PRRs can detect different PAMPs in distinct cellular compartments, *e.g.* double-stranded RNA (dsRNA) in endosomes is detected by Toll-like receptor 3 (TLR3), and in the cytoplasm by retinoic-acid-inducible gene I (RIG-I) (Fig. 1.8). Detection of PAMPs triggers innate immune responses through the activation of various transcription factors *e.g.* nuclear factor-κB (NF-κB) and IFN-regulatory factor 3 (IRF-3) (Trinchieri & Sher, 2007). Detection of viral components results in the production of cytokines, chemokines, and interferons, this is known as antiviral state. Produced type I IFNs, which acts both in autocrine and

paracrine manners, activate the Janus kinase (JAK)-signal transducer and activator of transcription (STAT) signalling pathway that leads to the transcription of antiviral IFN-stimulated genes (ISGs) (Schoggins & Rice, 2011). Many viruses evolved various ways to evade PRR detection and activation of the antiviral state (Rajsbaum & Garcia-Sastre, 2013). Also HIV-1 evades innate immunity sensors in its natural targets T-cells and macrophages (Rasaiyaah *et al*, 2013; Yan *et al*, 2010).

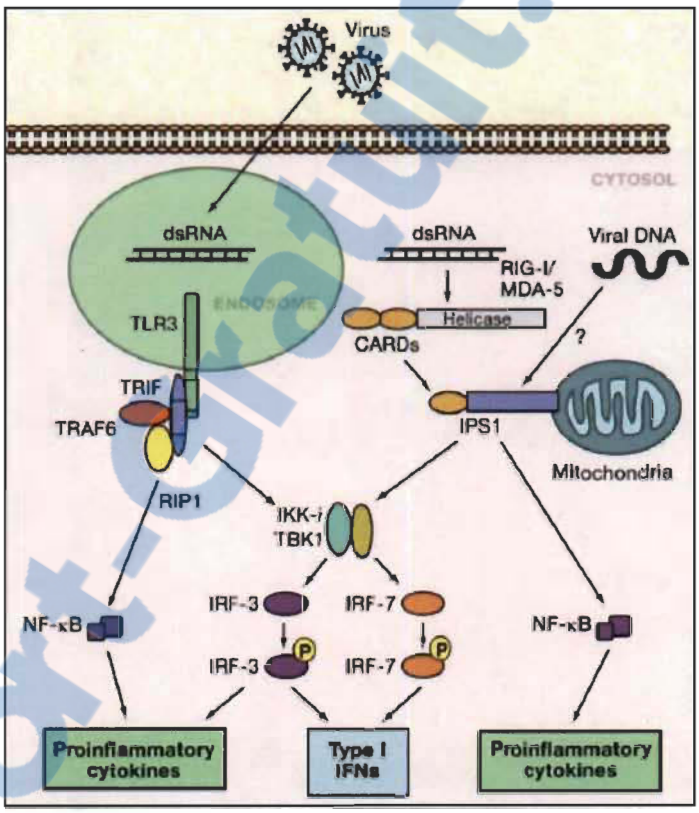

Figure 1.8 Mechanisms of Viral Detection in dendritic cells.
Viral PAMPs (pathogen-associated molecular patterns), such as dsRNA, are detected by various PRR (pattern recognition receptors) either in the cytosol (RIG-I) or in endosomes (TLR3), which induces proinflammatory cytokines and type I IFNs. TLR3 – Toll-like receptor 3; TRIF – TIR-domain-containing adapter-inducing interferon-β; TRAF6 – TNF receptor associated factor 6; RIP1 – Receptor-interacting protein 1; NF-κB - nuclear factor kappa-light-chain-enhancer of activated B cells; IKK *i* – IκB kinase *i*; TBK1 – TANK-binding kinase 1; IRF - Interferon regulatory factor; RIG-I – retinoic acid-inducible gene 1; MDA-5 Melanoma Differentiation-Associated protein 5; CARDs – Caspase activation and recruitment domains; IPS1 – interferon-beta promoter stimulator 1.
Image source: (Akira *et al*, 2006).

1.3.1 Restriction factors

Restriction factors are proteins belonging to ISGs that dominantly act to specifically inhibit pathogens (Harris *et al*, 2012). So far, several restriction factors targeting HIV-1 have been described: TRIM5α (Hatziioannou *et al*, 2004; Stremlau *et al*, 2004), bone marrow stromal cell antigen 2 (BST-2/Tetherin) (Neil *et al*, 2008), apolipoprotein B mRNA-editing, enzyme-catalytic, polypeptide-like 3 (APOBEC3) (Lecossier *et al*, 2003; Mangeat *et al*, 2003), SAM domain and HD domain-containing protein 1 (SAMHD1) (Hrecka *et al*, 2011; Laguette *et al*, 2011) and myxovirus resistance 2 (Mx2/MxB) (Goujon *et al*, 2013; Kane *et al*, 2013; Liu *et al*, 2013). Most of these factors are counteracted by HIV-1 proteins. The restriction factor Tetherin, which acts by preventing viral budding, is counteracted by Vpu (Neil *et al*, 2008; Varthakavi *et al*, 2003). The function of APOBEC3 proteins is counteracted by the viral protein Vif (Sheehy *et al*, 2002). In the absence of Vif APOBEC3 gets incorporated into budding HIV-1 virions and upon the second round of infection causes hypermutations during viral reverse transcription (Lecossier *et al*, 2003; Mangeat *et al*, 2003). HIV-2 does not encode Vpu protein, but instead carries Vpx, whose role was described as counteracting the restriction factor SAMHD1 (Hrecka *et al*, 2011; Laguette *et al*, 2011). SAMHD1 decreases HIV-1 infectivity in myeloid cells, such as macrophages and dendritic cells, by decreasing dNTP levels, which prevents viral reverse transcription (Goldstone *et al*, 2011; Powell *et al*, 2011). Notably, the restriction factor TRIM5α, which will be discussed later on, is not known to be antagonized by any viral protein. Little is known about the mechanism of MxB-mediated inhibition, except that its block is prior to viral integration. Interestingly, MxB function was mapped to the CA protein (Busnadiego *et al*, 2014; Goujon *et al*, 2013; Liu *et al*, 2013) and it was recently proposed that MxB might prevent HIV-1 uncoating (Fricke *et al*, 2014).

1.3.2 The TRIM family of proteins

The tripartite motif (TRIM) family of proteins encompasses multiple members involved in many cellular processes, such as proliferation, differentiation, signalling and innate immune response. The human genome contains around 100 genes coding for

TRIM proteins and many of them are synthesized as multiple isoforms. All TRIM proteins have a common N-terminal tripartite motif comprising three domains: RING ('really interesting new gene'), one or two B-boxes and coiled-coil, and therefore are often referred to as RBCC proteins. The C terminus of the proteins vary among the members and consist of one or two domains, such as SPRY (also known as PRYSPRY or B30.2) or Fibronectin III (FN3) (Fig. 1.9). Usually, the C-terminal domain determines the function of the whole protein, while RBCC works as an executive module (Han *et al*, 2011; Nisole *et al*, 2005; Reymond *et al*, 2001).

Many of the TRIM proteins are involved in the antiviral defence, such as TRIM5α (Hatziioannou *et al*, 2004; Keckesova *et al*, 2004; Stremlau *et al*, 2004; Yap *et al*, 2004), TRIM11 (Uchil *et al*, 2008), TRIM19 (promyelocytic leukemia protein, PML) (Chelbi-Alix *et al*, 1998; Regad *et al*, 2001), TRIM21 (Hauler *et al*, 2012), TRIM22 (Kajaste-Rudnitski *et al*, 2011), TRIM25 (Gack *et al*, 2007) and TRIM28 (KRAB-associated protein 1, Kap-1) (Wolf & Goff, 2007). The majority, if not all, TRIM proteins are involved in modulation of immune responses, however they can act in diverse ways, *e.g.* TRIM5α directly interacts with a restriction-sensitive virus (Sebastian & Luban, 2005; Stremlau *et al*, 2006), TRIM11 inhibits viral entry (Uchil *et al*, 2008) and TRIM25 is essential for the ability of RIG-I to trigger the innate immune response following detection of cytosolic viral RNA (Gack *et al*, 2007).

1.3.3 TRIM5α

One of the most studied members of the TRIM family is TRIM5α that belongs to ISGs (Asaoka *et al*, 2005). It was initially discovered as a cytoplasmic factor from Old World monkeys that inhibits HIV-1 replication (Hatziioannou *et al*, 2004; Stremlau *et al*, 2004). Further studies revealed that TRIM5α works in a virus-specific, species-specific manner. For example, rhesus macaque TRIM5α inhibits HIV-1, but not macaque SIV, whereas human TRIM5α inhibits N-tropic murine leukemia virus (N-MLV) and equine infectious anemia virus (EIAV), but neither B-tropic murine

leukemia virus (B-MLV) nor HIV-1 (Hatziioannou *et al*, 2004; Keckesova *et al*, 2004; Perron *et al*, 2004; Stremlau *et al*, 2004; Yap *et al*, 2004).

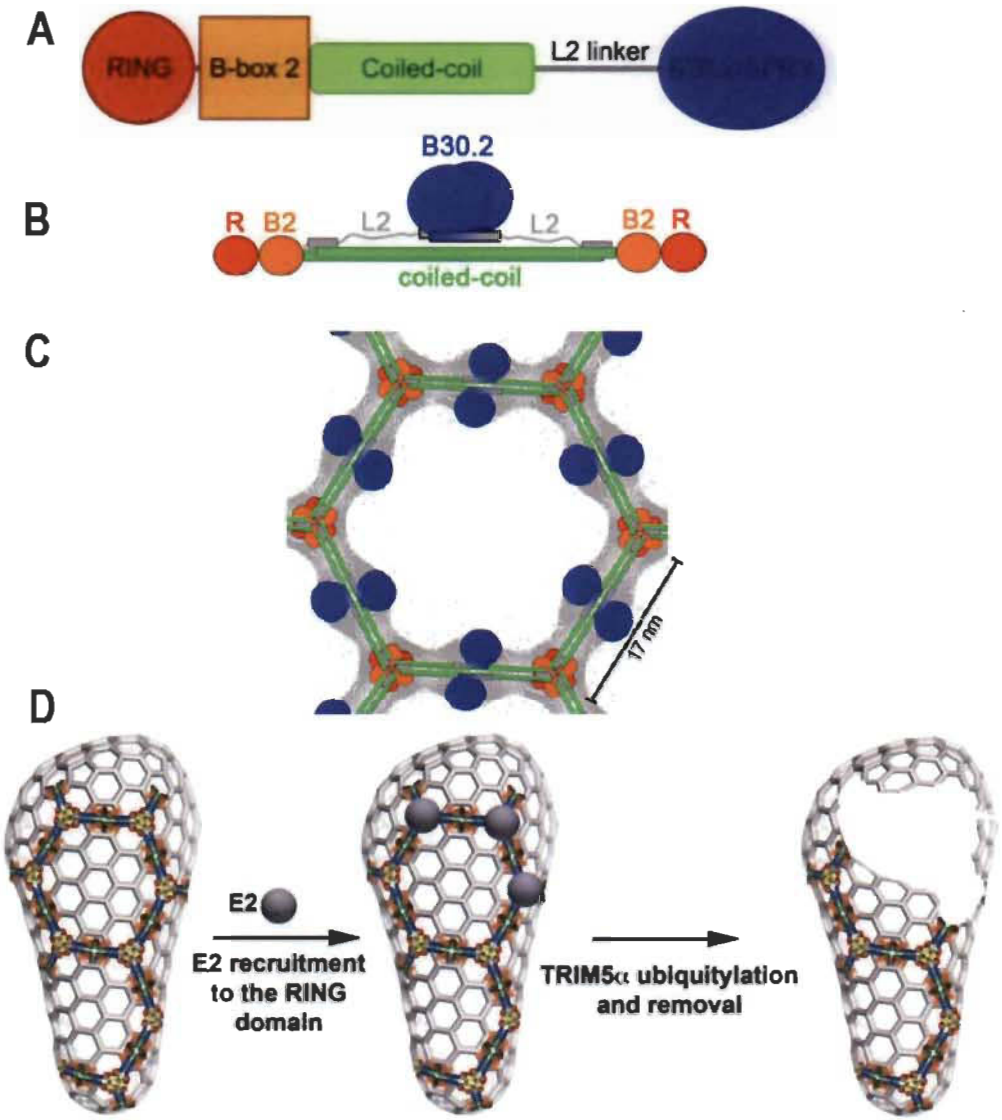

Figure 1.9 **Structure of TRIM5α and the current model of its action.**
(A) Linear diagram representing domain organization of TRIM5α. (B) Schematic model of the full-length TRIM5α dimer. The domain colors are the same as in (A). (C) Schematic model ofthe TRIM5α hexagonal lattice, showing the deduced positions of the different domains and overlaid with the cryoEM projection map (gray contours). (D) A model in which TRIM5α proteins form a hexagonal lattice around the capsid core that triggers auto-ubiquitylation of TRIM5α and its proteasomal degradation, which leads to tearing apart the capsid core. E2 – ubiquitin-conjugating enzyme.
Image sources: (Diaz-Griffero, 2011; Sanchez *et al*, 2014).

TRIM5 as a member of the tripartite family contains the three domains: RING, one B-box and coiled-coil, while its splice α additionally encodes a SPRY domain at the C terminus (Fig. 1.9A) (Reymond *et al*, 2001). Two additional linker sequences are found in the protein, between RING and B-box and between coiled-coil and SPRY.

1.3.3.1 Mechanism of action

Following entry of a restriction-sensitive virus into the cytoplasm, TRIM5α binds the incoming viral core *via* its SPRY domain (Nakayama *et al*, 2005; Sawyer *et al*, 2005; Stremlau *et al*, 2005; Yap *et al*, 2005). This interaction is host-specific, virus-specific and is determined by both SPRY domain and viral CA (Ohkura *et al*, 2006; Song *et al*, 2005b). A few consequences of this interaction can be observed as early as a few minutes post viral entry (Perez-Caballero *et al*, 2005). The CA core is quickly disassembled, which is linked with the decreased amounts of reverse transcription products (Perron *et al*, 2007; Roa *et al*, 2012; Stremlau *et al*, 2006). This is likely due to E3 ubiquitin ligase activity of the RING domain that results in TRIM5α auto-ubiquitylation and its proteasomal degradation, which is thought to tear the viral CA core apart (Fig. 1.9D) (Diaz-Griffero *et al*, 2006; Langelier *et al*, 2008; Lukic *et al*, 2011; Pertel *et al*, 2011; Rold & Aiken, 2008). Auto-ubiquitylation is important, but not essential, for TRIM5α restriction potency (Javanbakht *et al*, 2005; Lienlaf *et al*, 2011). Indeed, although a pharmacological inhibition of the proteasome rescues reverse transcription and seemingly normal stability of the CA core infectivity is still greatly inhibited (Anderson *et al*, 2006; Diaz-Griffero *et al*, 2006; Wu *et al*, 2006). Additionally, mutations in the RING domain that abrogate the ability of TRIM5α to inhibit reverse transcription and destabilize the CA core still allow potent retroviral restriction (Roa *et al*, 2012). This could be due to a sequestration of the incoming virus in cytoplasmic bodies (CBs; discussed below) formed by TRIM5α (Campbell *et al*, 2008; Danielson *et al*, 2012).

TRIM5α forms a hexagonal lattice around the CA core (Ganser-Pornillos *et al*, 2011) and binds to a conical core, rather than to a monomeric CA protein (Sebastian &

Luban, 2005; Zhao *et al*, 2011) (Fig. 1.9C-D). Interestingly, TRIM5α is thought to recognize multiple epitopes on the core interface and its action resembles antigen recognition by IgM antibodies (Biris *et al*, 2012). While monomeric TRIM5α weakly interacts with the CA structure, assembled TRIM5α proteins have very high avidity (Biris *et al*, 2013; Biris *et al*, 2012). Coiled-coil domain is required for homodimerization of TRIM5α proteins, which is necessary for the avidity of TRIM5α (Ganser-Pornillos *et al*, 2011; Kar *et al*, 2008; Langelier *et al*, 2008; Zhao *et al*, 2011). Interestingly, Linker2 was also linked to the ability of TRIM5α to self-associate (Sastri *et al*, 2010). Initial reports hypothesized that the dimers associate with each other laterally, whereas recent emerging reports suggest that this interaction is anti-parallel (Goldstone *et al*, 2014; Pornillos, 2014; Sanchez *et al*, 2014) (Fig. 1.9B). In the new model, the TRIM5α dimer would homo-associate anti-parallely *via* strong interactions between coiled-coil domains and helixes H3, which is contained in linker2. The B-box domain is responsible for higher-order multimerization, which is essential for full retroviral restriction (Diaz-Griffero *et al*, 2007b; Diaz-Griffero *et al*, 2009; Ganser-Pornillos *et al*, 2011; Javanbakht *et al*, 2005; Nepveu-Traversy *et al*, 2009).

1.3.3.2 Cell biology of TRIM5α

In the cytoplasm, over-expressed TRIM5α proteins form so-called cytoplasmic bodies (CBs) (Stremlau *et al*, 2004). It is uncertain if these structures reflect the real intracellular state of TRIM5α proteins, and their role in the retroviral restriction remains unclear, some studies deny their relevance (Perez-Caballero *et al*, 2005; Song *et al*, 2005a). Indeed, as endogenous levels of TRIM5α proteins are often too low to allow IF detection, most of the observations came from imaging of over-expressed proteins. The probable reason that CBs are observed is due to their ability to multimerize. However, these CBs were described as highly dynamic structures constantly associating and disassociating with each other (Campbell *et al*, 2007a). TRIM5α CBs co-localize with microtubules and undergo curvilinear movements along them. Additionally, live-cell imaging demonstrated that TRIM5α proteins self-associate around incoming restriction-sensitive viruses (Campbell *et al*, 2008). In the cytoplasm, TRIM5α CBs were shown to

co-localize with several proteins involved in proteasomal degradation pathway (Campbell *et al*, 2008; Danielson *et al*, 2012; Lukic *et al*, 2011). Additionally, in the presence of a restriction-sensitive virus this co-localization increases (Danielson *et al*, 2012). Moreover, TRIM5α proteins were shown to shuttle between the cytoplasm and the nucleus, although their predominant localization is cytoplasmic (Diaz-Griffero *et al*, 2011). When present in the nucleus, TRIM5α co-localize with PML/TRIM19 nuclear bodies (Diaz-Griffero *et al*, 2011). Therefore, although the possibility cannot be excluded that CBs formed by TRIM5α are artifacts stemming from protein over-expression (Song *et al*, 2005a), it is unlikely that these kind of dead artifacts would be as highly dynamic as those described by Campbell *et al*. (Campbell *et al*, 2007a).

TRIM5α has an additional role in mediating innate immune response, as it has been proposed to be a PRR (Pertel *et al*, 2011). TRIM5α promotes the innate immune signalling *via* activator protein 1 (AP-1) and NF-κB (Nepveu-Traversy & Berthoux, 2014; Pertel *et al*, 2011; Tareen & Emerman, 2011).

1.3.4 TRIMCyp

TRIMCyp is a protein related to TRIM5α that independently emerged in some monkeys by retrotransposition of the *cyclophilin A (CypA)* pseudogene sequence into the *TRIM5* locus, replacing the *SPRY* sequence (Nisole *et al*, 2004; Sayah *et al*, 2004; Wilson *et al*, 2008). This protein binds the CA core through its CypA domain and potently inhibits retroviruses in a virus-specific, species-specific manner, *e.g.* TRIMCyp from owl monkeys inhibits HIV-1 (Sayah *et al*, 2004), African green monkey SIV and feline immunodeficiency virus (FIV) (Lin & Emerman, 2006), while TRIMCyp arising in some rhesus macaques inhibits HIV-2 and FIV, but not HIV-1 (Wilson *et al*, 2008). TRIMCyp-mediated restriction can be inhibited by the specific CypA inhibitor cyclosporin A (CsA).

The next section briefly introduces the importance and rationale for conducting the following research. Also outlined are the hypotheses and specific objectives for the studies, as well as a summary of obtained results.

1.4 Importance, hypotheses and objectives

Despite the great progress in HIV-1 research, infection with this AIDS-causing virus remains incurable. Current antiretroviral therapies have many side effects and inconveniences, such as daily, life-long administration (Flepp *et al*, 2001). Additionally, the ability of HIV-1 to mutate and acquire multidrug resistance is tremendous (Abram *et al*, 2010). Whereas no sterilizing cure is accessible, new drugs have to be developed to keep up with this host-pathogen race. In particular, a new class of pharmaceuticals would be advantageous, targeting a different step of viral replication than currently used drugs. Promising new target for HIV-1 treatment seems to be the viral CA core, as evidence demonstrated that disrupting the incoming CA core inhibits infectivity (Forshey *et al*, 2002; Shi *et al*, 2011; Stremlau *et al*, 2004; Stremlau *et al*, 2006). Very little is known about the process of HIV-1 uncoating and how it employs cellular partners. It is crucial to gain more insight in this unexplored area in order to enable the development of novel drugs to target it.

While new drugs have to be developed, it is unlikely that they could ever become curative; taking into account that HIV-1 establishes reservoirs in long-living cells. The restriction factor TRIM5α could point to new approaches towards finding a sterilizing cure. Importantly, it has been suggested that TRIM5α could be employed in gene therapy approach targeting HIV-1 (Anderson, 2013). Gaining detailed knowledge about this protein is important as it could contribute to finding a cure to HIV-1 infection.

1.4.1 Objective I: To study the involvement of microtubules and dynein motor complexes in TRIM5α-mediated restriction

Both HIV-1 and TRIM5α CBs associate with and move along microtubules (Campbell *et al*, 2007a; McDonald *et al*, 2002). Additionally, HIV-1 uses the dynein motor complex for its route the nucleus (McDonald *et al*, 2002). Here, we hypothesized that the microtubule network could be a platform enabling TRIM5α to meet restriction-sensitive viruses. In this study, we investigated the role of microtubules and dynein motor complexes in the restriction of retroviruses mediated by TRIM5α. Interventions

disrupting microtubule dynamics and the function of the dynein motor complex partially rescued retroviral restriction, without affecting TRIM5α stability or causing excessive cytotoxicity. These interventions affected the dynamics of TRIM5α cytoplasmic bodies and decreased TRIM5α ability to destabilize incoming retroviral core. In conclusion, we found that both the microtubule network and the dynein motor complex are involved in the TRIM5α-mediated restriction of retroviruses.

1.4.2 Objective II: To study the involvement of microtubules and dynein motor complexes in HIV-1 uncoating

Following its entry to the cytoplasm, replication of HIV-1 is dependent on the cellular machinery. The incoming CA core is thought to be transported towards the nucleus *via* microtubules and dynein motor complexes (McDonald *et al*, 2002). During that time the CA core likely recruits cellular proteins to shield its genomic material from the hostile cellular environment (Lahaye *et al*, 2013; Rasaiyaah *et al*, 2013). Initially, cellular factors likely stabilize the HIV-1 CA core until it reaches the NPC, through which HIV-1 enters the nucleus (Fricke *et al*, 2013; Guth & Sodroski, 2014). A handful of cellular partners for HIV-1 uncoating have been described (De Iaco *et al*, 2013; Fricke *et al*, 2013; Guth & Sodroski, 2014; Li *et al*, 2009; Misumi *et al*, 2010; Shah *et al*, 2013). Here, based on the observations in the manuscript presented in Chapter II, we hypothesized that dynein-dependent transport along microtubules might be involved in HIV-1 uncoating. Indeed, pharmacological abrogation of microtubule dynamics and depletion of DHC led to an accumulation of HIV-1 CA *foci* in infected cells observed by IF. We also employed the fate-of-capsid assay, which allows for the isolation of particulate viral cores from infected cells (Perron *et al*, 2004). Perturbation of either microtubule dynamics or dynein-dependent transport resulted in a transient increase in the amount of pelletable (particulate) HIV-1 CA cores. In conclusion, we found that dynein-dependent transport along microtubules of HIV-1 might be linked with its uncoating.

Chapter II contains a study that demonstrates that microtubules and dynein motor complexes are involved in the retroviral restriction mediated by TRIM5α.

CHAPTER II

FUNCTIONAL EVIDENCE FOR THE INVOLVEMENT OF MICROTUBULES AND DYNEIN MOTOR COMPLEXES IN TRIM5α-MEDIATED RESTRICTION OF RETROVIRUSES

PAULINA PAWLICA, VALERIE LE SAGE[1], NOLWENN POCCARDI, MICHEL J. TREMBLAY[2], ANDREW J. MOULAND[1], LIONEL BERTHOUX

Published on 5th of March 2014 in *Journal of virology*

2.1 Contributions

L.B. designed the study. L.B., P.P. and A.J.M interpreted the results and prepared the manuscript. M.J.T shared materials. P.P. performed 95% of the experiments. V.L.S and N.P. performed 5% of the experiments.

2.2 Abstract

The tripartite motif (TRIM) family of proteins includes the TRIM5α antiretroviral restriction factor. TRIM5α from many Old World and some New World monkeys can restrict the human immunodeficiency virus type 1 (HIV-1), while human TRIM5α restricts N-tropic Murine Leukemia Virus (N-MLV). TRIM5α forms highly dynamic cytoplasmic bodies (CBs) that associate with and translocate on microtubules. However, the functional involvement of microtubules or other cytoskeleton-associated factors in the viral restriction process had not been shown. Here, we demonstrate the dependency of TRIM5α-mediated restriction on microtubule-mediated transport. Pharmacological

[1] HIV-1 RNA Trafficking Laboratory, Lady Davis Institute at the Jewish General Hospital and Department of Medicine, McGill University.

[2] Centre de Recherche en Infectiologie, Centre de Recherche du CHU de l'Université Laval.

disruption of the microtubule network using nocodazole or disabling it using paclitaxel decreased restriction of N-MLV and HIV-1 by human or simian alleles of TRIM5α, respectively. In addition, pharmacological inhibition of dynein motor complexes using erythro-9-(2-hydroxy-3-nonyl)adenine (EHNA) and siRNA-mediated depletion of the dynein heavy chain (DHC) similarly decreased TRIM5α-mediated restriction. The loss in restriction resulting from either the disassembly of microtubules or the disruption of dynein motor activity was seen for both endogenous and over-expressed TRIM5α and was not due to differences in protein stability or cell viability. Both nocodazole treatment and DHC depletion interfered with the dynamics of TRIM5α CBs, increasing their size and altering their intracellular localization. In addition, nocodazole, paclitaxel and DHC depletion were all found to increase the stability of HIV-1 cores in infected cells, providing an alternative explanation for the decreased restriction. In conclusion, association with microtubules and the translocation activity of dynein motor complexes are required to achieve efficient restriction by TRIM5α.

2.3 Importance

The primate innate cellular defenses against infection by retroviruses include a protein named TRIM5α, belonging to the family of restriction factors. TRIM5α is present in the cytoplasm where it can intercept incoming retroviruses shortly after their entry. How TRIM5α manages to be present at the appropriate subcytoplasmic location to interact with its target is unknown. We hypothesized that TRIM5α, either as a soluble protein or a high-molecular-weight complex (the cytoplasmic body) is transported within the cytoplasm by a molecular motor called the dynein complex, itself known to interact with and move along microtubules. Our results show that destructuring microtubules or crippling their function decreased the capacity of human or simian TRIM5α to restrict their retroviral targets. Inhibiting dynein motor activity, or reducing the expression of a key component of this complex, similarly affected TRIM5α-mediated restriction. Thus, we have identified specific cytoskeleton structures involved in innate antiretroviral defenses.

2.4 Introduction

Members of the tripartite motif (TRIM) family of proteins have been described to exhibit antiviral properties (Hauler *et al*, 2012; Kajaste-Rudnitski *et al*, 2011; Uchil *et al*, 2008; Wolf & Goff, 2007). The best-known member is TRIM5α, first characterized as a factor from Rhesus macaque (rhTRIM5α) that potently inhibits human immunodeficiency virus 1 (HIV-1) (Stremlau *et al*, 2004). Other TRIM5α orthologs from some New World and Old World monkeys also provide protection against HIV-1 infection (Hatziioannou *et al*, 2004; Keckesova *et al*, 2004; Song *et al*, 2005b). Human TRIM5α (huTRIM5α), while not having the ability to restrict HIV-1, protects against N-tropic murine leukemia virus (N-MLV) and equine infectious anaemia virus (EIAV) (Hatziioannou *et al*, 2004; Keckesova *et al*, 2004; Perron *et al*, 2004; Rahm *et al*, 2011; Yap *et al*, 2004). Expression of TRIM5α is induced by type 1 interferons, supporting their role as innate immunity effectors (Asaoka *et al*, 2005; Carthagena *et al*, 2008). In addition, TRIM5α acts as an innate sensor of retroviral infections, triggering an antiviral signalling pathway that can lead to interferon production (Pertel *et al*, 2011; Tareen & Emerman, 2011).

Retroviral restriction is initiated by specific recognition of the N-terminal domain of incoming retroviral capsid (CA) proteins by the B30.2/PRYSPRY domain of TRIM5α (Sebastian & Luban, 2005; Stremlau *et al*, 2006a). TRIM5α binds to intact CA cores rather than monomeric CA proteins (Ganser-Pornillos *et al*, 2011) and as a result of this interaction, replication is impaired by several effector mechanisms [rewieved in: (Luban, 2007; Nisole *et al*, 2005; Towers, 2007)]. So far two major TRIM5α-mediated blocks have been described. The first one is accelerated disassembly of the retroviral CA core accompanied by a decrease in amounts of reverse transcription products (Bérubé *et al*, 2007; Perron *et al*, 2007; Roa *et al*, 2012; Stremlau *et al*, 2006a). As a consequence of the disassembly induced by TRIM5α, core components such as the viral RNA and integrase are solubilized or degraded (Kutluay *et al*, 2013). This restriction effector mechanism also involves the degradation of TRIM5α by the proteasome in presence of the restricted virus (Rold & Aiken, 2008). Accordingly, treatment with proteasome inhibitors restores seemingly normal disassembly of the viral core and rescues the

production of viral cDNA (Anderson *et al*, 2006; Diaz-Griffero *et al*, 2007; Kutluay *et al*, 2013). However, proteasome inhibition does not fully rescue infectivity in restrictive conditions, pointing to the existence of a second, proteasome-independent restriction mechanism. The precise mechanism of this second block is still unclear but access of the viral DNA to the nucleus is inhibited (Anderson *et al*, 2006; Wu *et al*, 2006). This could be related to the 'sequestration' of incoming retroviruses in CBs formed by TRIM5α proteins (Campbell *et al*, 2008; Danielson *et al*, 2012).

TRIM5α contains a coiled-coil domain responsible for protein dimerization and a B-box domain important for the higher order organized states that probably promote the formation of CBs (Kar *et al*, 2008; Li & Sodroski, 2008). CBs were described as dynamic structures constantly associating and disassociating with each other, exchanging TRIM5α proteins with a pool of proteins diffused in the cytoplasm (Campbell *et al*, 2007), and their size depends on the level of TRIM5α expression (Perez-Caballero *et al*, 2005). The role of CBs in retroviral restriction is still unclear and some reports refute their relevance in this process (Perez-Caballero *et al*, 2005; Song *et al*, 2005a). Indeed, no CBs have been detected at endogenous TRIM5α expression levels, and it is possible that some observed CBs are artifacts stemming from protein over-expression (Song *et al*, 2005a). On the other hand, TRIM5α CBs were found to co-localize with ubiquitin (Campbell *et al*, 2008), proteasomal subunits (Danielson *et al*, 2012; Lukic *et al*, 2011) and p62/Sequestosome-1 (O'Connor *et al*, 2010). p62 is an important adaptor protein with a role in cell signalling and protein degradation [reviewed in (Moscat *et al*, 2007; Seibenhener *et al*, 2007)]. Additionally, TRIM5α proteins form bodies that enclose incoming restriction-sensitive viruses and closely resemble pre-existing CBs (Campbell *et al*, 2008). Collectively, these observations suggest that TRIM5α CBs are relevant to restriction mechanisms.

The microtubule network, a component of the cellular cytoskeleton, is made of highly dynamic filaments built of tubulin α/β heterodimers and plays multiple roles in the cell, including intra-cellular transport, organelle positioning and cell division (de Forges *et al*, 2012). Microtubules provide platforms for molecular motors, which enable

active transport through the dense cytoplasm of the cell. The dynein motor complex [reviewed in (Hook & Vallee, 2006)] is a microtubule-associated molecular motor that transports various cellular cargos towards the microtubule-organizing center (MTOC) at the minus-end of microtubules. The MTOC is found in the vicinity of the nucleus except during cell division. Several viruses, including HIV-1, were described to recruit dynein motor complexes for their transport during the early stages of their replication [reviewed in (Dodding & Way, 2011; Hsieh *et al*, 2010; Mouland & Milev, 2012)]. TRIM5α CBs also associate with microtubules and their movements along these filaments have been observed (Campbell *et al*, 2007). However, a functional role for this association has not been demonstrated, nor have the molecular motors responsible for TRIM5α movement been identified. Here we asked whether the integrity of microtubules was functionally important for restriction to occur. In addition, we investigated the role of the dynein motor in this process. Using pharmacological and genetic approaches coupled with imaging analyses, we provide evidence that both microtubules and dynein motor activity are important for the restriction process mediated by TRIM5α.

2.5 Materials and methods

Cells, pharmaceuticals and antibodies. Human embryonic kidney 293T cells, human epithelial carcinoma HeLa cells, human U373-derived MAGI cells, Rhesus macaque kidney FRhK-4 cells and feline renal CRFK cells were maintained in Dulbecco's modified Eagle's medium (DMEM) with high glucose, supplemented with 10% fetal bovine serum (FBS) and antibiotics at 37°C, 5% CO_2. All cell culture reagents were from HyClone (Thermo Scientific, Logan, UT). HeLa cells stably expressing FLAG-tagged TRIM5 proteins were generated by retroviral transduction as described previously (Bérubé *et al*, 2007; Pham *et al*, 2010). Nocodazole, paclitaxel (taxol), erythro-9-(2-hydroxy-3-nonyl)adenine (EHNA), 2,3-Bis-(2-Methoxy-4-Nitro-5-Sulfophenyl)-2H-Tetrazolium-5-Carboxanilide (XTT), phenazine methosulfate (PMS), heparin sodium salt and cycloheximide were provided by Sigma (St Louis, MI). Anti-DHC rabbit polyclonal antibodies were from Santa Cruz (Dallas, TX). The HRP-conjugated mouse anti-actin antibody was from Sigma. Capsid (CA, p24) was detected

using a mouse monoclonal antibody (clone 183) from the AIDS Research and Reference Reagent Program. The FLAG epitope was detected using the M2 mouse monoclonal antibody (Sigma) or the M2 rabbit polyclonal antibody from Cell Signaling (Danvers, MA). HRP-conjugated goat anti-rabbit and goat anti-mouse antibodies used as secondary antibodies in western blots were all from Santa Cruz.

Plasmid DNAs and retroviral vectors production. The plasmid encoding a GFP-tagged version of α-tubulin (Rusan *et al*, 2001) was a gift from Ali Saib. To produce viral vectors, 10-cm culture dishes of sub-confluent HEK293T cells were co-transfected using polyethylenimine (25,000 kDa, Polyscience) with the appropriate plasmids as follows. For wild-type (WT) or the G89V CA mutant of HIV-$1_{CMV-GFP}$, we used 10 μg of $pTRIP_{CMV-GFP}$, 10 μg of WT or G89V pΔR8.9 and 5 μg of pMD-G; for N-MLV_{GFP} and B-MLV_{GFP}, we used 10 μg of pCNCG, 5 μg of pMD-G and 10 μg of pCIG3N (N-MLV_{GFP}) or pCIG3B (B-MLV_{GFP}); for HIV-$1_{NL43-GFP}$, we used 10 μg of pNL-GFP and 5 μg of pMD-G; for $SIV_{mac-GFP}$, 10 μg of $pSIV_{mac-GFP}$ and 5 μg of pMD-G (Berthoux *et al*, 2005a; Berthoux *et al*, 2004; Berthoux *et al*, 2005b; Berthoux *et al*, 2003; Bérubé *et al*, 2007; Naviaux *et al*, 1996; Pham *et al*, 2010; Sebastian *et al*, 2006; Zufferey *et al*, 1997). $pNL4.3_{IRES-GFP}$ (Imbeault *et al*, 2009) encodes a version of the HIV-1 NL4-3 strain (Adachi *et al*, 1986) expressing GFP in addition to the viral proteins, and was a gift from David N. Levy. Production of the corresponding virus (HIV-$1_{NL43-IRES-GFP}$) was done by transfecting 10 μg of the plasmid in sub-confluent HEK293T cells in a 75-cm flask. Media were changed 16 h post transfection and virus-containing supernatants were collected after an additional 32 h of culture. All viral stocks were clarified by centrifugation for 5 min at 400 x *g*. All viral vectors were titrated in permissive CRFK cell using GFP expression as a marker of successful transduction. In some experiments, reverse transcriptase activity was measured on virus stocks using the EnzCheck kit (Molecular Probes) according to the manufacturer's instructions.

Viral challenges, pharmacological treatments and RNA interference. Cells were seeded in 24-well plates at 1 x 10^5 cells/well (HeLa, CRFK, MAGI) or

5×10^4 cells/well (FRhK-4), and were challenged the next day with various retroviral vectors (HIV-$1_{CMV\text{-}GFP}$, HIV-1_{G89V}, HIV-$1_{NL43\text{-}GFP}$, $SIV_{mac\text{-}GFP}$, N-MLV_{GFP} or B-MLV_{GFP}) or a replication-competent retrovirus (HIV-$1_{NL43\text{-}IRES\text{-}GFP}$). When applicable, cells were pre-treated for 15 min with nocodazole, paclitaxel or EHNA, and infections were then performed in presence of these drugs. Media were changed after 16 h, and 48 h post-infection cells were trypsinized and fixed in 2% formaldehyde (Fisher Scientific) in phosphate buffer saline (PBS). The % of GFP-positive cells were then determined by analyzing 1×10^4 to 3×10^4 cells on a FC500 MPL cytometer (Beckman Coulter) using the CXP software. For the siRNA treatments, 2×10^5 cells were plated in each 3.5-cm of a 6-well plate and transfected with 40 nM of siRNA using DharmaFECT 1 (Dharmacon). The siRNA against heavy chain of dynein (DHC) was previously described (Lehmann *et al*, 2009) and targets the following sequence: 5'GATCAAACATGACGGAATT. The control siRNA (purchased from Dharmacon) was designed to target a luciferase sequence (5'CGTACGCGGAATACTTCGATT) absent in the human genome. 48 h post transfection, cells were seeded in 24-well plates and were challenged the next day with retroviral vectors as described above.

Stability assay. 1×10^6 HeLa cells stably expressing FLAG-rhTRIM5α were seeded in 6-well plates one day prior to the experiment. For the siRNA treatments, cells were transfected 48 h before seeding, as described above. Cells were pre-treated for 1 h with 100 μg/ml of cycloheximide, then treated with the indicated drugs without removing cycloheximide and harvested at the indicated time points. Drug concentrations were as follows: nocodazole, 0.1 μM; paclitaxel, 0.1 μM, EHNA, 600 μM. Cells were lysed in cold stability buffer (100 mM Tris-HCl pH 8.0, 100 mM NaCl, 0.5% NP-40) supplemented with Complete protease inhibitor cocktail (Roche, Bale, Switzerland) and processed for western blotting. rhTRIM5α was detected using the anti-FLAG rabbit polyclonal antibody.

Viability assay. 1×10^4 HeLa or 5×10^3 FRhK-4 cells were seeded per well in 96-well plates. The next day, cells were washed with PBS and wells were replenished with 100 μl of DMEM without phenol red supplemented with serum and serial dilutions

of the tested drugs. After 16 h of incubation, 100 µl of the PBS solution containing 50 µg of XTT and 6 µg of PMS were added. Cells were incubated 2- 4 hours at 37ºC, then the absorbance was read at 490 nm on a Synergy HT (BioTek) plate reader and corrected for background value determined on blank samples.

Fate-of-capsid assay. To analyze post-entry capsid disassembly, a protocol adapted from Stremlau *et al* (Perron *et al*, 2004) was used as described earlier (Keckesova *et al*, 2004). Briefly, 3 x 10^6 HeLa cells seeded in 10-cm dishes were infected with HIV-$1_{CMV\text{-}GFP}$ at a multiplicity of infection (MOI) of ~2 as calculated on the permissive control cells. 2 h later, virus-containing supernatants were removed and cells were rinsed once in PBS followed by a gentle trypsinization treatment (1:1 trypsin:PBS mixture for 10 sec at room temperature). Fresh medium containing the appropriate drugs was then added, and cells were incubated at 37°C, 5% CO_2 for an additional 4 hours. Cells were then trypsinized and resuspended in ice-cold lysis buffer (100 µM Tris-HCl pH 8.0, 0.4 mM KCl, 2 µM EDTA, Roche's Complete protease inhibitor) and disrupted with a dounce homogenizer. Whole cell Lysate (WCL) samples were collected at this point. In order to remove cell debris and nuclei, lysates were centrifuged for 5 min at 1,000 x *g*, 4°C, and then layered on top of a 50% sucrose cushion prepared in STE buffer (100 mM NaCl, 10 mM Tris-HCl pH 8.0, 1 mM EDTA). Particulate viral cores were sedimented by ultracentrifugation in a Sorval WX Ultra 100 ultracentrifuge at 175,000 x *g* for 2 h at 4°C. Pellets were resuspended in denaturing gel loading buffer and processed for CA western blotting together with whole cell lysates. Post-centrifugation supernatants were collected from the fraction above the sucrose cushion, excluding the sucrose:supernatant interface.

Immunofluorescence (IF) microscopy. For the analysis of the localization patterns of LAMP-1 and microtubules, 2 x 10^5 cells (HeLa) or 1 x 10^5 cells (FRhK-4) were seeded on glass coverslips placed in 3.5-cm wells. For siRNA treatments, cells were transfected 48 h prior to seeding as described above. For the cells expressing GFP-tubulin, 2 µg of the plasmid were transfected per well 24 h prior to seeding. The day after seeding, cell were fixed (siRNA treatment) or incubated for 2 h with drugs

(nocodazole, paclitaxel, EHNA) and then fixed. Fixation was done for 10 min in pre-warmed 4% formaldehyde-DMEM at 37°C, then cells were washed once in PBS, blocked in 1X blocking solution (Roche, Bale, Switzerland) and stained or not for LAMP-1 for 1 h at room temperature. Primary rabbit LAMP-1 antibodies were described previously (Lehmann *et al*, 2009) and diluted 1:1000. LAMP-1 was revealed using the AlexaFluor594-conjugated donkey anti-rabbit secondary antibody (Molecular Probes, Eugene, OR). Cell nuclei were stained with DAPI (Invitrogen), then washed with PBS and mounted on glass slides using ImmunoMount (Thermo-Fisher Scientific). Microscopy was performed using a microscope (DM16000B; Leica) equipped with a spinning disk confocal head (WaveFX; Quorum Technologies, Guelph, Ontario), a 63X (1.4 numerical aperture oil immersion) plan apochromat objective lens, and an EM charge-coupled device camera (ImageEM; Hamamatsu Photonics, Boston, MA). The Volocity Imaging software (v4.3.2; PerkinElmer, Waltham, MA) was used as acquisition software. Image analyses were performed using the Imaris software v7.4 (Bitplane Inc., South Windsor, CT). We estimated the effect of EHNA treatment or DHC depletion by counting the % of cells (n = 100-300 in two experiments) exhibiting predominant LAMP juxtanuclear staining versus cells exhibiting mostly peripheral staining, as described earlier (Lehmann *et al*, 2009).

For the analysis of TRIM5α CBs and of microtubules, HeLa cells in 3.5-cm wells were transfected or not with siRNAs directed against DHC or Luciferase as described above. The next day, cells were additionally transfected or not with 2 μg of pGFP-tubulin per well, using polyethyleneimine. The next day, 2 x 10^5 of these cells were seeded on glass coverslips placed in 3.5-cm wells. 24 h later, the cells were treated or not with nocodazole for 4 h and then fixed and processed for IF staining. Fixation was done for 10 min in 4% formaldehyde-DMEM in 37°C, followed by three washes with ice-cold PBS. Cells were then permeabilized by treatment with 0.1% Triton X-100, 0.1 mM sodium citrate for 1-2 min on ice. Cells were then washed again three times with PBS and treated with 10% normal goat serum (Sigma) containing 0.3 M glycine (Sigma) for 30 min at RT. This was followed by a 4-hours incubation with a murine antibody against the FLAG epitope diluted 1:400 in PBS containing 10% normal goat

serum. Cells were washed five times and fluorescently stained with the Alexa594-conjugated goat anti-mouse antibody (Molecular Probes) at a 1:200 dilution. Cells were washed five times in PBS before mounting in Vectashield (Vector Laboratories, Burlington, Ontario). Hoechst33342 (0.8 μg/ml; Molecular Probes) was added along with the penultimate PBS wash to reveal DNA. Z-stacks were acquired on the AxioObserver Microscope (Carl Zeiss, Jena, Germany) equipped with the Apotome module and median Z-stacks were retained for analysis. For the analysis of TRIM5α CB sizes, FLAG foci in a given cell were manually outlined in the AxioVision software for calculation of the surface. A minimum of 100 and up to 214 CBs from 10 randomly chosen cells were included in the analysis. For the analysis of TRIM5α CB localization, the cell's edge was outlined and for each FLAG foci in a given cell, we measured the closest distance to the nuclear membrane and the closest distance to the plasma membrane, using Axiovision. A minimum of 85 and up to 440 CBs from a minimum of 5 randomly chosen cells were included in the analysis. To avoid human bias, CBs size and localization analyses were performed blindly by students not otherwise involved in this project, using image files that had coded names. For the analysis of TRIM5α-microtubules co-localization, images were acquired using the Apotome in Raw Data mode to allow for subsequent deconvolution, which was done using the AxioVision software (Carl-Zeiss).

2.6 Results

Nocodazole and paclitaxel treatments rescue infectivity of retroviruses restricted by endogenous TRIM5α. In order to determine whether the microtubule network has a functional role in retroviral restrictions mediated by TRIM5α, we used nocodazole and paclitaxel, pharmacological agents that prevent the polymerization of microtubules (Luduena & Roach, 1991) or block their dynamics by preventing disassembly (Jordan & Wilson, 2004), respectively. First we tested the effect of nocodazole and paclitaxel on restriction of HIV-1 or N-MLV at multiple drug concentrations (Fig. 2.1). In this set of experiments, we infected human HeLa cells with N-MLV$_{GFP}$, a huTRIM5α-sensitive N-tropic MLV vector expressing GFP and, as a

control, its restriction-insensitive B-tropic counterpart (B-MLV). Similarly, we infected Rhesus macaque FRhK-4 cells with a rhTRIM5α-sensitive HIV-1 vector expressing GFP or, as a control, with $SIV_{mac\text{-}GFP}$, a rhTRIM5α-insensitive simian immunodeficiency virus (SIV) strain mac239-based vector also expressing GFP. These infections were done using virus doses that had been previously determined to result in 0.1% to 1% infected (GFP-positive) cells in the absence of drug. In these experimental conditions, we found that both nocodazole and paclitaxel increased GFP transduction by the restricted virus while having little effect on infection by the unrestricted control virus (Fig. 2.1). Specifically, nocodazole treatment of cells increased N-MLV infection of HeLa cells by up to 45.2-fold, and was active at a large range of concentrations peaking at about 0.1 μM (Fig. 2.1A). Nocodazole also increased the permissiveness of FRhK-4 cells to infection by $HIV\text{-}1_{NL43\text{-}GFP}$ by up to 8.5-fold (Fig. 2.1B). In these cells, nocodazole was active at higher concentrations (> 0.5 μM). Nocodazole slightly increased infection by the unrestricted retroviral vector ($B\text{-}MLV_{GFP}$ or $SIV_{mac\text{-}GFP}$) in both cell lines, but the magnitude of this effect reached ≤ 4-fold and ≤ 2-fold in HeLa and FRhK-4 cells, respectively (Fig. 2.1). This subtle enhancement in infection might be the result of cell cycle arrest mediated by nocodazole (Groschel & Bushman, 2005). Similar to nocodazole, paclitaxel increased N-MLV infection of HeLa cells by up to 33.1-fold (Fig. 2.1A). This enhancement was seen for all drug concentrations tested in HeLa cells, peaking at ~0.1 μM. Paclitaxel increased HIV-1 infection of FRhK-4 cells by up to 7.9-fold (Fig. 2.1B), and similar to nocodazole, higher concentrations of the drug (≥ 1μM) needed to be used in this cell line in order to observe an effect on restriction. Paclitaxel slightly increased the infection of FRhK-4 cells by $SIV_{mac\text{-}GFP}$ (Fig. 2.1B) but, conversely, decreased B-MLV infectivity in HeLa cells at concentrations > 6 μM (Fig. 2.1A).

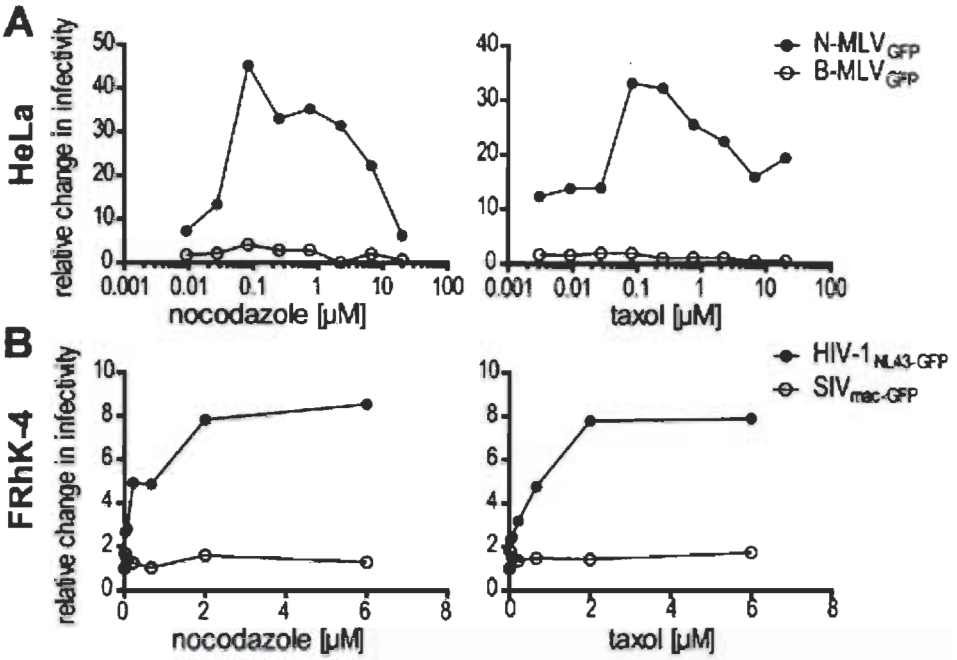

Figure 2.1 **Drug concentration-dependent enhancement of permissiveness to infection by TRIM5α-restricted retroviral vectors in human and simian cells.**
HeLa cells (A) and FRhK-4 cells (B) were infected with single doses of the indicated viral vectors in the absence or presence of increasing amounts of nocodazole or paclitaxel (taxol) for 16 h. The amounts of viruses used were adjusted to obtain in the vicinity of 0.1 to 1% of infected cells in the absence of the drug and yielded 0.09% (N-MLV$_{GFP}$), 0.38% (B-MLV$_{GFP}$), 0.85% (HIV-1$_{NL43-GFP}$) and 1.23% (SIV$_{mac-GFP}$) infected cells. The % of infected (GFP-positive) cells were determined by flow cytometry 2 d post infection and results are presented as -fold changes in infectivity relative to the relevant untreated controls.

Partial inhibition of TRIM5α-mediated restriction by disruption of the microtubule network. The experiments shown in Fig. 2.1 indicated that disruption of microtubules by nocodazole or paclitaxel treatments could increase infection by TRIM5α-sensitive viruses but not TRIM5α-insensitive ones. However, these results did not allow us to quantify the extent of inhibition conferred by nocodazole or paclitaxel treatments, relative to the magnitude of restriction itself. They also did not allow us to analyze whether the effect seen was dependent on the MOI used. Therefore, we performed virus dose-dependent experiments using fixed drug concentrations. We used nocodazole and paclitaxel concentrations that corresponded to their peak of anti-

restriction activity as determined in Fig. 2.1. When the virus amounts used were normalized according to infectivity in non-restrictive CRFK cells (CRFK Infectious Units [IU]), we found N-MLV$_{GFP}$ to be to ~500-times less infectious than B-MLV$_{GFP}$ in HeLa cells (Fig. 2.2A), reflecting the expected level of N-MLV restriction by endogenous huTRIM5α in these cells (Keckesova *et al*, 2004). Permissiveness to the huTRIM5α-insensitive B-MLV vector was not significantly affected by either nocodazole or paclitaxel treatments, regardless of the virus amounts used (Fig. 2.2A). In contrast, N-MLV infectivity was increased by up to 65-fold following nocodazole treatment and 71-fold following paclitaxel treatment (Fig. 2.2A). In other words, nocodazole and paclitaxel reduced restriction of N-MLV to only about 20-fold in HeLa cells. In these cells, the effects of nocodazole and paclitaxel on N-MLV were the greatest when a relatively small amount of virus was used (5 CRFK IU), while there was only a ~7-fold increase in N-MLV infection at MOIs 10-times higher (Fig. 2.2A). These observations probably reflect the fact that saturation of endogenous huTRIM5α by large amounts of N-MLV capsids partly suppresses restriction in the absence of pharmacological treatment.

As expected, HIV-1$_{NL43\text{-}GFP}$ was strongly restricted (~1000-fold) relative to SIV$_{mac\text{-}GFP}$ in macaque FRhK-4 cells, when the two viruses were normalized according to their infectious titers in CRFK cells (Fig. 2.2B) (Berthoux *et al*, 2005b; Besnier *et al*, 2002). Nocodazole and paclitaxel had no effect on infection by SIV$_{mac\text{-}GFP}$, regardless of the amount of virus used (Fig. 2.2B). In contrast, both nocodazole and paclitaxel increased infection by HIV-1$_{NL43\text{-}GFP}$ in these cells by 16- to 17-fold at low MOIs. When the virus dose used was > 100 CRFK IU, the enhancing effect of nocodazole and paclitaxel was smaller, which again was probably due to saturation of TRIM5α by incoming capsids. The cyclophilin A (CypA) binding loop of CA is a major determinant of HIV-1 sensitivity to restriction by TRIM5α (Lin & Emerman, 2008), and the CA-G89V mutant, which abrogates CypA binding (Yoo *et al*, 1997), is known to be less susceptible to restriction by rhTRIM5α (Berthoux *et al*, 2005b; Stremlau *et al*, 2006b). Thus, we hypothesized that nocodazole and paclitaxel treatments would have a smaller enhancing effect on CA-G89V HIV-1 compared to its WT counterpart. Indeed, we

found that in subsaturating conditions (<200 CRFK IU), nocodazole and paclitaxel increased WT HIV-$1_{CMV\text{-}GFP}$ by ~10-fold (5.6- to 16-fold) and ~7.5-fold (4.7- to 10.5-fold), respectively (Fig. 2.2C). In contrast, nocodazole and paclitaxel increased infectivity of the mutant virus by only ~3.7-fold (2.3- to 5.0-fold) and ~3.4-fold (2.0- to 5.7-fold), respectively (Fig. 2.2C).

In order to verify that nocodazole and paclitaxel had the expected effect on the microtubule network in the cell lines used, we transfected a construct expressing a GFP-α-tubulin fusion in HeLa and FRhK-4 cells and then treated the cells with the same concentrations of nocodazole and paclitaxel as used in Fig. 2.2A-C. The cells were then processed for IF analysis (Fig. 2.2D). Nocodazole prevents polymerization of microtubules (Luduena & Roach, 1991) and consequently, microtubules appeared shortened and/or disassociated; most of the signal was diffuse and distributed throughout the cytoplasm (Fig. 2.2D). Paclitaxel, on the other hand, binds to microtubule polymers to prevent their disassembly (Jordan & Wilson, 2004), resulting in the formation of abnormal microtubules bundles (Hornick *et al*, 2008), a phenotype that was observed in both HeLa and FRhK-4 cell lines (Fig. 2.2D). Collectively, the data in Figures 2.1 and 2.2 show that disrupting the dynamics (either assembly or disassembly) of microtubules results in a decrease of restriction by endogenous TRIM5α without inhibiting it completely. Interestingly, when drug concentrations were optimized, we observed that nocodazole and paclitaxel had very similar effects on N-MLV or HIV-1 (Fig. 2.2A-C), suggesting that disruption of the microtubule network inhibited TRIM5α regardless of the drug's mechanism of action.

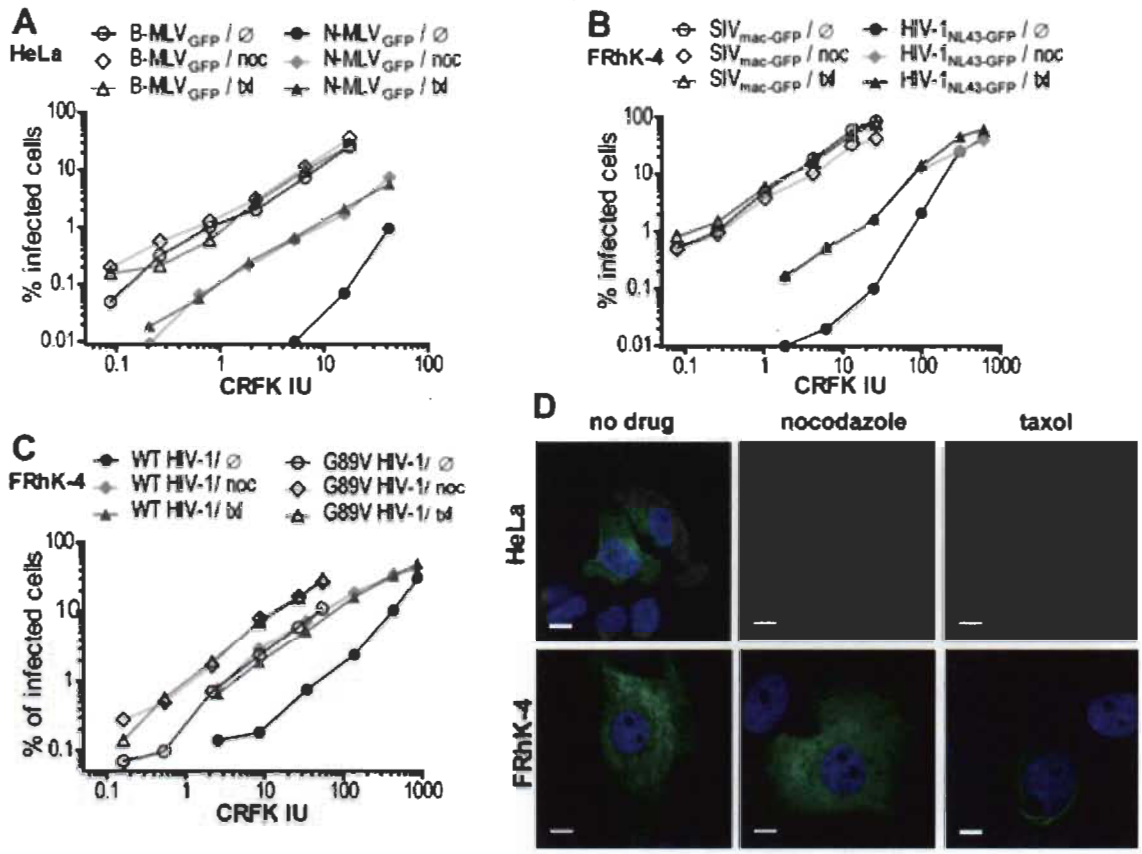

Figure 2.2 **Pharmacological disruption of microtubules decreases endogenous TRIM5α-mediated retroviral restriction.**

(A to C) Effect of nocodazole (noc) and paclitaxel (txl) on restriction. Human HeLa cells (A) or macaque FRhK-4 cells (B, C) were infected with multiples doses of N-MLV$_{GFP}$, B-MLV$_{GFP}$, HIV-1$_{NL43-GFP}$ or SIV$_{mac-GFP}$ as indicated. In (C), FRhK-4 cells were infected with WT HIV-1$_{CMV-GFP}$ or with the CA-G89V mutant of this vector. Infections were performed for 16 h and in the absence of drug or in the presence of either nocodazole or paclitaxel. Nocodazole was used at 0.1 μM in HeLa cells and 6 μM in FRhK-4 cells, and paclitaxel was used at 0.1 μM in HeLa cells and 2 μM at FRhK-4 cells. The x-axis in each graph represents the amounts of virus used expressed in infectious units (IU) based on infectious titers calculated for each virus in permissive feline CRFK cells. Infected (GFP-expressing) cells were detected by flow cytometry 2 d post-infection. (D) IF microscopy analysis of microtubules in treated cells. HeLa and FRhK-4 cells were transfected with GFP-α-tubulin, and 2 d later subjected to two-hour drug treatments using the same concentrations as above, and then fixed. GFP fluorescence was observed by IF microscopy, along with DNA which was stained using DAPI (blue staining). The bar on the images represents 10 μm. A representative image from each condition is presented. Taxol – paclitaxel.

Pharmacological inhibition of dynein function rescues the infectivity of TRIM5α-restricted retroviruses. TRIM5α CBs are associated with microtubules and their movements within the cytoplasm seem to be at least partly dependent upon them (Campbell *et al*, 2007). However, the molecular motors driving TRIM5α CBs movements along microtubules are not known. We hypothesized that dynein played a role in TRIM5α localization and contributed to its antiretroviral activity. We first infected HeLa cells with N- or B-MLV$_{GFP}$ viral vectors in the presence of increasing concentrations of EHNA (Fig. 2.3A), a drug that inhibits the ATPase activity associated with the heavy chain of axonemal and cytoplasmic dyneins (Penningroth *et al*, 1982; Zhang *et al*, 2012). In the presence of EHNA, N-MLV$_{GFP}$ infectivity increased by up to 22-fold compared to the vehicle control, while the EHNA treatment caused a drug concentration-dependent decrease in permissiveness to B-MLV (Fig. 2.3A). In macaque FRhK-4 cells, EHNA increased permissiveness to HIV-1$_{NL43\text{-}GFP}$ by up to 18.5-fold in a drug concentration-dependent fashion (Fig. 2.3B). By contrast, EHNA slightly decreased (less than 2-fold) infection by the restriction-insensitive SIV$_{mac\text{-}GFP}$. We then performed the reverse experiments, infecting the cells at a fixed EHNA concentration but using multiple MOIs. Viruses were equalized as before, based on their titers in the non-restrictive CRFK cells. In HeLa cells, treatment with 600 μM of EHNA had no effect on B-MLV$_{GFP}$ infectivity, but it increased permissiveness to N-MLV$_{GFP}$ infection by up to 22-fold, depending on the MOI (Fig. 2.3C). In FRhK-4 cells (Fig. 2.3D), EHNA (1.2 mM) enhanced HIV-1$_{NL43\text{-}GFP}$ infection at subsaturating MOIs (≤100 CRFK IUs) by 7.5-fold on average (3.2- to 13.5-fold). In contrast, EHNA caused a reduction in SIV$_{mac\text{-}GFP}$ infectivity to ~0.4-fold the untreated control (Fig. 2.3D). Thus, the magnitude of HIV-1 enhancement by EHNA in FRhK-4 cells is probably underestimated in this experiment due to the negative effect of the drug on infectivity, as seen with SIV$_{mac\text{-}GFP}$. In order to verify that the EHNA treatments indeed affected dynein function, we analyzed the subcellular distribution of LAMP-1, a marker for late endosomes (Fukuda, 1991). Impairment of dynein function causes a shift of late endosomes towards the cell periphery, as previously described by us (Lehmann *et al*, 2009) and others (Burkhardt *et al*, 1997). Cells were stained for LAMP-1 following treatment or not with 600 μM (HeLa) or 1.2 mM (FRhK-4) of EHNA. We then counted the number of cells exhibiting

a juxtanuclear localization of LAMP-1 versus the ones with peripheral localization (Fig. 2.3E). In the DMSO-treated control cells, the localization of LAMP-1 was predominantly juxtanuclear. Specifically, 92% ± 2.1 (standard deviation) HeLa cells and 87% ± 1.5 FRhK-4 cells had juxtanuclear LAMP-1. As exemplified in Fig. 2.3E, EHNA treatment caused a significant decrease in juxtanuclear LAMP-1, to 11% ± 4.6 in HeLa cells and 8.6% ± 1.7 in FRhK-4 cells. In conclusion, EHNA can rescue both N-MLV and HIV-1 from restriction by different orthologs of endogenously expressed TRIM5α, but does not totally block restriction.

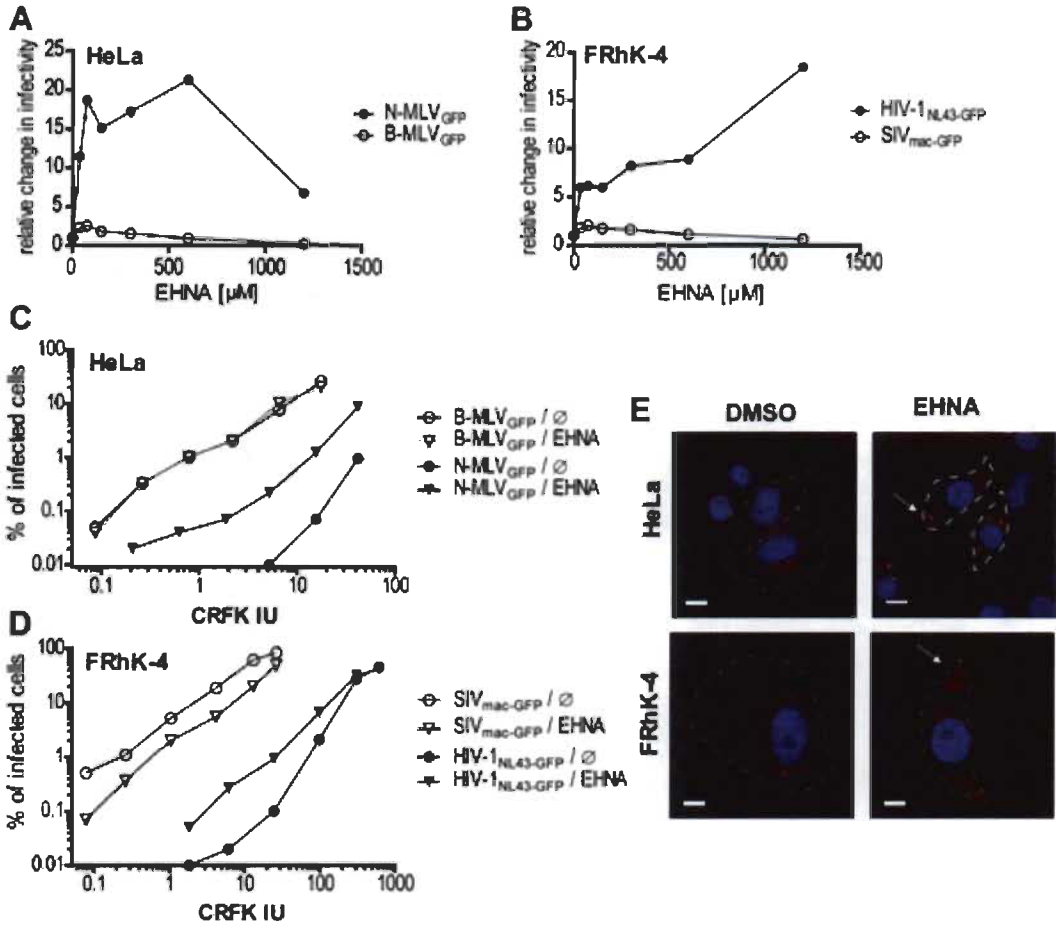

Figure 2.3 Pharmacological disruption of dynein motor function decreases endogenous TRIM5α-mediated retroviral restriction.
(A, B) Dose-dependent effect of EHNA on restriction. Human HeLa cells (A) and macaque FRhK-4 cells (B) were infected for 16 h with a single dose of the indicated viruses in the presence of increasing concentrations of EHNA. The amounts of viruses used were the same as in Fig. 2.1. Infected (GFP-expressing) cells were detected by flow cytometry 2 d post

infection. (C, D) Virus dose-dependent effect of EHNA on restriction. Human HeLa cells (C) and macaque FRhK-4 cells (D) were infected for 16 h with multiples doses of the indicated viruses in the presence or absence of EHNA at 600 μM (HeLa) or 1.2 mM (FRhK-4). The x-axis represents the amounts of virus used expressed in infectious units (IU) based on infectious titers calculated for each virus in permissive feline CRFK cells. Infected (GFP-expressing) cells were detected by flow cytometry 2 d later. (E) IF microscopy analysis of LAMP-1 distribution. HeLa and FRhK-4 cells were treated for 2 h with EHNA or left untreated, then fixed and stained for the lysosomal marker LAMP-1 (red) and DNA (blue). Cell edges are outlined and examples of localization shift caused by impaired dynein function are indicated by white arrows. A representative image from each condition is presented. The bar on the image panels represents 10 μm.

Depletion of dynein heavy chain counteracts TRIM5α-mediated retroviral restriction. In order to directly test the hypothesis that dynein function is important for TRIM5α-mediated restriction, we depleted DHC by transfection of a siRNA, as described previously (Lehmann *et al*, 2009). Knocking down DHC is known to disrupt all dynein-mediated transport activities, and it can also affect the assembly of microtubules by inhibiting the anterograde transport of microtubule complexes (He *et al*, 2005). HeLa cells were transfected with a siRNA targeting DHC or with an irrelevant siRNA targeting luciferase (Luc). Knockdown of DHC was efficient (Fig. 2.4A), resulting in an 85.4% (± 6.7%) reduction in protein levels as estimated by western blotting in 4 independent experiments. In addition, DHC depletion caused a redistribution of LAMP-1 from juxtanuclear to peripheral (Fig. 2.4B), similar to what we had previously published (Lehmann *et al*, 2009). Specifically, 86.6% of HeLa cells transfected with the control siRNA had juxtanuclear staining, compared with 35.5% for the cells transfected with the siRNA targeting DHC. As shown Fig. 2.4C, DHC knockdown caused a significant increase in HeLa permissiveness to N-MLV$_{GFP}$ infection at all MOIs examined (4.6-fold on average; range, 4.0- to 6.0-fold), while having no effect on infection by B-MLV$_{GFP}$. Thus, dynein motor complexes are involved in the restriction of N-MLV by endogenous huTRIM5α. Since dynein's transport function is dependent on microtubules, we predicted that combining pharmacological disruption of microtubules and DHC depletion would have non-additive effects. Therefore, we analyzed the permissiveness to infection by N-MLV$_{GFP}$ and B-MLV$_{GFP}$ of

cells depleted or not for DHC, in the presence of nocodazole or paclitaxel. As shown in Fig. 2.4D, nocodazole alone increased N-MLV infection by an average of 23-fold (range, 11- to 34-fold) while dual treatment with nocodazole and DHC siRNAs resulted in a slightly smaller increase in N-MLV_{GFP} infectivity (13-fold on average; range, 8- to 19-fold). Treatment with paclitaxel resulted in an average increase of 16.7-fold (range: 13- to 24-fold) in permissiveness to N-MLV_{GFP}, and the enhancement effect was only slightly bigger (23-fold; range, 18- to 28-fold) when DHC depletion was combined with paclitaxel treatment (Fig. 2.4E). Altogether, the results in Fig. 2.4D and 2.4E show that disruption of the microtubule network and DHC depletion had non-additive effects on the restriction of N-MLV by endogenous huTRIM5α. None of the treatments or combinations of treatments had a significant effect on the infectivity of the non-restricted B-MLV_{GFP} control (Fig. 2.4C-E).

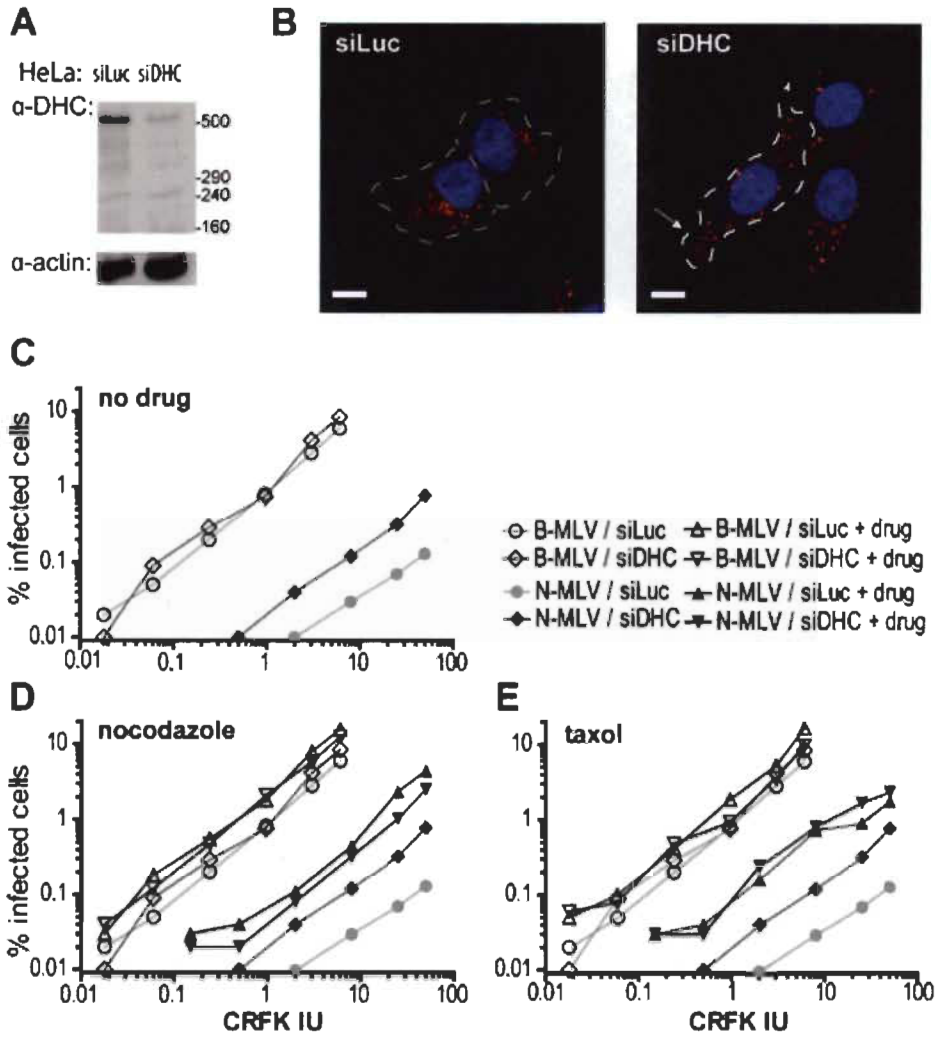

Figure 2.4 **DHC depletion decreases TRIM5α-mediated retroviral restriction and has no effect on cells treated with nocodazole or paclitaxel.**
(A) Western blot analysis of DHC expression in HeLa cells 48 h after transfection of the indicated siRNAs. Actin was analyzed as a loading control. (B) IF microscopy analysis of LAMP-1. LAMP-1 was stained 72 h post siRNAs transfection (red) and DNA was stained using DAPI (blue). Cell edges are outlined and a LAMP-1 distribution shift caused by impaired dynein function is indicated by a white arrow. A representative image is shown for each condition. The bar on the image panels represents 10 μm. (C) Effect of DHC knockdown on restriction. Human HeLa cells were transfected with siRNAs against dynein heavy chain (siDHC), or against luciferase (siLuc) as a control. 72 h later, cells were infected for 16 h with multiple doses of N- or B-MLV$_{GFP}$. Infected cells were detected by flow cytometry 2 d after infection. The x-axis shows the amounts of virus used expressed in CRFK infectious units. (D, E) Effect of combining siRNA transfections with 0.25 μM of nocodazole (D) or 0.1 μM of paclitaxel (taxol) (E). Infections were performed and analyzed as in panel C, and panels C-E all share the same legend.

Inhibition of HIV-1 restriction by over-expressed rhTRIM5α in human cells is counteracted by depletion of dynein heavy chain or microtubules disruption. The experiments shown in Fig. 2.1 to 2.4 indicate that restriction of HIV-1 or N-MLV by endogenous huTRIM5α or rhTRIM5α cells is partly suppressed by DHC knockdown or by pharmacological disruption of microtubules using nocodazole or paclitaxel. We therefore decided to determine whether these interventions would also inhibit HIV-1 restriction in cells in which exogenous FLAG-tagged rhTRIM5α was over-expressed. rhTRIM5α was expressed in HeLa cells through retroviral transfer, and non-transduced cells were eliminated by puromycin treatment. We infected the transduced cells with the restriction-sensitive HIV-1 vectors HIV-$1_{CMV\text{-}GFP}$ and HIV-$1_{NL43\text{-}GFP}$ as well as the rhTRIM5α-insensitive $SIV_{mac\text{-}GFP}$ (Fig. 2.5A). The two vectors used differ in that HIV-$1_{CMV\text{-}GFP}$ does not carry the viral products Vpr, Nef, Vif and Vpu, and no viral proteins are expressed following integration (Naldini *et al*, 1996). In contrast, HIV-$1_{NL43\text{-}GFP}$ encodes all HIV-1 proteins with the exception of Env and Nef, and viral proteins are expressed in infected cells (He *et al*, 1997). Restriction was observed for both viruses in HeLa-rhTRIM5α cells, compared with $SIV_{mac\text{-}GFP}$ and after normalization of viral stocks according to their titers on CRFK cells (Fig. 2.5A). Specifically, HIV-$1_{CMV\text{-}GFP}$ and HIV-$1_{NL43\text{-}GFP}$ were restricted ~40-fold and between ~48- and 78-fold, respectively. Nocodazole and paclitaxel increased permissiveness to HIV-$1_{CMV\text{-}GFP}$ by 10.1-fold and 9.8-fold, on average, and they increased permissiveness to HIV-$1_{NL43\text{-}GFP}$ by an average of 17.8-fold and 15.6-fold, respectively (Fig. 2.5A). None of the drug treatments had a significant effect on infection by $SIV_{mac\text{-}GFP}$, although paclitaxel seemed to increase HIV-1 infectivity at relatively low MOIs and decrease it at relatively high MOIs (Fig. 2.5A). Next, we used FLAG-rhTRIM5α transduced HeLa cells transfected with the control (luciferase-targeting) siRNA or with the siRNA targeting DHC (Fig. 2.5B). In this experiment, restriction of HIV-$1_{NL43\text{-}GFP}$ by rhTRIM5α was particularly high (>1,000-fold). We found that cells depleted of DHC were more permissive to infection by HIV-$1_{NL43\text{-}GFP}$ than cells transfected with the control siRNA (an 11.1-fold increase on average). In contrast, DHC knockdown slightly decreased infection by the control $SIV_{mac\text{-}GFP}$ vector (Fig. 2.5B).

In the next set of experiments (Fig. 2.5C-F), we compared the effect of nocodazole, paclitaxel and DHC depletion on the permissiveness to HIV-1 of cells transduced with FLAG-rhTRIM5α or with a non-restrictive control (huTRIM5α). The expression levels of huTRIM5α and rhTRIM5α were found to be comparable (Fig. 2.5F). Cells were infected at an MOI leading to approximately 1% infected cells in the absence of treatment, as in Fig. 2.1. Addition of nocodazole increased permissiveness of HeLa-rhTRIM5α to HIV-$1_{CMV\text{-}GFP}$ by 5.3-fold ± 0.21 (Fig. 2.5C), while it had a much smaller effect on HeLa transduced with the 'empty' vector (1.5-fold ± 0.04) or HeLa transduced with huTRIM5α (1.46-fold ± 0.10). Likewise, treating the cells with paclitaxel increased permissiveness to HIV-$1_{CMV\text{-}GFP}$ by 3.9-fold ± 0.33 (Fig. 2.5D), while it slightly decreased infection of HeLa-vector and HeLa-huTRIM5α cells (0.6 fold ± 0.13 and 0.63-fold ± 0.12, respectively). Depleting DHC similarly increased permissiveness to HIV-$1_{CMV\text{-}GFP}$ in cells expressing rhTRIM5α (4.2-fold ± 0.38) while having no effect in cells expressing the human ortholog (Fig. 2.5E). In conclusion, microtubule disruption with nocodazole and paclitaxel treatment and DHC depletion specifically inhibited the restriction of HIV-1 by exogenously expressed rhTRIM5α in human cells.

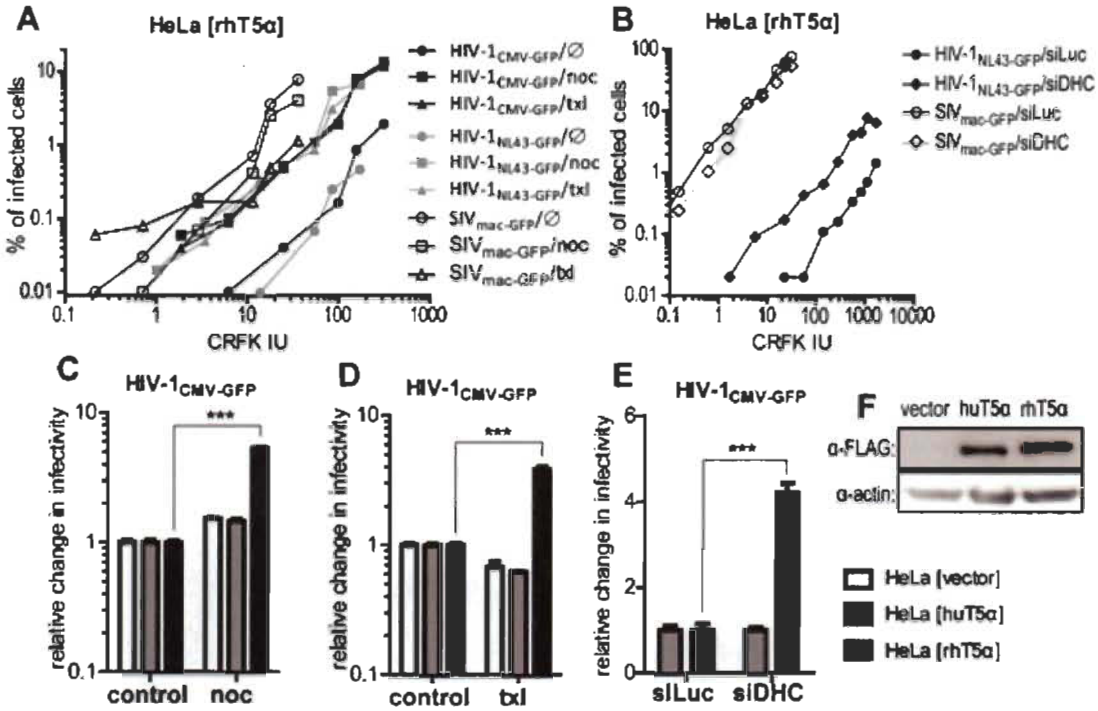

Figure 2.5 Inhibition of HIV-1 restriction by rhTRIM5α exogenously expressed in HeLa cells.

(A) Effect of nocodazole (noc) and paclitaxel (txl) on the restriction of HIV-1 vectors at multiple virus doses. HeLa cells stably expressing FLAG-tagged rhTRIM5α (rhT5α) were infected for 16 h with multiple amounts of the indicated vectors in the presence or absence of 0.1 μM of nocodazole or paclitaxel. Virus doses were normalized according to titers in CRFK cells. % of infected cells were analyzed 2 d post infection. (B) Effect of DHC depletion on the restriction of HIV-$1_{NL43\text{-}GFP}$. HeLa cells stably expressing rhTRIM5α (rhT5α) were transfected with siRNAs targeting DHC (siDHC) or, as a control, luciferase (siLuc). The efficiency of DHC knockdown was similar to that in Fig. 2.4A (not shown). Cells were then infected for 16 h with HIV-$1_{NL43\text{-}GFP}$ or $SIV_{mac\text{-}GFP}$, and the % of infected cells were determined 2 d later. (C, D) Effect of nocodazole or paclitaxel treatment on the infectivity of HIV-$1_{CMV\text{-}GFP}$ in cells expressing HIV-1 restrictive or non-restrictive TRIM5α alleles. HeLa cells transduced as indicated with FLAG-tagged huTRIM5α (huT5α), rhTRIM5α (rhT5α) or with the empty vector were treated or not with 0.1 μM of nocodazole (C) or paclitaxel (D). Cells were simultaneously infected in triplicates with single doses of HIV-$1_{CMV\text{-}GFP}$ adjusted to yield ~1-10% of infected cells in the absence of the drug. Infectivities obtained in the absence of drugs were as follows: for (C), HeLa [vector], 1.23 ± 0.09%; HeLa [huT5α], 2.14 ± 0.81%; HeLa [rhT5α], 0.82 ± 0.06%; for (D), HeLa [vector], 6.84 ± 0.14%; HeLa [huT5α], 6.58 ± 0.27%; HeLa [rhT5α], 2.79 ± 0.19%. Infected cells were detected by flow cytometry 2 d post infection and results are presented as -fold changes relative to the

relevant untreated controls (relative change in infectivity). (E) Effect of DHC depletion on restriction. HeLa cells stably expressing huTRIM5α or rhTRIM5α were transfected with siRNAs against DHC (siDHC) or against luciferase (siLuc) as a control and infected 72 h later in triplicates with single doses of the viral vector HIV-$1_{CMV\text{-}GFP}$ for 16 h. Virus doses were adjusted to obtain ~1% of infected cells for the siLuc control and yielded 1.61% ± 0.29 infected HeLa [huT5α] cells and 0.30 ± 0.08% infected HeLa [rhT5α] cells. Infected cells were detected by flow cytometry 2 d post infection and results are presented as -fold changes relative to the relevant untreated controls (relative change in infectivity). *** indicates $P < 0.0001$ in a Student *t* test. (F) Western blotting analysis of cells stably transduced with FLAG-tagged huTRIM5α and rhTRIM5α, with actin as a loading control.

Nocodazole and paclitaxel inhibit TRIM5α-mediated restriction of an HIV-1 vector bearing autologous envelope proteins. The experiments shown in Fig. 2.1 to 2.5 were all performed using VSV G-pseudotyped vectors. TRIM5α-mediated restriction is not known to be affected by the mode of virus entry, nonetheless we decided to verify that nocodazole and paclitaxel would inhibit the TRIM5α-mediated restriction of a virus bearing its autologous envelope. For that, we used a fully infectious HIV-1 clone (HIV-$1_{NL43\text{-}IRES\text{-}GFP}$) encoding GFP in addition to all the other viral proteins. Human MAGI cells (Vodicka *et al*, 1997), which are U373 (glioblastoma) cells stably expressing the HIV-1 receptors and thus are permissive for HIV-1 infection, were retrovirally transduced to express huTRIM5α or rhTRIM5α. rhTRIM5α was expressed at higher levels as compared to huTRIM5α (Fig. 2.6B), which may reflect intrinsic differences in expression levels of the two proteins, since similar observations were made in other cellular contexts (Bérubé *et al*, 2007; Pham *et al*, 2010). HIV-1 was restricted ~41-fold in the cells transduced with rhTRIM5α compared to control ('empty' vector-transduced) cells, while as expected, it was not restricted in cells transduced with huTRIM5α (not shown). Cells transduced with either of the two TRIM5α orthologs or transduced with the empty vector were then infected with HIV-$1_{NL43\text{-}IRES\text{-}GFP}$ using amounts of the virus leading to approximately 0.1% infected cells and in the presence or absence of drug treatment. As shown Fig. 2.6A, nocodazole and paclitaxel increased the capacity of HIV-1 to infect cells transduced with rhTRIM5α by 6.1-fold ± 1.7 and 12.1-fold ± 4.5, respectively. The drugs had no significant effect on HIV-1 infectivity in

the non-restrictive control cells. Thus, integrity of the microtubule network is important for efficient restriction by TRIM5α regardless of the mechanism of virus entry.

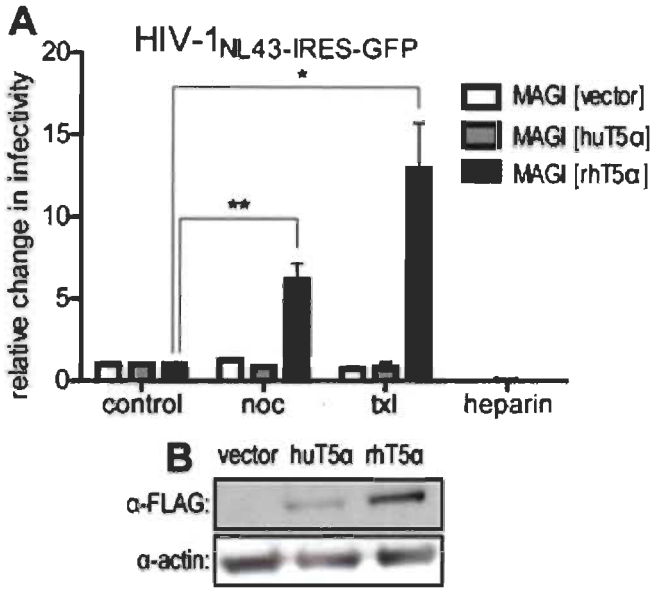

Figure 2.6 Nocodazole and paclitaxel inhibit TRIM5α-mediated restriction of non-pseudotyped HIV-1.
(A) MAGI cells transduced with FLAG-tagged huTRIM5α (huT5α), rhTRIM5α (rhT5α) or with the empty vector were treated or not with 0.25 μM nocodazole (noc) or 0.1 μM paclitaxel (txl). As a control, cells were also infected in presence of the fusion inhibitor heparin (20 μg/ml). Cells were infected in triplicates with single doses of HIV-$1_{NL43\text{-}IRES\text{-}GFP}$. The amounts of virus used were adjusted to obtain ~0.1% of infected cells in the absence of the drug and yielded 0.22% ± 0.025 infected MAGI [vector] cells, 0.16% ± 0.03 infected MAGI [huT5α] cells and 0.043% ± 0.006 infected MAGI [rhT5α] cells. Supernatants were replaced with fresh medium containing heparin 16 h post infection in order to prevent re-infections. Infected (GFP-positive) cells were detected by flow cytometry 2 d post infection and results are presented as -fold changes in the % of infected cells relative to the relevant untreated controls (relative change in infectivity). * and ** indicate $P = 0.0134$ and $P = 0.0068$ in a Student t test, respectively. (B) Western blot analysis of FLAG-huTRIM5α and FLAG-rhTRIM5α expression in stably transduced MAGI cells. Actin was analyzed as a loading control.

Loss of restriction is not caused by decreased TRIM5α stability nor by decreased cellular viability. Next, we investigated a possible impact of the treatments on the turnover/stability of TRIM5α. HeLa cells stably expressing FLAG-rhTRIM5α

were either subjected to treatment with vehicle, nocodazole, paclitaxel or EHNA, or transfected with DHC or control siRNAs, using the same conditions as before. De novo mRNA translation was inhibited using cycloheximide, and we monitored the decrease in protein levels for TRIM5α and for actin as a control (Fig. 2.7A-B). We found that the turnover of TRIM5α was not affected by the various treatments used. EHNA slightly decreased TRIM5α levels at a single time-point (1 h of cycloheximide treatment) while DHC depletion also slightly decreased TRIM5α levels at 3 and 4.5 h of cycloheximide treatment (Fig. 2.7A). However, the results derived from several experiments revealed that these effects were not statistically significant (Fig. 2.7B).

Nocodazole, paclitaxel and EHNA disrupt essential cellular functions and it was thus important to insure that the loss of restriction observed in our experimental conditions was not an artifact caused by gross cytotoxic effects. In all our infectivity assays, drugs are added for only 16 h and then removed, since only the first hours of infection are relevant to mechanisms of TRIM5α-mediated restriction. Thus, we examined cellular viability following 16-hour treatments of HeLa and FRhK-4 cells with increasing concentrations of nocodazole, paclitaxel and EHNA (Fig. 2.7C). Viability was monitored using the XTT assay, a colorimetric method to measure cellular metabolic activity, specifically the activity of dehydrogenase enzymes (Scudiero *et al*, 1988). Both nocodazole and paclitaxel caused a progressive but relatively modest loss in viability, obviously reflecting a concentration-dependent inhibition of cell division (Jordan *et al*, 1992; Sorger *et al*, 1997). At the relatively low concentrations used for infectivity assays, nocodazole caused a ~19% decrease in the viability of HeLa cells and a ~32% decrease in the viability of FRhK-4 cells (Fig. 2.7C). Similarly, paclitaxel caused a ~23% decrease in the viability of HeLa cells and a ~20% decrease in the viability of FRhK-4 cells at the concentrations used in our restriction assays (Fig. 2.7C). In both cases, the concentrations used were well below the threshold at which the decrease in viability becomes sharper, probably reflecting the occurrence of cytotoxic mechanisms in addition to the inhibition of cell division. Based on our XTT data, we would estimate these cytopathic effects to take place at above ~30 μM for nocodazole, ~20 μM for paclitaxel. We obtained a different pattern for EHNA: in both HeLa and

FRhK-4 cells, viability decreased slowly to reach 85-90% of the control levels at 1 mM of the drug, but the drop in viability was much sharper at higher concentrations, and viability was fully lost at ~5 mM (Fig. 2.7C). At the concentrations used in our infectivity assays (600 μM in HeLa cells, 1.2 mM in FRhK-4 cells), EHNA caused a ~12% decrease in viability in HeLa cells, 8% in FRhK-4 cells (Fig. 2.7C). Thus, even though these concentrations are close to the concentrations at which viability starts declining sharply, cellular viability is still at the level of untreated cells, and it is unlikely that the effects of EHNA on restriction result from its cytotoxicity.

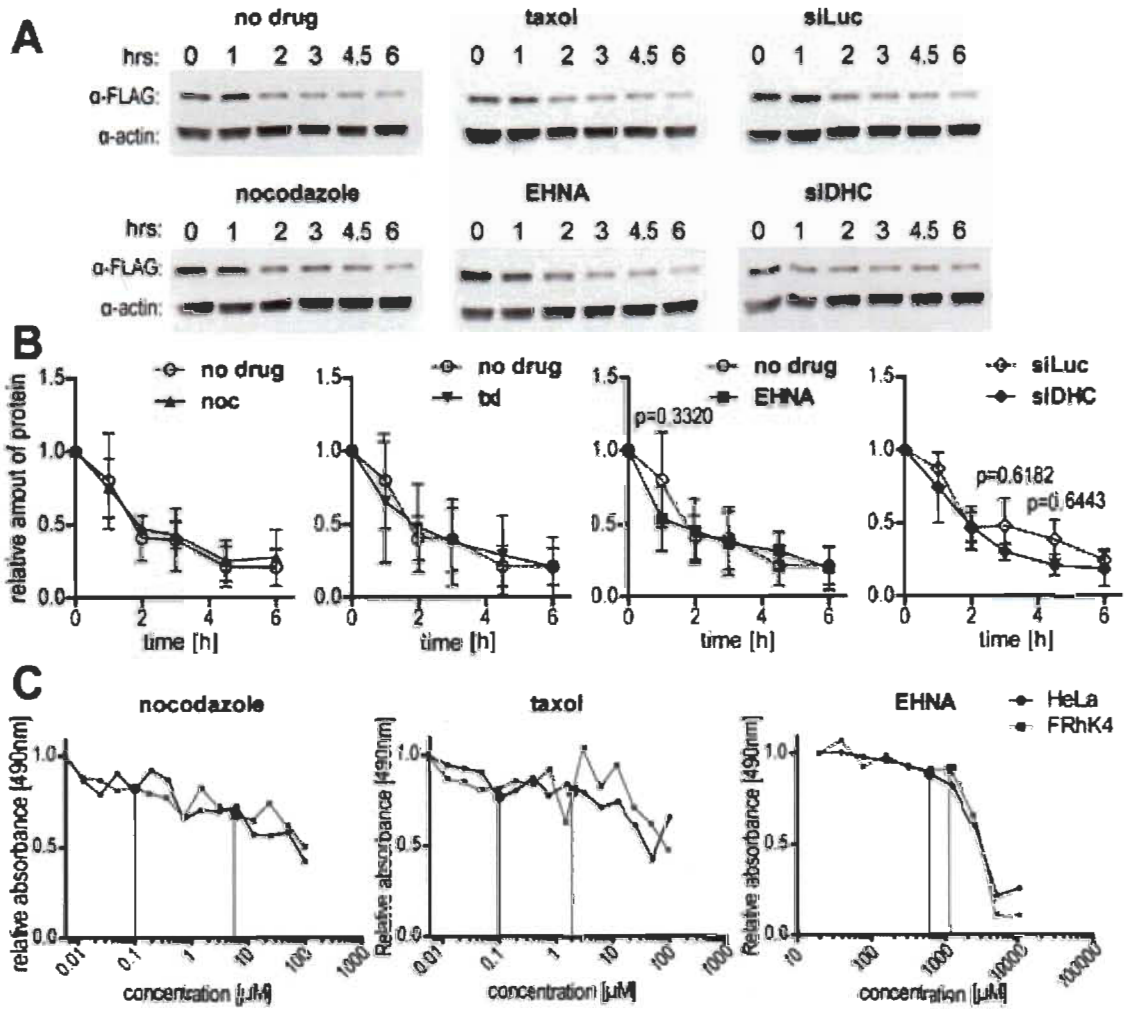

Figure 2.7 Effect of treatments on TRIM5α stability and cell viability.
(A) Effect on rhTRIM5α protein levels. HeLa cells stably expressing FLAG-tagged rhTRIM5α were treated with nocodazole (0.1 μM), paclitaxel (taxol) (0.1 μM), EHNA (600 μM) and concomitantly treated

with cycloheximide. Alternatively, cells were transfected with luciferase- or DHC-targeting siRNAs like before and treated with cycloheximide 72 h later. The efficiency of DHC knockdown was similar to that in Fig. 2.4A (not shown). Protein lysates were prepared at the indicated time points following the beginning of drug treatments. Lysates were subjected to Western blotting to detect FLAG-rhTRIM5α and actin. One representative experiment out of 3 independent experiments is shown. (B) Analysis of FLAG-rhTRIM5α protein turnover. FLAG-rhTRIM5α bands detected by Western blotting were quantified by densitometry and normalized to actin levels and then to the value obtained at the '0' time point; ctl, control; noc, nocodazole; txl, paclitaxel. Average data from 3 independent experiments with standard deviations are shown. The P-values indicated on the graphs were calculated using a Student *t* test for the three conditions at which an effect could be observed: EHNA treatment (1 h) and DHC siRNA transfection (3 h and 4.5 h). (C) Cell viability assay. HeLa and FRhK-4 cells were treated with multiple concentrations of the indicated drugs for 16 h and cell viability was then determined using the XTT assay and normalized using the value obtained in absence of drug as a reference. Vertical lines indicate the drug concentrations used in this study, for each combination of drug and cell line.

DHC depletion, nocodazole treatment and paclitaxel treatment stabilize post-entry HIV-1 cores. A characteristic effect of TRIM5α-mediated post-entry retroviral restriction is the increase in the CA core disassembly of restriction-sensitive retroviruses, i.e. a decrease in core stability. We used the well-established fate-of-capsid assay (Bérubé *et al*, 2007; Ohkura *et al*, 2011; Stremlau *et al*, 2006a) to analyze the impact of nocodazole treatment, paclitaxel treatment and DHC depletion on TRIM5α-mediated core disassembly. HeLa cells expressing rhTRIM5α or mock-transduced with the empty vector were exposed to HIV-$1_{NL43\text{-}GFP}$ in the presence or the absence of nocodazole, paclitaxel or DHC siRNA. The efficiency of DHC knockdown was the same as in Fig. 2.4A (not shown). Cells were lysed and core-associated (pelletable) CA was isolated by ultracentrifugation through a sucrose cushion. The relative amounts of core-associated, soluble (post-centrifugation supernatant-associated) and total (whole cell lysate, WCL) CAp24 were assessed by densitometry of western blots from three independent experiments (Fig. 2.8). The amounts of pelletable CA recovered were estimated relative to total CA or relative to soluble CA. As a control, cells were infected with a vector devoid of envelope proteins and thus incompetent for entry. Both virus

preparations were normalized using a reverse transcription assay to insure equal virus input. In the absence of the VSV G envelope, no or little CA signal was detectable in the infected cells, confirming that the CA detected was not associated with unfused viral particles (Fig. 2.8A-C). As expected and in the absence of treatment, the relative amounts of pelletable CA cores were reduced in cells expressing rhTRIM5α, compared to the control cells transduced with the empty vector (Fig. 2.8A-C). Specifically, the pellet/WCL CA ratio was reduced by 85.9% (± 9.0), 70.4% (± 14.0) and 75.7% (± 23.0) in the experiments shown Fig. 2.8A, 2.8B and 2.8C, respectively. Similarly, the pellet/supernatant CA ratio was reduced by 85.0% (± 12.7), 72.2% (± 11.5) and 88.4% (± 9.1) in cells expressing rhTRIM5α (Fig. 2.8A-C, right panels).

We observed that all the treatments used had a stabilizing effect on post-entry CA cores, both in permissive (control) cells and in restrictive (TRIM5α-expressing) cells (Fig. 2.8A-C). However, the increase in stability mediated by DHC depletion and paclitaxel treatment was greater in rhTRIM5α-expressing cells than in control cells, consistent with the ability of these treatments to rescue infection. Specifically, DHC depletion increased the pellet/WCL CA ratio by 1.28-fold in control cells while this increase was of 3.10-fold in rhTRIM5α-expressing cells (Fig. 2.8A). Similarly, DHC depletion increased the pellet/supernatant CA ratio by 2.11-fold in control cells and by 5.78-fold in rhTRIM5α-expressing cells (Fig. 2.8A). Paclitaxel treatment increased the pellet/WCL CA ratio by 1.61-fold in control cells while the corresponding increase in rhTRIM5α-expressing cells was 2.52-fold. Similarly, paclitaxel increased the pellet/supernatant CA ratio by 1.46-fold in control cells and 3.87-fold in rhTRIM5α-expressing cells (Fig. 2.8B). We obtained different effects for nocodazole, since treatment with this drug sharply increased CA core stability both in permissive and restrictive conditions (Fig. 2.8C). Specifically, nocodazole increased the pellet/WCL CA ratio by 3.94-fold in control cells and by 2.83-fold in rhTRIM5α-expressing cells. Similarly, the pellet/supernatant CA ratio was increased by 3.77-fold in control cells and by about the same amount (4.05-fold) in rhTRIM5α-expressing cells treated with this drug (Fig. 2.8C). Therefore, disrupting the microtubule network or the dynein heavy chain motor has a stabilizing effect on post-entry HIV-1 cores, which may decrease their

susceptibility to TRIM5α-mediated restriction. In addition, the magnitude of this stabilizing effect was greater in cells expressing rhTRIM5α under treatment by paclitaxel or DHC siRNAs, which is consistent with these interventions specifically increasing HIV-1 infectivity in restrictive conditions. Nocodazole treatment increased post-entry HIV-1 cores stability equally in permissive and restrictive conditions, but its effects in permissive conditions was also much stronger (3.94-fold) compared to DHC depletion (1.28-fold) or paclitaxel treatment (1.61-fold), perhaps masking the specific effect on restriction (see Discussion).

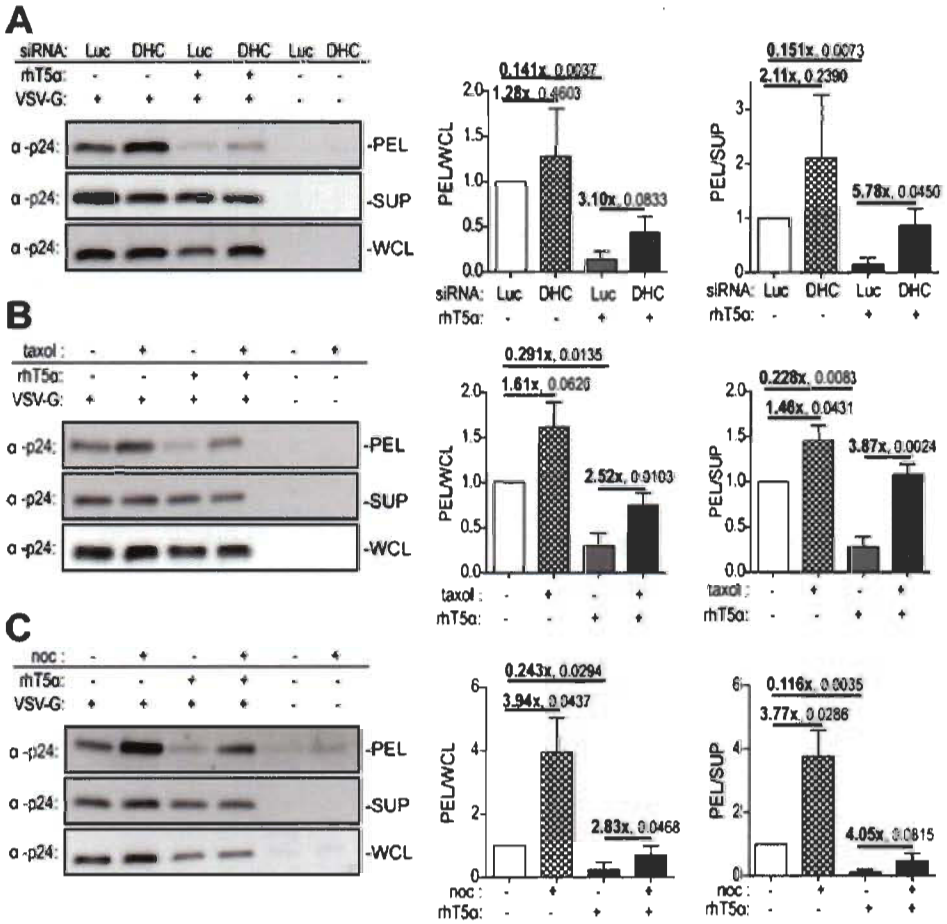

Figure 2.8 **DHC depletion, paclitaxel treatment and nocodazole treatment increase the stability of HIV-1 cores in permissive or restrictive conditions.**

(A) HeLa cells stably expressing rhTRIM5α (rhT5α) or transduced with the empty vector were transfected with the indicated siRNAs and 72 h later infected with HIV-$1_{NL43\text{-}GFP}$ or an entry-incompetent version of this vector lacking the VSV G envelope protein. Supernatants were replaced

by fresh medium 2 h post infection and cells were lysed after an additional 4 h of incubation. Pre-cleared lysates were layered on sucrose cushions and particulate viral CA cores were pelleted by ultracentrifugation. Proteins in post-centrifugation pellets (PEL), supernatants (SUP) and whole cell lysates (WCL) were analyzed by Western blotting to detect CA (p24). Bands corresponding to p24 were quantified by densitometry and plotted as pellet/WCL and pellet/supernatant ratios, relative to the non-restrictive untreated control. Average data from 3 independent experiments with standard deviations are shown. -fold changes and P-values (calculated using a Student *t* test) are shown for specific pairs of data. (B) Same as (A), but cells were treated or not with 0.1 μM paclitaxel (txl) during the 2 h of infection and during the 4 h of incubation. (C) Same as (B), but cells were treated or not with 0.1 μM nocodazole (noc).

Effect of nocodazole treatment and DHC depletion on the size and localization of TRIM5 CBs. The capacity of nocodazole treatment and DHC depletion to reduce TRIM5α-mediated restriction could stem from effects on the dynamics of TRIM5α, which would affect the size and/or localization of CBs. HeLa cells stably expressing FLAG-tagged rhTRIM5α were treated with nocodazole or depleted for DHC and then stained for FLAG (Fig. 2.9A-B). The settings were adjusted to reveal CBs but not the diffuse FLAG signal. The size (area) of CBs (Fig. 2.9C) and their relative distances to the nucleus and to the 'edge-of-cell' (Fig. 2.9D) were calculated as detailed in 'Materials and Methods'. Nocodazole treatment and DHC knockdown increased the average size of rhTRIM5α CBs by 33.9 ± 7.8% and 52.6 ± 8.9%, respectively (Fig. 2.9C). In addition, rhTRIM5α CBs were found to be 31.5 ± 3.7% closer to the nucleus following nocodazole treatment (Fig. 2.9D). In contrast, DHC depletion caused a significant rhTRIM5α CBs localization shift (14.2 ± 2.8%) towards the plasma membrane (Fig. 2.9D). The results presented in Fig. 2.9 show that the microtubule network is important for the dynamics of TRIM5α CBs. Depletion of DHC and disruption of microtubules can have distinct effects on TRIM5α CBs, but the increased peripheral localization of CBs seen upon DHC depletion suggests that dynein motor complexes are responsible for their retrograde transport. To test more directly whether dynein is involved in the association of TRIM5α CBs with microtubules, we co-transfected HeLa cells stably expressing FLAG-rhTRIM5α with siRNAs targeting either DHC or an irrelevant control and with a plasmid expressing GFP-α-tubulin, then stained

for FLAG (Fig. 2.9E-F). Images were acquired with the Apotome system and deconvolved to facilitate analysis, and co-localization was quantified from multiple randomly chosen cells. The depletion of DHC resulted in a modest (23% ± 0.3) yet statistically significant decrease in the co-localization of rhTRIM5α CBs and microtubules (Fig. 2.9G). Altogether, these results suggest that dynein motor complexes are involved in the association of TRIM5α CBs with microtubules and in the retrograde transport of either TRIM5α CBs.

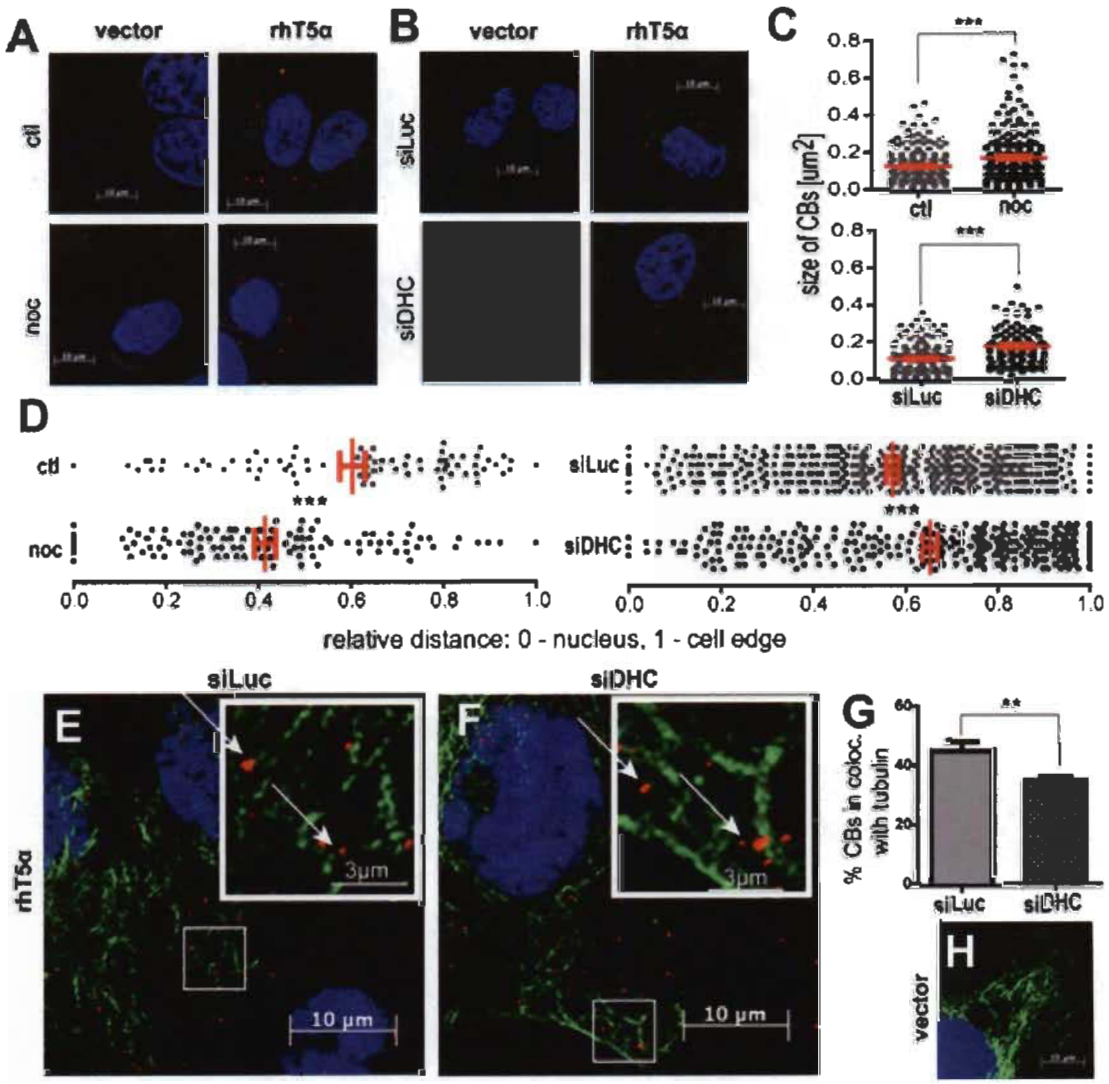

Figure 2.9 **Influence of DHC depletion and nocodazole treatment on the localization and dynamics of rhTRIM5α cytoplasmic bodies (CBs).** (A, B) IF microscopy. HeLa cells transduced with FLAG-tagged rhT5α and control cells transduced with the empty vector were (A) seeded on

glass coverslips and 24 h later treated or not with 2 μM of nocodazole for 6 h, or (B) transfected with 40 nM of siRNAs targeting DHC or Luc and 48 h later seeded on glass coverslips and incubated for an additional 24 h. Cells were fixed and immunostained for FLAG (red). DNA was stained with Hoechst33342 (blue). Representative images are shown. (C) Sizes of CBs. All CBs were outlined in cells from a minimum of 5 randomly chosen fields and their area was calculated using an image analysis software (AxioVision). Red bars show the standard error of the mean (SEM). *** indicates $P \leq 0.0001$ in a Student t test analysis. (D) The relative localization of all TRIM5α CBs from a minimum of 5 randomly chosen cells was calculated using the formula x/(x+y), where x is the shortest distance to the nucleus and y is the shortest distance to the cell's edge. SEM are shown as red bars, and *** indicates $P \leq 0.0001$. (E-G) Co-localization of rhT5α CBs and microtubules. (E) HeLa cells transduced with FLAG-tagged rhTRIM5α were transfected with siRNAs targeting Luc or DHC and 24 h later cells were additionally transfected with a plasmid expressing GFP-α-tubulin. The next day, cells were seeded on glass coverslips and grown for 24 h. Cells were fixed and immunostained for FLAG (red) and DNA (blue). (F) Same as (E), except that cells were transduced with the empty vector and were transfected with the luciferase-targeting siRNA. Representative images are shown. Boxes in the top right corner show enlarged regions outlined on the images, and white arrows show examples of GFP-tubulin/FLAG-TRIM5α co-localizations. (G) Events of co-localization were quantified as a % of total CBs in 10 randomly chosen fields. Bars represent the mean values from analyzed cells with SEM (** indicates $P < 0.005$).

2.7 Discussion

In this work, we examined the importance of microtubules and of the microtubule-associated dynein motor complexes in the restriction of HIV-1 and N-MLV by TRIM5α. Pharmacological and siRNA-mediated depletion studies clearly show that the capacity of TRIM5α to efficiently restrict incoming retroviruses is dependent on intact microtubules and a functioning dynein motor complex (Fig. 2.1 to 2.6). This was true regardless of (i) the retrovirus and TRIM5α ortholog studied, (ii) whether TRIM5α was expressed at endogenous levels or over-expressed through stable transduction, and (iii) the mechanism of virus entry. Nocodazole and paclitaxel, two drugs that disrupt the structure of the microtubule network through different mechanisms, had very similar, sometimes identical effects on retroviral restriction levels (Fig. 2.2, 2.4). DHC depletion generally had a smaller effect on restriction than treatment with nocodazole or paclitaxel

(Fig. 2.4), which may be due to the observed incomplete knockdown (Fig. 2.4A). However, DHC depletion did not synergistically inhibit TRIM5α in the presence of either nocodazole (Fig. 2.4D) or paclitaxel (Fig. 2.4E), implying that these treatments all affected the same pathway. Finally, the observed impact of microtubules or dynein disruption on virus restriction was not caused by gross differences in expression levels or TRIM5α stability (Fig. 2.7A-B) and was not a putative artifact stemming from cytotoxicity (Fig. 2.7C).

Destabilization of the viral CA core upon interaction with TRIM5α is a hallmark of restriction and occurs in the hours following virus entry. We observed that DHC depletion, nocodazole treatment and paclitaxel treatment all increased the relative amounts of pelletable CA, both in permissive and restrictive conditions. This indicates that these treatments increase the stability of post-entry HIV-1 CA cores. To our knowledge, this effect of interventions altering the cytoskeleton on HIV-1 disassembly had never been investigated before. Although the mechanism behind HIV-1 post-entry CA core stabilization is unclear, it could contribute to making HIV-1 partly resistant to TRIM5α, by counteracting the destabilizing effect of TRIM5α (Black & Aiken, 2010). The increase in the relative amounts of core-associated CA induced by DHC depletion or paclitaxel treatment was greater in cells expressing rhTRIM5α compared to control cells (Fig. 2.8A, 2.8B). This is consistent with these treatments specifically increasing HIV-1 infectivity in restrictive conditions. The results with nocodazole were more ambiguous, as this drug strongly increased the relative levels of core-associated CA (a 3- to 4-fold increase) both in permissive and restrictive conditions (Fig. 2.8C). This apparent lack of specificity of nocodazole in this assay might be due to compounding effects of the drug. For instance, nocodazole could increase the apparent stability in permissive conditions through an additional mechanism that does not take place in restrictive conditions, hence masking the restriction-specific effect that is seen with DHC siRNAs or paclitaxel. Consistent with this, nocodazole increased the relative amounts of core-associated CA in permissive cells about twice as much as DHC depletion or paclitaxel treatment did.

Nocodazole treatment increased the size of TRIM5α CBs and caused them to be positioned closer to the nucleus (Fig. 2.9), which is consistent with previous observations by Diaz-Griffero *et al.* (Diaz-Griffero *et al*, 2006). These data suggest that nocodazole interferes with the dynamics of TRIM5α CBs, perhaps by preventing the exchange of TRIM5α proteins between diffuse cytoplasmic population and CBs-associated population (Campbell *et al*, 2007). DHC depletion increased the average size of rhTRIM5α CBs (Fig. 2.9C), but also caused CBs to accumulate towards the cell periphery (Fig. 2.9D). In addition, there was a modest but significant decrease in the association between microtubules and rhTRIM5α (Fig. 2.9G). Altogether, these results suggest that the dynein motor translocates rhTRIM5α CBs on microtubules and is at least partly responsible for their retrograde transport. When DHC is depleted, rhTRIM5α CBs may shift towards the periphery of cells due to interactions with other molecular motors, such as the reverse polarity motor kinesin, which performs anterograde transport and can transport the same cargos as dynein does (Muller *et al*, 2008). Alternatively, DHC depletion could enhance the association of rhTRIM5α with late endosomes, as was observed previously for components of the HIV-1 ribonucleoprotein such as Gag and the genomic RNA (Lehmann *et al*, 2009). Nocodazole treatment and DHC depletion showed distinct phenotypes with regard to TRIM5α-mediated CA core disassembly (Fig. 2.8) and TRIM5α CBs localization (Fig. 2.9D), yet their effects on restriction are clearly not additive (Fig. 2.4). Thus, it is likely that these phenotypic differences simply reflect different mechanisms of action by which the two treatments inhibit a single pathway.

Perhaps surprisingly, the various interventions used in this study generally had little effect on the transduction of HIV-1, SIVmac and MLV vectors in permissive conditions. Nocodazole was originally reported to modestly inhibit the early stages of HIV-1 infectivity in MAGI cells (Bukrinskaya *et al*, 1998). However, other studies demonstrated a lack of HIV-1 sensitivity to this drug in human embryo kidney 293T cells (Daniel *et al*, 2005) and in CEM T cells (Yoder *et al*, 2011). At first glance, such a lack of inhibition by nocodazole contradicts a role for microtubules in HIV-1 post-entry intracellular transport (McDonald *et al*, 2002). However, the existence of a population of nocodazole-resistant microtubules, which are less dynamic, has been described (Schulze

& Kirschner, 1987), raising the possibility that HIV-1 uses these specific microtubules for its transport. Likewise, depleting DHC had a small effect on the infection of human permissive HeLa cells by an SIVmac vector (Fig. 2.5B) and no effect was seen on infection of HeLa cells by B-MLV (Fig. 2.4C) or HIV-1 (Fig. 2.5E) vectors. To the best of our knowledge, the only published evidence of a functional role for dynein motor complexes in HIV-1 post-entry transport consisted in the injection of an antibody interfering with dynein motor function, leading to a ~50% decrease in HIV-1 movements toward the nucleus (McDonald *et al*, 2002); however, this observation was not supported by infectivity data. Clearly, the precise mechanism of retroviral capsids transport toward the nucleus is yet to be determined (Mouland & Milev, 2012). Regardless, our results show that disruption of the microtubule network and DHC depletion affect TRIM5α-mediated restriction without strongly impairing infectivity in permissive cells, firmly establishing specificity. The effects seen on restriction probably stem from effects on TRIM5α localization (Fig. 2.9), on CA stability (Fig. 2.8), or a combination of both.

2.8 Acknowledgements

We thank Maximilian Webers, Marie Leclerc, Maxime Veillette, Réjean Cantin, Pascal Jalaguier, Alexandre Deshière and Mélodie B. Plourde for providing technical help. We thank Natacha Mérindol, Mélodie B. Plourde and Marie-Édith Nepveu-Traversy for a critical reading of this manuscript. We acknowledge David N. Levy (University of Alabama at Birmingham), and Ali Saib (Université Paris, France) for sharing plasmid DNAs. The following reagents were obtained through the NIH AIDS Research and Reference Reagent Program, Division of AIDS, NIAID, NIH: nevirapine (cat#4666), clone 183 p24 antibodies (cat#3537, contributed by Bruce Chesebro). M.J.T. holds a tier 1 Canada Research Chair in Human Immuno-Retrovirology. This work was supported by grants from the Canadian Institutes of Health Research to A.J.M. (MOP-56974), M.J.T. (MOP-110960) and L.B. (MOP-102712).

2.9 References

Adachi A, Gendelman HE, Koenig S, Folks T, Willey R, Rabson A, Martin MA (1986) Production of acquired immunodeficiency syndrome-associated retrovirus in human and nonhuman cells transfected with an infectious molecular clone. *Journal of virology* 59: 284-291

Anderson JL, Campbell EM, Wu X, Vandegraaff N, Engelman A, Hope TJ (2006) Proteasome inhibition reveals that a functional preintegration complex intermediate can be generated during restriction by diverse TRIM5 proteins. *Journal of virology* 80: 9754-9760

Asaoka K, Ikeda K, Hishinuma T, Horie-Inoue K, Takeda S, Inoue S (2005) A retrovirus restriction factor TRIM5alpha is transcriptionally regulated by interferons. *Biochemical and biophysical research communications* 338: 1950-1956

Berthoux L, Sebastian S, Sayah DM, Luban J (2005a) Disruption of human TRIM5alpha antiviral activity by nonhuman primate orthologues. *Journal of virology* 79: 7883-7888

Berthoux L, Sebastian S, Sokolskaja E, Luban J (2004) Lv1 inhibition of human immunodeficiency virus type 1 is counteracted by factors that stimulate synthesis or nuclear translocation of viral cDNA. *Journal of virology* 78: 11739-11750

Berthoux L, Sebastian S, Sokolskaja E, Luban J (2005b) Cyclophilin A is required for TRIM5alpha-mediated resistance to HIV-1 in Old World monkey cells. *Proceedings of the National Academy of Sciences of the United States of America* 102: 14849-14853

Berthoux L, Towers GJ, Gurer C, Salomoni P, Pandolfi PP, Luban J (2003) As(2)O(3) enhances retroviral reverse transcription and counteracts Ref1 antiviral activity. *Journal of virology* 77: 3167-3180

Bérubé J, Bouchard A, Berthoux L (2007) Both TRIM5alpha and TRIMCyp have only weak antiviral activity in canine D17 cells. *Retrovirology* 4: 68

Besnier C, Takeuchi Y, Towers G (2002) Restriction of lentivirus in monkeys. *Proceedings of the National Academy of Sciences of the United States of America* 99: 11920-11925

Black LR, Aiken C (2010) TRIM5alpha disrupts the structure of assembled HIV-1 capsid complexes in vitro. *Journal of virology* 84: 6564-6569

Bukrinskaya A, Brichacek B, Mann A, Stevenson M (1998) Establishment of a functional human immunodeficiency virus type 1 (HIV-1) reverse transcription complex involves the cytoskeleton. *The Journal of experimental medicine* 188: 2113-2125

Burkhardt JK, Echeverri CJ, Nilsson T, Vallee RB (1997) Overexpression of the dynamitin (p50) subunit of the dynactin complex disrupts dynein-dependent maintenance of membrane organelle distribution. *The Journal of cell biology* 139: 469-484

Campbell EM, Dodding MP, Yap MW, Wu X, Gallois-Montbrun S, Malim MH, Stoye JP, Hope TJ (2007) TRIM5 alpha cytoplasmic bodies are highly dynamic structures. *Molecular biology of the cell* 18: 2102-2111

Campbell EM, Perez O, Anderson JL, Hope TJ (2008) Visualization of a proteasome-independent intermediate during restriction of HIV-1 by rhesus TRIM5alpha. *The Journal of cell biology* 180: 549-561

Carthagena L, Parise MC, Ringeard M, Chelbi-Alix MK, Hazan U, Nisole S (2008) Implication of TRIM alpha and TRIMCyp in interferon-induced anti-retroviral restriction activities. *Retrovirology* 5: 59

Daniel R, Marusich E, Argyris E, Zhao RY, Skalka AM, Pomerantz RJ (2005) Caffeine inhibits human immunodeficiency virus type 1 transduction of nondividing cells. *Journal of virology* 79: 2058-2065

Danielson CM, Cianci GC, Hope TJ (2012) Recruitment and dynamics of proteasome association with rhTRIM5alpha cytoplasmic complexes during HIV-1 infection. *Traffic* 13: 1206-1217

de Forges H, Bouissou A, Perez F (2012) Interplay between microtubule dynamics and intracellular organization. *The international journal of biochemistry & cell biology* 44: 266-274

Diaz-Griffero F, Kar A, Lee M, Stremlau M, Poeschla E, Sodroski J (2007) Comparative requirements for the restriction of retrovirus infection by TRIM5alpha and TRIMCyp. *Virology* 369: 400-410

Diaz-Griffero F, Li X, Javanbakht H, Song B, Welikala S, Stremlau M, Sodroski J (2006) Rapid turnover and polyubiquitylation of the retroviral restriction factor TRIM5. *Virology* 349: 300-315

Dodding MP, Way M (2011) Coupling viruses to dynein and kinesin-1. *The European Molecular Biology Organization journal* 30: 3527-3539

Fukuda M (1991) Lysosomal membrane glycoproteins. Structure, biosynthesis, and intracellular trafficking. *The Journal of biological chemistry* 266: 21327-21330

Ganser-Pornillos BK, Chandrasekaran V, Pornillos O, Sodroski JG, Sundquist WI, Yeager M (2011) Hexagonal assembly of a restricting TRIM5alpha protein. *Proceedings of the National Academy of Sciences of the United States of America* 108: 534-539

Groschel B, Bushman F (2005) Cell cycle arrest in G2/M promotes early steps of infection by human immunodeficiency virus. *Journal of virology* 79: 5695-5704

Hatziioannou T, Perez-Caballero D, Yang A, Cowan S, Bieniasz PD (2004) Retrovirus resistance factors Ref1 and Lv1 are species-specific variants of TRIM5alpha. *Proceedings of the National Academy of Sciences of the United States of America* 101: 10774-10779

Hauler F, Mallery DL, McEwan WA, Bidgood SR, James LC (2012) AAA ATPase p97/VCP is essential for TRIM21-mediated virus neutralization. *Proceedings of the National Academy of Sciences of the United States of America* 109: 19733-19738

He J, Chen Y, Farzan M, Choe H, Ohagen A, Gartner S, Busciglio J, Yang X, Hofmann W, Newman W, Mackay CR, Sodroski J, Gabuzda D (1997) CCR3 and CCR5 are co-receptors for HIV-1 infection of microglia. *Nature* 385: 645-649

He Y, Francis F, Myers KA, Yu W, Black MM, Baas PW (2005) Role of cytoplasmic dynein in the axonal transport of microtubules and neurofilaments. *The Journal of cell biology* 168: 697-703

Hook P, Vallee RB (2006) The dynein family at a glance. *Journal of cell science* 119: 4369-4371

Hornick JE, Bader JR, Tribble EK, Trimble K, Breunig JS, Halpin ES, Vaughan KT, Hinchcliffe EH (2008) Live-cell analysis of mitotic spindle formation in taxol-treated cells. *Cell motility and the cytoskeleton* 65: 595-613

Hsieh MJ, White PJ, Pouton CW (2010) Interaction of viruses with host cell molecular motors. *Current opinion in biotechnology* 21: 633-639

Imbeault M, Lodge R, Ouellet M, Tremblay MJ (2009) Efficient magnetic bead-based separation of HIV-1-infected cells using an improved reporter virus system reveals that p53 up-regulation occurs exclusively in the virus-expressing cell population. *Virology* 393: 160-167

Jordan MA, Thrower D, Wilson L (1992) Effects of vinblastine, podophyllotoxin and nocodazole on mitotic spindles. Implications for the role of microtubule dynamics in mitosis. *Journal of cell science* 102 (Pt 3): 401-416

Jordan MA, Wilson L (2004) Microtubules as a target for anticancer drugs. *Nature reviews Cancer* 4: 253-265

Kajaste-Rudnitski A, Marelli SS, Pultrone C, Pertel T, Uchil PD, Mechti N, Mothes W, Poli G, Luban J, Vicenzi E (2011) TRIM22 inhibits HIV-1 transcription independently of its E3 ubiquitin ligase activity, Tat, and NF-kappaB-responsive long terminal repeat elements. *Journal of virology* 85: 5183-5196

Kar AK, Diaz-Griffero F, Li Y, Li X, Sodroski J (2008) Biochemical and biophysical characterization of a chimeric TRIM21-TRIM5alpha protein. *Journal of virology* 82: 11669-11681

Keckesova Z, Ylinen LM, Towers GJ (2004) The human and African green monkey TRIM5alpha genes encode Ref1 and Lv1 retroviral restriction factor activities. *Proceedings of the National Academy of Sciences of the United States of America* 101: 10780-10785

Kutluay SB, Perez-Caballero D, Bieniasz PD (2013) Fates of Retroviral Core Components during Unrestricted and TRIM5-Restricted Infection. *PLoS Pathogens* 9: e1003214

Lehmann M, Milev MP, Abrahamyan L, Yao XJ, Pante N, Mouland AJ (2009) Intracellular transport of human immunodeficiency virus type 1 genomic RNA and viral production are dependent on dynein motor function and late endosome positioning. *The Journal of biological chemistry* 284: 14572-14585

Li X, Sodroski J (2008) The TRIM5alpha B-box 2 domain promotes cooperative binding to the retroviral capsid by mediating higher-order self-association. *Journal of virology* 82: 11495-11502

Lin TY, Emerman M (2008) Determinants of cyclophilin A-dependent TRIM5 alpha restriction against HIV-1. *Virology* 379: 335-341

Luban J (2007) Cyclophilin A, TRIM5, and resistance to human immunodeficiency virus type 1 infection. *Journal of virology* 81: 1054-1061

Luduena RF, Roach MC (1991) Tubulin sulfhydryl groups as probes and targets for antimitotic and antimicrotubule agents. *Pharmacology & therapeutics* 49: 133-152

Lukic Z, Hausmann S, Sebastian S, Rucci J, Sastri J, Robia SL, Luban J, Campbell EM (2011) TRIM5alpha associates with proteasomal subunits in cells while in complex with HIV-1 virions. *Retrovirology* 8: 93

McDonald D, Vodicka MA, Lucero G, Svitkina TM, Borisy GG, Emerman M, Hope TJ (2002) Visualization of the intracellular behavior of HIV in living cells. *The Journal of cell biology* 159: 441-452

Moscat J, Diaz-Meco MT, Wooten MW (2007) Signal integration and diversification through the p62 scaffold protein. *Trends in biochemical sciences* 32: 95-100

Mouland AJ, Milev MP (2012) Role of Dynein in Viral Pathogenesis. In *Dyneins: structure, biology and disease*, King SM (ed), 561-583, pp 561-583. Elsevier

Muller MJ, Klumpp S, Lipowsky R (2008) Tug-of-war as a cooperative mechanism for bidirectional cargo transport by molecular motors. *Proceedings of the National Academy of Sciences of the United States of America* 105: 4609-4614

Naldini L, Blomer U, Gage FH, Trono D, Verma IM (1996) Efficient transfer, integration, and sustained long-term expression of the transgene in adult rat brains injected with a lentiviral vector. *Proceedings of the National Academy of Sciences of the United States of America* 93: 11382-11388

Naviaux RK, Costanzi E, Haas M, Verma IM (1996) The pCL vector system: rapid production of helper-free, high-titer, recombinant retroviruses. *Journal of virology* 70: 5701-5705

Nisole S, Stoye JP, Saib A (2005) TRIM family proteins: retroviral restriction and antiviral defence. *Nature Reviews Microbiology* 3: 799-808

O'Connor C, Pertel T, Gray S, Robia SL, Bakowska JC, Luban J, Campbell EM (2010) p62/sequestosome-1 associates with and sustains the expression of retroviral restriction factor TRIM5alpha. *Journal of virology* 84: 5997-6006

Ohkura S, Goldstone DC, Yap MW, Holden-Dye K, Taylor IA, Stoye JP (2011) Novel escape mutants suggest an extensive TRIM5alpha binding site spanning the entire outer surface of the murine leukemia virus capsid protein. *PLoS Pathogens* 7: e1002011

Penningroth SM, Cheung A, Bouchard P, Gagnon C, Bardin CW (1982) Dynein ATPase is inhibited selectively in vitro by erythro-9-[3-2-(hydroxynonyl)]adenine. *Biochemical and biophysical research communications* 104: 234-240

Perez-Caballero D, Hatziioannou T, Zhang F, Cowan S, Bieniasz PD (2005) Restriction of human immunodeficiency virus type 1 by TRIM-CypA occurs with rapid kinetics and independently of cytoplasmic bodies, ubiquitin, and proteasome activity. *Journal of virology* 79: 15567-15572

Perron MJ, Stremlau M, Lee M, Javanbakht H, Song B, Sodroski J (2007) The human TRIM5alpha restriction factor mediates accelerated uncoating of the N-tropic murine leukemia virus capsid. *Journal of virology* 81: 2138-2148

Perron MJ, Stremlau M, Song B, Ulm W, Mulligan RC, Sodroski J (2004) TRIM5alpha mediates the postentry block to N-tropic murine leukemia viruses in human cells. *Proceedings of the National Academy of Sciences of the United States of America* 101: 11827-11832

Pertel T, Hausmann S, Morger D, Zuger S, Guerra J, Lascano J, Reinhard C, Santoni FA, Uchil PD, Chatel L, Bisiaux A, Albert ML, Strambio-De-Castillia C, Mothes W, Pizzato M, Grutter MG, Luban J (2011) TRIM5 is an innate immune sensor for the retrovirus capsid lattice. *Nature* 472: 361-365

Pham QT, Bouchard A, Grutter MG, Berthoux L (2010) Generation of human TRIM5alpha mutants with high HIV-1 restriction activity. *Gene Therapy* 17: 859-871

Rahm N, Yap M, Snoeck J, Zoete V, Munoz M, Radespiel U, Zimmermann E, Michielin O, Stoye JP, Ciuffi A, Telenti A (2011) Unique spectrum of activity of prosimian TRIM5alpha against exogenous and endogenous retroviruses. *Journal of virology* 85: 4173-4183

Roa A, Hayashi F, Yang Y, Lienlaf M, Zhou J, Shi J, Watanabe S, Kigawa T, Yokoyama S, Aiken C, Diaz-Griffero F (2012) RING domain mutations uncouple TRIM5alpha restriction of HIV-1 from inhibition of reverse transcription and acceleration of uncoating. *Journal of virology* 86: 1717-1727

Rold CJ, Aiken C (2008) Proteasomal degradation of TRIM5alpha during retrovirus restriction. *PLoS Pathogens* 4: e1000074

Rusan NM, Fagerstrom CJ, Yvon AM, Wadsworth P (2001) Cell cycle-dependent changes in microtubule dynamics in living cells expressing green fluorescent protein-alpha tubulin. *Molecular biology of the cell* 12: 971-980

Schulze E, Kirschner M (1987) Dynamic and stable populations of microtubules in cells. *The Journal of cell biology* 104: 277-288

Scudiero DA, Shoemaker RH, Paull KD, Monks A, Tierney S, Nofziger TH, Currens MJ, Seniff D, Boyd MR (1988) Evaluation of a soluble tetrazolium/formazan assay for cell growth and drug sensitivity in culture using human and other tumor cell lines. *Cancer research* 48: 4827-4833

Sebastian S, Luban J (2005) TRIM5alpha selectively binds a restriction-sensitive retroviral capsid. *Retrovirology* 2: 40

Sebastian S, Sokolskaja E, Luban J (2006) Arsenic counteracts human immunodeficiency virus type 1 restriction by various TRIM5 orthologues in a cell type-dependent manner. *Journal of virology* 80: 2051-2054

Seibenhener ML, Geetha T, Wooten MW (2007) Sequestosome 1/p62--more than just a scaffold. *Federation of European Biochemical Societies letters* 581: 175-179

Song B, Diaz-Griffero F, Park DH, Rogers T, Stremlau M, Sodroski J (2005a) TRIM5alpha association with cytoplasmic bodies is not required for antiretroviral activity. *Virology* 343: 201-211

Song B, Javanbakht H, Perron M, Park DH, Stremlau M, Sodroski J (2005b) Retrovirus restriction by TRIM5alpha variants from Old World and New World primates. *Journal of virology* 79: 3930-3937

Sorger PK, Dobles M, Tournebize R, Hyman AA (1997) Coupling cell division and cell death to microtubule dynamics. *Current opinion in cell biology* 9: 807-814

Stremlau M, Owens CM, Perron MJ, Kiessling M, Autissier P, Sodroski J (2004) The cytoplasmic body component TRIM5alpha restricts HIV-1 infection in Old World monkeys. *Nature* 427: 848-853

Stremlau M, Perron M, Lee M, Li Y, Song B, Javanbakht H, Diaz-Griffero F, Anderson DJ, Sundquist WI, Sodroski J (2006a) Specific recognition and accelerated uncoating of retroviral capsids by the TRIM5alpha restriction factor. *Proceedings of the National Academy of Sciences of the United States of America* 103: 5514-5519

Stremlau M, Song B, Javanbakht H, Perron M, Sodroski J (2006b) Cyclophilin A: an auxiliary but not necessary cofactor for TRIM5alpha restriction of HIV-1. *Virology* 351: 112-120

Tareen SU, Emerman M (2011) Human Trim5alpha has additional activities that are uncoupled from retroviral capsid recognition. *Virology* 409: 113-120

Towers GJ (2007) The control of viral infection by tripartite motif proteins and cyclophilin A. *Retrovirology* 4: 40

Uchil PD, Quinlan BD, Chan WT, Luna JM, Mothes W (2008) TRIM E3 ligases interfere with early and late stages of the retroviral life cycle. *PLoS Pathogens* 4: e16

Vodicka MA, Goh WC, Wu LI, Rogel ME, Bartz SR, Schweickart VL, Raport CJ, Emerman M (1997) Indicator cell lines for detection of primary strains of human and simian immunodeficiency viruses. *Virology* 233: 193-198

Wolf D, Goff SP (2007) TRIM28 mediates primer binding site-targeted silencing of murine leukemia virus in embryonic cells. *Cell* 131: 46-57

Wu X, Anderson JL, Campbell EM, Joseph AM, Hope TJ (2006) Proteasome inhibitors uncouple rhesus TRIM5alpha restriction of HIV-1 reverse transcription and infection. *Proceedings of the National Academy of Sciences of the United States of America* 103: 7465-7470

Yap MW, Nisole S, Lynch C, Stoye JP (2004) Trim5alpha protein restricts both HIV-1 and murine leukemia virus. *Proceedings of the National Academy of Sciences of the United States of America* 101: 10786-10791

Yoder A, Guo J, Yu D, Cui Z, Zhang XE, Wu Y (2011) Effects of microtubule modulators on HIV-1 infection of transformed and resting CD4 T cells. *Journal of virology* 85: 3020-3024

Yoo S, Myszka DG, Yeh C, McMurray M, Hill CP, Sundquist WI (1997) Molecular recognition in the HIV-1 capsid/cyclophilin A complex. *Journal of molecular biology* 269: 780-795

Zhang W, Greene W, Gao SJ (2012) Microtubule- and dynein-dependent nuclear trafficking of rhesus rhadinovirus in rhesus fibroblasts. *Journal of virology* 86: 599-604

Zufferey R, Nagy D, Mandel RJ, Naldini L, Trono D (1997) Multiply attenuated lentiviral vector achieves efficient gene delivery in vivo. *Nature Biotechnology* 15: 871-875

The next chapter contains a study in preparation that demonstrates the involvement of microtubules and dynein motor complexes in HIV-1 uncoating.

CHAPTER III

INHIBITION OF MICROTUBULE- AND DYNEIN-DEPENDENT TRANSPORT COUNTERACTS HIV-1 UNCOATING

PAULINA PAWLICA, LIONEL BERTHOUX

Manuscript in preparation

3.1 Contributions

P.P. and L.B. designed the study, interpreted the results and prepared the manuscript. P.P. performed the experiments.

3.2 Abstract

Retroviral capsid cores undergo uncoating during their transport toward the nucleus and/or after reaching the nuclear membrane. Here we investigate the role of the microtubule network and dynein-dependent transport in HIV-1 uncoating. We used the pharmacological agents nocodazole and paclitaxel (formerly named taxol) to inhibit microtubule dynamics, while dynein-mediated transport was perturbed either by depletion of dynein heavy chain (DHC) or by p50/dynamitin over-expression. In immunofluorescence microscopy experiments, we detected an accumulation of CA foci in HIV-1 infected cells following DHC depletion or microtubule perturbation. Using a fate-of-capsid assay to monitor HIV-1 CA core disassembly in infected cells, we observed an increase in the amounts of pelletable CA cores following treatments with nocodazole or paclitaxel, DHC depletion and p50/dynamitin over-expression. Our results show that inhibiting microtubules dynamics or dynein-mediated transport

interferes with uncoating in the cytoplasm of infected cells, suggesting a functional link between HIV-1 transport and uncoating.

Keywords: HIV-1; uncoating; capsid; microtubules; dynein

3.3 Introduction

The mature CA core of human immunodeficiency virus 1 (HIV-1) is a ~60 nm x 120 nm (Briggs *et al*, 2003) cone-shaped protein lattice, encasing viral genomic RNA, enzymes (integrase and reverse transcriptase) and other viral proteins [reviewed in (Briggs & Krausslich, 2011)]. It is composed of ~1000 CA monomers (Pornillos *et al*, 2011) arranged in ~170 hexamers and 12 pentamers through interactions involving their N-terminal domains (Pornillos *et al*, 2009), whereas C-terminal domains are important for homodimerization that connects the rings into a lattice (Gamble *et al*, 1997). In addition to viral proteins, the CA core also encloses many cellular components originating from the producer cells, such as APOBEC3G [reviewed in (Ott, 2008)].

Following receptor-mediated entry into the cytoplasm, HIV-1 undergoes tightly regulated processes that prepare the virus for nuclear import and integration of its genetic material into host DNA. The nucleoprotein complex formed before completing reverse transcription (RT) is usually referred to as the reverse transcription complex (RTC), which is later transformed into the pre-integration complex (PIC). RT is thought to be initiated within 30 min post virus entry (Goff, 2001) by a still unknown mechanism. Before, during or after RT, the CA core must be disassembled in a process called 'uncoating'. The precise timing and location of uncoating remain unclear; some reports propose that it occurs in the cytoplasm (Hulme *et al*, 2011; McDonald *et al*, 2002), while others suggest that uncoating takes place at the nuclear pore (Arhel *et al*, 2007; Rasaiyaah *et al*, 2013; Schaller *et al*, 2011). It is possible that a small fraction of CA proteins remain associated with PICs and are transported to the nucleus (Zhou *et al*, 2011), and CA has been identified as a determinant for HIV-1 integration site specificity (Schaller *et al*, 2011). These hypotheses are not mutually exclusive considering that

uncoating could take place in several well-orchestrated steps instead of being a rapid single-step process (Ambrose & Aiken, 2014). Additionally, recent lines of evidence indicate that uncoating is linked with RT (Hulme *et al*, 2011; Roa *et al*, 2012; Yang *et al*, 2013) and suggest that RT triggers uncoating (Hulme *et al*, 2011; Zhang *et al*, 2000). However, it cannot be excluded that RT initiation itself depends on prior destabilization or increased permeability of the CA core after entry into the cytoplasm (Zhang *et al*, 1998). Alternatively, uncoating could be triggered by an as yet unknown cellular factor (Auewarakul *et al*, 2005).

Numerous studies indicate that CA is the main viral determinant for uncoating. Mutations resulting in either hypostable or hyperstable CA cores almost completely abolish viral infectivity despite normal virion protein content (Forshey *et al*, 2002). Additionally, the retroviral restriction factors TRIM5α and TRIMCyp inhibit viral infection (Sayah *et al*, 2004; Stremlau *et al*, 2004) through binding to and destabilization of incoming CA cores, in essence causing 'premature uncoating' (Stremlau *et al*, 2006). Furthermore, the HIV-1 small-molecule inhibitor PF-3450074 (PF74) inhibits HIV-1 infectivity specifically by destabilizing the CA core (Shi *et al*, 2011). Uncoating is also likely dependent on cellular factors, but these remain mostly elusive (Ambrose & Aiken, 2014). A few cellular partners that interact with the HIV-1 CA core were characterized and some were proposed to modulate uncoating, such as cyclophilin A (CypA) (Li *et al*, 2009; Shah *et al*, 2013), nucleoprotein RanBP2/Nup358 (Schaller *et al*, 2011), transportin 3 (TNPO3) (Shah *et al*, 2013), cleavage and polyadenylation specific factor 6 (CPSF6) (De Iaco *et al*, 2013) and PDZ Domain-containing 8 (Guth & Sodroski, 2014).

Similarly to other viruses [reviewed in (Slonska *et al*, 2012)], HIV-1 hijacks the cell's cytoskeleton and associated molecular motors for its trafficking towards the nucleus [reviewed in (Gaudin *et al*, 2013)]. The microtubule network and microtubule-associated dynein motor complexes were proposed to transport HIV-1 RTCs towards the nucleus (McDonald *et al*, 2002). Specifically, HIV-1 translocation on microtubules was evidenced by live microscopy, and was inhibited by micro-injection of anti-dynein antibodies (McDonald *et al*, 2002). Recently, one team reported that HIV-1 induces the

formation of and co-localizes with a stable sub-population of microtubules whose disruption abolishes infectivity (Sabo *et al*, 2013). Thus, the microtubule network seems to be important for HIV-1 trafficking and infectivity.

In this study, we hypothesized that uncoating of the HIV-1 CA core and its trafficking towards the nucleus were linked mechanisms. Our results suggest a role for the microtubule network and dynein motor complexes in HIV-1 uncoating.

3.4 Results

Disruption of the dynein motor complex and the microtubule network causes an accumulation of CA foci in infected cells. We used immunofluorescence (IF) microscopy with a monoclonal antibody to analyze the presence of CA foci in human HeLa cells infected with VSV G-pseudotyped HIV-$1_{CMV\text{-}GFP}$ or in human MAGI cells infected with HIV-1_{NL43}, and in the presence of treatments disrupting the microtubule network or dynein motor function. Such CA foci detected in acute infection conditions are thought to be individual viruses that are not or only partially uncoated (Arhel *et al*, 2007; Campbell *et al*, 2007; Hulme *et al*, 2011; McDonald *et al*, 2002). HeLa cells transfected with siRNAs targeting either the dynein heavy chain (DHC) mRNA (Lehmann *et al*, 2009; Pawlica *et al*, 2014) or the non-relevant luciferase (Luc) mRNA (Pawlica *et al*, 2014) were infected with the VSV G-pseudotyped lentiviral vector HIV-$1_{CMV\text{-}GFP}$ for 4 h, at which point the virus was removed and cells were incubated for an additional 2 h. DHC depletion was efficient as assessed by Western blotting, since transfection of DHC siRNA led to a reduction of ~ 85.4% ± 6.7 (n = 10) in protein levels (Fig. 3.1A). Upon staining infected cells using an antibody against CA, we detected distinct foci as expected, that were absent from mock-infected cells (Fig. 3.1B). DHC depletion caused an increase in the amounts of these foci. Specifically, the average number of CA foci per cell increased ~2.5-fold following DHC depletion, from 6.98 ± 0.818 to 17.4 ± 2.88 (P = 0.0038) (Fig. 3.1C). Moreover, CA foci tended to accumulate in the cell periphery, as evidenced by measuring relative distances to the nucleus (calculated using the formula x/(x+y) where x is the shortest distance to the nucleus and

y the shortest distance to the cell's edge). The median relative distance to the nucleus changed significantly ($P < 0.0001$) from 0.44 (95% CI, 0.39-0.52) for the Luc siRNA-transfected control cells to 0.83 (95% CI, 0.79-0.84) for cells transfected with DHC siRNA (Fig. 3.1D). A similar accumulation of viral RTCs in the cell periphery was observed upon transfection of anti-dynein antibodies prior to infection (McDonald *et al*, 2002).

HIV-1 virions pseudotyped with VSV G are delivered through clathrin-mediated endocytosis (Sun *et al*, 2005) and are further released into the cytoplasm following acidification of endosomes (Blumenthal *et al*, 1987). Clathrin-mediated entry relies mainly on actin filaments (Cureton *et al*, 2009), while maturation of endosomes involves microtubules (Lakadamyali *et al*, 2006) and possibly the dynein motor complex (Lehmann *et al*, 2009). Therefore, in order to confirm that the effects observed in Fig. 3.1B-D were not stemming from pseudotyping, we repeated the experiment using a virus harboring an autologous HIV-1 envelope. U373-derived MAGI cells (Vodicka *et al*, 1997) were infected with the replication-competent HIV-1_{NL43}. Since dynein-mediated movements are microtubule-dependent [reviewed in (Kikkawa, 2013)], we also disrupted microtubule dynamics using nocodazole and paclitaxel, which inhibit microtubule polymerization (Luduena & Roach, 1991) or their disassembly (Schiff *et al*, 1979), respectively. We previously established low-toxicity effective concentrations of these drugs (Pawlica *et al*, 2014). MAGI cells were infected for 2 h with HIV-1_{NL43} and in the presence of the various treatments or left uninfected (Fig. 3.1E). We observed a significant increase in the amount of CA foci per cell following DHC depletion (Fig 3.1F). Specifically, the average number of CA foci per cell was 16.07 ± 2.27 in cells transfected with DHC siRNA compared to 5.4 ± 0.41 in control cells ($P = 0.0001$). Pharmacological disruption of microtubules also resulted in a significant increase in the number of CA foci per cell, as we observed 14.47 ± 2.05 ($P = 0.0001$) and 10.08 ± 1.30 ($P = 0.0007$) cores per cell in the presence of paclitaxel and nocodazole, respectively (Fig. 3.1F). Accordingly, another study also reported an accumulation of CA foci following nocodazole treatment (Arhel *et al*, 2007). CA foci were predominantly found in proximity to the nucleus of control cells (Luc siRNA), with a median relative distance

to the nucleus of 0.30 (95% CI, 0.26-0.37) (Fig. 3.1G). Like before, DHC depletion caused a significant ($P < 0.0001$) shift in the distribution of CA cores towards the cell periphery; CA foci were found at a median relative distance of 0.70 (95% CI, 0.63-0.75). These observations confirm that the effects reported in Fig. 3.1B-D did not result from pseudotyping, and suggest that the dynein motor complex might be involved in HIV-1 core disassembly. As shown Fig. 3.1G, nocodazole and paclitaxel treatments also resulted in a shift of CA foci localization towards the periphery of the cytoplasm, although this effect was more pronounced with paclitaxel. The different effects of nocodazole and paclitaxel can be explained by differences in the mechanism of action of these two pharmacological agents, with nocodazole causing microtubule disassembly while paclitaxel prevents their depolymerisation (Schiff *et al*, 1979) and inhibits dynein-mediated translocation (Nilsson & Wallin, 1998). Collectively, the results shown in Fig. 3.1 suggest that dynein motor complexes and the microtubule network influence both HIV-1 retrograde transport and CA core stability in infected cells, irrespective of the mode of viral entry.

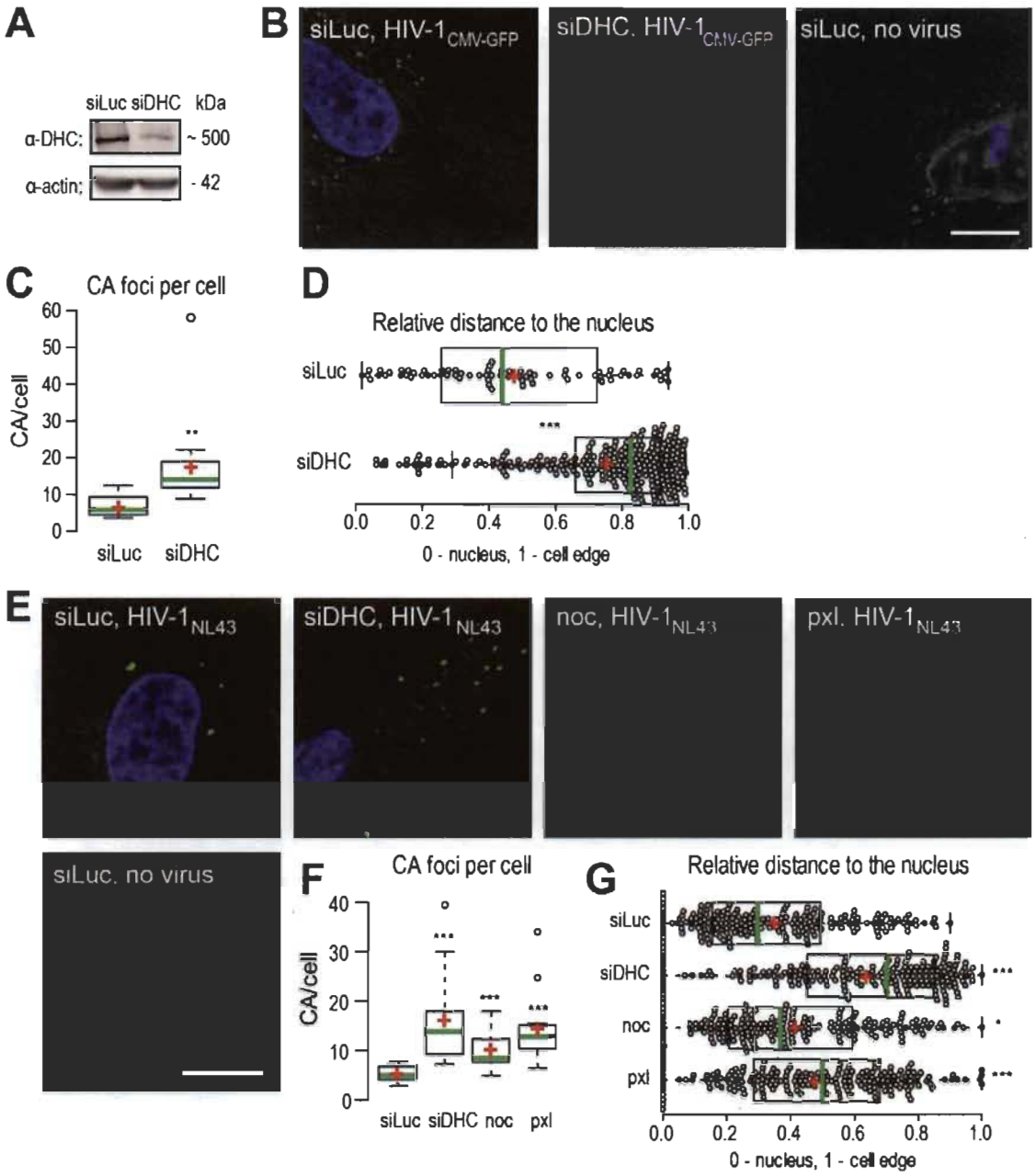

Figure 3.1 **Dynein heavy chain (DHC) depletion and microtubule perturbation cause the accumulation of HIV-1 CA cores in infected cells and alter their subcellular distribution.**

(A) HeLa cells were transfected with siRNAs targeting either dynein heavy chain (siDHC) or luciferase (siLuc) as a control, and DHC expression was analyzed 2 days later by Western blotting. (B) IF microscopy observations of CA foci following infection with VSV G-pseudotyped HIV-1. HeLa cells were transfected with the indicated siRNAs and 72 h later were infected or not with VSV G-pseudotyped HIV-$1_{CMV-GFP}$ in the presence of MG132. At 4 h p.i., supernatants were

replaced with virus-free medium supplemented with MG132. Cells were fixed 6 h p.i. and stained to detect CA (green) or DNA (blue). The outline of cells was revealed by low-exposure bright-field microscopy. Representative images are shown. The white bar represents 10 μm. (C) Box plots showing total amounts of CA foci per cell. The total numbers of CA foci and nuclei in 10 randomly chosen fields were counted and the CA foci/nuclei ratios were calculated. 375 and 1047 CA foci were counted for siLuc and siDHC, respectively. Center green lines show the medians; box limits indicate the 25th and 75th percentiles as determined by R software; whiskers extend 1.5 times the interquartile range from the 25th and 75th percentiles; and red crosses represent sample means. **, $P \leq 0.001$ in a Student *t*-test. (D) Box plots showing the relative localization of CA foci in 10 randomly chosen cells, calculated using the formula x/(x+y) where x is the shortest distance to the nucleus and y is the shortest distance to the cell's edge. Data points are plotted as open circles; center green lines show the medians; box limits indicate the 25th and 75th percentiles as determined by R software; whiskers extend 1.5 times the interquartile range from the 25th and 75th percentiles; and red crosses represent sample means. *** indicates $P \leq 0.0001$ in a Student *t*-test analysis. (E) IF microscopy observation of CA foci following infection with HIV-1 bearing an autologous envelope. MAGI cells were either transfected with siDHC or siLuc 72 h prior to infection, or were pretreated for 15 min with 2 μM of nocodazole (noc) or 0.1 μM of paclitaxel (pxl), and then infected with HIV-1_{NL43} in the presence of MG132. Cells were fixed 2 h later and stained as in (B). The white bars represent 10 μm. (F) The total amounts of CA foci per cell were calculated as in (C). At least 250 and up to 800 CA foci were counted for each condition (***, $P \leq 0.0001$). (G) Relative cellular distribution of CA foci, analyzed as in (D) (* and *** indicate $P < 0.05$ and $P \leq 0.0001$, respectively).

Analyzing uncoating using the fate-of-capsid assay. As an independent experimental approach to analyze uncoating, we used the well described fate-of-capsid biochemical assay (Perron *et al*, 2004; Stremlau *et al*, 2006) that allows isolation of post-entry CA cores from infected cells, by ultracentrifugation of pre-cleared cell lysates through a sucrose cushion. This assay has been used mostly to study the destabilization of HIV-1 cores caused by TRIM5 proteins (Bérubé *et al*, 2007; Pawlica *et al*, 2014; Stremlau *et al*, 2006). We performed a preliminary experiment to analyze whether nocodazole and paclitaxel would affect uncoating as analyzed by fate-of-capsid. In this experiment, we additionally used a VSV G-devoid, entry-defective control virus (De Iaco *et al*, 2013; Stremlau *et al*, 2006; Tipper & Sodroski, 2013) to confirm that the fate-

of-capsid assay detects primarily post-entry viruses. Such 'bald' particles can interact non-specifically with the cellular plasma membrane and can be internalized by endocytosis, but cannot enter the cytosol (Marechal *et al*, 1998). As expected, envelope-devoid HIV-$1_{NL43\text{-}GFP}$ virions were not infectious in HeLa cells (Fig. 3.2A), but had normal CA content (Fig. 3.2B). HeLa cells pretreated or not with nocodazole or paclitaxel were infected with either HIV-$1_{NL43\text{-}GFP}$ or its envelope-devoid counterpart for 1 h, at which time point supernatants were replaced with fresh media containing the appropriate drugs, and we analyzed the presence of CAp24 in whole cell lysates (WCL), pellets and supernatants after an additional 5 h of incubation (Fig. 3.2C). Pellets contain particulate, not-yet uncoated CA cores while supernatants contain soluble CA proteins. The 6-hours timing was chosen because we had previously observed an increase in amounts of pelletable HIV-1 CA cores in cells infected for the same amount of time and treated with nocodazole, paclitaxel or DHC siRNA (Pawlica *et al*, 2014). As expected, it was possible to detect CAp24 in all fractions of cells infected with the VSV G-pseudotyped vector (Fig. 3.2C). For the envelope-devoid virus, bands corresponding to CAp24 were barely detectable in WCL and this signal likely corresponded to virions attached to the cellular membrane or trapped in endosomal compartments. However, CAp24 was not detected in particulate or soluble forms following ultracentrifugation, suggesting that the fate-of-capsid assay detects primarily CA that has entered the cytoplasm, at least in the conditions employed here. Additionally, nocodazole and paclitaxel did not cause unspecific virus entry. Interestingly, we observed an increase in the amounts of pelletable CA cores upon treatment with these two drugs of cells infected with the VSV G-pseudotyped virus, compared to untreated cells. Specifically, pellet/supernatant and pellet/WCL ratios increased by 2.6-fold and 2.9-fold, respectively, following nocodazole treatment (Fig. 3.2D). Likewise, paclitaxel increased these ratios by 2.0-fold and 2.5-fold (Fig. 3.2D). These results suggest that both drugs alter HIV-1 CA core disassembly.

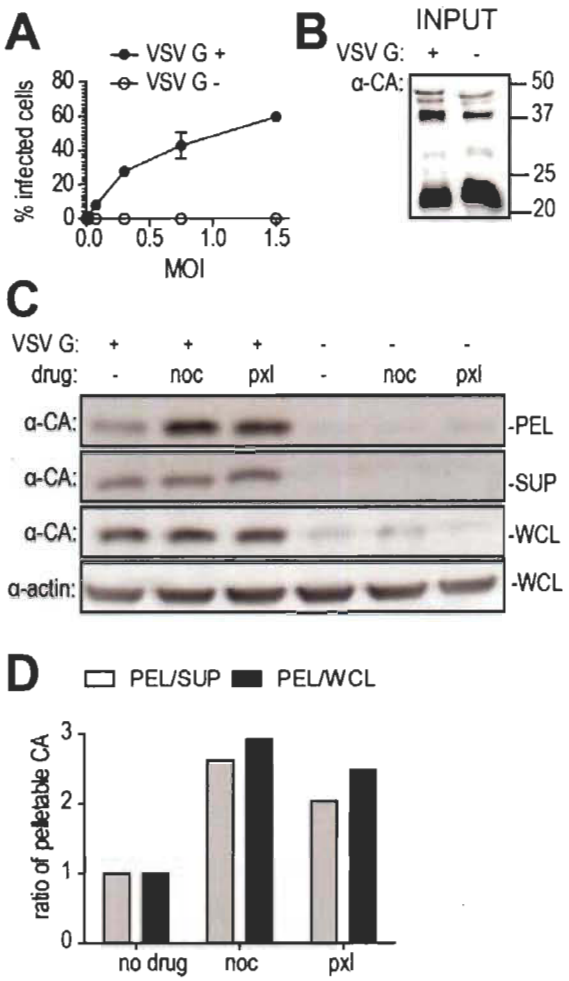

Figure 3.2 **Analysis of HIV-1 uncoating using the fate-of-capsid assay.**
(A) Percentages of HeLa cells expressing GFP following infection with increasing amounts of HIV-$1_{NL43\text{-}GFP}$ pseudotyped with VSV G or devoid of an envelope as indicated. The virus preparations were equalized by RT activity and the amounts of virus used are shown as MOI units, as calculated for the VSV G-pseudotyped virus. (B) The viral preparations used in (A) and normalized by RT assay were concentrated by ultracentrifugation and analyzed by Western blotting to detect CA. (C, D) Fate-of-capsid assay. HeLa cells were infected with HIV-$1_{NL43\text{-}GFP}$ bearing VSV G or not (MOI ~2 as calculated for the VSV G-pseudotyped virus) and in the presence or absence of nocodazole (noc; 0.1 μM) or paclitaxel (pxl; 0.1 μM). Supernatants were replaced with virus-free media containing the appropriate drugs 1 h p.i., and cells were incubated for an additional 5 h, then lysed and fate-of-capsid was performed. Western blot analyses of HIV-1 CAp24 in the ultracentrifugation pellets (PEL), supernatants (SUP) and whole-cell lysates (WCL) are shown. Levels of actin in WCLs were also analyzed. (D) CAp24 bands shown in (C) were quantified by densitometry and plotted as pellet/WCL or pellet/supernatant ratios normalized to the no-drug control.

DHC depletion and nocodazole treatment both alter HIV-1 uncoating. In order to gain more insight in the timing of HIV-1 uncoating and how it is affected by DHC depletion and nocodazole treatment, a time-course fate-of-capsid assay was performed (Fig. 3.3A, B). HeLa cells transfected with siRNAs targeting either DHC or Luc, or treated with nocodazole were infected with equal amounts of VSV G-pseudotyped HIV-$1_{NL43\text{-}GFP}$ for 1 h and then lysed immediately or placed in virus-free medium and lysed at 3, 6, 12 and 24 h post infection (p.i.). To track relative changes in the amounts of particulate (pelletable) CA core, the different time points were analyzed side by side by CA Western blotting. To enable comparison between different conditions, equal amounts of a CAp24-containing reference sample were loaded on the different gels (Fig. 3.3A). Only pelletable fractions were analyzed at all time points, but the CAp24 content in WCLs, as analyzed at 3 h p.i., confirmed equal input (Fig. 3.3A). The amounts of particulate CAp24 determined by densitometry were then normalized to the reference sample and plotted (Fig. 3.3B). These amounts of particulate CA likely reflect a balance between the dynamics of CA core release from endosomes and its uncoating. In the control cells transfected with Luc siRNA, the relative amounts of particulate CA peaked at 6 h p.i. but were smaller at 12 h p.i. (Fig. 3.3A, B), suggesting that as expected (Arhel *et al*, 2007; Hulme *et al*, 2011), uncoating had taken place for most RTCs by that time. CAp24 content did not decrease further between 12 and 24 h p.i. (Fig. 3.3A), a probable result of de novo Gag synthesis in the infected cells. For that reason, the 24 h time point was not included in the analysis shown in Fig. 3.3B. Increased levels of pelletable CA were observed at 6 h p.i. in cells treated with nocodazole or transfected with DHC siRNA (Fig. 3.3A, B). Specifically, nocodazole treatment and DHC depletion increased CAp24 content in the pelletable fraction by ~1.7-fold ($P = 0.017$) and ~1.5-fold ($P = 0.059$) relative to the control cells, respectively (Fig. 3.3B). This is consistent with the results shown in Fig. 3.2C and with our previous report showing an increase in relative amounts of CA cores 6 h p.i. following DHC depletion or treatment with nocodazole and paclitaxel (Pawlica *et al*, 2014). Interestingly, the increase in amounts of particulate CA caused by DHC depletion appeared to be transient, since it was not observed at 12 h p.i. On the other hand, nocodazole treatment also increased the amounts of CA cores at 12 h p.i. Specifically, at

this time point the CAp24 content in the pelletable fractions of cells treated with nocodazole was ~3 times that observed in the control cells (P = 0.013). Collectively, these results confirm that perturbation of microtubule dynamics and disruption of dynein motor complexes increase the relative amounts of CA cores in infected cells, suggesting impaired or delayed HIV-1 uncoating.

We performed an additional experiment, focusing on the 6 h and 9 h p.i. time points, that also included paclitaxel treatment. Results were plotted as pellet/WCL ratios normalized to the no-treatment control (Fig. 3.3C). As expected, an increase in pelletable/total CA ratios could be observed at 6 h p.i. as a result of nocodazole or paclitaxel treatments or DHC depletion (an increase of ~2.4-fold, ~2.8-fold and ~2.4-fold compared to the control cells, respectively). DHC depletion did not have an effect on CA core stability at 9 h p.i., confirming that the effect seen was transient (Fig. 3.3A, B). Perturbation of microtubule dynamics with nocodazole and paclitaxel led to a more persistent increase in pelletable CA cores. Indeed, at 9 h p.i. pellet/WCL ratios in nocodazole- and paclitaxel-treated cells were ~2.5-fold and ~2.3-fold higher, respectively, than for the untreated control. In summary, microtubule perturbation and DHC depletion both counteract uncoating, although the effect appears to be more prolonged for the former than for the latter.

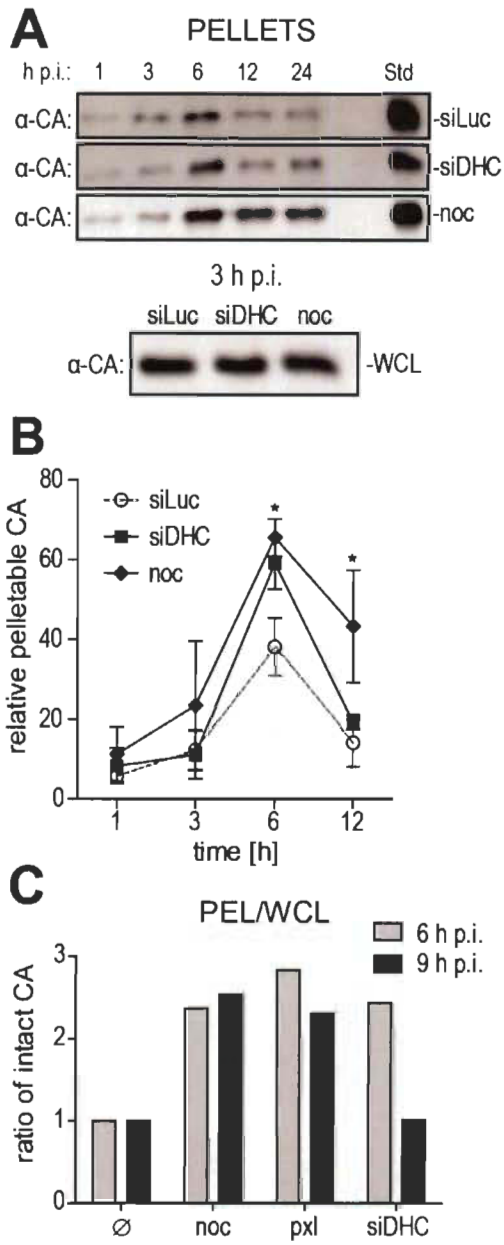

Figure 3.3 **DHC depletion and nocodazole treatment affect HIV-1 uncoating.** (A, B) Time-course fate-of-capsid assay. (A) HeLa cells were transfected with siRNAs targeting DHC (siDHC) or luciferase (siLuc), or were pretreated with 2 μM of nocodazole (noc), and were infected with HIV-$1_{NL43\text{-}GFP}$ (MOI ~2 as calculated on the untreated cells). Supernatants were removed 1 h p.i. and replaced with fresh media containing nocodazole, if applicable, and fate-of-capsid was performed 1, 3, 6, 12 and 24 h p.i. Shown are Western blot analyses of CAp24 at 3 h p.i. in WCL (lower panel) and at various times in ultracentrifugation pellets (upper panels). Identical amounts of a control CAp24-containing sample were included in each gel as an internal standard ('Std'). (B) Bands corresponding to pelletable CAp24 were quantified by densitometry up to

12 h p.i. and plotted after normalization to the standard. The error bars correspond to standard deviations of duplicates. * indicates $P < 0.05$ in a two-way ANOVA analysis, when compared to the untreated (siLuc) control at the same time points. (C) Fate-of-capsid analysis at 6 h and 9 h p.i. HeLa cells transfected with DHC siRNA or treated with nocodazole (0.1 μM) or paclitaxel (0.1 μM) were infected with HIV-$1_{NL43\text{-}GFP}$ (MOI ~2). Supernatants were replaced with fresh media containing the appropriate drugs 1 h p.i., and fate-of-capsid was performed at 6 or 9 h p.i. Bands corresponding to CAp24 detected by Western blotting in pellets and WCLs were quantified by densitometry, and the -fold differences in pellet/WCL ratio relative to the untreated control (ø) are shown for each time-point.

Disruption of the dynactin complex interferes with HIV-1 uncoating. As an additional approach to disrupt dynein-dependent transport, we over-expressed p50/dynamitin (p50), a subunit of the dynactin complex responsible for binding cargos to the dynein motor. p50 over-expression results in the disassembly of the dynactin complex, thereby disrupting cargo binding to the dynein motor and inhibiting dynein-dependent transport (Burkhardt *et al*, 1997; Melkonian *et al*, 2007). The efficiency of p50 transfection was confirmed by Western blotting (Fig. 3.4A). We analyzed the effect of p50 over-expression on HIV-1 uncoating at 6 h p.i., since the maximal effect of DHC depletion on CA cores was observed at this time point (Fig. 3.3). As a control, we used the small-molecule CA inhibitor PF-3450074 (PF74), known to disrupt HIV-1 infectivity through destabilization of the CA core (Shi *et al*, 2011). p50 transfection resulted in increased amounts of pelletable CA cores isolated at 6 h p.i. from cells infected with HIV-$1_{NL43\text{-}GFP}$ (Fig. 3.4B). The pellet/WCL ratio was 2.3-fold (± 0.097, $n = 2$) higher than for control cells transfected with an irrelevant plasmid (Fig. 3.4C). As expected, PF-3450074 caused a decrease (3.7-fold) in the amounts of pelletable CA (Fig. 3.4B-C). p50 transfection had no significant effect on HIV-1 infectivity, while PF-3450074 decreased permissiveness to HIV-1 by ~150- to ~550-fold, depending on the MOI used (Fig. 3.4D) and as previously reported (Blair *et al*, 2010). These results confirm that disruption of dynein-dependent transport counteracts uncoating, but the lack of an effect on infectivity suggests that uncoating is delayed rather than abrogated.

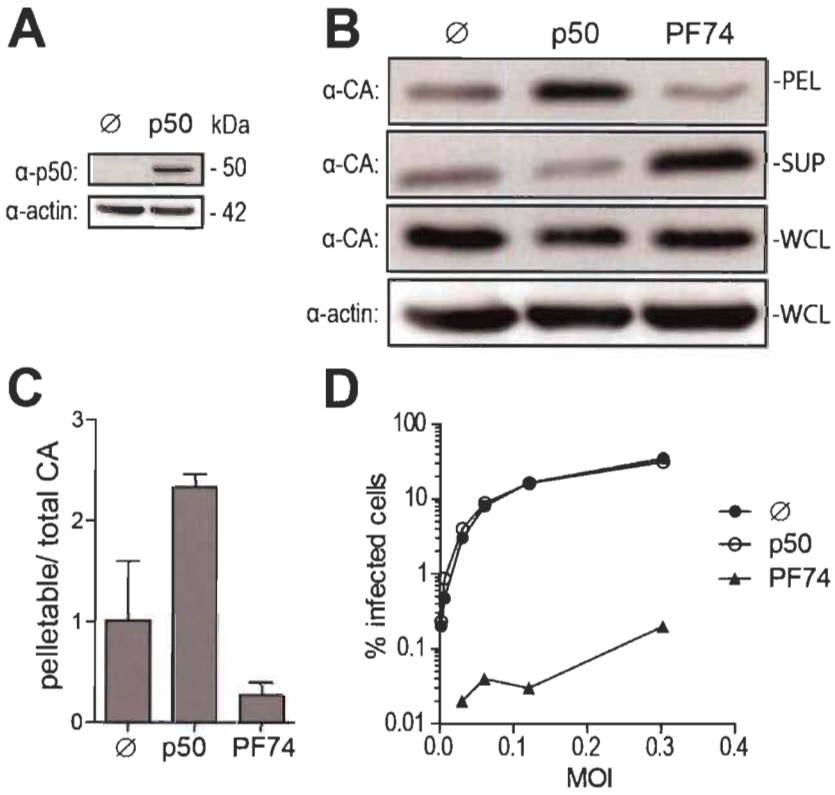

Figure 3.4 **Over-expression of p50/dynamitin affects HIV-1 uncoating.** (A) Western blot analysis of p50 and actin expression in HeLa cells 2 days after transfection with a plasmid encoding p50 or an irrelevant plasmid (pMIP; ø). (B, C) Fate-of-capsid analysis. (B) HeLa cells transfected with a p50 expression construct or with pMIP (ø), or treated with 10 μM of PF-3450074 (PF74), were infected with HIV-$1_{NL43\text{-}GFP}$ (MOI ~2 as calculated in the untreated cells). Supernatants were replaced with virus-free media containing PF-3450074, if applicable, at 1 h p.i. and fate-of-capsid was performed at 6 h p.i. Shown are Western blot analyses of CAp24 in pellets, supernatants and WCLs. Levels of actin in WCLs were also analyzed. (C) CAp24 bands were quantified by densitometry from an experiment done in a duplicate, and pelletable/WCL ratios were calculated and are shown as -fold changes relative to the untreated control, with standard deviations. (D) Infectivity. HeLa cells treated as in (B) were infected with increasing amounts of HIV-$1_{NL43\text{-}GFP}$. Supernatants were replaced with virus-free, drug-free medium 16 h p.i. The percentages of GFP-expressing cells were analyzed 2 days p.i. by flow cytometry.

Nocodazole does not stabilize the intrinsically hypostable CA mutant K203A.

Next, we asked what would be the effect of nocodazole-mediated core stabilization on CA mutants that confer increased or decreased stability to virion-associated CA cores

(Forshey *et al*, 2002). Thus, we analyzed the effect of nocodazole treatment on cores produced with CA mutants E45A and K203A, using the fate-of-capsid assay. HeLa cells were infected with equal amounts of WT or CA-mutated HIV-$1_{R9\Delta E}$ (as normalized by RT assay) and in the presence or absence of nocodazole, and infection was stopped after 1 h. Fate-of-capsid was performed immediately on half of the cells, while the remaining cells were kept in culture for 11 additional hours in the absence or presence of nocodazole (Fig. 3.5A). CAp24 bands were quantified by densitometry and results were plotted as pellet/WCL ratios (Fig. 3.5B). At 1 h p.i., many virions would still be attached on the outside of cells or trapped in endocytic vesicles, or would have just entered the cells without having undergone uncoating yet; thus, we expected that the phenotypes observed at that point would mirror those seen when analyzing the stability of virion-associated cores for these two mutants (Forshey *et al*, 2002). Indeed, the relative levels of pelletable CA at 1 h p.i. were ~1.6-fold higher for E45A HIV-$1_{R9\Delta E}$ and ~3.3-fold smaller for the K203A mutant, compared to the WT control. These results are consistent with the reported in vitro behavior of these mutants (Forshey *et al*, 2002). Nocodazole had no major effect on pellet/WCL ratios at 1 h p.i. Relative to the WT control, levels of pelletable K203A CAp24 were almost undetectable at 12 h p.i (Fig. 3.5), probably indicating spontaneous uncoating over time. However, levels of pelletable CA at 12 h p.i. were also low for the hyperstable E45A mutant, compared with the WT (Fig. 3.5B), perhaps due to increased susceptibility to a cellular restriction mechanism for this mutant (Rasaiyaah *et al*, 2013). Nocodazole increased the relative amounts of pelletable CA by ~2.8-fold for the WT and ~6.5-fold for the E45A mutant (Fig. 3.5B). However, nocodazole did not increase the relative levels of pelletable K203A CA cores at 12 h p.i. These results confirm the stabilizing effect of nocodazole treatment on CA cores and indicate that this drug does not counteract spontaneous uncoating stemming from intrinsic instability.

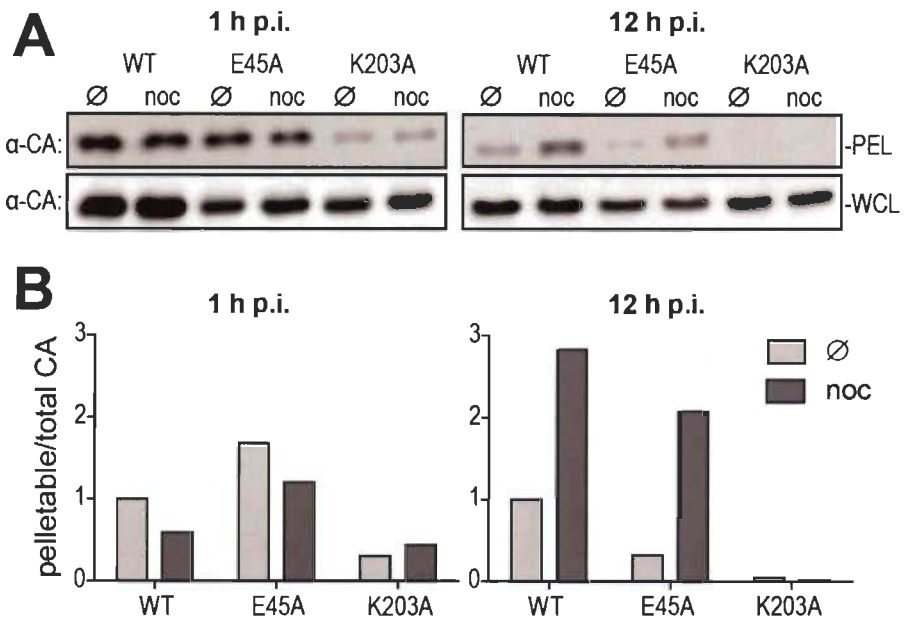

Figure 3.5 Nocodazole increases the relative amounts of E45A CA cores in infected cells, but has no effect on the intrinsically hypostable CA mutant K203A.

(A) HeLa cells were pretreated or not with 0.25 μM of nocodazole and infected with equal amounts of VSV G-pseudotyped WT, E45A or K203A HIV-$1_{R9\Delta E}$ (normalized by RT assay). Half of the cells were lysed at 1 h p.i. and the rest were incubated for an additional 11 h in fresh medium containing nocodazole if applicable, then lysed. Fate-of-capsid was performed, and pellet- and WCL-associated CA were analyzed by Western blotting. (B) CAp24 bands were quantified by densitometry and plotted as pellet/WCL ratios.

3.5 Discussion

Previous articles showed that HIV-1 uncoating could be modulated by CA interactions with cellular factors such as CPSF6 (De Iaco *et al*, 2013) and cyclophilin A (Li *et al*, 2009). In this article, we demonstrate that functional disruption of the microtubule network and dynein motors increases the amounts of HIV-1 CA cores in cells, most likely reflecting delayed uncoating caused by inhibition of their transport towards the nucleus. As observed using IF microscopy, DHC depletion significantly increased the amounts of CA foci and resulted in their accumulation in the cell periphery. These results are consistent with the hypothesis that HIV-1 can use dynein motors to translocate on microtubules towards the nucleus (McDonald *et al*, 2002).

Similarly, nocodazole and paclitaxel treatments resulted in an increase in the relative distance of CA foci from the nucleus and also increased the frequency of these foci, suggesting that fewer cores underwent uncoating. Furthermore, fate-of-capsid experiments revealed that DHC depletion and disruption of dynein-dependent transport by p50 over-expression transiently increased the amounts of CA cores. Thus, dynein motor complexes seem to be involved not only in HIV-1 trafficking but also in uncoating. However, neither DHC depletion (not shown) nor p50 over-expression had a significant effect on HIV-1 infectivity, which is consistent with our previous observations (Pawlica *et al*, 2014) and is explained by the fact that the effect of these interventions on uncoating seem to be transient. The effect of nocodazole and paclitaxel treatments on HIV-1 uncoating was more prolonged, though our experimental setting did not allow us to analyze time points beyond 12 h p.i. These drugs did not significantly affect infectivity in the cell lines used here (data not shown), consistent with previous reports (Bukrinskaya *et al*, 1998; Pawlica *et al*, 2014; Yoder *et al*, 2011), also suggesting that uncoating was delayed by the treatments rather than disrupted altogether. These observations can be partly explained by the use of a more stable (nocodazole-resistant) sub-population of microtubules by HIV-1, as proposed by others (Sabo *et al*, 2013). Alternatively, HIV-1 CA core retrograde transport could proceed by microtubule-independent mechanisms, such as translocation on actin microfilaments (Yoder *et al*, 2011). Thus, we propose that inhibition of dynein- and microtubule-mediated transport delays uncoating until the virus reaches the juxtanuclear region by employing alternative transportation strategies.

The uncoating inhibition phenotype reported here stands in sharp contrast with the effect of the CA E45A mutation, which enhances the stability of CA cores purified from virions, but abrogates HIV-1 infectivity (Forshey *et al*, 2002). We show that despite being more stable in infected cells than their WT counterpart when analyzed at 1 h, most E45A CA cores are 'lost' by 12 h p.i., which may reflect their sensitivity to a cellular restriction factor, by disruption of interactions between incoming CA cores and cellular partners shielding them (Rasaiyaah *et al*, 2013). Nocodazole treatment increased the amounts of E45A CA cores at 12 h p.i, suggesting that this mutant is not impaired in its

interactions with the microtubule network. On the other hand, nocodazole did not stabilize the intrinsically hypostable K203A mutant, suggesting that this mutant undergoes spontaneous disassembly independently of its retrograde transport.

It has been reported that HIV-1 CA cores can reach the vicinity of the nucleus within two hours of infection (Arhel, 2010; Arhel *et al*, 2007; McDonald *et al*, 2002), and uncoating appears to be initiated during this transport (Hulme *et al*, 2011), but is not completed before reaching the nuclear pore complex (Arhel *et al*, 2007; Rasaiyaah *et al*, 2013). Our results support the notion that when microtubules/dynein-dependent transport is inhibited, both retrograde transport and uncoating are simultaneously delayed; longitudinal live microscopy experiments might be needed to definitely prove this hypothesis. Interestingly, a member of the PDZ domain-containing family, the putative microtubule-interacting protein PDZD8, was recently reported to stabilize HIV-1 CA cores (Guth & Sodroski, 2014). In agreement with this report, we propose that during dynein-dependent transport along microtubules, the HIV-1 CA core is stabilized by PDZD8 and/or other cellular proteins, remaining intact or only partially uncoated, and completes its uncoating only after being transferred to actin filaments in the vicinity of the nucleus (Arhel *et al*, 2007; Hulme *et al*, 2011). Our study suggests that uncoating is functionally linked to intracytoplasmic transport of the CA core.

3.6 Methods

Cells, pharmaceuticals and antibodies. Human embryonic kidney 293T (HEK293T) cells, epithelial carcinoma HeLa cells and human U373-derived MAGI cells (Vodicka *et al*, 1997) were maintained in Dulbecco's modified Eagle's medium (DMEM) with high glucose, supplemented with 10% fetal bovine serum (FBS) and antibiotics at 37°C, 5% CO_2. All cell culture reagents were from HyClone (Thermo Scientific, Logan, UT). Nocodazole, paclitaxel and MG132 were from Sigma (St Louis, MI), while PF-3450074 was provided by Pfizer (New York, NY). Rabbit polyclonal antibodies against dynein heavy chain and p50/dynamitin were from Santa Cruz (Dallas, TX) and Millipore (Billerica, MA), respectively. Capsid (CA, p24) was detected using a

mouse monoclonal antibody (clone 183, cat#3537) from the AIDS Research and Reference Reagent Program. The HRP-conjugated mouse anti-actin antibody was from Sigma. HRP-conjugated goat anti-rabbit and goat anti-mouse antibodies used as secondary antibodies in Western blots were all from Santa Cruz.

Plasmid DNAs, retrovirus production and reverse transcriptase assay. $pR9\Delta E_{WT}$, $pR9\Delta E_{E45A}$ and $pR9\Delta E_{K203A}$, plasmids encoding Δ env HIV-1 vectors and bearing capsid stability mutations, were generously provided by Chistopher Aiken (Forshey *et al*, 2005), while p50/dynamitin-HA was a gift from Tina Schroer (Schrader *et al*, 2000). To produce viral vectors, 10-cm culture dishes or 75-cm flasks of sub-confluent HEK293T cells were co-transfected using polyethylenimine (PEI; MW 25,000, Polyscience, Niles, IL) with the appropriate plasmids, as follows: for the replication-competent $HIV\text{-}1_{NL43}$, 20 μg of pNL4-3; for the viral vector $HIV\text{-}1_{CMV\text{-}GFP}$, $pTRIP_{CMV\text{-}GFP}$ (10 μg), pΔR8.9 (10 μg) and pMD-G (5 μg); for $HIV\text{-}1_{NL43\text{-}GFP}$, pNL-GFP (10 μg) and pMD-G (5 μg); for the envelope-devoid $HIV\text{-}1_{NL43\text{-}GFP}$, pNL-GFP (10 μg); for the $HIV\text{-}1_{R9\Delta E}$ constructs, the appropriate pR9ΔE (20 μg) and pMD-G (5 μg) (Aiken, 1997; Berthoux *et al*, 2003; Naviaux *et al*, 1996; Zufferey *et al*, 1997). Media were changed 16 h post transfection and virus-containing supernatants were collected after an additional 1.5 d of culture. Viral stocks were clarified by centrifugation for 5 min at 400 x *g*. In some experiments, reverse transcriptase activity was measured on virus stocks using the EnzCheck kit (Molecular Probes, Eugene, OR) according to the manufacturer's instructions.

Viral challenges. Cells were seeded in 24-well plates at 2×10^5 cells per well and challenged the next day with the appropriate GFP-expressing viral vectors. When applicable, cells were pre-treated for 15 min with nocodazole, paclitaxel or PF-3450074, and supernatants were replaced with fresh medium 16 h post infection (p.i.) Cells were trypsinized 48 h p.i. and fixed in 2% formaldehyde (Fisher Scientific, Waltham, MA). The percentages of GFP-positive cells were then determined by analyzing 10^4 to 3×10^4 cells on a FC500 MPL cytometer (Beckman Coulter, Brea, CA) using the CXP Software (Beckman Coulter).

siRNA and plasmid DNA transfection. For the siRNA treatments, 10^6 cells were seeded in a 10 cm dish in Opti-MEM (Gibco, Carlsbad, CA) and transfected the next day with 40 nM of siRNA using DharmaFECT 1 (Dharmacon, Lafayette, CO). The siRNA targeting the sequence 5'GATCAAACATGACGGAATT of the dynein heavy chain (DHC), has been described before (Lehmann *et al*, 2009; Pawlica *et al*, 2014) and was purchased from Qiagen (Venlo, Netherlands). A control siRNA (5'CGTACGCGGAATACTTCGATT) targeting the luciferase mRNA (Pawlica *et al*, 2014) was purchased from Dharmacon. 48 h post transfection, cells were seeded in 24-well plates and infected the next day with HIV-1 vectors as described above. For p50 over-expression, 10^6 cells seeded in a 10-cm dish were PEI transfected with 5 µg of p50/dynamitin-HA or an irrelevant plasmid (pMIP). Cells were seeded in 24-well plates 24 h later and challenged with viral vectors the next day.

Immunofluorescence (IF) microscopy. 2 x 10^5 HeLa or MAGI cells were seeded on glass coverslips placed in 3.5-cm wells and were infected the next day at a high multiplicity of infection (MOI) of vesicular stomatitis virus glycoprotein (VSV G)-pseudotyped HIV-$1_{CMV\text{-}GFP}$ (HeLa) or replication-competent HIV-1_{NL43} (MAGI) in the presence of 1 µg/ml MG132 and various treatments. For depletion experiments, siRNAs were transfected 72 h prior to infection while cells were pre-treated with nocodazole or paclitaxel 15 min prior to infection. Infections were carried out for 2 h (HIV-1_{NL43}) or 4 h followed by a 2-h incubation in fresh medium (HIV-$1_{CMV\text{-}GFP}$). Cells were then fixed for 30 min in 4% formaldehyde-DMEM, followed by 3 washes with ice-cold phosphate buffer saline (PBS) and permeabilized for 2 min on ice in 0.1% Triton X-100, 0.1 mM sodium citrate. Cells were then washed again three times with PBS and treated with 10% normal goat serum (Sigma, St Louis, MI) containing 0.3 M glycine (Sigma) for 30 min at room temperature. This was followed by a 4-hours incubation with antibodies against CA (1:100 dilution) in PBS containing 10% normal goat serum. Cells were washed five times and fluorescently stained with AlexaFluor488-conjugated goat anti-mouse (Molecular Probes, Eugene, OR) diluted 1:200 in normal goat serum-containing PBS. Cells were then washed five times in PBS before mounting in Vectashield (Vector Laboratories, Peterborough, UK). Hoechst33342 (0.8 µg/ml; Molecular Probes) was

added along with the penultimate PBS wash to reveal DNA. Z-stacks were acquired on an AxioObserver Microscope (Carl Zeiss, Jena, Germany) equipped with an ApoTome module, and the median optical slice of a Z-stack was analyzed.

Fate-of-capsid assay. To analyze post-entry CA uncoating, a protocol adapted from Perron *et al* (Perron *et al*, 2004) was used and has been described in details before (Bérubé *et al*, 2007; Pawlica *et al*, 2014). 4 x 10^6 HeLa cells were seeded in 10-cm dishes. In some cases, HeLa cells were previously transfected with siRNAs or p50/dynamitin. The next day, if applicable, cells were pretreated 15 min with pharmacological agents and infected with HIV-$1_{NL43\text{-}GFP}$ or HIV-$1_{R9\Delta E}$ [wild-type (WT) or CA-mutated]. The MOI used for HIV-$1_{NL43\text{-}GFP}$ was ~2. WT, CA-E45A and CA-K203A HIV-$1_{R9\Delta E}$ vectors were equalized using reverse transcriptase (RT) assay. The amounts of envelope-devoid HIV-$1_{NL43\text{-}GFP}$ and its VSV G-pseudotyped counterpart were also normalized by RT assay. Unless otherwise specified, supernatants were replaced with fresh media containing the appropriate drugs 1 h p.i. Cells were collected by trypsinization at different time points. Cells were washed in ice-cold PBS and resuspended in 1.5 ml of ice-cold lysis buffer [100 µM Tris-HCl (pH 8.0), 0.4 mM KCl, 2 µM EDTA, Roche's Complete protease inhibitor] and disrupted with a Dounce homogenizer. Whole-cell Lysate (WCL) samples were collected at this point. Lysates were centrifuged for 5 min 1,000 x *g*, 4°C to remove cell debris and nuclei, and supernatants were layered on top of a 50% sucrose cushion prepared in STE buffer [100 mM NaCl, 10 mM Tris-HCl (pH 8.0), 1 mM EDTA]. Particulate viral cores were sedimented by ultracentrifugation in a Sorval WX Ultra 100 ultracentrifuge at 175,000 x *g* for 2 h at 4°C. In some experiments, post-ultracentrifugation supernatants were collected. Pellets were resuspended in 80 µl of 1X denaturing loading buffer and processed for CA Western blotting together with WCLs.

Statistical analysis. All statistical analyses were done in Graph Prism 5 (GraphPad Software, Inc., La Jolla, CA, USA). The box blot representations in Fig. 3.1 were generated with the R software (Spitzer *et al*, 2014).

3.7 Acknowledgements

We thank Réjean Cantin, Maxime Veillette and Mélodie B. Plourde for providing technical help. We thank Natacha Mérindol and Marie-Édith Nepveu-Traversy for a critical reading of this manuscript. We are grateful to Chistopher Aiken (Vanderbilt University School of Medicine) and Trina Schroer (Johns Hopkins University) for sharing plasmid DNA. We thank Michel Tremblay (Centre de Recherche du CHU de l'université Laval) for allowing us to use his BSLIII laboratory facilities. The following reagent was obtained through the NIH AIDS Research and Reference Reagent Program, Division of AIDS, NIAID, NIH: clone 183 p24 antibody (cat#3537, contributed by Bruce Chesebro). PF-3450074 was a gift from Pfizer. This work was supported by Canadian Institutes of Health Research operating grant MOP-102712 (L.B.).

3.8 References

Aiken C (1997) Pseudotyping human immunodeficiency virus type 1 (HIV-1) by the glycoprotein of vesicular stomatitis virus targets HIV-1 entry to an endocytic pathway and suppresses both the requirement for Nef and the sensitivity to cyclosporin A. *Journal of virology* 71: 5871-5877

Ambrose Z, Aiken C (2014) HIV-1 uncoating: connection to nuclear entry and regulation by host proteins. *Virology* 454-455:371-9

Arhel N (2010) Revisiting HIV-1 uncoating. *Retrovirology* 7: 96

Arhel NJ, Souquere-Besse S, Munier S, Souque P, Guadagnini S, Rutherford S, Prevost MC, Allen TD, Charneau P (2007) HIV-1 DNA Flap formation promotes uncoating of the pre-integration complex at the nuclear pore. *The European Molecular Biology Organization journal* 26: 3025-3037

Auewarakul P, Wacharapornin P, Srichatrapimuk S, Chutipongtanate S, Puthavathana P (2005) Uncoating of HIV-1 requires cellular activation. *Virology* 337: 93-101

Berthoux L, Towers GJ, Gurer C, Salomoni P, Pandolfi PP, Luban J (2003) As(2)O(3) enhances retroviral reverse transcription and counteracts Ref1 antiviral activity. *Journal of virology* 77: 3167-3180

Bérubé J, Bouchard A, Berthoux L (2007) Both TRIM5alpha and TRIMCyp have only weak antiviral activity in canine D17 cells. *Retrovirology* 4: 68

Blair WS, Pickford C, Irving SL, Brown DG, Anderson M, Bazin R, Cao J, Ciaramella G, Isaacson J, Jackson L, Hunt R, Kjerrstrom A, Nieman JA, Patick AK, Perros M, Scott AD, Whitby K, Wu H, Butler SL (2010) HIV capsid is a tractable target for small molecule therapeutic intervention. *PLoS Pathogens* 6: e1001220

Blumenthal R, Bali-Puri A, Walter A, Covell D, Eidelman O (1987) pH-dependent fusion of vesicular stomatitis virus with Vero cells. Measurement by dequenching of octadecyl rhodamine fluorescence. *The Journal of biological chemistry* 262: 13614-13619

Briggs JA, Krausslich HG (2011) The molecular architecture of HIV. *Journal of molecular biology* 410: 491-500

Briggs JA, Wilk T, Welker R, Krausslich HG, Fuller SD (2003) Structural organization of authentic, mature HIV-1 virions and cores. *The European Molecular Biology Organization journal* 22: 1707-1715

Bukrinskaya A, Brichacek B, Mann A, Stevenson M (1998) Establishment of a functional human immunodeficiency virus type 1 (HIV-1) reverse transcription complex involves the cytoskeleton. *The Journal of experimental medicine* 188: 2113-2125

Burkhardt JK, Echeverri CJ, Nilsson T, Vallee RB (1997) Overexpression of the dynamitin (p50) subunit of the dynactin complex disrupts dynein-dependent maintenance of membrane organelle distribution. *The Journal of cell biology* 139: 469-484

Campbell EM, Perez O, Melar M, Hope TJ (2007) Labeling HIV-1 virions with two fluorescent proteins allows identification of virions that have productively entered the target cell. *Virology* 360: 286-293

Cureton DK, Massol RH, Saffarian S, Kirchhausen TL, Whelan SP (2009) Vesicular stomatitis virus enters cells through vesicles incompletely coated with clathrin that depend upon actin for internalization. *PLoS Pathogens* 5: e1000394

De Iaco A, Santoni F, Vannier A, Guipponi M, Antonarakis S, Luban J (2013) TNPO3 protects HIV-1 replication from CPSF6-mediated capsid stabilization in the host cell cytoplasm. *Retrovirology* 10: 20

Forshey BM, Shi J, Aiken C (2005) Structural requirements for recognition of the human immunodeficiency virus type 1 core during host restriction in owl monkey cells. *Journal of virology* 79: 869-875

Forshey BM, von Schwedler U, Sundquist WI, Aiken C (2002) Formation of a human immunodeficiency virus type 1 core of optimal stability is crucial for viral replication. *Journal of virology* 76: 5667-5677

Gamble TR, Yoo S, Vajdos FF, von Schwedler UK, Worthylake DK, Wang H, McCutcheon JP, Sundquist WI, Hill CP (1997) Structure of the carboxyl-terminal dimerization domain of the HIV-1 capsid protein. *Science* 278: 849-853

Gaudin R, Alencar BC, Arhel N, Benaroch P (2013) HIV trafficking in host cells: motors wanted! *Trends in cell biology* 23: 652-662

Goff SP (2001) Intracellular trafficking of retroviral genomes during the early phase of infection: viral exploitation of cellular pathways. *The journal of gene medicine* 3: 517-528

Guth CA, Sodroski J (2014) Contribution of PDZD8 to Stabilization of the Human Immunodeficiency Virus (HIV-1) Capsid. *Journal of virology* 88: 4612-23

Hulme AE, Perez O, Hope TJ (2011) Complementary assays reveal a relationship between HIV-1 uncoating and reverse transcription. *Proceedings of the National Academy of Sciences of the United States of America* 108: 9975-9980

Kikkawa M (2013) Big steps toward understanding dynein. *The Journal of cell biology* 202: 15-23

Lakadamyali M, Rust MJ, Zhuang X (2006) Ligands for clathrin-mediated endocytosis are differentially sorted into distinct populations of early endosomes. *Cell* 124: 997-1009

Lehmann M, Milev MP, Abrahamyan L, Yao XJ, Pante N, Mouland AJ (2009) Intracellular transport of human immunodeficiency virus type 1 genomic RNA and viral production are dependent on dynein motor function and late endosome positioning. *The Journal of biological chemistry* 284: 14572-14585

Li Y, Kar AK, Sodroski J (2009) Target cell type-dependent modulation of human immunodeficiency virus type 1 capsid disassembly by cyclophilin A. *Journal of virology* 83: 10951-10962

Luduena RF, Roach MC (1991) Tubulin sulfhydryl groups as probes and targets for antimitotic and antimicrotubule agents. *Pharmacology & therapeutics* 49: 133-152

Marechal V, Clavel F, Heard JM, Schwartz O (1998) Cytosolic Gag p24 as an index of productive entry of human immunodeficiency virus type 1. *Journal of Virology* 72: 2208-2212

McDonald D, Vodicka MA, Lucero G, Svitkina TM, Borisy GG, Emerman M, Hope TJ (2002) Visualization of the intracellular behavior of HIV in living cells. *The Journal of cell biology* 159: 441-452

Melkonian KA, Maier KC, Godfrey JE, Rodgers M, Schroer TA (2007) Mechanism of dynamitin-mediated disruption of dynactin. *The Journal of biological chemistry* 282: 19355-19364

Naviaux RK, Costanzi E, Haas M, Verma IM (1996) The pCL vector system: rapid production of helper-free, high-titer, recombinant retroviruses. *Journal of virology* 70: 5701-5705

Nilsson H, Wallin M (1998) Microtubule aster formation by dynein-dependent organelle transport. *Cell motility and the cytoskeleton* 41: 254-263

Ott DE (2008) Cellular proteins detected in HIV-1. *Reviews in medical virology* 18: 159-175

Pawlica P, Le Sage V, Poccardi N, Tremblay MJ, Mouland AJ, Berthoux L (2014) Functional evidence for the involvement of microtubules and dynein motor complexes in TRIM5alpha-mediated restriction of retroviruses. *Journl of virology* 88: 5661-5676

Perron MJ, Stremlau M, Song B, Ulm W, Mulligan RC, Sodroski J (2004) TRIM5alpha mediates the postentry block to N-tropic murine leukemia viruses in human cells. *Proceedings of the National Academy of Sciences of the United States of America* 101: 11827-11832

Pornillos O, Ganser-Pornillos BK, Kelly BN, Hua Y, Whitby FG, Stout CD, Sundquist WI, Hill CP, Yeager M (2009) X-ray structures of the hexameric building block of the HIV capsid. *Cell* 137: 1282-1292

Pornillos O, Ganser-Pornillos BK, Yeager M (2011) Atomic-level modelling of the HIV capsid. *Nature* 469: 424-427

Rasaiyaah J, Tan CP, Fletcher AJ, Price AJ, Blondeau C, Hilditch L, Jacques DA, Selwood DL, James LC, Noursadeghi M, Towers GJ (2013) HIV-1 evades innate immune recognition through specific cofactor recruitment. *Nature* 503: 402-405

Roa A, Hayashi F, Yang Y, Lienlaf M, Zhou J, Shi J, Watanabe S, Kigawa T, Yokoyama S, Aiken C, Diaz-Griffero F (2012) RING domain mutations uncouple TRIM5alpha restriction of HIV-1 from inhibition of reverse transcription and acceleration of uncoating. *Journal of virology* 86: 1717-1727

Sabo Y, Walsh D, Barry DS, Tinaztepe S, de Los Santos K, Goff SP, Gundersen GG, Naghavi MH (2013) HIV-1 induces the formation of stable microtubules to enhance early infection. *Cell host & microbe* 14: 535-546

Sayah DM, Sokolskaja E, Berthoux L, Luban J (2004) Cyclophilin A retrotransposition into TRIM5 explains owl monkey resistance to HIV-1. *Nature* 430: 569-573

Schaller T, Ocwieja KE, Rasaiyaah J, Price AJ, Brady TL, Roth SL, Hue S, Fletcher AJ, Lee K, KewalRamani VN, Noursadeghi M, Jenner RG, James LC, Bushman FD, Towers GJ (2011) HIV-1 capsid-cyclophilin interactions determine nuclear import pathway, integration targeting and replication efficiency. *PLoS Pathogens* 7: e1002439

Schiff PB, Fant J, Horwitz SB (1979) Promotion of microtubule assembly in vitro by taxol. *Nature* 277: 665-667

Schrader M, King SJ, Stroh TA, Schroer TA (2000) Real time imaging reveals a peroxisomal reticulum in living cells. *Journal of cell science* 113 (Pt 20): 3663-3671

Shah VB, Shi J, Hout DR, Oztop I, Krishnan L, Ahn J, Shotwell MS, Engelman A, Aiken C (2013) The host proteins transportin SR2/TNPO3 and cyclophilin A exert opposing effects on HIV-1 uncoating. *Journal of Virology* 87: 422-432

Shi J, Zhou J, Shah VB, Aiken C, Whitby K (2011) Small-molecule inhibition of human immunodeficiency virus type 1 infection by virus capsid destabilization. *Journal of virology* 85: 542-549

Slonska A, Polowy R, Golke A, Cymerys J (2012) Role of cytoskeletal motor proteins in viral infection. *Postępy higieny i medycyny doświadczalnej (Online)* 66: 810-817

Spitzer M, Wildenhain J, Rappsilber J, Tyers M (2014) BoxPlotR: a web tool for generation of box plots. *Nature methods* 11: 121-122

Stremlau M, Owens CM, Perron MJ, Kiessling M, Autissier P, Sodroski J (2004) The cytoplasmic body component TRIM5alpha restricts HIV-1 infection in Old World monkeys. *Nature* 427: 848-853

Stremlau M, Perron M, Lee M, Li Y, Song B, Javanbakht H, Diaz-Griffero F, Anderson DJ, Sundquist WI, Sodroski J (2006) Specific recognition and accelerated uncoating of retroviral capsids by the TRIM5alpha restriction factor. *Proceedings of the National Academy of Sciences of the United States of America* 103: 5514-5519

Sun X, Yau VK, Briggs BJ, Whittaker GR (2005) Role of clathrin-mediated endocytosis during vesicular stomatitis virus entry into host cells. *Virology* 338: 53-60

Tipper C, Sodroski J (2013) Enhanced autointegration in hyperstable simian immunodeficiency virus capsid mutants blocked after reverse transcription. *Journal of Virology* 87: 3628-3639

Vodicka MA, Goh WC, Wu LI, Rogel ME, Bartz SR, Schweickart VL, Raport CJ, Emerman M (1997) Indicator cell lines for detection of primary strains of human and simian immunodeficiency viruses. *Virology* 233: 193-198

Yang Y, Fricke T, Diaz-Griffero F (2013) Inhibition of reverse transcriptase activity increases stability of the HIV-1 core. *Journal of Virology* 87: 683-687

Yoder A, Guo J, Yu D, Cui Z, Zhang XE, Wu Y (2011) Effects of microtubule modulators on HIV-1 infection of transformed and resting CD4 T cells. *Journal of virology* 85: 3020-3024

Zhang H, Dornadula G, Orenstein J, Pomerantz RJ (2000) Morphologic changes in human immunodeficiency virus type 1 virions secondary to intravirion reverse transcription: evidence indicating that reverse transcription may not take place within the intact viral core. *Journal of human virology* 3: 165-172

Zhang H, Dornadula G, Pomerantz RJ (1998) Natural endogenous reverse transcription of HIV-1. *Journal of reproductive immunology* 41: 255-260

Zhou L, Sokolskaja E, Jolly C, James W, Cowley SA, Fassati A (2011) Transportin 3 promotes a nuclear maturation step required for efficient HIV-1 integration. *PLoS Pathogens* 7: e1002194

Zufferey R, Nagy D, Mandel RJ, Naldini L, Trono D (1997) Multiply attenuated lentiviral vector achieves efficient gene delivery in vivo. *Nature Biotechnology* 15: 871-875

Chapter IV contains a summary and discussion of the results described in Chapters II and III. Additionally, in this chapter new directions and perspectives of the studies are described.

CHAPTER IV

CONCLUSIONS

4.1 The involvement of microtubules and dynein motor complexes in TRIM5α-mediated restriction

In the study in Chapter II, we examined the importance of microtubules and dynein motors in TRIM5α-mediated restriction. We found that both microtubules and dynein motor complexes were relevant for the ability of TRIM5α to fully inhibit retroviral infection. To disrupt the microtubule network we used the pharmacological agents nocodazole and paclitaxel, while the dynein motor was inhibited either by EHNA treatment or by DHC depletion. Perturbation of microtubules and dynein motor complexes decreased the ability of TRIM5α to inhibit retroviruses and impaired its hallmark feature: the destabilization of viral CA cores. Additionally, these treatments affected dynamics of cytoplasmic bodies (CBs) formed by TRIM5α proteins. DHC depletion also decreased the co-localization of these structures with microtubules.

4.1.1 How might TRIM5α use microtubules?

TRIM5α CBs, similarly to HIV-1, most likely use microtubules for their transport and/or correct localization. Thus, microtubules are likely a platform for the encounter of TRIM5α proteins and incoming restriction-sensitive retroviruses. The hypothesis that TRIM5α CBs use microtubules is supported by their altered dynamics following disruptions of these filaments. While it appears to be certain that TRIM5α CBs associate with microtubules, the role of the dynein motor complexes as a mediator of this association is not fully understood. The effects of DHC depletion on the localization of TIRM5α CBs and their co-localization with microtubules were moderate. This can be explained by two factors. First, the siRNA-mediated DHC knockdown was not complete and thus unaffected dynein motor complexes could still mediate the interaction of

TRIM5α CBs with microtubules. Secondly, the dynein motor complex might be one of two, or more, co-factors responsible for these interactions. Indeed, the majority of cargos for molecular motors associate simultaneously with kinesins and dyneins (Gross, 2004), and sometimes these molecular motors share an adaptor complex, *e.g.* the dynactin complex (Deacon *et al*, 2003). Of note, the 'tug-of-war' theory (Hendricks *et al*, 2010; Muller *et al*, 2008) seems to be well illustrated in this study when upon a depletion of the dynein motor its cargos (TRIM5α CBs) are probably pulled by the kinesin motor towards the cell periphery.

Interestingly, the treatments targeting either microtubules or dynein motor complexes did not significantly affect the replication of retroviruses in non-restrictive conditions. This seems to be counter-intuitive, as both of these cytoskeletal components were suggested to be responsible for the transport of HIV-1 virus. However, the base for these suggestions were IF observations and were not supported by infectivity data (McDonald *et al*, 2002). On the contrary, initial reports described little or no effects of microtubule-targeting drugs on HIV-1 infectivity (Bukrinskaya *et al*, 1998; Daniel *et al*, 2005; Yoder *et al*, 2011). Only recently has it been proposed that for its transport HIV-1 uses a stable sub-population of microtubules (Sabo *et al*, 2013). Regardless of the lack of an effect of these treatments on HIV-1 transduction, the role of nocodazole- and paclitaxel-sensitive microtubules in TRIM5α-mediated restriction is certain, as these drugs decrease it.

Microtubule disruption did not completely abolish the full capacity of TRIM5α to restrict retroviruses; the loss in the initial restriction potency varied, depending on a cell line, and was between 16 and 71%. This could be explained by several factors. First, the pharmacological agents nocodazole and paclitaxel probably do not alter all microtubules in the cell and the drug-resistant microtubules are present in the cell following these treatments (Bre *et al*, 1987; Schulze & Kirschner, 1987). While HIV-1 likely exploits stable microtubules for its transport (Sabo *et al*, 2013), it remains unknown which types of microtubules are used by TRIM5α. The diversity of microtubules in one cell is vast and is regulated by the presence of different microtubule-associated proteins and post-

translational modifications. TRIM5α might use various subsets of microtubules, some of which could be nocodazole- and paclitaxel-sensitive. Secondly, TRIM5α can block a restriction-sensitive virus in more than one way. The microtubules and dynein motor complexes could be involved in only one step of TRIM5α-mediated restriction, while other steps like activation of the innate immune signaling could still be active (Pertel *et al*, 2011; Tareen & Emerman, 2011).

The results acquired in the fate-of-capsid assay suggest that microtubules and dynein motor complexes could enable the initial contact between TRIM5α proteins and restriction-sensitive viruses. However, the possibility that this contact could still take place, but the subsequent proteasome-dependent degradation of TRIM5α is inhibited cannot be ruled out. Nonetheless, proteasome inhibitors restore seemingly normal stability of the HIV-1 core without greatly rescuing viral infectivity (Anderson *et al*, 2006; Diaz-Griffero *et al*, 2007a; Kutluay *et al*, 2013), while the treatments targeting microtubules and dynein motor complexes significantly increase infectivity.

4.1.2 Future experiments

In order to address more completely the role of dynein motor complexes in TRIM5α-mediated restriction it would be important to look at the restriction upon additional disabling of kinesin motor complexes. As an initial approach it should be possible to inhibit the function of the kinesin motor complex by one of many inhibitors (Brier *et al*, 2004; Hewitt *et al*, 2010; Kapoor & Mitchison, 1999; Kawaguchi & Ishiwata, 2001; Smith *et al*, 2013). Although the pharmacological agents could be informative, more in-depth studies would be required to determine which of the 45 kinesins might be involved. To suggest some candidates, the knowledge about other members from the TRIM family could be helpful, *e.g.* TRIM60/RNF33 associates with the kinesin-2 family (KIF3A and KIF3B (Huang *et al*, 2012)) and TRIM3/BERP associates with KIF21B (Labonte *et al*, 2013).

Experiments aimed at establishing the effects of microtubule/dynein disrupting agents on the role of TRIM5α proteasome-dependent degradation should be peerformed. TRIM5α CBs were shown to co-localize with many proteins involved in the proteasomal degradation pathway (Campbell *et al*, 2008; Danielson *et al*, 2012; Lukic *et al*, 2011). Firstly, it would be interesting to look at the co-localization of these structures upon treatments targeting either microtubules or dynein motors. Additionally, as this co-localization is increased in the presence of a restriction-sensitive virus (Danielson *et al*, 2012), it would be also informative to perform similar observations following infection. Another experiment relating to the same question would be to look at the turnover of TRIM5α. It is known that the turnover of TRIM5α is greatly increased in the presence of a restriction-sensitive virus (Diaz-Griffero *et al*, 2006) and it would be interesting to look at this process following disruptions of microtubules and dynein motor complexes.

Moreover, it would be tempting to investigate whether TRIM5α, like HIV-1, uses a stable sub-population of microtubules. It could be informative to look at TRIM5α-mediated restriction while depleting EB1, which is responsible for the formation of the stable sub-population of microtubules used by HIV-1 (Gouveia & Akhmanova, 2010).

Additionally, a new small-molecule antagonists of cytoplasmic dynein was recently discovered, called ciliobrevin (Firestone *et al*, 2012). Employing this drug could simplify experimental procedures, eliminating the necessity of depleting DHC for each experiment.

Very interesting data could be generated by performing real-time IF imaging. TRIM5α CBs are described as dynamic structures constantly undergoing homo- fusions and fissions (Campbell *et al*, 2007a). It would be informative to observe how these processes are altered by inhibiting either microtubules or dynein motor complexes. Additionally, TRIM5α CBs can sequester incoming restriction-sensitive viruses (Campbell *et al*, 2008) and thus it would be interesting to monitor this process in real-time in the presence of treatments modifying either microtubules or molecular motors.

Interestingly, some of the TRIM family members, such as MID1/TRIM18, possess a so-called COS box which mediates microtubule binding (Short & Cox, 2006). This domain is directly downstream coiled-coil, precedes C-terminal functional domains, and is necessary for direct binding to microtubules. TRIM proteins from are known, not only to homodimerize, but also to heteredimerize (Reymond *et al*, 2001). Taking these two facts together, it could be interesting to examine if TRIM5α could interact with microtubules *via* one of the proteins from TRIM family that contains the COS box. Perhaps an over-expression of *e.g.* MID1 could inhibit TRIM5-mediated restriction through competition for binding to microtubules.

4.2 The involvement of microtubules and dynein motor complexes in HIV-1 uncoating

In Chapter III, we presented a study based upon which we proposed that microtubules and dynein motor complexes are important for HIV-1 uncoating. In brief, we disrupted microtubules using the pharmacological agents nocodazole and paclitaxel, and disabled dynein-mediated transport by either siRNA targeting DHC or by p50 over-expression. Following these treatments in cells infected with HIV-1 we noted increases in the amounts of (i) CA *foci* observed by IF and (ii) pelletable (particulate) CA cores by employing the fate-of-capsid assay. We hypothesize that these results reflect impaired or delayed HIV-1 uncoating.

Intriguingly, we observed that the disruption of nocodazole-sensitive microtubules seems to increase the amounts/stability of HIV-1 CA cores, while it was proposed that HIV-1 uses a stable sub-population of microtubules (Sabo *et al*, 2013). We can only speculate about how to explain this discrepancy. It is not fully understood how HIV-1 traffics in the cytoplasm. It is likely that it uses, in addition to the stable sub-population of microtubules, other cytoskeletal components, *e.g.* actin microfilaments. It has been suggested that HIV-1 associates with actin filaments upon its entry and in the proximity of the NPC (Arhel *et al*, 2006; McDonald *et al*, 2002; Zamborlini *et al*, 2007). Some reports even suggested that HIV-1 might mainly use actin microfilaments for its route to

the nucleus (Yoder *et al*, 2011). It is likely that for its transport to the nucleus HIV-1 could use both actin filaments and microtubules, and this would explain why we observed only a delay in HIV-1 core uncoating. Additionally, the lack of an effect on HIV-1 infectivity following the disruption of microtubules and dynein motor complexes might be explained by the cellular context. HeLa cells used in this study likely lack either cytosolic receptors that sense HIV-1 cDNA or elements in the downstream signaling pathway that would induce type I interferon (IFN) response, *e.g.* cyclic GMP-AMP synthase cGAS or STING (Rasaiyaah *et al*, 2013; Yan *et al*, 2010). These immune sensors are present in natural HIV-1 targets *e.g.* macrophages (Lahaye *et al*, 2013; Rasaiyaah *et al*, 2013). It was reported that N74D and P90A CA mutants, which are unable to recruit cellular partners shielding the core and thus enabling the evasion of the innate detection, fail to replicate in macrophages, but infect HeLa cells (Fig. 4.1). Thus, it would be important to perform experiments in cells that are natural HIV-1 targets. It would be also very interesting to look at possible uncoating defects of the mutants impaired for the recruitment of cellular partners, such as N74D and P90A CA.

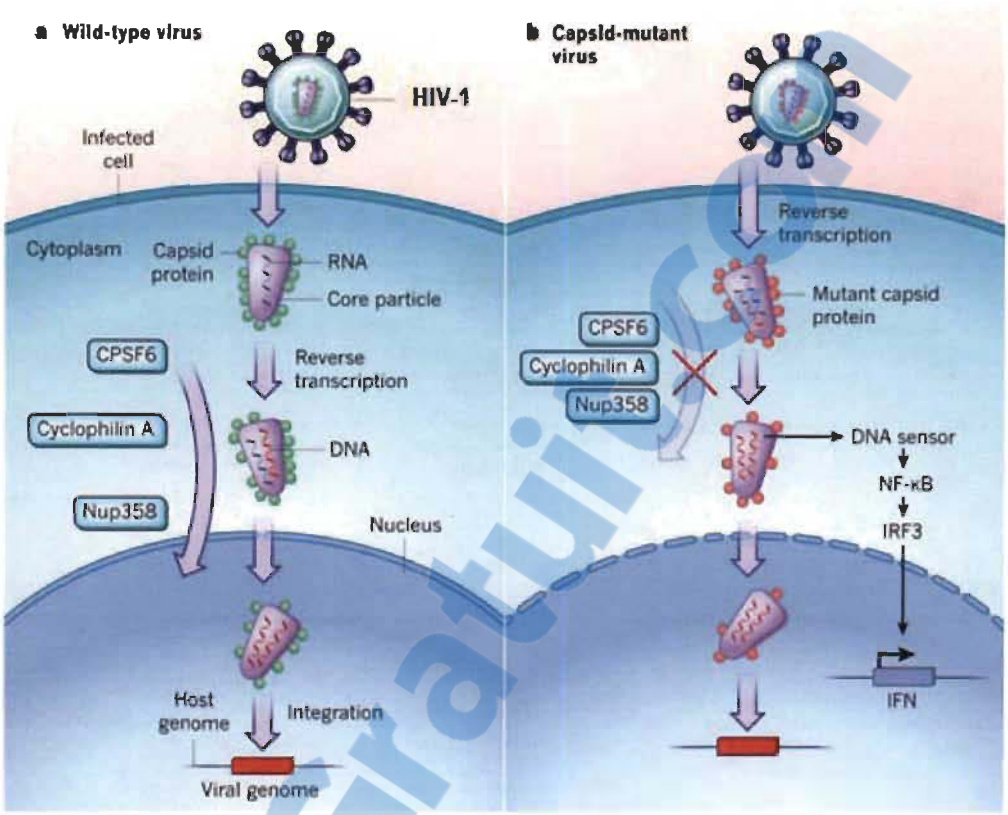

Figure 4.1 Retroviral evasion of immune detection.
a) Upon infection of macrophages, WT HIV-1 CA core interacts with host-cell proteins, including CPSF6, cyclophilin A and Nup358, which prevents the induction of IFN response. b) HIV-1 viruses carrying mutations in CA proteins that block the proteins' interactions with host proteins may traffic differently within the cell, and reverse transcription may occur prematurely, allowing recognition of viral DNA by host-cell sensors that induce a signaling pathway (involving the transcription factors NF-κB and IRF-3) leading to IFN production.
Image source: (Goff, 2013; Rasaiyaah *et al*, 2013).

4.2.1 Trafficking of HIV-1 and its uncoating

Microtubules and dynein motor complexes are thought to be involved in the transport of HIV-1 towards the nucleus and the results from the study in Chapter III suggest that these structures are also implicated in the uncoating of its CA core. It is thus probable that the transport of HIV-1 and its uncoating are linked. Importantly, uncoating might not be initiated during the transport of HIV-1 towards the nucleus, but only after this transport is complete. The association of the CA core with microtubules and dynein

complexes could even promote its stabilization. Recent reports have demonstrated that cellular components stabilize the post-entry HIV-1 CA core (Fricke *et al*, 2013; Guth & Sodroski, 2014), and uncoating might take place after the virus reaches the NPC (Ambrose & Aiken, 2014; Arhel *et al*, 2007; Rasaiyaah *et al*, 2013; Schaller *et al*, 2011). Many reports evidence that CA proteins must be present at these later stage, as they interact with Nup358 and Nup153 (Matreyek *et al*, 2013; Schaller *et al*, 2011), have a role in nuclear entry (Yamashita & Emerman, 2004; Yamashita *et al*, 2007) and are connected with integration site specificity (Schaller *et al*, 2011). It is possible that, similarly to CypA (Li *et al*, 2009; Shah *et al*, 2013), CPSF6 (Shah *et al*, 2013) and PDZD8 (Guth & Sodroski, 2014), dynein-dependent transport would promote stabilization of CA cores until they reach the NPC. The currently emerging hypothesis suggests that in the proximity of the NPC, CPSF6 and CypA would disassociate from the CA core, which would be transferred to Nup358 and Nup153, allowing for uncoating (Ambrose & Aiken, 2014; Rasaiyaah *et al*, 2013; Schaller *et al*, 2011; Shah *et al*, 2013). TNPO3 would have a role in sequestering CPSF6 and CypA (De Iaco *et al*, 2013; Shah *et al*, 2013). This hypothesis would be additionally supported by the fact that these proteins share the same CA-binding interface (Price *et al*, 2012).

The recently discovered PDZD8 protein is a moesin-interacting factor and a potential regulator of microtubule stability (Henning *et al*, 2010). This protein has been shown to stabilize the HIV-1 CA core (Guth & Sodroski, 2014). It is also possible that this protein could be involved in HIV-1 transport towards the nucleus. Interestingly, in neurons, a trimetric complex of PDZ proteins, mLin-2, mLin-7 and mLin-10, mediates binding of N-methyl-D-aspartate (NMDA) receptors to the kinesin family member 17 (KIF17) (Fig. 4.2) (Setou *et al*, 2000). Thus, maybe PDZD8 could take part in the HIV-1 CA core binding to the dynein motor complex?

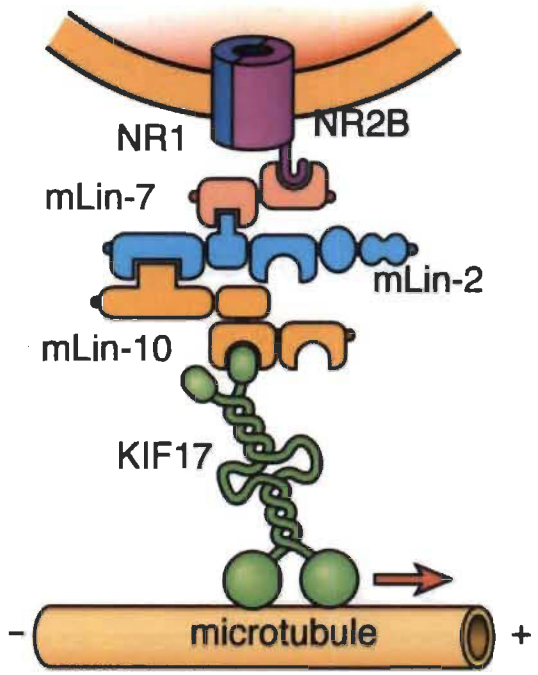

Figure 4.2 **Model of the NMDA receptor transporting machinery.**
NR1 and NR2B – subunits of NMDA (N-methyl-D-aspartate) receptor.
Image source: (Setou *et al*, 2000).

In conclusion, the relationship between HIV-1 uncoating and its transport to the nucleus remains unclear. Very likely they are linked, as the disruptions of microtubules and dynein motor complexes seem to affect uncoating. Additional experiments must be performed in order to outline a more precise model of how these structures are involved in HIV-1 uncoating.

4.2.2 Future experiments

In order to provide more conclusive answers referring to the involvement of microtubules and dynein motor complexes in HIV-1 uncoating a few additional experiments should be considered.

First, it would be very important to look at HIV-1 uncoating and infectivity in its natural cellular targets: macrophages, dendritic cells and lymphocytes. We might have missed an important consequence of microtubule and dynein disruptions on HIV-1

infectivity due to the employment of HeLa cells. Similarly, CA mutants N74D and P90A were thought not to impair HIV-1 infectivity until monocyte-derived macrophages (MDM) were used (Rasaiyaah *et al*, 2013).

Secondly, as actin microfilaments also have a role in HIV-1 transport (Arhel *et al*, 2006; McDonald *et al*, 2002; Yoder *et al*, 2011; Zamborlini *et al*, 2007) it would be important to look at HIV-1 uncoating upon disrupting these structures. There are many available pharmacological agents targeting actin filaments, such as cytochalasin D (Casella *et al*, 1981) or latrunculin B (Coue *et al*, 1987). It would be especially interesting in the case of T-cells as they do not have a robust microtubule cytoskeleton (Yoder *et al*, 2011) and it is possible that HIV-1 transport towards the nucleus might be more dependent on actin filaments. Additionally, simultaneous disruption of microtubule and actin filaments could be very interesting.

Furthermore, a possible effect of disrupting microtubules and dynein motor complexes on the fusion of the HIV-1 Env with the plasma membrane should be investigated. It is possible that interfering with the cytoskeleton might affect this step. These experiments might be especially significant, when VSV G-pseudotyped virions are used as they enter *via* endosomes which requires microtubules for their maturation (Lakadamyali *et al*, 2006).

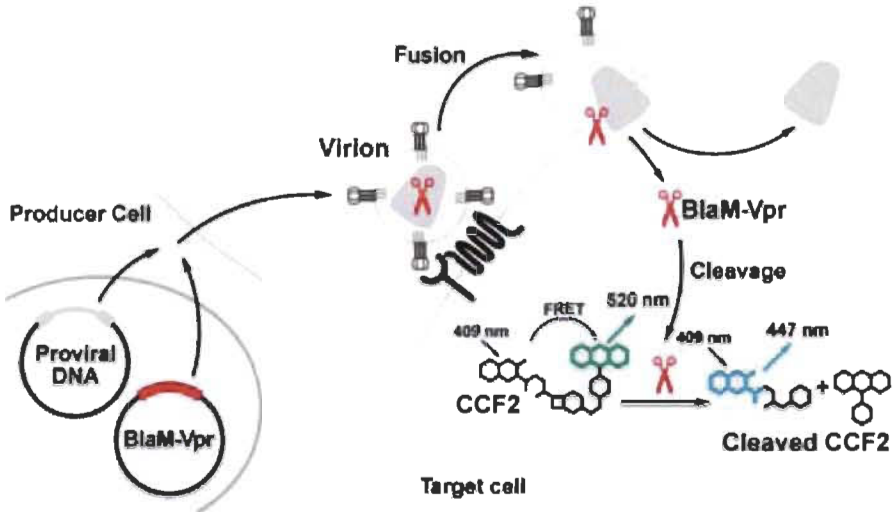

Figure 4.3 Schematic overview of viral fusion assay.
Producer cells are co-transfected with plasmids encoding HIV-1 provirus and β-lactamase-Vpr (BlaM-Vpr) chimera. Target cells are infected with BlaM-Vpr virions and then loaded with self-quenching CCF2/AM dye, which diffuses passively into cells. In the cell, excitation of the dye at 409 nm leads to fluorescent resonance energy transfer (FRET) producing green emission (520 nm). However, if β-lactam ring (green) is cleaved by BlaM, FRET is blocked and blue emission (447 nm) is detected. Cells can be discriminated by IF or FACS.
Image source: (Cavrois *et al*, 2002).

Already established assays would enable looking at fusion of the viral and plasma membranes (Cavrois *et al*, 2002; Smith *et al*, 2014), and an example of such an assay is shown in Fig. 4.3. In principle, a successful fusion is detected by a cleavage of a fluorescent dye localized in the cytoplasm by a β-lactamase enclosed inside an incoming virion.

An interesting insight in uncoating could be obtained through another approach, the 'CsA washout assay' (Fig. 4.4) (Hulme & Hope, 2014). This assay employs owl monkey cells (OMK) that endogenously express TRIMCyp. Normally, TRIMCyp binds the post-entry HIV-1 CA core and destabilizes it, resulting in loss of infectivity. When CsA is present, it binds TRIMCyp and prevents its activity against HIV-1. In theory, this assay should allow tracking uncoating by removing CsA at different times post infection; coated viral complexes are still restricted by TRIMCyp, while uncoated

particles are able to infect the cell. The advantage of this assay is that it detects only the cores that enter the cytoplasm.

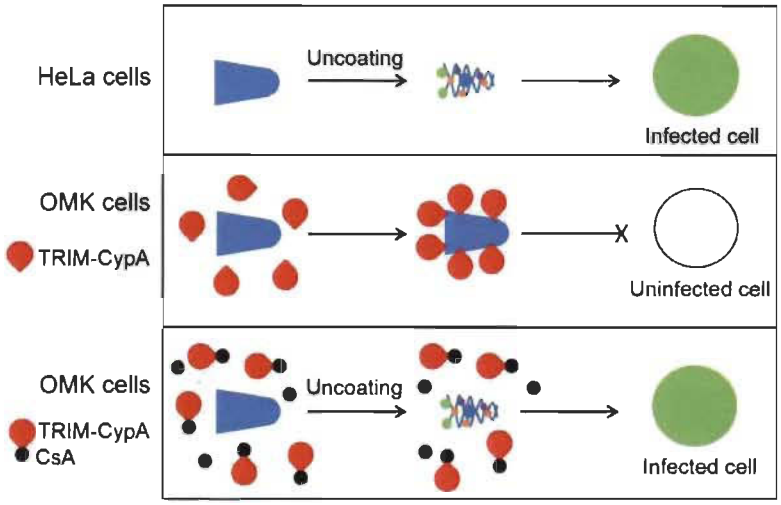

Figure 4.4 The principle of CsA washout assay.
HIV-1 uncoats and infects HeLa cells which can be detected by FACS. In owl monkey OMK cells TRIM-CypA (TRIMCyp) binds to the CA core and restricts HIV-1 infection (middle panel). HIV-1 can infect OMK cells in the presence of cyclosporine A (CsA) which binds TRIM-CypA and prevents its binding to the HIV-1 capsid (bottom panel).
Image source: (Hulme & Hope, 2014).

Moreover, while in the study presented in Chapter III the IF observations were performed with a virus bearing autologous HIV-1 Env, all subsequent fate-of-capsid experiments were performed with a VSV G-pseudotyped virus. It would be of extreme interest to perform these experiments with HIV-1 bearing its autologous Env. This, however, might cause certain difficulties as working with a replication-competent virus requires the use of minimum Biosafety Level II+ (BSLII+) facilities, which in the case of fate-of-capsid would have to contain all the necessary equipment, *e.g.* an ultracentrifuge. Alternatively, this kind of experiment could be done with a replication-impaired vector produced with in *trans* encoded HIV-1 Env. However it must be noted that viruses using HIV-1 Env for their entry have significantly lower infectivity yield than those pseudotyped with VSV G. To our knowledge all published fate-of-capsid assays were done with VSV G-pseudotyped vectors.

Finally, in the future it would also be of interest to try to determine how HIV-1 interacts with the dynein motor complex - whether this is a direct or indirect interaction, through adaptor complexes. If HIV-1 interacts directly with the dynein motor complex it would be important to characterize the nature of this interaction, *e.g.* which chain of the dynein motor interacts with which HIV-1 protein. Although HIV-1 CA appears to be a valid candidate for this interaction, some preliminary results presented last year at the 9th International Retroviral Nucleocapsid Protein and Assembly Symposium in Montreal by Yao *et al.* indicated that HIV-1 might associate with dynein light chain 1 (LC8- type 1) *via* integrase (Yao *et al*, 2013).

4.3 Perspectives: Gene therapy targeting HIV-1 using TRIM5α

The case of the Berlin patient (described in the section 1.1.3) provided a proof-of-concept of the possibility that replacing the patient's cells permissive to HIV-1 with cells resistant to it can result in a sterilizing cure. Recently, the first clinical trial studying an autologous T-cell transplant, with *ex vivo* disrupted *CCR5* genes, was completed, proving the safety of that approach, though with a moderate efficacy (Tebas *et al*, 2014). The patients, following the infusion of modified cells, were subjected to a cessation of antiretroviral therapy, and while none of them was able to control the virus, the modified T-cells had longer survival times when compared with the autologous ones (Tebas *et al*, 2014). TRIM5α is thought to be a great candidate for gene therapy aimed at treating HIV-1 infection (Anderson, 2013). It could be accomplished by modifying the existing human *TRIM5* gene (Pham *et al*, 2010; Yap *et al*, 2005) or introducing a human version of TRIMCyp (Neagu *et al*, 2009).

4.4 Perspectives: development of new classes of drugs

Some small molecules, *e.g.* PF-3450074 (PF74) were shown to destabilize the post-entry HIV-1 CA core inhibiting HIV-1 infectivity (Blair *et al*, 2010; Shi *et al*, 2011). Other molecules binding to the same CA site, BI-1 and BI-2, that *in vitro* stabilized CA-NC tubes also inhibited HIV-1 infectivity (Lamorte *et al*, 2013). The

effects of these drugs on HIV-1 replication confirmed that uncoating can be a new area of investigation for antiviral therapeutics targeting HIV-1. Uncoating remains one of the least explored aspects of HIV-1 replication, thus it is important to obtain more detailed knowledge about this process.

4.5 Final conclusions

The studies presented in this thesis offer novel and important input into the field of HIV-1 pathogen-host interaction. This research contributes to the state of knowledge about the replication of HIV-1 and the mechanism of action of the restriction factor TRIM5α. Hopefully, these studies will contribute to future development of new approaches to treat HIV-1 infection.

REFERENCES

Abram ME, Ferris AL, Shao W, Alvord WG, Hughes SH (2010) Nature, position, and frequency of mutations made in a single cycle of HIV-1 replication. *Journal of virology* 84: 9864-9878

Aiken C, Konner J, Landau NR, Lenburg ME, Trono D (1994) Nef induces CD4 endocytosis: requirement for a critical dileucine motif in the membrane-proximal CD4 cytoplasmic domain. *Cell* 76: 853-864

Akira S, Uematsu S, Takeuchi O (2006) Pathogen recognition and innate immunity. *Cell* 124: 783-801

Alberts B (2002) *Molecular biology of the cell*, 4th ed. New York: Garland Science.

Alkhatib G, Combadiere C, Broder CC, Feng Y, Kennedy PE, Murphy PM, Berger EA (1996) CC CKR5: a RANTES, MIP-1alpha, MIP-1beta receptor as a fusion cofactor for macrophage-tropic HIV-1. *Science* 272: 1955-1958

Ambrose JC, Li W, Marcus A, Ma H, Cyr R (2005) A minus-end-directed kinesin with plus-end tracking protein activity is involved in spindle morphogenesis. *Molecular biology of the cell* 16: 1584-1592

Ambrose Z, Aiken C (2014) HIV-1 uncoating: connection to nuclear entry and regulation by host proteins. *Virology*

Anderson JL, Campbell EM, Wu X, Vandegraaff N, Engelman A, Hope TJ (2006) Proteasome inhibition reveals that a functional preintegration complex intermediate can be generated during restriction by diverse TRIM5 proteins. *Journal of virology* 80: 9754-9760

Anderson JS (2013) Using TRIM5alpha as an HIV therapeutic: the alpha gene? *Expert Opinion on Biological Therapy*13: 1029-1038

Anglemyer A, Rutherford GW, Baggaley RC, Egger M, Siegfried N (2011) Antiretroviral therapy for prevention of HIV transmission in HIV-discordant couples. *The Cochrane database of systematic reviews*: CD009153

Arhel N (2010) Revisiting HIV-1 uncoating. *Retrovirology* 7: 96

Arhel N, Genovesio A, Kim KA, Miko S, Perret E, Olivo-Marin JC, Shorte S, Charneau P (2006) Quantitative four-dimensional tracking of cytoplasmic and nuclear HIV-1 complexes. *Nature methods* 3: 817-824

Arhel NJ, Souquere-Besse S, Munier S, Souque P, Guadagnini S, Rutherford S, Prevost MC, Allen TD, Charneau P (2007) HIV-1 DNA Flap formation promotes uncoating of the pre-integration complex at the nuclear pore. *The European Molecular Biology Organization journal* 26: 3025-3037

Asaoka K, Ikeda K, Hishinuma T, Horie-Inoue K, Takeda S, Inoue S (2005) A retrovirus restriction factor TRIM5alpha is transcriptionally regulated by interferons. *Biochemical and biophysical research communications* 338: 1950-1956

Auvert B, Taljaard D, Lagarde E, Sobngwi-Tambekou J, Sitta R, Puren A (2005) Randomized, controlled intervention trial of male circumcision for reduction of HIV infection risk: the ANRS 1265 Trial. *PLoS medicine* 2: e298

Barre-Sinoussi F, Chermann JC, Rey F, Nugeyre MT, Chamaret S, Gruest J, Dauguet C, Axler-Blin C, Vezinet-Brun F, Rouzioux C, Rozenbaum W, Montagnier L (1983) Isolation of a T-lymphotropic retrovirus from a patient at risk for acquired immune deficiency syndrome (AIDS). *Science* 220: 868-871

Batonick M, Favre M, Boge M, Spearman P, Honing S, Thali M (2005) Interaction of HIV-1 Gag with the clathrin-associated adaptor AP-2. *Virology* 342: 190-200

Bérubé J, Bouchard A, Berthoux L (2007) Both TRIM5alpha and TRIMCyp have only weak antiviral activity in canine D17 cells. *Retrovirology* 4: 68

Biris N, Tomashevski A, Bhattacharya A, Diaz-Griffero F, Ivanov DN (2013) Rhesus monkey TRIM5alpha SPRY domain recognizes multiple epitopes that span several capsid monomers on the surface of the HIV-1 mature viral core. *Journal of molecular biology* 425: 5032-5044

Biris N, Yang Y, Taylor AB, Tomashevski A, Guo M, Hart PJ, Diaz-Griffero F, Ivanov DN (2012) Structure of the rhesus monkey TRIM5alpha PRYSPRY domain, the HIV capsid recognition module. *Proceedings of the National Academy of Sciences of the United States of America* 109: 13278-13283

Blair WS, Pickford C, Irving SL, Brown DG, Anderson M, Bazin R, Cao J, Ciaramella G, Isaacson J, Jackson L, Hunt R, Kjerrstrom A, Nieman JA, Patick AK, Perros M, Scott AD, Whitby K, Wu H, Butler SL (2010) HIV capsid is a tractable target for small molecule therapeutic intervention. *PLoS Pathogens* 6: e1001220

Bouchard P, Penningroth SM, Cheung A, Gagnon C, Bardin CW (1981) erythro-9-[3-(2-Hydroxynonyl)]adenine is an inhibitor of sperm motility that blocks dynein ATPase and protein carboxylmethylase activities. *Proceedings of the National Academy of Sciences of the United States of America* 78: 1033-1036

Bre MH, Kreis TE, Karsenti E (1987) Control of microtubule nucleation and stability in Madin-Darby canine kidney cells: the occurrence of noncentrosomal, stable detyrosinated microtubules. *The Journal of cell biology* 105: 1283-1296

Brier S, Lemaire D, Debonis S, Forest E, Kozielski F (2004) Identification of the protein binding region of S-trityl-L-cysteine, a new potent inhibitor of the mitotic kinesin Eg5. *Biochemistry* 43: 13072-13082

Briggs JA, Simon MN, Gross I, Krausslich HG, Fuller SD, Vogt VM, Johnson MC (2004) The stoichiometry of Gag protein in HIV-1. *Nature Structural & Molecular Biology* 11: 672-675

Briggs JA, Wilk T, Welker R, Krausslich HG, Fuller SD (2003) Structural organization of authentic, mature HIV-1 virions and cores. *The European Molecular Biology Organization journal* 22: 1707-1715

Bukrinskaya A, Brichacek B, Mann A, Stevenson M (1998) Establishment of a functional human immunodeficiency virus type 1 (HIV-1) reverse transcription complex involves the cytoskeleton. *Journal of Experimental Medicine* 188: 2113-2125

Bukrinsky MI, Sharova N, McDonald TL, Pushkarskaya T, Tarpley WG, Stevenson M (1993) Association of integrase, matrix, and reverse transcriptase antigens of human immunodeficiency virus type 1 with viral nucleic acids following acute infection. *Proceedings of the National Academy of Sciences of the United States of America* 90: 6125-6129

Burkhardt JK, Echeverri CJ, Nilsson T, Vallee RB (1997) Overexpression of the dynamitin (p50) subunit of the dynactin complex disrupts dynein-dependent maintenance of membrane organelle distribution. *The Journal of cell biology* 139: 469-484

Busnadiego I, Kane M, Rihn SJ, Preugschas HF, Hughes J, Blanco-Melo D, Strouvelle VP, Zang TM, Willett BJ, Boutell C, Bieniasz PD, Wilson SJ (2014) Host and viral determinants of Mx2 antiretroviral activity. *Journal of virology* 88: 7738-7752

Buss F, Kendrick-Jones J (2008) How are the cellular functions of myosin VI regulated within the cell? *Biochemical and biophysical research communications* 369: 165-175

Campbell EM, Dodding MP, Yap MW, Wu X, Gallois-Montbrun S, Malim MH, Stoye JP, Hope TJ (2007a) TRIM5 alpha cytoplasmic bodies are highly dynamic structures. *Molecular biology of the cell* 18: 2102-2111

Campbell EM, Perez O, Anderson JL, Hope TJ (2008) Visualization of a proteasome-independent intermediate during restriction of HIV-1 by rhesus TRIM5alpha. *The Journal of cell biology* 180: 549-561

Campbell EM, Perez O, Melar M, Hope TJ (2007b) Labeling HIV-1 virions with two fluorescent proteins allows identification of virions that have productively entered the target cell. *Virology* 360: 286-293

Camus G, Segura-Morales C, Molle D, Lopez-Verges S, Begon-Pescia C, Cazevieille C, Schu P, Bertrand E, Berlioz-Torrent C, Basyuk E (2007) The clathrin adaptor complex AP-1 binds HIV-1 and MLV Gag and facilitates their budding. *Molecular biology of the cell* 18: 3193-3203

Cantalupo G, Alifano P, Roberti V, Bruni CB, Bucci C (2001) Rab-interacting lysosomal protein (RILP): the Rab7 effector required for transport to lysosomes. *The European Molecular Biology Organization journal* 20: 683-693

Cardo DM, Culver DH, Ciesielski CA, Srivastava PU, Marcus R, Abiteboul D, Heptonstall J, Ippolito G, Lot F, McKibben PS, Bell DM (1997) A case-control study of HIV seroconversion in health care workers after percutaneous exposure. Centers for Disease Control and Prevention Needlestick Surveillance Group. *The New England journal of medicine* 337: 1485-1490

Casella JF, Flanagan MD, Lin S (1981) Cytochalasin D inhibits actin polymerization and induces depolymerization of actin filaments formed during platelet shape change. *Nature* 293: 302-305

Cavrois M, De Noronha C, Greene WC (2002) A sensitive and specific enzyme-based assay detecting HIV-1 virion fusion in primary T lymphocytes. *Nature Biotechnology* 20: 1151-1154

CDC (1981) Pneumocystis pneumonia–Los Angeles. *Morbidity and Mortality Weekly Report* 30: 250-252

CDC (1982) Update on acquired immune deficiency syndrome (AIDS). *Morbidity and Mortality Weekly Report* 31: 507-514

Chelbi-Alix MK, Quignon F, Pelicano L, Koken MH, de The H (1998) Resistance to virus infection conferred by the interferon-induced promyelocytic leukemia protein. *Journal of virology* 72: 1043-1051

Chun TW, Engel D, Berrey MM, Shea T, Corey L, Fauci AS (1998) Early establishment of a pool of latently infected, resting CD4(+) T cells during primary HIV-1 infection. *Proceedings of the National Academy of Sciences of the United States of America* 95: 8869-8873

Clavel F, Guetard D, Brun-Vezinet F, Chamaret S, Rey MA, Santos-Ferreira MO, Laurent AG, Dauguet C, Katlama C, Rouzioux C, *et al.* (1986) Isolation of a new human retrovirus from West African patients with AIDS. *Science* 233: 343-346

Clavel F, Mansinho K, Chamaret S, Guetard D, Favier V, Nina J, Santos-Ferreira MO, Champalimaud JL, Montagnier L (1987) Human immunodeficiency virus type 2 infection associated with AIDS in West Africa. *The New England journal of medicine* 316: 1180-1185

Coffin JM, Hughes SH, Varmus H (1997) *Retroviruses*, Plainview, N.Y.: Cold Spring Harbor Laboratory Press.

Cohen J (2013) HIV/AIDS. Early treatment may have cured infant of HIV infection. *Science* 339: 1134

Cohen S, Au S, Pante N (2011) How viruses access the nucleus. *Biochimica et biophysica acta* 1813: 1634-1645

Coue M, Brenner SL, Spector I, Korn ED (1987) Inhibition of actin polymerization by latrunculin A. *Federation of European Biochemical Societies letters* 213: 316-318

Dalgleish AG, Beverley PC, Clapham PR, Crawford DH, Greaves MF, Weiss RA (1984) The CD4 (T4) antigen is an essential component of the receptor for the AIDS retrovirus. *Nature* 312: 763-767

Daniel R, Marusich E, Argyris E, Zhao RY, Skalka AM, Pomerantz RJ (2005) Caffeine inhibits human immunodeficiency virus type 1 transduction of nondividing cells. *Journal of virology* 79: 2058-2065

Danielson CM, Cianci GC, Hope TJ (2012) Recruitment and dynamics of proteasome association with rhTRIM5alpha cytoplasmic complexes during HIV-1 infection. *Traffic* 13: 1206-1217

De Cock KM, Adjorlolo G, Ekpini E, Sibailly T, Kouadio J, Maran M, Brattegaard K, Vetter KM, Doorly R, Gayle HD (1993) Epidemiology and transmission of HIV-2. Why there is no HIV-2 pandemic. *Jama* 270: 2083-2086

De Cock KM, Fowler MG, Mercier E, de Vincenzi I, Saba J, Hoff E, Alnwick DJ, Rogers M, Shaffer N (2000) Prevention of mother-to-child HIV transmission in resource-poor countries: translating research into policy and practice. *Jama* 283: 1175-1182

de Forges H, Bouissou A, Perez F (2012) Interplay between microtubule dynamics and intracellular organization. *The international journal of biochemistry & cell biology* 44: 266-274

De Iaco A, Santoni F, Vannier A, Guipponi M, Antonarakis S, Luban J (2013) TNPO3 protects HIV-1 replication from CPSF6-mediated capsid stabilization in the host cell cytoplasm. *Retrovirology* 10: 20

Deacon SW, Serpinskaya AS, Vaughan PS, Lopez Fanarraga M, Vernos I, Vaughan KT, Gelfand VI (2003) Dynactin is required for bidirectional organelle transport. *The Journal of cell biology* 160: 297-301

Decroly E, Vandenbranden M, Ruysschaert JM, Cogniaux J, Jacob GS, Howard SC, Marshall G, Kompelli A, Basak A, Jean F, *et al.* (1994) The convertases furin and PC1 can both cleave the human immunodeficiency virus (HIV)-1 envelope glycoprotein gp160 into gp120 (HIV-1 SU) and gp41 (HIV-I TM). *The Journal of biological chemistry* 269: 12240-12247

Decroly E, Wouters S, Di Bello C, Lazure C, Ruysschaert JM, Seidah NG (1996) Identification of the paired basic convertases implicated in HIV gp160 processing based on in vitro assays and expression in CD4(+) cell lines. *The Journal of biological chemistry* 271: 30442-30450

Deng H, Liu R, Ellmeier W, Choe S, Unutmaz D, Burkhart M, Di Marzio P, Marmon S, Sutton RE, Hill CM, Davis CB, Peiper SC, Schall TJ, Littman DR, Landau NR (1996) Identification of a major co-receptor for primary isolates of HIV-1. *Nature* 381: 661-666

Derry WB, Wilson L, Jordan MA (1995) Substoichiometric binding of taxol suppresses microtubule dynamics. *Biochemistry* 34: 2203-2211

Di Nunzio F, Danckaert A, Fricke T, Perez P, Fernandez J, Perret E, Roux P, Shorte S, Charneau P, Diaz-Griffero F, Arhel NJ (2012) Human nucleoporins promote HIV-1 docking at the nuclear pore, nuclear import and integration. *PloS one* 7: e46037

Diaz-Griffero F, Gallo DE, Hope TJ, Sodroski J (2011) Trafficking of some old world primate TRIM5alpha proteins through the nucleus. *Retrovirology* 8: 38

Diaz-Griffero F, Kar A, Lee M, Stremlau M, Poeschla E, Sodroski J (2007a) Comparative requirements for the restriction of retrovirus infection by TRIM5alpha and TRIMCyp. *Virology* 369: 400-410

Diaz-Griffero F, Kar A, Perron M, Xiang SH, Javanbakht H, Li X, Sodroski J (2007b) Modulation of retroviral restriction and proteasome inhibitor-resistant turnover by changes in the TRIM5alpha B-box 2 domain. *Journal of virology* 81: 10362-10378

Diaz-Griffero F, Li X, Javanbakht H, Song B, Welikala S, Stremlau M, Sodroski J (2006) Rapid turnover and polyubiquitylation of the retroviral restriction factor TRIM5. *Virology* 349: 300-315

Diaz-Griffero F, Qin XR, Hayashi F, Kigawa T, Finzi A, Sarnak Z, Lienlaf M, Yokoyama S, Sodroski J (2009) A B-box 2 surface patch important for TRIM5alpha self-association, capsid binding avidity, and retrovirus restriction. *Journal of virology* 83: 10737-10751

Dismuke DJ, Aiken C (2006) Evidence for a functional link between uncoating of the human immunodeficiency virus type 1 core and nuclear import of the viral preintegration complex. *Journal of virology* 80: 3712-3720

Dodding MP, Way M (2011) Coupling viruses to dynein and kinesin-1. *The European Molecular Biology Organization journal* 30: 3527-3539

Dong X, Li H, Derdowski A, Ding L, Burnett A, Chen X, Peters TR, Dermody TS, Woodruff E, Wang JJ, Spearman P (2005) AP-3 directs the intracellular trafficking of HIV-1 Gag and plays a key role in particle assembly. *Cell* 120: 663-674

Dragic T, Litwin V, Allaway GP, Martin SR, Huang Y, Nagashima KA, Cayanan C, Maddon PJ, Koup RA, Moore JP, Paxton WA (1996) HIV-1 entry into CD4+ cells is mediated by the chemokine receptor CC-CKR-5. *Nature* 381: 667-673

Ellis RJ (2001) Macromolecular crowding: an important but neglected aspect of the intracellular environment. *Current opinion in structural biology* 11: 114-119

Farnet CM, Haseltine WA (1991) Determination of viral proteins present in the human immunodeficiency virus type 1 preintegration complex. *Journal of virology* 65: 1910-1915

Feng Y, Broder CC, Kennedy PE, Berger EA (1996) HIV-1 entry cofactor: functional cDNA cloning of a seven-transmembrane, G protein-coupled receptor. *Science* 272: 872-877

Finzi A, Orthwein A, Mercier J, Cohen EA (2007) Productive human immunodeficiency virus type 1 assembly takes place at the plasma membrane. *Journal of virology* 81: 7476-7490

Firestone AJ, Weinger JS, Maldonado M, Barlan K, Langston LD, O'Donnell M, Gelfand VI, Kapoor TM, Chen JK (2012) Small-molecule inhibitors of the AAA+ ATPase motor cytoplasmic dynein. *Nature* 484: 125-129

Flepp M, Schiffer V, Weber R, Hirschel B (2001) Modern anti-HIV therapy. *Swiss medical weekly* 131: 207-213

Forshey BM, von Schwedler U, Sundquist WI, Aiken C (2002) Formation of a human immunodeficiency virus type 1 core of optimal stability is crucial for viral replication. *Journal of virology* 76: 5667-5677

Foth BJ, Goedecke MC, Soldati D (2006) New insights into myosin evolution and classification. *Proceedings of the National Academy of Sciences of the United States of America* 103: 3681-3686

Freed EO (1998) HIV-1 gag proteins: diverse functions in the virus life cycle. *Virology* 251: 1-15

Fricke T, Brandariz-Nunez A, Wang X, Smith AB, 3rd, Diaz-Griffero F (2013) Human cytosolic extracts stabilize the HIV-1 core. *Journal of virology* 87: 10587-10597

Fricke T, White TE, Schulte B, de Souza Aranha Vieira DA, Dharan A, Campbell EM, Brandariz-Nunez A, Diaz-Griffero F (2014) MxB binds to the HIV-1 core and prevents the uncoating process of HIV-1. *Retrovirology* 11: 68

Friedman-Kien AE (1981) Disseminated Kaposi's sarcoma syndrome in young homosexual men. *Journal of the American Academy of Dermatology* 5: 468-471

Friedman JR, Webster BM, Mastronarde DN, Verhey KJ, Voeltz GK (2010) ER sliding dynamics and ER-mitochondrial contacts occur on acetylated microtubules. *The Journal of cell biology* 190: 363-375

Fu W, Rein A (1993) Maturation of dimeric viral RNA of Moloney murine leukemia virus. *Journal of virology* 67: 5443-5449

Gack MU, Shin YC, Joo CH, Urano T, Liang C, Sun L, Takeuchi O, Akira S, Chen Z, Inoue S, Jung JU (2007) TRIM25 RING-finger E3 ubiquitin ligase is essential for RIG-I-mediated antiviral activity. *Nature* 446: 916-920

Gallo RC, Salahuddin SZ, Popovic M, Shearer GM, Kaplan M, Haynes BF, Palker TJ, Redfield R, Oleske J, Safai B, *et al.* (1984) Frequent detection and isolation of cytopathic retroviruses (HTLV-III) from patients with AIDS and at risk for AIDS. *Science* 224: 500-503

Gamble TR, Yoo S, Vajdos FF, von Schwedler UK, Worthylake DK, Wang H, McCutcheon JP, Sundquist WI, Hill CP (1997) Structure of the carboxyl-terminal dimerization domain of the HIV-1 capsid protein. *Science* 278: 849-853

Ganser-Pornillos BK, Chandrasekaran V, Pornillos O, Sodroski JG, Sundquist WI, Yeager M (2011) Hexagonal assembly of a restricting TRIM5alpha protein. *Proceedings of the National Academy of Sciences of the United States of America* 108: 534-539

Gaudin R, Alencar BC, Arhel N, Benaroch P (2013) HIV trafficking in host cells: motors wanted! *Trends in cell biology* 23: 652-662

Gennerich A, Vale RD (2009) Walking the walk: how kinesin and dynein coordinate their steps. *Current opinion in cell biology* 21: 59-67

Gigant B, Wang C, Ravelli RB, Roussi F, Steinmetz MO, Curmi PA, Sobel A, Knossow M (2005) Structural basis for the regulation of tubulin by vinblastine. *Nature* 435: 519-522

Goff SP (2013) HIV: Slipping under the radar. *Nature* 503: 352-353

Goldstone DC, Ennis-Adeniran V, Hedden JJ, Groom HC, Rice GI, Christodoulou E, Walker PA, Kelly G, Haire LF, Yap MW, de Carvalho LP, Stoye JP, Crow YJ, Taylor IA, Webb M (2011) HIV-1 restriction factor SAMHD1 is a deoxynucleoside triphosphate triphosphohydrolase. *Nature* 480: 379-382

Goldstone DC, Walker PA, Calder LJ, Coombs PJ, Kirkpatrick J, Ball NJ, Hilditch L, Yap MW, Rosenthal PB, Stoye JP, Taylor IA (2014) Structural studies of postentry restriction factors reveal antiparallel dimers that enable avid binding to the HIV-1 capsid lattice. *Proceedings of the National Academy of Sciences of the United States of America* 111: 9609-9614

Gottlieb MS (2006) Pneumocystis pneumonia--Los Angeles. 1981. *American journal of public health* 96: 980-981; discussion 982-983

Goujon C, Moncorge O, Bauby H, Doyle T, Ward CC, Schaller T, Hue S, Barclay WS, Schulz R, Malim MH (2013) Human MX2 is an interferon-induced post-entry inhibitor of HIV-1 infection. *Nature* 502: 559-562

Gouveia SM, Akhmanova A (2010) Cell and molecular biology of microtubule plus end tracking proteins: end binding proteins and their partners. *International review of cell and molecular biology* 285: 1-74

Greene WC, Peterlin BM (2002) Charting HIV's remarkable voyage through the cell: Basic science as a passport to future therapy. *Nature Medicine* 8: 673-680

Gross SP (2004) Hither and yon: a review of bi-directional microtubule-based transport. *Physical biology* 1: R1-11

Guth CA, Sodroski J (2014) Contribution of PDZD8 to Stabilization of the Human Immunodeficiency Virus (HIV-1) Capsid. *Journal of virology*

Hallett TB, Alsallaq RA, Baeten JM, Weiss H, Celum C, Gray R, Abu-Raddad L (2011) Will circumcision provide even more protection from HIV to women and men? New estimates of the population impact of circumcision interventions. *Sexually transmitted infections* 87: 88-93

Han K, Lou DI, Sawyer SL (2011) Identification of a genomic reservoir for new TRIM genes in primate genomes. *PLoS genetics* 7: e1002388

Harris RS, Hultquist JF, Evans DT (2012) The restriction factors of human immunodeficiency virus. *The Journal of biological chemistry* 287: 40875-40883

Hatziioannou T, Perez-Caballero D, Yang A, Cowan S, Bieniasz PD (2004) Retrovirus resistance factors Ref1 and Lv1 are species-specific variants of TRIM5alpha. *Proceedings of the National Academy of Sciences of the United States of America* 101: 10774-10779

Hauler F, Mallery DL, McEwan WA, Bidgood SR, James LC (2012) AAA ATPase p97/VCP is essential for TRIM21-mediated virus neutralization. *Proceedings of the National Academy of Sciences of the United States of America* 109: 19733-19738

He Y, Francis F, Myers KA, Yu W, Black MM, Baas PW (2005) Role of cytoplasmic dynein in the axonal transport of microtubules and neurofilaments. *The Journal of cell biology* 168: 697-703

Hendricks AG, Lazarus JE, Perlson E, Gardner MK, Odde DJ, Goldman YE, Holzbaur EL (2012) Dynein tethers and stabilizes dynamic microtubule plus ends. *Current Biology* 22: 632-637

Hendricks AG, Perlson E, Ross JL, Schroeder HW, 3rd, Tokito M, Holzbaur EL (2010) Motor coordination via a tug-of-war mechanism drives bidirectional vesicle transport. *Current Biology* 20: 697-702

Henning MS, Morham SG, Goff SP, Naghavi MH (2010) PDZD8 is a novel Gag-interacting factor that promotes retroviral infection. *Journal of virology* 84: 8990-8995

Hewitt L, Tighe A, Santaguida S, White AM, Jones CD, Musacchio A, Green S, Taylor SS (2010) Sustained Mps1 activity is required in mitosis to recruit O-Mad2 to the Mad1-C-Mad2 core complex. *The Journal of cell biology* 190: 25-34

Hirokawa N, Noda Y, Tanaka Y, Niwa S (2009) Kinesin superfamily motor proteins and intracellular transport. *Nature Reviews Molecular Cell Biology* 10: 682-696

Hrecka K, Hao C, Gierszewska M, Swanson SK, Kesik-Brodacka M, Srivastava S, Florens L, Washburn MP, Skowronski J (2011) Vpx relieves inhibition of HIV-1 infection of macrophages mediated by the SAMHD1 protein. *Nature* 474: 658-661

Huang CJ, Huang CC, Chang CC (2012) Association of the testis-specific TRIM/RBCC protein RNF33/TRIM60 with the cytoplasmic motor proteins KIF3A and KIF3B. *Molecular Cell Biochemistry* 360: 121-131

Hulme AE, Hope TJ (2014) The cyclosporin A washout assay to detect HIV-1 uncoating in infected cells. *Methods Molecular Biology* 1087: 37-46

Hulme AE, Perez O, Hope TJ (2011) Complementary assays reveal a relationship between HIV-1 uncoating and reverse transcription. *Proceedings of the National Academy of Sciences of the United States of America* 108: 9975-9980

Hutter G, Nowak D, Mossner M, Ganepola S, Mussig A, Allers K, Schneider T, Hofmann J, Kucherer C, Blau O, Blau IW, Hofmann WK, Thiel E (2009) Long-term control of HIV by CCR5 Delta32/Delta32 stem-cell transplantation. *The New England journal of medicine* 360: 692-698

Hutter G, Thiel E (2011) Allogeneic transplantation of CCR5-deficient progenitor cells in a patient with HIV infection: an update after 3 years and the search for patient no. 2. *AIDS* 25: 273-274

Hymes KB, Cheung T, Greene JB, Prose NS, Marcus A, Ballard H, William DC, Laubenstein LJ (1981) Kaposi's sarcoma in homosexual men-a report of eight cases. *Lancet* 2: 598-600

Imamula K, Kon T, Ohkura R, Sutoh K (2007) The coordination of cyclic microtubule association/dissociation and tail swing of cytoplasmic dynein. *Proceedings of the National Academy of Sciences of the United States of America* 104: 16134-16139

Iyengar S, Hildreth JE, Schwartz DH (1998) Actin-dependent receptor colocalization required for human immunodeficiency virus entry into host cells. *Journal of virology* 72: 5251-5255

Janeway C (2001) *Immunobiology 5 : the immune system in health and disease*, 5th edn. New York: Garland Pub.

Javanbakht H, Diaz-Griffero F, Stremlau M, Si Z, Sodroski J (2005) The contribution of RING and B-box 2 domains to retroviral restriction mediated by monkey TRIM5alpha. *The Journal of biological chemistry* 280: 26933-26940

Jones JD, Dangl JL (2006) The plant immune system. *Nature* 444: 323-329

Jordan A, Bisgrove D, Verdin E (2003) HIV reproducibly establishes a latent infection after acute infection of T cells in vitro. *The European Molecular Biology Organization journal* 22: 1868-1877

Kajaste-Rudnitski A, Marelli SS, Pultrone C, Pertel T, Uchil PD, Mechti N, Mothes W, Poli G, Luban J, Vicenzi E (2011) TRIM22 inhibits HIV-1 transcription independently of its E3 ubiquitin ligase activity, Tat, and NF-kappaB-responsive long terminal repeat elements. *Journal of virology* 85: 5183-5196

Kane M, Yadav SS, Bitzegeio J, Kutluay SB, Zang T, Wilson SJ, Schoggins JW, Rice CM, Yamashita M, Hatziioannou T, Bieniasz PD (2013) MX2 is an interferon-induced inhibitor of HIV-1 infection. *Nature* 502: 563-566

Kao SY, Calman AF, Luciw PA, Peterlin BM (1987) Anti-termination of transcription within the long terminal repeat of HIV-1 by tat gene product. *Nature* 330: 489-493

Kapoor TM, Mitchison TJ (1999) Allele-specific activators and inhibitors for kinesin. *Proceedings of the National Academy of Sciences of the United States of America* 96: 9106-9111

Kar AK, Diaz-Griffero F, Li Y, Li X, Sodroski J (2008) Biochemical and biophysical characterization of a chimeric TRIM21-TRIM5alpha protein. *Journal of virology* 82: 11669-11681

Karageorgos L, Li P, Burrell C (1993) Characterization of HIV replication complexes early after cell-to-cell infection. *AIDS research and human retroviruses* 9: 817-823

Kardon JR, Vale RD (2009) Regulators of the cytoplasmic dynein motor. *Nature Reviews Molecular Cell Biology* 10: 854-865

Kawaguchi K, Ishiwata S (2001) Nucleotide-dependent single- to double-headed binding of kinesin. *Science* 291: 667-669

Keckesova Z, Ylinen LM, Towers GJ (2004) The human and African green monkey TRIM5alpha genes encode Ref1 and Lv1 retroviral restriction factor activities. *Proceedings of the National Academy of Sciences of the United States of America* 101: 10780-10785

Kimpton J, Emerman M (1992) Detection of replication-competent and pseudotyped human immunodeficiency virus with a sensitive cell line on the basis of activation of an integrated beta-galactosidase gene. *Journal of virology* 66: 2232-2239

Kirschner M, Mitchison T (1986) Beyond self-assembly: from microtubules to morphogenesis. *Cell* 45: 329-342

Klatzmann D, Barre-Sinoussi F, Nugeyre MT, Danquet C, Vilmer E, Griscelli C, Brun-Veziret F, Rouzioux C, Gluckman JC, Chermann JC, *et al.* (1984a) Selective tropism of lymphadenopathy associated virus (LAV) for helper-inducer T lymphocytes. *Science* 225: 59-63

Klatzmann D, Champagne E, Chamaret S, Gruest J, Guetard D, Hercend T, Gluckman JC, Montagnier L (1984b) T-lymphocyte T4 molecule behaves as the receptor for human retrovirus LAV. *Nature* 312: 767-768

Kogan M, Rappaport J (2011) HIV-1 accessory protein Vpr: relevance in the pathogenesis of HIV and potential for therapeutic intervention. *Retrovirology* 8: 25

Komarova Y, De Groot CO, Grigoriev I, Gouveia SM, Munteanu EL, Schober JM, Honnappa S, Buey RM, Hoogenraad CC, Dogterom M, Borisy GG, Steinmetz MO, Akhmanova A (2009) Mammalian end binding proteins control persistent microtubule growth. *The Journal of cell biology* 184: 691-706

Krishnan L, Matreyek KA, Oztop I, Lee K, Tipper CH, Li X, Dar MJ, Kewalramani VN, Engelman A (2010) The requirement for cellular transportin 3 (TNPO3 or TRN-SR2) during infection maps to human immunodeficiency virus type 1 capsid and not integrase. *Journal of virology* 84: 397-406

Krogan NJ. (2011) Pathogenic Landscape of HIV. http://www.ucsf.edu/news/2011/12/11163/pathogenic-landscape-hiv.

Kueh HY, Mitchison TJ (2009) Structural plasticity in actin and tubulin polymer dynamics. *Science* 325: 960-963

Kutluay SB, Perez-Caballero D, Bieniasz PD (2013) Fates of Retroviral Core Components during Unrestricted and TRIM5-Restricted Infection. *PLoS pathogens* 9: e1003214

Kuznetsov YG, Victoria JG, Robinson WE, Jr., McPherson A (2003) Atomic force microscopy investigation of human immunodeficiency virus (HIV) and HIV-infected lymphocytes. *Journal of virology* 77: 11896-11909

Labonte D, Thies E, Pechmann Y, Groffen AJ, Verhage M, Smit AB, van Kesteren RE, Kneussel M (2013) TRIM3 regulates the motility of the kinesin motor protein KIF21B. *PloS one* 8: e75603

Laguette N, Sobhian B, Casartelli N, Ringeard M, Chable-Bessia C, Segeral E, Yatim A, Emiliani S, Schwartz O, Benkirane M (2011) SAMHD1 is the dendritic- and myeloid-cell-specific HIV-1 restriction factor counteracted by Vpx. *Nature* 474: 654-657

Lahaye X, Satoh T, Gentili M, Cerboni S, Conrad C, Hurbain I, El Marjou A, Lacabaratz C, Lelievre JD, Manel N (2013) The capsids of HIV-1 and HIV-2 determine immune detection of the viral cDNA by the innate sensor cGAS in dendritic cells. *Immunity* 39: 1132-1142

Lakadamyali M, Rust MJ, Zhuang X (2006) Ligands for clathrin-mediated endocytosis are differentially sorted into distinct populations of early endosomes. *Cell* 124: 997-1009

Lamorte L, Titolo S, Lemke CT, Goudreau N, Mercier JF, Wardrop E, Shah VB, von Schwedler UK, Langelier C, Banik SS, Aiken C, Sundquist WI, Mason SW (2013) Discovery of novel small-molecule HIV-1 replication inhibitors that stabilize capsid complexes. *Antimicrob Agents Chemother* 57: 4622-4631

Langelier CR, Sandrin V, Eckert DM, Christensen DE, Chandrasekaran V, Alam SL, Aiken C, Olsen JC, Kar AK, Sodroski JG, Sundquist WI (2008) Biochemical characterization of a recombinant TRIM5alpha protein that restricts human immunodeficiency virus type 1 replication. *Journal of virology* 82: 11682-11694

Lecossier D, Bouchonnet F, Clavel F, Hance AJ (2003) Hypermutation of HIV-1 DNA in the absence of the Vif protein. *Science* 300: 1112

Lehmann M, Milev MP, Abrahamyan L, Yao XJ, Pante N, Mouland AJ (2009) Intracellular transport of human immunodeficiency virus type 1 genomic RNA and viral production are dependent on dynein motor function and late endosome positioning. *The Journal of biological chemistry* 284: 14572-14585

Lehmann MJ, Sherer NM, Marks CB, Pypaert M, Mothes W (2005) Actin- and myosin-driven movement of viruses along filopodia precedes their entry into cells. *The Journal of cell biology* 170: 317-325

Leopold PL, Kreitzer G, Miyazawa N, Rempel S, Pfister KK, Rodriguez-Boulan E, Crystal RG (2000) Dynein- and microtubule-mediated translocation of adenovirus serotype 5 occurs after endosomal lysis. *Human Gene Therapy* 11: 151-165

Lewis PF, Emerman M (1994) Passage through mitosis is required for oncoretroviruses but not for the human immunodeficiency virus. *Journal of virology* 68: 510-516

Li Y, Kar AK, Sodroski J (2009) Target cell type-dependent modulation of human immunodeficiency virus type 1 capsid disassembly by cyclophilin A. *Journal of virology* 83: 10951-10962

Lienlaf M, Hayashi F, Di Nunzio F, Tochio N, Kigawa T, Yokoyama S, Diaz-Griffero F (2011) Contribution of E3-ubiquitin ligase activity to HIV-1 restriction by TRIM5alpha(rh): structure of the RING domain of TRIM5alpha. *Journal of virology* 85: 8725-8737

Lin TY, Emerman M (2006) Cyclophilin A interacts with diverse lentiviral capsids. *Retrovirology* 3: 70

Liu KC, Chibwesha CJ (2013) Intrapartum management for prevention of mother-to-child transmission of HIV in resource-limited settings: a review of the literature. *African journal of reproductive health* 17: 107-117

Liu R, Paxton WA, Choe S, Ceradini D, Martin SR, Horuk R, MacDonald ME, Stuhlmann H, Koup RA, Landau NR (1996) Homozygous defect in HIV-1 coreceptor accounts for resistance of some multiply-exposed individuals to HIV-1 infection. *Cell* 86: 367-377

Liu Z, Pan Q, Ding S, Qian J, Xu F, Zhou J, Cen S, Guo F, Liang C (2013) The interferon-inducible MxB protein inhibits HIV-1 infection. *Cell host & microbe* 14: 398-410

Lodish HF (2004) *Molecular cell biology*, 5th edn. New York: W.H. Freeman.

Luby-Phelps K (2000) Cytoarchitecture and physical properties of cytoplasm: volume, viscosity, diffusion, intracellular surface area. *International review of cytology* 192: 189-221

Luduena RF (1998) Multiple forms of tubulin: different gene products and covalent modifications. *International review of cytology* 178: 207-275

Lukic Z, Hausmann S, Sebastian S, Rucci J, Sastri J, Robia SL, Luban J, Campbell EM (2011) TRIM5alpha associates with proteasomal subunits in cells while in complex with HIV-1 virions. *Retrovirology* 8: 93

Mandelkow E, Mandelkow EM (1995) Microtubules and microtubule-associated proteins. *Current opinion in cell biology* 7: 72-81

Mangeat B, Turelli P, Caron G, Friedli M, Perrin L, Trono D (2003) Broad antiretroviral defence by human APOBEC3G through lethal editing of nascent reverse transcripts. *Nature* 424: 99-103

Marraffini LA, Sontheimer EJ (2010) CRISPR interference: RNA-directed adaptive immunity in bacteria and archaea. *Nature reviews Genetics* 11: 181-190

Martin-Serrano J, Zang T, Bieniasz PD (2003) Role of ESCRT-I in retroviral budding. *Journal of virology* 77: 4794-4804

Martinez NW, Xue X, Berro RG, Kreitzer G, Resh MD (2008) Kinesin KIF4 regulates intracellular trafficking and stability of the human immunodeficiency virus type 1 Gag polyprotein. *Journal of virology* 82: 9937-9950

Matreyek KA, Yucel SS, Li X, Engelman A (2013) Nucleoporin NUP153 phenylalanine-glycine motifs engage a common binding pocket within the HIV-1 capsid protein to mediate lentiviral infectivity. *PLoS Pathogens* 9: e1003693

McDonald D, Vodicka MA, Lucero G, Svitkina TM, Borisy GG, Emerman M, Hope TJ (2002) Visualization of the intracellular behavior of HIV in living cells. *The Journal of cell biology* 159: 441-452

McKenney RJ, Huynh W, Tanenbaum ME, Bhabha G, Vale RD (2014) Activation of cytoplasmic dynein motility by dynactin-cargo adapter complexes. *Science* 345: 337-341

Melikyan GB (2014) HIV entry: a game of hide-and-fuse? *Current opinion in virology* 4C: 1-7

Milev MP, Brown CM, Mouland AJ (2010) Live cell visualization of the interactions between HIV-1 Gag and the cellular RNA-binding protein Staufen1. *Retrovirology* 7: 41

Misumi S, Inoue M, Dochi T, Kishimoto N, Hasegawa N, Takamune N, Shoji S (2010) Uncoating of human immunodeficiency virus type 1 requires prolyl isomerase Pin1. *The Journal of biological chemistry* 285: 25185-25195

Mitchison T, Kirschner M (1984) Dynamic instability of microtubule growth. *Nature* 312: 237-242

Muller MJ, Klumpp S, Lipowsky R (2008) Tug-of-war as a cooperative mechanism for bidirectional cargo transport by molecular motors. *Proceedings of the National Academy of Sciences of the United States of America* 105: 4609-4614

Nabel G, Baltimore D (1987) An inducible transcription factor activates expression of human immunodeficiency virus in T cells. *Nature* 326: 711-713

Nakayama EE, Miyoshi H, Nagai Y, Shioda T (2005) A specific region of 37 amino acid residues in the SPRY (B30.2) domain of African green monkey TRIM5alpha determines species-specific restriction of simian immunodeficiency virus SIVmac infection. *Journal of virology* 79: 8870-8877

Neagu MR, Ziegler P, Pertel T, Strambio-De-Castillia C, Grutter C, Martinetti G, Mazzucchelli L, Grutter M, Manz MG, Luban J (2009) Potent inhibition of HIV-1 by TRIM5-cyclophilin fusion proteins engineered from human components. *The Journal of clinical investigation* 119: 3035-3047

Neil SJ, Zang T, Bieniasz PD (2008) Tetherin inhibits retrovirus release and is antagonized by HIV-1 Vpu. *Nature* 451: 425-430

Nepveu-Traversy ME, Berthoux L (2014) The conserved sumoylation consensus site in TRIM5alpha modulates its immune activation functions. *Virus research* 184: 30-38

Nepveu-Traversy ME, Berube J, Berthoux L (2009) TRIM5alpha and TRIMCyp form apparent hexamers and their multimeric state is not affected by exposure to restriction-sensitive viruses or by treatment with pharmacological inhibitors. *Retrovirology* 6: 100

Neuwald AF, Aravind L, Spouge JL, Koonin EV (1999) AAA+: A class of chaperone-like ATPases associated with the assembly, operation, and disassembly of protein complexes. *Genome research* 9: 27-43

Nguyen DG, Booth A, Gould SJ, Hildreth JE (2003) Evidence that HIV budding in primary macrophages occurs through the exosome release pathway. *The Journal of biological chemistry* 278: 52347-52354

NIH. (2012) HIV Replication Cycle. In Diseases NIoAaI (ed.), http://www.niaid.nih.gov/topics/HIVAIDS/Understanding/Biology/pages/hivreplicationcycle.aspx.

Nisole S, Lynch C, Stoye JP, Yap MW (2004) A Trim5-cyclophilin A fusion protein found in owl monkey kidney cells can restrict HIV-1. *Proceedings of the National Academy of Sciences of the United States of America* 101: 13324-13328

Nisole S, Stoye JP, Saib A (2005) TRIM family proteins: retroviral restriction and antiviral defence. *Nature reviews* 3: 799-808

Ohkura S, Yap MW, Sheldon T, Stoye JP (2006) All three variable regions of the TRIM5alpha B30.2 domain can contribute to the specificity of retrovirus restriction. *Journal of virology* 80: 8554-8565

Organization. GWH (2007) WHO case definitions of HIV for surveillance and revised clinical staging and immunological classification of HIV-related disease in adults and children.

Ott DE (2008) Cellular proteins detected in HIV-1. *Reviews in medical virology* 18: 159-175

Palmisano L, Vella S (2011) A brief history of antiretroviral therapy of HIV infection: success and challenges. *Annali dell'Istituto superiore di sanita* 47: 44-48

Pawlica P, Le Sage V, Poccardi N, Tremblay MJ, Mouland AJ, Berthoux L (2014) Functional evidence for the involvement of microtubules and dynein motor complexes in TRIM5alpha-mediated restriction of retroviruses. *Journal of virology* 88: 5661-5676

Pelchen-Matthews A, Kramer B, Marsh M (2003) Infectious HIV-1 assembles in late endosomes in primary macrophages. *The Journal of cell biology* 162: 443-455

Penningroth SM, Cheung A, Bouchard P, Gagnon C, Bardin CW (1982) Dynein ATPase is inhibited selectively in vitro by erythro-9-[3-2-(hydroxynonyl)]adenine. *Biochemical and biophysical research communications* 104: 234-240

Perez-Caballero D, Hatziioannou T, Zhang F, Cowan S, Bieniasz PD (2005) Restriction of human immunodeficiency virus type 1 by TRIM-CypA occurs with rapid kinetics and independently of cytoplasmic bodies, ubiquitin, and proteasome activity. *Journal of virology* 79: 15567-15572

Perron MJ, Stremlau M, Lee M, Javanbakht H, Song B, Sodroski J (2007) The human TRIM5alpha restriction factor mediates accelerated uncoating of the N-tropic murine leukemia virus capsid. *Journal of virology* 81: 2138-2148

Perron MJ, Stremlau M, Song B, Ulm W, Mulligan RC, Sodroski J (2004) TRIM5alpha mediates the postentry block to N-tropic murine leukemia viruses in human cells. *Proceedings of the National Academy of Sciences of the United States of America* 101: 11827-11832

Pertel T, Hausmann S, Morger D, Zuger S, Guerra J, Lascano J, Reinhard C, Santoni FA, Uchil PD, Chatel L, Bisiaux A, Albert ML, Strambio-De-Castillia C, Mothes W, Pizzato M, Grutter MG, Luban J (2011) TRIM5 is an innate immune sensor for the retrovirus capsid lattice. *Nature* 472: 361-365

Petit C, Giron ML, Tobaly-Tapiero J, Bittoun P, Real E, Jacob Y, Tordo N, De The H, Saib A (2003) Targeting of incoming retroviral Gag to the centrosome involves a direct interaction with the dynein light chain 8. *Journal of cell science* 116: 3433-3442

Pfister KK, Fisher EM, Gibbons IR, Hays TS, Holzbaur EL, McIntosh JR, Porter ME, Schroer TA, Vaughan KT, Witman GB, King SM, Vallee RB (2005) Cytoplasmic dynein nomenclature. *The Journal of cell biology* 171: 411-413

Pham QT, Bouchard A, Grutter MG, Berthoux L (2010) Generation of human TRIM5alpha mutants with high HIV-1 restriction activity. *Gene Therapy* 17: 859-871

Pollard VW, Malim MH (1998) The HIV-1 Rev protein. *Annual review of microbiology* 52: 491-532

Popovic M, Sarngadharan MG, Read E, Gallo RC (1984) Detection, isolation, and continuous production of cytopathic retroviruses (HTLV-III) from patients with AIDS and pre-AIDS. *Science* 224: 497-500

Pornillos O (2014) Crystal Structure of a TRIM Coiled-Coil: Implications for HIV-1 Capsid Recognition by TRIM5α. In *Conference On Retroviruses And Opportunistic Infections*. Boston

Pornillos O, Ganser-Pornillos BK, Kelly BN, Hua Y, Whitby FG, Stout CD, Sundquist WI, Hill CP, Yeager M (2009) X-ray structures of the hexameric building block of the HIV capsid. *Cell* 137: 1282-1292

Pornillos O, Ganser-Pornillos BK, Yeager M (2011) Atomic-level modelling of the HIV capsid. *Nature* 469: 424-427

Powell RD, Holland PJ, Hollis T, Perrino FW (2011) Aicardi-Goutieres syndrome gene and HIV-1 restriction factor SAMHD1 is a dGTP-regulated deoxynucleotide triphosphohydrolase. *The Journal of biological chemistry* 286: 43596-43600

Price AJ, Fletcher AJ, Schaller T, Elliott T, Lee K, KewalRamani VN, Chin JW, Towers GJ, James LC (2012) CPSF6 defines a conserved capsid interface that modulates HIV-1 replication. *PLoS Pathogens* 8: e1002896

Radtke K, Dohner K, Sodeik B (2006) Viral interactions with the cytoskeleton: a hitchhiker's guide to the cell. *Cellular microbiology* 8: 387-400

Radtke K, Kieneke D, Wolfstein A, Michael K, Steffen W, Scholz T, Karger A, Sodeik B (2010) Plus- and minus-end directed microtubule motors bind simultaneously to herpes simplex virus capsids using different inner tegument structures. *PLoS Pathogens* 6: e1000991

Rajsbaum R, Garcia-Sastre A (2013) Viral evasion mechanisms of early antiviral responses involving regulation of ubiquitin pathways. *Trends Microbiology* 21: 421-429

Rasaiyaah J, Tan CP, Fletcher AJ, Price AJ, Blondeau C, Hilditch L, Jacques DA, Selwood DL, James LC, Noursadeghi M, Towers GJ (2013) HIV-1 evades innate immune recognition through specific cofactor recruitment. *Nature* 503: 402-405

Ratner L, Haseltine W, Patarca R, Livak KJ, Starcich B, Josephs SF, Doran ER, Rafalski JA, Whitehorn EA, Baumeister K, *et al.* (1985) Complete nucleotide sequence of the AIDS virus, HTLV-III. *Nature* 313: 277-284

Ravelli RB, Gigant B, Curmi PA, Jourdain I, Lachkar S, Sobel A, Knossow M (2004) Insight into tubulin regulation from a complex with colchicine and a stathmin-like domain. *Nature* 428: 198-202

Reeves JD, Doms RW (2002) Human immunodeficiency virus type 2. *Journal of General Virology* 83: 1253-1265

Regad T, Saib A, Lallemand-Breitenbach V, Pandolfi PP, de The H, Chelbi-Alix MK (2001) PML mediates the interferon-induced antiviral state against a complex retrovirus via its association with the viral transactivator. *The European Molecular Biology Organization journal* 20: 3495-3505

Rerks-Ngarm S, Pitisuttithum P, Nitayaphan S, Kaewkungwal J, Chiu J, Paris R, Premsri N, Namwat C, de Souza M, Adams E, Benenson M, Gurunathan S, Tartaglia J, McNeil JG, Francis DP, Stablein D, Birx DL, Chunsuttiwat S, Khamboonruang C, Thongcharoen P, Robb ML, Michael NL, Kunasol P, Kim JH (2009) Vaccination with ALVAC and AIDSVAX to prevent HIV-1 infection in Thailand. *The New England journal of medicine* 361: 2209-2220

Reymond A, Meroni G, Fantozzi A, Merla G, Cairo S, Luzi L, Riganelli D, Zanaria E, Messali S, Cainarca S, Guffanti A, Minucci S, Pelicci PG, Ballabio A (2001) The tripartite motif family identifies cell compartments. *The European Molecular Biology Organization journal* 20: 2140-2151

Roa A, Hayashi F, Yang Y, Lienlaf M, Zhou J, Shi J, Watanabe S, Kigawa T, Yokoyama S, Aiken C, Diaz-Griffero F (2012) RING domain mutations uncouple TRIM5alpha restriction of HIV-1 from inhibition of reverse transcription and acceleration of uncoating. *Journal of virology* 86: 1717-1727

Roberts AJ, Kon T, Knight PJ, Sutoh K, Burgess SA (2013) Functions and mechanics of dynein motor proteins. *Nature Reviews Molecular Cell Biology* 14: 713-726

Rodriguez OC, Schaefer AW, Mandato CA, Forscher P, Bement WM, Waterman-Storer CM (2003) Conserved microtubule-actin interactions in cell movement and morphogenesis. *Nature cell biology* 5: 599-609

Roe T, Reynolds TC, Yu G, Brown PO (1993) Integration of murine leukemia virus DNA depends on mitosis. *The European Molecular Biology Organization journal* 12: 2099-2108

Rogers SL, Rogers GC, Sharp DJ, Vale RD (2002) Drosophila EB1 is important for proper assembly, dynamics, and positioning of the mitotic spindle. *The Journal of cell biology* 158: 873-884

Rold CJ, Aiken C (2008) Proteasomal degradation of TRIM5alpha during retrovirus restriction. *PLoS pathogens* 4: e1000074

Sabo Y, Walsh D, Barry DS, Tinaztepe S, de Los Santos K, Goff SP, Gundersen GG, Naghavi MH (2013) HIV-1 induces the formation of stable microtubules to enhance early infection. *Cell host & microbe* 14: 535-546

Saez-Cirion A, Bacchus C, Hocqueloux L, Avettand-Fenoel V, Girault I, Lecuroux C, Potard V, Versmisse P, Melard A, Prazuck T, Descours B, Guergnon J, Viard JP, Boufassa F, Lambotte O, Goujard C, Meyer L, Costagliola D, Venet A, Pancino G, Autran B, Rouzioux C (2013) Post-treatment HIV-1 controllers with a long-term virological remission after the interruption of early initiated antiretroviral therapy ANRS VISCONTI Study. *PLoS Pathogens* 9: e1003211

Sanchez JG, Okreglicka K, Chandrasekaran V, Welker JM, Sundquist WI, Pornillos O (2014) The tripartite motif coiled-coil is an elongated antiparallel hairpin dimer. *Proceedings of the National Academy of Sciences of the United States of America* 111: 2494-2499

Sandefur S, Varthakavi V, Spearman P (1998) The I domain is required for efficient plasma membrane binding of human immunodeficiency virus type 1 Pr55Gag. *Journal of virology* 72: 2723-2732

Sastri J, O'Connor C, Danielson CM, McRaven M, Perez P, Diaz-Griffero F, Campbell EM (2010) Identification of residues within the L2 region of rhesus TRIM5alpha that are required for retroviral restriction and cytoplasmic body localization. *Virology* 405: 259-266

Sawyer SL, Wu LI, Emerman M, Malik HS (2005) Positive selection of primate TRIM5alpha identifies a critical species-specific retroviral restriction domain. *Proceedings of the National Academy of Sciences of the United States of America* 102: 2832-2837

Sayah DM, Sokolskaja E, Berthoux L, Luban J (2004) Cyclophilin A retrotransposition into TRIM5 explains owl monkey resistance to HIV-1. *Nature* 430: 569-573

Schaller T, Ocwieja KE, Rasaiyaah J, Price AJ, Brady TL, Roth SL, Hue S, Fletcher AJ, Lee K, KewalRamani VN, Noursadeghi M, Jenner RG, James LC, Bushman FD, Towers GJ (2011) HIV-1 capsid-cyclophilin interactions determine nuclear import pathway, integration targeting and replication efficiency. *PLoS Pathogens* 7: e1002439

Schiff PB, Horwitz SB (1981) Taxol assembles tubulin in the absence of exogenous guanosine 5'-triphosphate or microtubule-associated proteins. *Biochemistry* 20: 3247-3252

Schliwa M, Ezzell RM, Euteneuer U (1984) erythro-9-[3-(2-Hydroxynonyl)]adenine is an effective inhibitor of cell motility and actin assembly. *Proceedings of the National Academy of Sciences of the United States of America* 81: 6044-6048

Schoggins JW, Rice CM (2011) Interferon-stimulated genes and their antiviral effector functions. *Current opinion in virology* 1: 519-525

Schroder AR, Shinn P, Chen H, Berry C, Ecker JR, Bushman F (2002) HIV-1 integration in the human genome favors active genes and local hotspots. *Cell* 110: 521-529

Schulze E, Kirschner M (1987) Dynamic and stable populations of microtubules in cells. *The Journal of cell biology* 104: 277-288

Sebastian S, Luban J (2005) TRIM5alpha selectively binds a restriction-sensitive retroviral capsid. *Retrovirology* 2: 40

Setou M, Nakagawa T, Seog DH, Hirokawa N (2000) Kinesin superfamily motor protein KIF17 and mLin-10 in NMDA receptor-containing vesicle transport. *Science* 288: 1796-1802

Shah VB, Shi J, Hout DR, Oztop I, Krishnan L, Ahn J, Shotwell MS, Engelman A, Aiken C (2013) The host proteins transportin SR2/TNPO3 and cyclophilin A exert opposing effects on HIV-1 uncoating. *Journal of virology* 87: 422-432

Sharp PM, Bailes E, Chaudhuri RR, Rodenburg CM, Santiago MO, Hahn BH (2001) The origins of acquired immune deficiency syndrome viruses: where and when? *Philosophical transactions of the Royal Society of London Series B, Biological sciences* 356: 867-876

Sharp PM, Hahn BH (2011) Origins of HIV and the AIDS pandemic. *Cold Spring Harbor perspectives in medicine* 1: a006841

Sharp PM, Shaw GM, Hahn BH (2005) Simian immunodeficiency virus infection of chimpanzees. *Journal of virology* 79: 3891-3902

Sheehy AM, Gaddis NC, Choi JD, Malim MH (2002) Isolation of a human gene that inhibits HIV-1 infection and is suppressed by the viral Vif protein. *Nature* 418: 646-650

Shi J, Zhou J, Shah VB, Aiken C, Whitby K (2011) Small-molecule inhibition of human immunodeficiency virus type 1 infection by virus capsid destabilization. *Journal of virology* 85: 542-549

Short KM, Cox TC (2006) Subclassification of the RBCC/TRIM superfamily reveals a novel motif necessary for microtubule binding. *The Journal of biological chemistry* 281: 8970-8980

Smith DK, Grohskopf LA, Black RJ, Auerbach JD, Veronese F, Struble KA, Cheever L, Johnson M, Paxton LA, Onorato IM, Greenberg AE (2005) Antiretroviral postexposure prophylaxis after sexual, injection-drug use, or other nonoccupational exposure to HIV in the United States: recommendations from the U.S. Department of Health and Human Services. *MMWR Recommendations and reports : Morbidity and mortality weekly report Recommendations and reports / Centers for Disease Control* 54: 1-20

Smith EB, Ogert RA, Pechter D, Villafania A, Abbondanzo SJ, Lin K, Rivera-Gines A, Rebsch-Mastykarz C, Monsma FJ, Jr. (2014) HIV cell fusion assay: phenotypic screening tool for the identification of HIV entry inhibitors via CXCR4. *Journal of biomolecular screening* 19: 108-118

Smith TE, Hong W, Zachariah MM, Harper MK, Matainaho TK, Van Wagoner RM, Ireland CM, Vershinin M (2013) Single-molecule inhibition of human kinesin by adociasulfate-13 and -14 from the sponge Cladocroce aculeata. *Proceedings of the National Academy of Sciences of the United States of America* 110: 18880-18885

Song B, Diaz-Griffero F, Park DH, Rogers T, Stremlau M, Sodroski J (2005a) TRIM5alpha association with cytoplasmic bodies is not required for antiretroviral activity. *Virology* 343: 201-211

Song B, Gold B, O'Huigin C, Javanbakht H, Li X, Stremlau M, Winkler C, Dean M, Sodroski J (2005b) The B30.2(SPRY) domain of the retroviral restriction factor TRIM5alpha exhibits lineage-specific length and sequence variation in primates. *Journal of virology* 79: 6111-6121

Stremlau M, Owens CM, Perron MJ, Kiessling M, Autissier P, Sodroski J (2004) The cytoplasmic body component TRIM5alpha restricts HIV-1 infection in Old World monkeys. *Nature* 427: 848-853

Stremlau M, Perron M, Lee M, Li Y, Song B, Javanbakht H, Diaz-Griffero F, Anderson DJ, Sundquist WI, Sodroski J (2006) Specific recognition and accelerated uncoating of retroviral capsids by the TRIM5alpha restriction factor. *Proceedings of the National Academy of Sciences of the United States of America* 103: 5514-5519

Stremlau M, Perron M, Welikala S, Sodroski J (2005) Species-specific variation in the B30.2(SPRY) domain of TRIM5alpha determines the potency of human immunodeficiency virus restriction. *Journal of virology* 79: 3139-3145

Su X, Ohi R, Pellman D (2012) Move in for the kill: motile microtubule regulators. *Trends in cell biology* 22: 567-575

Sun X, Whittaker GR (2007) Role of the actin cytoskeleton during influenza virus internalization into polarized epithelial cells. *Cellular microbiology* 9: 1672-1682

Sundquist WI, Krausslich HG (2012) HIV-1 assembly, budding, and maturation. *Cold Spring Harbor perspectives in medicine* 2: a006924

Sung. (2006) Cytoplasmic Dynein and Cell Polarity. *The Sung Lab*, cornellcelldevbiology.org/sung/researchcytoplasmic.html.

Suomalainen M, Nakano MY, Keller S, Boucke K, Stidwill RP, Greber UF (1999) Microtubule-dependent plus- and minus end-directed motilities are competing processes for nuclear targeting of adenovirus. *The Journal of cell biology* 144: 657-672

Tan J, Sattentau QJ (2013) The HIV-1-containing macrophage compartment: a perfect cellular niche? *Trends Microbiology* 21: 405-412

Tang Y, Winkler U, Freed EO, Torrey TA, Kim W, Li H, Goff SP, Morse HC, 3rd (1999) Cellular motor protein KIF-4 associates with retroviral Gag. *Journal of virology* 73: 10508-10513

Tareen SU, Emerman M (2011) Human Trim5alpha has additional activities that are uncoupled from retroviral capsid recognition. *Virology* 409: 113-120

Tebas P, Stein D, Tang WW, Frank I, Wang SQ, Lee G, Spratt SK, Surosky RT, Giedlin MA, Nichol G, Holmes MC, Gregory PD, Ando DG, Kalos M, Collman RG, Binder-Scholl G, Plesa G, Hwang WT, Levine BL, June CH (2014) Gene editing of CCR5 in autologous CD4 T cells of persons infected with HIV. *The New England journal of medicine* 370: 901-910

Tipper C, Sodroski J (2013) Enhanced autointegration in hyperstable simian immunodeficiency virus capsid mutants blocked after reverse transcription. *Journal of virology* 87: 3628-3639

Trinchieri G, Sher A (2007) Cooperation of Toll-like receptor signals in innate immune defence. *Nature Reviews Immunology* 7: 179-190

Uchil PD, Quinlan BD, Chan WT, Luna JM, Mothes W (2008) TRIM E3 ligases interfere with early and late stages of the retroviral life cycle. *PLoS Pathogens* 4: e16

UNAIDS. (2010) UNAIDS report on the global AIDS epidemic 2010. WHO Library Cataloguing-in-Publication Data.

UNAIDS. (2013) UNAIDS report on the global AIDS epidemic 2013. WHO Library Cataloguing-in-Publication Data.

Vaid N, Langan KM, Maude RJ (2013) Post-exposure prophylaxis in resource-poor settings: review and recommendations for pre-departure risk assessment and planning for expatriate healthcare workers. *Tropical medicine & international health : TM & IH* 18: 588-595

Vale RD (2003) The molecular motor toolbox for intracellular transport. *Cell* 112: 467-480

van Leeuwen H, Elliott G, O'Hare P (2002) Evidence of a role for nonmuscle myosin II in herpes simplex virus type 1 egress. *Journal of virology* 76: 3471-3481

Varthakavi V, Smith RM, Bour SP, Strebel K, Spearman P (2003) Viral protein U counteracts a human host cell restriction that inhibits HIV-1 particle production. *Proceedings of the National Academy of Sciences of the United States of America* 100: 15154-15159

Verhey KJ, Gaertig J (2007) The tubulin code. *Cell Cycle* 6: 2152-2160

Verhey KJ, Hammond JW (2009) Traffic control: regulation of kinesin motors. *Nature Reviews Molecular Cell Biology* 10: 765-777

Viard M, Parolini I, Sargiacomo M, Fecchi K, Ramoni C, Ablan S, Ruscetti FW, Wang JM, Blumenthal R (2002) Role of cholesterol in human immunodeficiency virus type 1 envelope protein-mediated fusion with host cells. *Journal of virology* 76: 11584-11595

Wain-Hobson S, Sonigo P, Danos O, Cole S, Alizon M (1985) Nucleotide sequence of the AIDS virus, LAV. *Cell* 40: 9-17

Welte MA (2004) Bidirectional transport along microtubules. *Current Biology* 14: R525-537

Wilson SJ, Webb BL, Ylinen LM, Verschoor E, Heeney JL, Towers GJ (2008) Independent evolution of an antiviral TRIMCyp in rhesus macaques. *Proceedings of the National Academy of Sciences of the United States of America* 105: 3557-3562

Wolf D, Goff SP (2007) TRIM28 mediates primer binding site-targeted silencing of murine leukemia virus in embryonic cells. *Cell* 131: 46-57

Wolfstein A, Nagel CH, Radtke K, Dohner K, Allan VJ, Sodeik B (2006) The inner tegument promotes herpes simplex virus capsid motility along microtubules in vitro. *Traffic* 7: 227-237

Wu X, Anderson JL, Campbell EM, Joseph AM, Hope TJ (2006) Proteasome inhibitors uncouple rhesus TRIM5alpha restriction of HIV-1 reverse transcription and infection. *Proceedings of the National Academy of Sciences of the United States of America* 103: 7465-7470

Wyma DJ, Kotov A, Aiken C (2000) Evidence for a stable interaction of gp41 with Pr55(Gag) in immature human immunodeficiency virus type 1 particles. *Journal of virology* 74: 9381-9387

Xiao PJ, Samulski RJ (2012) Cytoplasmic trafficking, endosomal escape, and perinuclear accumulation of adeno-associated virus type 2 particles are facilitated by microtubule network. *Journal of virology* 86: 10462-10473

Xu H, Franks T, Gibson G, Huber K, Rahm N, De Castillia CS, Luban J, Aiken C, Watkins S, Sluis-Cremer N, Ambrose Z (2013) Evidence for biphasic uncoating during HIV-1 infection from a novel imaging assay. *Retrovirology* 10: 70

Xu K, Schwarz PM, Luduena RF (2002) Interaction of nocodazole with tubulin isotypes. *Drug Development Research* 55: 91-96

Yamashita M, Emerman M (2004) Capsid is a dominant determinant of retrovirus infectivity in nondividing cells. *Journal of virology* 78: 5670-5678

Yamashita M, Perez O, Hope TJ, Emerman M (2007) Evidence for direct involvement of the capsid protein in HIV infection of nondividing cells. *PLoS Pathogens* 3: 1502-1510

Yan N, Regalado-Magdos AD, Stiggelbout B, Lee-Kirsch MA, Lieberman J (2010) The cytosolic exonuclease TREX1 inhibits the innate immune response to human immunodeficiency virus type 1. *Nature immunology* 11: 1005-1013

Yang Y, Fricke T, Diaz-Griffero F (2013) Inhibition of reverse transcriptase activity increases stability of the HIV-1 core. *Journal of virology* 87: 683-687

Yao X, Jayappa KD, Mouland A, Ao Z (2013). Contribution of a microtubule associated dynein proteins for HIV-1 reverse transcription and replication. *9th International Retroviral Nucleocapsid Protein and Assembly Symposium*; Montreal.

Yap MW, Nisole S, Lynch C, Stoye JP (2004) Trim5alpha protein restricts both HIV-1 and murine leukemia virus. *Proceedings of the National Academy of Sciences of the United States of America* 101: 10786-10791

Yap MW, Nisole S, Stoye JP (2005) A single amino acid change in the SPRY domain of human Trim5alpha leads to HIV-1 restriction. *Current Biology* 15: 73-78

Yarchoan R, Broder S (1987) Development of antiretroviral therapy for the acquired immunodeficiency syndrome and related disorders. A progress report. *The New England journal of medicine* 316: 557-564

Yoder A, Guo J, Yu D, Cui Z, Zhang XE, Wu Y (2011) Effects of microtubule modulators on HIV-1 infection of transformed and resting CD4 T cells. *Journal of virology* 85: 3020-3024

Zamborlini A, Lehmann-Che J, Clave E, Giron ML, Tobaly-Tapiero J, Roingeard P, Emiliani S, Toubert A, de The H, Saib A (2007) Centrosomal pre-integration latency of HIV-1 in quiescent cells. *Retrovirology* 4: 63

Zhang H, Dornadula G, Orenstein J, Pomerantz RJ (2000) Morphologic changes in human immunodeficiency virus type 1 virions secondary to intravirion reverse transcription: evidence indicating that reverse transcription may not take place within the intact viral core. *Journal of human virology* 3: 165-172

Zhang H, Dornadula G, Pomerantz RJ (1998) Natural endogenous reverse transcription of HIV-1. *Journal of reproductive immunology* 41: 255-260

Zhang W, Greene W, Gao SJ (2012) Microtubule- and dynein-dependent nuclear trafficking of rhesus rhadinovirus in rhesus fibroblasts. *Journal of virology* 86: 599-604

Zhao G, Ke D, Vu T, Ahn J, Shah VB, Yang R, Aiken C, Charlton LM, Gronenborn AM, Zhang P (2011) Rhesus TRIM5alpha disrupts the HIV-1 capsid at the inter-hexamer interfaces. *PLoS Pathogens* 7: e1002009

Zhou L, Sokolskaja E, Jolly C, James W, Cowley SA, Fassati A (2011) Transportin 3 promotes a nuclear maturation step required for efficient HIV-1 integration. *PLoS Pathogens* 7: e1002194

Zhu T, Korber BT, Nahmias AJ, Hooper E, Sharp PM, Ho DD (1998) An African HIV-1 sequence from 1959 and implications for the origin of the epidemic. *Nature* 391: 594-597

Annex A contains a published study, containing extended results from Chapter II, which demonstrates that the dynein motor complex is involved HIV-1 uncoating.

ANNEX A

CYTOPLASMIC DYNEIN PROMOTES HIV-1 UNCOATING

PAULINA PAWLICA, LIONEL BERTHOUX

Published on 4th of November 2014 in *Viruses*

A.1 Contributions

P.P. and L.B. conceived and designed the experiments; P.P. performed the experiments; P.P. and L.B. analyzed the data; P.P. and L.B. wrote the paper.

A.2 Abstract

Retroviral capsid (CA) cores undergo uncoating during their retrograde transport (toward the nucleus), and/or after reaching the nuclear membrane. However, whether HIV-1 CA core uncoating is dependent upon its transport is not understood. There is some evidence that HIV-1 cores retrograde transport involves cytoplasmic dynein complexes translocating on microtubules. Here we investigate the role of dynein-dependent transport in HIV-1 uncoating. To interfere with dynein function, we depleted dynein heavy chain (DHC) using RNA interference, and we over-expressed p50/dynamitin. In immunofluorescence microscopy experiments, DHC depletion caused an accumulation of CA foci in HIV-1 infected cells. Using a biochemical assay to monitor HIV-1 CA core disassembly in infected cells, we observed an increase in amounts of intact (pelletable) CA cores upon DHC depletion or p50 over-expression. Results from these two complementary assays suggest that inhibiting dynein-mediated transport interferes with HIV-1 uncoating in infected cells, indicating the existence of a functional link between HIV-1 transport and uncoating.

Keywords: HIV-1; uncoating; capsid; microtubules; dynein

A.3 Introduction

The mature CA core of human immunodeficiency virus 1 (HIV-1) is a ~60 nm x 120 nm (Briggs *et al*, 2003) cone-shaped protein lattice, encasing viral genomic RNA, enzymes (integrase and reverse transcriptase) and other viral proteins [reviewed in (Briggs & Krausslich, 2011)]. It is composed of ~1,000 CA monomers (Pornillos *et al*, 2011) arranged in ~170 hexamers and 12 pentamers through interactions involving their N-terminal domains (Pornillos *et al*, 2009), whereas the C-terminal domains are important for homodimerization that connects the rings into a lattice (Gamble *et al*, 1997). Following receptor-mediated entry into the cytoplasm, HIV-1 undergoes tightly regulated processes that prepare the virus for nuclear import and integration of its genetic material into host DNA. The nucleoprotein complex formed before completing reverse transcription (RT) is usually referred to as the reverse transcription complex (RTC), which is later transformed into the pre-integration complex. RT is thought to be initiated within 30 minutes post virus entry (Goff, 2001) by a still unknown mechanism. Before, during or after RT, the CA core must be disassembled in a process called 'uncoating'. The precise timing and location of uncoating remain unclear; some reports propose that it occurs in the cytoplasm (Hulme *et al*, 2011; McDonald *et al*, 2002), while others suggest that uncoating takes place at the nuclear pore (Arhel *et al*, 2007; Rasaiyaah *et al*, 2013; Schaller *et al*, 2011). It is possible that a small fraction of CA proteins remain associated with pre-integration complexes and are transported to the nucleus (Zhou *et al*, 2011). These hypotheses are not mutually exclusive considering that uncoating could take place through several sequential steps rather than through a rapid single-step process (Ambrose & Aiken, 2014). Additionally, recent lines of evidence indicate that uncoating is linked with RT (Hulme *et al*, 2011; Roa *et al*, 2012; Yang *et al*, 2013) and that RT may even trigger uncoating (Hulme *et al*, 2011; Zhang *et al*, 2000). However, RT initiation itself may depend on prior destabilization or increased permeability of the CA core after entry into the cytoplasm (Zhang *et al*, 1998). Alternatively, uncoating could be triggered by an as yet unknown cellular factor (Auewarakul *et al*, 2005).

Numerous studies indicate that CA is the main viral determinant for uncoating. Mutations resulting in either hypostable or hyperstable CA cores almost completely abolish viral infectivity despite normal virion protein content (Forshey *et al*, 2002). Additionally, the retroviral restriction factors TRIM5α and TRIMCyp inhibit viral infection (Sayah *et al*, 2004; Stremlau *et al*, 2004) through binding to and destabilization of incoming CA cores, in essence causing 'premature uncoating' (Stremlau *et al*, 2006). Furthermore, the HIV-1 small-molecule inhibitor PF-3450074 (PF74) inhibits HIV-1 infectivity specifically by destabilizing the CA core (Shi *et al*, 2011). Uncoating is also likely dependent on cellular factors, but these remain mostly elusive (Ambrose & Aiken, 2014). A few cellular partners that interact with the HIV-1 CA core were characterized and some were proposed to modulate uncoating, such as cyclophilin A (CypA) (Li *et al*, 2009b; Shah *et al*, 2013), nucleoprotein RanBP2/Nup358 (Schaller *et al*, 2011), transportin 3 (TNPO3) (Shah *et al*, 2013), cleavage and polyadenylation specific factor 6 (CPSF6) (De Iaco *et al*, 2013) and PDZ Domain-containing 8 (Guth & Sodroski, 2014).

Similarly to other viruses [reviewed in (Slonska *et al*, 2012)], HIV-1 hijacks the cell's cytoskeleton and associated molecular motors for its trafficking towards the nucleus [reviewed in (Gaudin *et al*, 2013)]. The microtubule network and microtubule-associated dynein motor complexes were proposed to transport HIV-1 RTCs toward the nucleus (McDonald *et al*, 2002). Specifically, HIV-1 translocation on microtubules was evidenced by live microscopy, and was inhibited by micro-injection of anti-dynein antibodies (McDonald *et al*, 2002). Recently, it was reported that HIV-1 induces the formation of and co-localizes with a stable sub-population of microtubules whose disruption abolishes infectivity (Sabo *et al*, 2013). Thus, the microtubule network seems to be important for HIV-1 trafficking and infectivity.

In this study, we hypothesized that uncoating of the HIV-1 CA core and its trafficking towards the nucleus were linked mechanisms. Our results suggest a role for dynein motor complexes in HIV-1 uncoating.

A.4 Results

Disruption of the Dynein Motor Complex Causes an Accumulation of CA Foci in Infected Cells. We used immunofluorescence (IF) microscopy to analyze the presence of CA foci, visualized using a CA monoclonal antibody, in human HeLa cells infected with HIV-$1_{CMV\text{-}GFP}$ pseudotyped with the glycoprotein of the vesicular stomatitis virus (VSV G) or in human MAGI cells infected with HIV-1_{NL43}. Such CA foci detected in acute infection conditions are thought to be individual viruses that are not or only partially uncoated (Arhel *et al*, 2007; Campbell *et al*, 2007; Hulme *et al*, 2011; McDonald *et al*, 2002). HeLa cells transfected with siRNAs targeting either the dynein heavy chain (DHC) mRNA (Lehmann *et al*, 2009; Pawlica *et al*, 2014) or the non-relevant luciferase (Luc) mRNA (Pawlica *et al*, 2014) were infected with HIV-$1_{CMV\text{-}GFP}$ for 2 h, at which point supernatants were removed and cells were incubated for an additional 4 hours. This timing was previously determined to allow for the efficient detection of cytoplasmic, unenveloped HIV-1 CA cores (data not shown and (Campbell *et al*, 2008)). DHC depletion was efficient as assessed by Western blotting, since transfection of DHC siRNA led to a reduction of ~85.4% ± 6.7% (n = 10) in protein levels (Figure 1A), which is consistent with previous observations that a large proportion of cells showed altered dynein-dependent transport in these conditions as seen by LAMP-1 staining (Pawlica *et al*, 2014). Upon staining infected cells using an anti-CA antibody, we detected distinct foci that were absent from mock-infected cells, as expected (Figure 1B). We analyzed the median slice from a Z-stack for each field, which removed the cytoplasm present on top of or underneath the nucleus from the analysis. DHC depletion caused an increase in the amounts of CA foci. Specifically, the average number of CA foci per cell increased ~2.5-fold following DHC depletion, from 6.98 ± 0.82 in control cells (n = 71 cells analyzed) to 17.4 ± 2.9 in DHC-depleted cells (n = 57) (P = 0.0038) (Figure 1C). Moreover, CA foci tended to accumulate in the cell periphery, as evidenced by measuring relative distances to the nucleus. The median relative distance to the nucleus changed significantly (P < 0.0001) from 0.44 (95% CI, 0.39–0.52) for the Luc siRNA-transfected control cells (P = 10) to 0.83 (95% CI, 0.79–0.84) for cells (n = 16) transfected with DHC siRNA (Figure 1D). A similar accumulation of

viral RTCs in the cell periphery was observed upon transfection of anti-dynein antibodies prior to infection (McDonald *et al*, 2002).

HIV-1 virions pseudotyped with VSV G are delivered through clathrin-mediated endocytosis (Sun *et al*, 2005) and are further released into the cytoplasm following acidification of endosomes (Blumenthal *et al*, 1987). Clathrin-mediated entry relies mainly on actin filaments (Cureton *et al*, 2009), while maturation of endosomes involves microtubules (Lakadamyali *et al*, 2006) and possibly the dynein motor complex (Lehmann *et al*, 2009). Therefore, in order to confirm that the effects observed in Figure 1B-D were not stemming from pseudotyping, we repeated the experiment using a virus harboring an autologous HIV-1 envelope. U373-derived MAGI cells (Vodicka *et al*, 1997) were infected with the replication-competent HIV-1_{NL43}. MAGI cells were transfected with the DHC-targeting siRNA or with the control siRNA and later infected with HIV-1_{NL43}, or left uninfected (Figure 1E). We used a shorter duration for the infection, as these non-pseudotyped viruses fuse primarily at the surface of cells and do not need to escape endosomes. We observed a significant increase in the amount of CA foci per cell following DHC depletion (Figure 1F). Specifically, the average number of CA foci per cell was 16.1 ± 2.3 in cells (n = 77) transfected with DHC siRNA compared to 5.4 ± 0.4 in control cells (n = 84) (P = 0.0001). CA foci were predominantly found in the vicinity of the nucleus in control cells (Luc siRNA), with a median relative distance to the nucleus of 0.30 (95% confidence interval, 0.26–0.37; n = 29 cells analyzed) (Figure 1G). As previously, DHC depletion caused a significant ($P < 0.0001$) shift in the distribution of CA cores towards the cell periphery; CA foci were found at a median relative distance of 0.70 (95% confidence interval, 0.63–0.75; n = 12 cells analyzed). These observations confirm that the effects reported in Figure 1B–D did not result from pseudotyping, and suggest that the dynein motor complex might not only be involved in the intracellular transport of CA cores (as reflected by the shift in relative distance) but also in their uncoating (as evidenced by their increased numbers). Collectively, the results shown in Figure 1 suggest that dynein motor complexes influence both HIV-1 retrograde transport and CA core stability in infected cells, irrespective of the mode of viral entry.

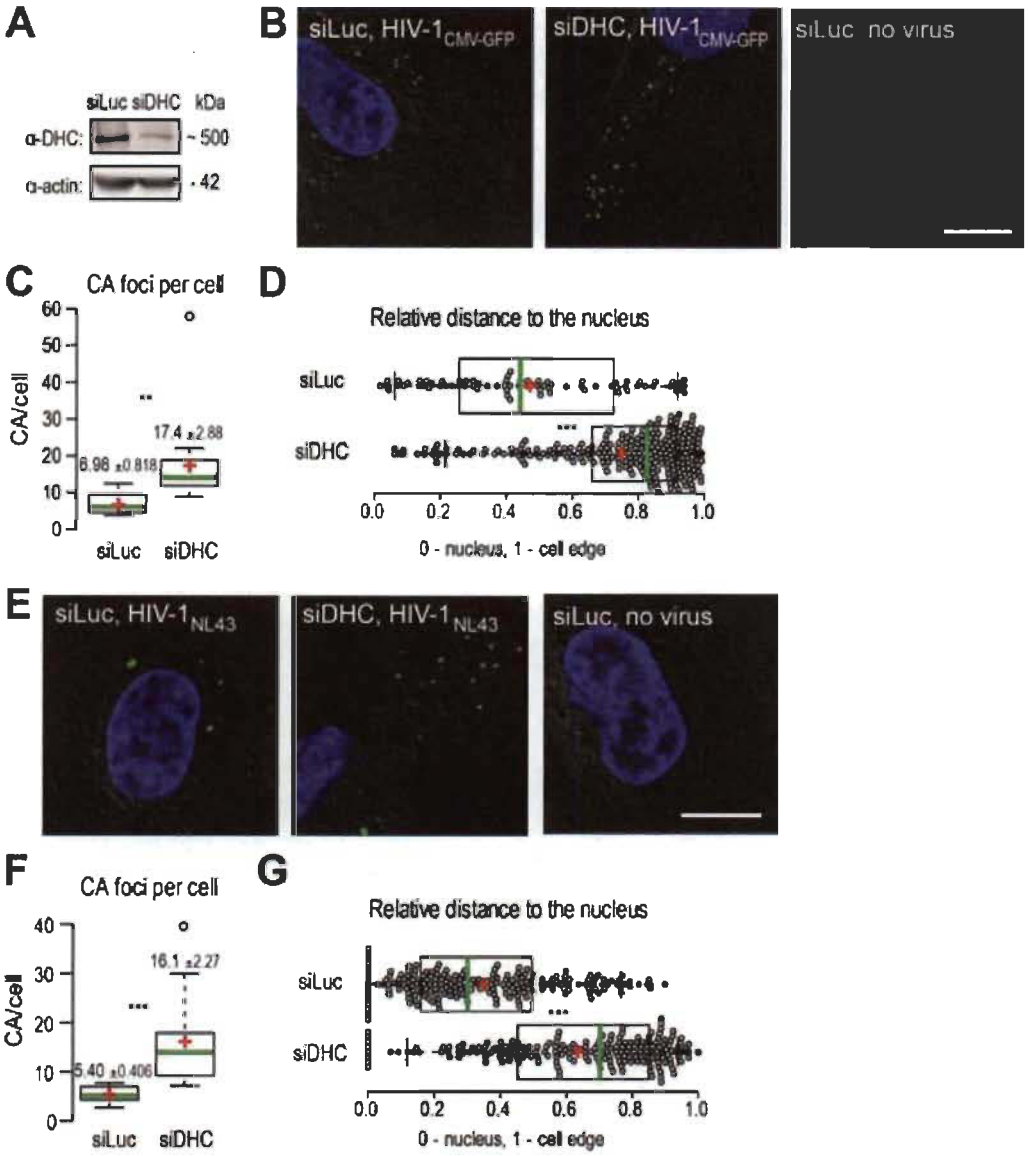

Figure 1. **Dynein heavy chain (DHC) depletion causes the accumulation of HIV-1 CA cores in infected cells and alters their subcellular distribution.**

(A) HeLa cells were transfected with siRNAs targeting either dynein heavy chain (siDHC) or luciferase (siLuc) as a control, and DHC expression was analyzed 2 days later by Western blotting; (B) Immunofluorescence microscopy observations of CA foci following infection with VSV G-pseudotyped HIV-1. HeLa cells were transfected with the indicated siRNAs and 72 h later were infected or not with VSV G-pseudotyped HIV-$1_{CMV\text{-}GFP}$ in the presence of MG132. At 4 h p.i., supernatants were replaced with virus-free medium. Cells were fixed 6 h p.i. and stained to detect CA (green) or DNA (blue). The outline of cells was revealed by low-exposure bright-field microscopy. Representative images are shown. The white bar represents 10 μm; (C) Box plots showing total amounts of CA foci per cell. The total numbers of CA foci

and nuclei in 10 randomly chosen fields were counted and the CA foci/nuclei ratios were calculated. 375 and 1047 CA foci were counted for siLuc and siDHC, respectively. Center green lines show the medians; box limits indicate the 25th and 75th percentiles as determined by R software; whiskers extend 1.5 times the interquartile range from the 25th and 75th percentiles; and red crosses represent sample means. ** indicates $P \leq 0.001$ in a Student *t*-test analysis; (D) Box plots showing the relative localization of CA foci in 10 randomly chosen cells, calculated using the formula x/(x + y) where x is the shortest distance to the nucleus edge and y is the shortest distance to the cell's edge in the two-dimensional cellular cross-section analyzed. Data points are plotted as open circles; center green lines show the medians; box limits indicate the 25th and 75th percentiles as determined by R software; whiskers extend 1.5 times the interquartile range from the 25th and 75th percentiles; and red crosses represent sample means. *** indicates $P \leq 0.0001$ in a Student *t*-test analysis; (E) Immunofluorescence microscopy observation of CA foci following infection with HIV-1 bearing an autologous envelope. MAGI cells were transfected with siDHC or siLuc prior to infection, and 72 h later were infected with HIV-1_{NL43} in the presence of MG132. Cells were fixed 2 h later and stained as in (B); The white bars represent 10 μm; (F) The total amounts of CA foci per cell were calculated as in (C); At least 250 CA foci were counted for each condition (*** indicates $P \leq 0.0001$); (G) Relative cellular distribution of CA foci, analyzed as in (D) (*** indicates $P \leq 0.0001$).

DHC Depletion Alters HIV-1 Uncoating, As Analyzed Using the Fate-of-Capsid Assay. As an independent, biochemical approach to analyze uncoating, we used the well described fate-of-capsid biochemical assay (Perron *et al*, 2004; Stremlau *et al*, 2006) that allows isolation of post-entry CA cores from infected cells, by ultracentrifugation of pre-cleared cell lysates through a sucrose cushion. This assay has been mostly used to study the destabilization of HIV-1 cores caused by TRIM5 proteins (Bérubé *et al*, 2007; Pawlica *et al*, 2014; Stremlau *et al*, 2006), but several reports established that it was a suitable tool to analyze uncoating in other contexts (Fricke *et al*, 2014; Li *et al*, 2009a; Lukic *et al*, 2014). In order to gain insight into the timing of HIV-1 uncoating and how it is affected by DHC depletion, a time-course fate-of-capsid assay was performed (Figure 2). HeLa cells transfected with siRNAs targeting either DHC or Luc were infected with equal amounts of VSV G-pseudotyped HIV-$1_{NL43\text{-}GFP}$ for a short period of time (1 h) and then lysed immediately or placed in virus-free medium and lysed at 3, 6, 12 and 24 h post infection (p.i.). This allowed us to analyze

uncoating in quasi-synchronized conditions. To track relative changes in the amounts of particulate (pelletable) CA core, samples from different time points were analyzed side by side by CA Western blotting. The CAp24 content in whole cell lysates, as analyzed at 3 h p.i., confirmed equal input (Figure 2A). To enable comparison between control and DHC-depleted conditions, equal amounts of a CAp24-containing reference sample were loaded on the different gels (Figure 2A). The amounts of particulate CAp24 determined by densitometry were then normalized to the reference sample and plotted (Figure 2B). These amounts of particulate CA likely reflect a balance between the dynamics of CA core release from endosomes and its uncoating. In the control cells transfected with Luc siRNA, the relative amounts of particulate CA peaked at 6 h p.i. but were smaller at 12 h p.i. (Figure 2A,B), suggesting that uncoating had taken place for most RTCs by that time, as expected (Arhel *et al*, 2007; Hulme *et al*, 2011). Increased levels of pelletable CA were observed at 6 h p.i. in cells transfected with DHC siRNA (Figure 2A,B). Specifically, DHC depletion increased CAp24 content in the pelletable fraction by ~1.5-fold ($P = 0.059$) relative to the control cells (Figure 2B). This is consistent with our previous report showing an increase in relative amounts of CA cores 6 h p.i. following DHC depletion or treatment with nocodazole and paclitaxel (Pawlica *et al*, 2014). Interestingly, the increase in amounts of particulate CA caused by DHC depletion appeared to be transient, suggesting that uncoating was delayed rather than fully impaired.

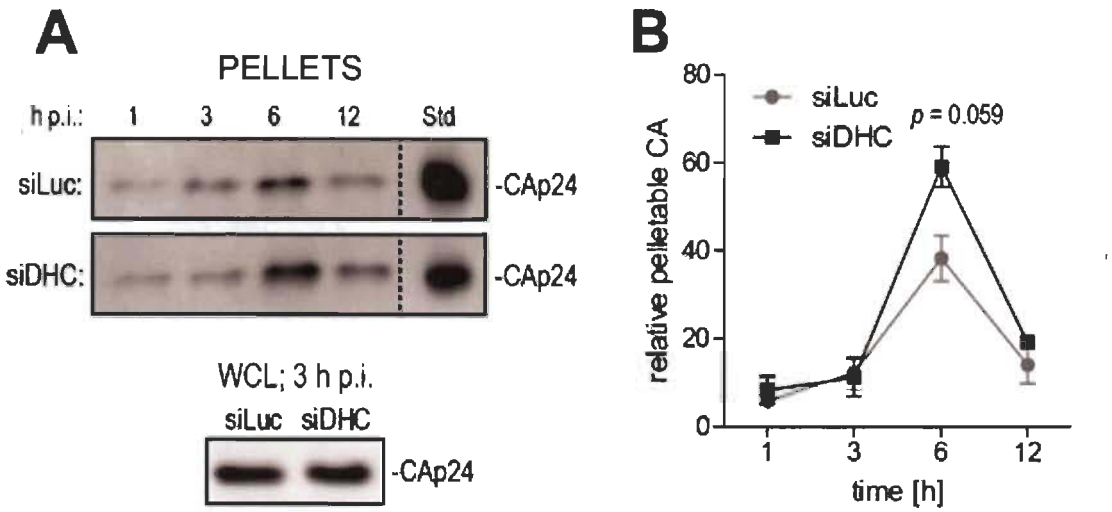

Figure 2. **DHC depletion affects HIV-1 uncoating as analyzed using the fate-of-capsid assay.**
(A) Time-course fate-of-capsid assay. HeLa cells were transfected with siRNAs targeting DHC (siDHC) or luciferase (siLuc) and then infected with HIV-$1_{NL43\text{-}GFP}$ for 1 h. Pelletable CA cores were isolated by ultracentrifugation at the indicated times after infection and analyzed by Western blotting (upper panels). Also shown is a Western blot analysis of CAp24 in whole cell lysates (WCLs) at 3 h p.i. (lower panel). Identical amounts of a control CAp24-containing sample were included in each gel as an internal standard ('Std'); (B) Bands corresponding to pelletable CAp24 were quantified by densitometry up to 12 h p.i. and plotted after normalization to the standard. Mean values from two independent experiments are shown, with standard errors of the mean (SEM).

Disruption of the dynactin complex interferes with HIV-1 uncoating. As an additional approach to disrupt dynein-dependent transport, we over-expressed p50/dynamitin (p50), a subunit of the dynactin complex responsible for binding cargos to the dynein motor. p50 over-expression results in the disassembly of the dynactin complex, thereby disrupting cargo binding to the dynein motor and inhibiting dynein-dependent transport (Burkhardt *et al*, 1997; Melkonian *et al*, 2007). The efficiency of p50 transfection was confirmed by Western blotting (Figure 3A). We analyzed the effect of p50 over-expression on HIV-1 uncoating at 6 h p.i., since the maximal effect of DHC depletion on CA cores was observed at this time point (Figure 2). As a control, we used the small-molecule CA inhibitor PF-3450074 (PF74), known to disrupt HIV-1 infectivity through destabilization of the CA core (Shi *et al*, 2011). p50 transfection resulted in increased amounts of pelletable CA cores isolated at 6 h p.i. from cells

infected with HIV-$1_{NL43\text{-}GFP}$ (Figure 3B). The pellet/whole cell lysate ratio was 2.3-fold (± 0.097, n = 2) higher than for control cells transfected with an irrelevant plasmid (Figure 3C). As expected, PF-3450074 caused a decrease (3.7-fold) in the amounts of pelletable CA (Figure 3B,C). p50 transfection had no significant effect on HIV-1 infectivity, while PF-3450074 decreased permissiveness to HIV-1 by ~150- to ~550-fold, depending on the MOI used (Figure 3D) and as previously reported (Blair *et al*, 2010). These results confirm that disruption of dynein-dependent transport counteracts uncoating, but the lack of an effect on infectivity suggests that uncoating is delayed rather than permanently impaired.

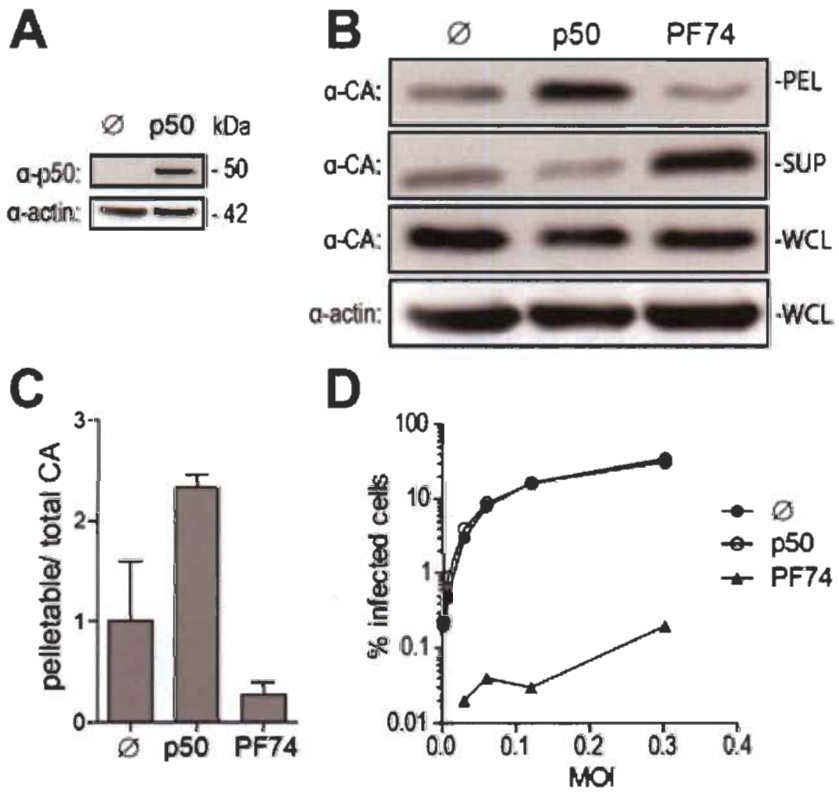

Figure 3. **Over-expression of p50/dynamitin affects HIV-1 uncoating.**
(A) Western blot analysis of p50 and actin expression in HeLa cells 2 days after transfection with a plasmid encoding p50 or an irrelevant plasmid (pMIP; ø); (B,C) Fate-of-capsid analysis; (B) HeLa cells transfected with a p50 expression construct or with pMIP (ø), or treated with 10 μM of PF-3450074 (PF74), were infected two days later with HIV-$1_{NL43\text{-}GFP}$. Supernatants were replaced with virus-free media, containing PF-3450074 where applicable, at 1 h p.i. and fate-of-capsid

was performed at 6 h p.i. Shown are Western blot analyses of CAp24 in pellets and whole cell lysates (WCLs). Levels of actin in whole cell lysates were also analyzed; (C) CAp24 bands were quantified by densitometry in two independent experiments, and pelletable/whole cell lysate ratios were calculated and are shown as -fold changes relative to the untreated control, with standard deviations; (D) Infectivity. HeLa cells treated as in (B) were infected with increasing amounts of HIV-$1_{NL43\text{-}GFP}$. Supernatants were replaced with virus-free, drug-free medium 16 h p.i. The percentages of GFP-expressing cells were analyzed 2 days p.i. by flow cytometry.

Dynein Depletion Reduces HIV-1 cDNA Levels. HIV-1 RT was suggested to be linked to uncoating of its CA core, as increased stabilization of CA cores was observed following inhibition of RT (Hulme *et al*, 2011; Yang *et al*, 2013). We therefore asked whether RT would be affected by treatments that have a stabilizing effect on CA cores. Quantitative PCR (qPCR) was performed on DNA isolated at various times from HeLa cells subjected or not to DHC depletion and infected with HIV-$1_{NL43\text{-}GFP}$. GFP DNA was quantified as a marker for late viral reverse transcribed DNA (Figure 4A). In control cells transfected with Luc siRNA, RT product levels peaked at 6 to 9 h p.i., which is consistent with previous reports (Butler *et al*, 2001; Kim *et al*, 1989; Zennou *et al*, 2000). In cells expressing owl monkey TRIMCyp, or treated with nevirapine, viral RT products were undetectable as expected (Bérubé *et al*, 2007) (Figure 4A). RT product levels in DHC-depleted cells at 6 hours p.i. were 0.65-fold ± 0.027 those in the control cells, a small but significant decrease. However, no reduction was apparent at 12 h p.i., suggesting that the defect in RT was transient, consistent with the uncoating results in Figure 2. We also analyzed 2-LTR circular RT products, which are a marker for nuclear reverse transcribed HIV-1 DNA (Pauza *et al*, 1994). Less 2-LTR products were detected in DHC-depleted cells compared with the control cells at early time-points, but no difference was seen at 12 h p.i. (Figure 4B). Altogether, our results suggest that a transient decrease (or delay) in uncoating is associated with a transient RT defect.

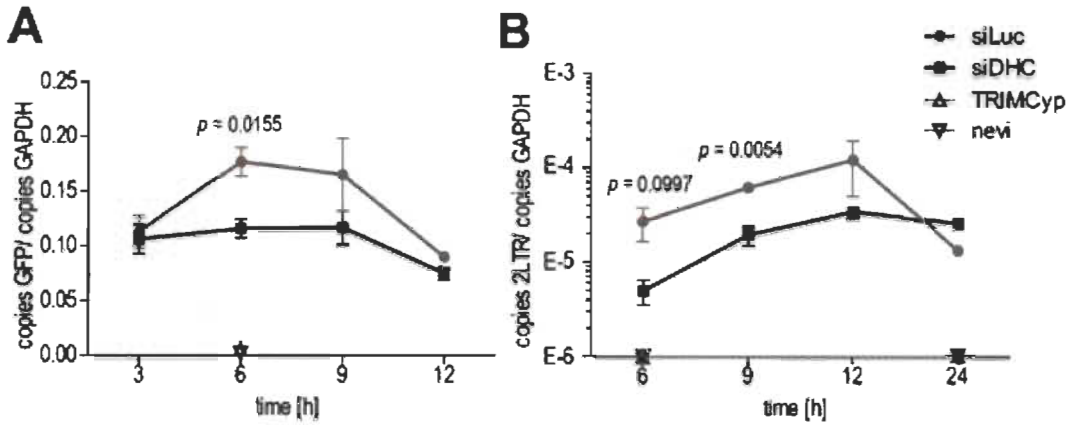

Figure 4. **DHC depletion reduces levels of HIV-1 reverse transcribed DNA.** (A,B) HeLa cells transfected with siRNAs targeting DHC (siDHC) or luciferase (siLuc), or treated with the RT inhibitor nevirapine (nevi; 20 μM), or stably expressing TRIMCyp (TCyp) were infected with HIV-$1_{NL43\text{-}GFP}$. Supernatants were removed 3 h p.i. and replaced with virus-free media containing the appropriate drugs; Total DNAs were extracted at 3, 6, 9, 12 and 24 h p.i. and quantitative PCR (qPCR) was performed to detect GFP as a marker for RT (A), or 2-LTR circles as a marker for nuclear transport (B). GAPDH DNA was quantified for normalization purposes. The results are presented as ratios of GFP copies/GAPDH copies or 2-LTR copies/GAPDH copies. Shown are the means with SEM for each time point, from triplicate infections.

A.5 Discussion

Previous articles showed that HIV-1 uncoating could be modulated by CA interactions with cellular factors such as CPSF6 (De Iaco *et al*, 2013) and cyclophilin A (Li *et al*, 2009b). In this article, we present data suggesting that functional disruption of cytoplasmic dynein transiently increases the amounts of HIV-1 CA cores in cells, most likely reflecting delayed uncoating caused by inhibition of their transport towards the nucleus. These observations are in agreement with a recent report by the Campbell laboratory (Lukic *et al*, 2014). In this latter study, the authors similarly observed a delay in uncoating when dynein was targeted using siRNAs, as analyzed using a fate-of-capsid assay and also using an elegant 'CsA withdrawal' assay that takes advantage of the fact that only intact CA cores can be inhibited by the restriction factor TRIMCyp in Owl monkey cells (Hulme *et al*, 2011; Hulme *et al*, 2014; Yufenyuy *et al*, 1013). Our p50 over-expression experiment provides additional evidence for the involvement of dynein

in HIV-1 uncoating. As observed using immunofluorescence microscopy, DHC depletion significantly increased the amounts of CA foci and resulted in their accumulation in the cell's periphery. These results are consistent with the hypothesis that HIV-1 can use dynein motors to translocate on microtubules towards the nucleus (McDonald *et al*, 2002). Furthermore, fate-of-capsid experiments revealed that DHC depletion and disruption of dynein-dependent transport by p50 over-expression transiently increased the amounts of CA cores. Thus, dynein motor complexes seem to be involved in both HIV-1 trafficking and in its uncoating, supporting the idea that the two processes are related (Ambrose *et al*, 2014; Fassati *et al*, 2012; Arhel, 2010). Along these lines, other authors previously reported that decreased uncoating resulting from mutations in CA correlated with decreased nuclear transport (De Iaco *et al*, 2014; Dismuke *et al*, 2006). Consistently, mutations in CA affect the process of nuclear transport or the involvement of specific cellular factors in this process (Dismuke *et al*, 2006; Krishnan *et al*, 2010; Meehan *et al*, 2014). Binding of the HIV-1 CA protein, as part of intact CA cores, to the nucleopore protein NUP358 could trigger an uncoating step (Bichel *et al*, 2013). Collectively, these observations suggest that dynein complexes contribute indirectly to uncoating by transporting the HIV-1 CA core to the vicinity of nucleopores where key uncoating steps occur. Interestingly, a member of the PDZ domain-containing family, the putative microtubule-interacting protein PDZD8, was recently reported to stabilize HIV-1 CA cores (Guth & Sodroski, 2013), raising the possibility that HIV-1 uncoating is actively inhibited during transport. Whether dynein complexes are involved in this stabilization remains to be investigated.

Neither DHC depletion (not shown) nor p50 over-expression (Figure 3) had a significant effect on HIV-1 infectivity in HeLa cells, as we previously reported (Pawlica *et al*, 2014) and consistent with the fact that the effects of these interventions on uncoating and RT seem to be transient (Figures 2 and 4). Although the effect of counteracting dynein on HIV-1 transport has long been known from live microscopy-based evidence (Mcdonald *et al*, 2002), it was not clear whether inhibiting dynein completely disrupts HIV-1 transport, and our results suggest that it does not. In their recent paper, however, Lukic *et al.* (2014) showed that pharmacological inhibition of

cytoplasmic dynein by Ciliobrevin D does decrease infectivity. Why does this drug have an effect on infectivity while two genetic approaches (DHC knockdown and p50 over-expression) do not, is unclear, but one could propose off-target effects of the drug on infectivity, independent of its effect on dynein. It is equally possible, however, that our genetic interventions did not fully disrupt dynein function and that low levels of cytoplasmic dynein complexes are sufficient to achieve transport, although in a delayed fashion. Alternatively, it is possible that HIV-1 CA core retrograde transport can proceed in the absence of functional dynein, albeit less efficiently, by dynein-independent or even microtubule-independent mechanisms, such as translocation on actin microfilaments (Yoder *et al*, 2011).

A.6 Methods

Cells, pharmaceuticals and antibodies. Human embryonic kidney 293T (HEK293T) cells, epithelial carcinoma HeLa cells and human U373-derived MAGI cells (Vodicka *et al*, 1997) were maintained in Dulbecco's modified Eagle's medium (DMEM) with high glucose, supplemented with 10% fetal bovine serum (FBS) and antibiotics at 37 °C, 5% CO_2. HeLa cells retrovirally transduced to stably express owl monkey TRIMCyp were described before before (Bérubé *et al*, 2007; Nepveu-Traversy *et al*, 2009). All cell culture reagents were from HyClone (Thermo Scientific, Logan, UT, USA). MG132 was from Sigma (St Louis, MI, USA), nevirapine (cat#4666) was from the AIDS Research and Reference Reagent Program, while PF-3450074 was provided by Pfizer (New York, NY, USA). Rabbit polyclonal antibodies against dynein heavy chain and p50/dynamitin were from Santa Cruz (Dallas, TX, USA) and Millipore (Billerica, MA, USA), respectively. Capsid (CA, p24) was detected using a mouse monoclonal antibody (clone 183, cat#3537) from the AIDS Research and Reference Reagent Program. The HRP-conjugated mouse anti-actin antibody was from Sigma. HRP-conjugated goat anti-rabbit and goat anti-mouse antibodies used as secondary antibodies in Western blots were from Santa Cruz.

Plasmid DNAs and retrovirus production. p50/dynamitin-HA was a gift from Tina Schroer (Schrader *et al*, 2000). To produce viral vectors, 10-cm culture dishes or 75-cm flasks of sub-confluent HEK293T cells were co-transfected using polyethylenimine (PEI; MW 25,000, Polyscience, Niles, IL, USA) with the appropriate plasmids, as follows: for the replication-competent HIV-1_{NL43}, 20 μg of pNL4-3; for the viral vector HIV-$1_{CMV\text{-}GFP}$, pTRIP-CMV-GFP (10 μg), pΔR8.9 (10 μg) and pMD-G (5 μg); for HIV-$1_{NL43\text{-}GFP}$, pNL-GFP (10 μg) and pMD-G (5 μg) (Berthoux *et al*, 2003; He *et al*, 1997; Naviaux *et al*, 1996; Zufferey *et al*, 1997). Media were changed 16 h post transfection and virus-containing supernatants were collected after an additional 1.5 days of culture. Viral stocks were clarified by centrifugation for 5 min at 400 × *g*.

Viral challenges. 10^6 cells seeded in a 10-cm dish were PEI transfected with 5 μg of p50/dynamitin-HA or an irrelevant plasmid (pMIP). 24 h later cells were seeded in 24-well plates at 2×10^5 cells per well and challenged with GFP-expressing viral vectors the next day. Where applicable, cells were pre-treated for 15 min with PF-3450074, and supernatants were replaced with fresh medium 16 h post infection (p.i.) Cells were trypsinized 48 h p.i. and fixed in 2% formaldehyde (Fisher Scientific, Waltham, MA, USA). The percentages of GFP-positive cells were then determined by analyzing 10^4 to 3×10^4 cells on a FC500 MPL cytometer (Beckman Coulter, Brea, CA, USA) using the CXP Software (Beckman Coulter).

siRNA transfection. 10^6 cells were seeded in a 10-cm dish in Opti-MEM (Gibco, Carlsbad, CA, USA) and transfected the next day with 40 nM of siRNA using DharmaFECT 1 (Dharmacon, Lafayette, CO, USA). The siRNA targeting the sequence 5'GATCAAACATGACGGAATT of (DHC), has been described before (Lehmann *et al*, 2009; Pawlica *et al*, 2014) and was purchased from Qiagen (Venlo, The Netherlands). A control siRNA (5'CGTACGCGGAATACTTCGATT) targeting the luciferase mRNA (Pawlica *et al*, 2014) was purchased from Dharmacon. 48 h post transfection, cells were seeded for the experiments.

Immunofluorescence (IF) microscopy. HeLa and MAGI cells were siRNA-transfected as detailed above. 72 h later, 2×10^5 cells were seeded on glass coverslips placed in 3.5-cm wells and were infected the next day at a multiplicity of infection (MOI) of ~1 with vesicular stomatitis virus glycoprotein (VSV G)-pseudotyped HIV-$1_{CMV\text{-}GFP}$ (HeLa) or replication-competent HIV-1_{NL43} (MAGI) in the presence of 1 μg/mL MG132. Infections were carried out for 2 h (HIV-1_{NL43}) or 4 h followed by a 2-h incubation in fresh medium (HIV-$1_{CMV\text{-}GFP}$). Cells were then fixed for 30 min in 4% formaldehyde-DMEM, followed by 3 washes with ice-cold phosphate buffer saline (PBS) and permeabilized for 2 min on ice in 0.1% Triton X-100, 0.1 mM sodium citrate. Cells were then washed again three times with PBS and treated with 10% normal goat serum (Sigma, St Louis, MI) containing 0.3 M glycine (Sigma) for 30 min at room temperature. This was followed by a 4-h incubation with antibodies against CA (1:100 dilution) in PBS containing 10% normal goat serum. Cells were washed five times and fluorescently stained with AlexaFluor488-conjugated goat anti-mouse (Molecular Probes, Eugene, OR, USA) diluted 1:200 in normal goat serum-containing PBS. Cells were then washed five times in PBS before mounting in Vectashield (Vector Laboratories, Peterborough, UK). Hoechst33342 (0.8 μg/mL; Molecular Probes) was added along with the penultimate PBS wash to reveal DNA. Z-stacks were acquired on an AxioObserver Microscope (Carl Zeiss Canada, Jena, Germany) equipped with the ApoTome module, and the median optical slice of each Z-stack was analyzed. For the calculation of relative distances to the nucleus, we proceeded as described previously (Pawlica *et al*, 2014). The nucleus edge was defined using Hoechst33342 staining, while the cell's edge was visualized by bright field microscopy. The shortest distances to the nucleus edge and to the cell's edge were calculated in 2D images of median optical slices and thus represent apparent, rather than real, shortest distances.

Fate-of-capsid assay. To analyze post-entry CA uncoating, a protocol adapted from Perron *et al* (Perron *et al*, 2004) was used and has been described in details before (Bérubé *et al*, 2007; Pawlica *et al*, 2014). 4×10^6 HeLa cells, previously transfected with siRNAs or p50 as described above, were seeded in 10-cm dishes. The next day, if applicable, cells were pretreated 15 min with PF-3450074 and infected with

HIV-$1_{NL43\text{-}GFP}$ at a MOI of ~2 and in presence or absence of PF-3450074. Supernatants were replaced with fresh media, containing PF-3450074 or not, 1 h p.i. Cells were collected by trypsinization at different time points, washed in ice-cold PBS and resuspended in 1.5 mL of ice-cold lysis buffer (100 µM Tris-HCl (pH 8.0), 0.4 mM KCl, 2 µM EDTA, Roche's Complete protease inhibitor) and disrupted with a Dounce homogenizer. Whole cell lysate samples were collected at this point. Lysates were centrifuged for 5 min 1000 × *g*, 4°C to remove cell debris and nuclei, and supernatants were layered on top of a 50% sucrose cushion prepared in STE buffer (100 mM NaCl, 10 mM Tris-HCl (pH 8.0), 1 mM EDTA). Particulate viral cores were sedimented by ultracentrifugation in a Sorval WX Ultra 100 ultracentrifuge at 175,000 × *g* for 2 h at 4 °C. Pellets were resuspended in 80 µL of 1X denaturing loading buffer and processed for CA Western blotting together with whole cell lysates.

Quantitative PCR of HIV-1 DNA. Cells were seeded in 12-well plates at 3×10^5 cells/well and infected with HIV-$1_{NL43\text{-}GFP}$ (MOI ~0.03 as calculated on the control permissive cells) depleted or not of DHC, as detailed above. Prior to infection, viral stocks were passed through 0.45-µm filters and pretreated for 1 h at 37 °C with 20 U/mL DNAse I (New England Biolabs) to prevent contamination by carry-over plasmid DNA. After 3 h, supernatants were replaced with fresh media, and cellular DNAs were isolated at various times using the DNeasy Blood and Tissue Kit (Qiagen, CA, USA). Purified DNAs were digested with 0.25 µL of DpnI (20 U/µL, New England Biolabs) for 1 h at 37 °C to help remove any remaining plasmid DNA. The absence of such contaminant DNA was verified by performing control infections in the presence of 80 µM of the RT inhibitor nevirapine. The primers and reaction conditions for detecting GFP, 2-LTR and GAPDH have been previously described (Veillette *et al*, 2013). In each experiment, a standard curve of the amplicon being measured was run in duplicates ranging from 30 to 3×10^5 copies plus a no-template control. Reactions contained 1x SensiFAST SYBR Lo-Rox (Bioline, UK), 300 nM forward and reverse primers, and 100–300 ng template DNA. Results were analyzed with the MxPro software (Agilent Technologies, CA, USA). Computed values for GFP and 2-LTR copy numbers were normalized to the amounts of GAPDH copy numbers for each sample.

Statistical analysis. All statistical analyses were done using GraphPad Prism version 5.00 for Windows, GraphPad Software, San Diego California USA, www.graphpad.com. The box blot representations in Figure 1 were generated using the R software (Spitzer et al, 2014).

A.7 Acknowledgements

We thank Mélodie B. Plourde and Natacha Mérindol for a critical reading of this manuscript. We thank Réjean Cantin, Maxime Veillette and Mélodie B. Plourde for providing technical help. We are grateful to Trina Schroer (Johns Hopkins University) for sharing plasmid DNA. We thank Michel J. Tremblay (Centre de Recherche du CHU de l'université Laval) for allowing us to use his BSLIII laboratory facilities. The following reagents were obtained through the NIH AIDS Research and Reference Reagent Program, Division of AIDS, NIAID, NIH: nevirapine (cat#4666) and clone 183 p24 antibody (cat#3537, contributed by Bruce Chesebro). PF-3450074 was a gift from Pfizer. This work was supported by Canadian Institutes of Health Research operating grant MOP-102712 (L.B.).

A.8 References

Ambrose Z, Aiken C (2014) HIV-1 uncoating: connection to nuclear entry and regulation by host proteins. *Virology* 454-455: 371-9

Arhel NJ, Souquere-Besse S, Munier S, Souque P, Guadagnini S, Rutherford S, Prevost MC, Allen TD, Charneau P (2007) HIV-1 DNA Flap formation promotes uncoating of the pre-integration complex at the nuclear pore. *The European Molecular Biology Organization journal* 26: 3025-3037

Auewarakul P, Wacharapornin P, Srichatrapimuk S, Chutipongtanate S, Puthavathana P (2005) Uncoating of HIV-1 requires cellular activation. *Virology* 337: 93-101

Berthoux L, Towers GJ, Gurer C, Salomoni P, Pandolfi PP, Luban J (2003) As(2)O(3) enhances retroviral reverse transcription and counteracts Ref1 antiviral activity. *Journal of virology* 77: 3167-3180

Bérubé J, Bouchard A, Berthoux L (2007) Both TRIM5alpha and TRIMCyp have only weak antiviral activity in canine D17 cells. *Retrovirology* 4: 68

Blair WS, Pickford C, Irving SL, Brown DG, Anderson M, Bazin R, Cao J, Ciaramella G, Isaacson J, Jackson L, Hunt R, Kjerrstrom A, Nieman JA, Patick AK, Perros M, Scott AD, Whitby K, Wu H, Butler SL (2010) HIV capsid is a tractable target for small molecule therapeutic intervention. *PLoS Pathogens* 6: e1001220

Blumenthal R, Bali-Puri A, Walter A, Covell D, Eidelman O (1987) pH-dependent fusion of vesicular stomatitis virus with Vero cells. Measurement by dequenching of octadecyl rhodamine fluorescence. *The Journal of biological chemistry* 262: 13614-13619

Briggs JA, Krausslich HG (2011) The molecular architecture of HIV. *Journal of molecular biology* 410: 491-500

Briggs JA, Wilk T, Welker R, Krausslich HG, Fuller SD (2003) Structural organization of authentic, mature HIV-1 virions and cores. *The European Molecular Biology Organization journal* 22: 1707-1715

Burkhardt JK, Echeverri CJ, Nilsson T, Vallee RB (1997) Overexpression of the dynamitin (p50) subunit of the dynactin complex disrupts dynein-dependent maintenance of membrane organelle distribution. *The Journal of cell biology* 139: 469-484

Butler SL, Hansen MS, Bushman FD (2001) A quantitative assay for HIV DNA integration in vivo. *Nature Medicine* 7: 631-634

Campbell EM, Perez O, Anderson JL, Hope TJ (2008) Visualization of a proteasome-independent intermediate during restriction of HIV-1 by rhesus TRIM5alpha. *The Journal of cell biology* 180: 549-561

Campbell EM, Perez O, Melar M, Hope TJ (2007) Labeling HIV-1 virions with two fluorescent proteins allows identification of virions that have productively entered the target cell. *Virology* 360: 286-293

Cureton DK, Massol RH, Saffarian S, Kirchhausen TL, Whelan SP (2009) Vesicular stomatitis virus enters cells through vesicles incompletely coated with clathrin that depend upon actin for internalization. *PLoS Pathogens* 5: e1000394

De Iaco A, Santoni F, Vannier A, Guipponi M, Antonarakis S, Luban J (2013) TNPO3 protects HIV-1 replication from CPSF6-mediated capsid stabilization in the host cell cytoplasm. *Retrovirology* 10: 20

Forshey BM, von Schwedler U, Sundquist WI, Aiken C (2002) Formation of a human immunodeficiency virus type 1 core of optimal stability is crucial for viral replication. *Journal of virology* 76: 5667-5677

Fricke T, White TE, Schulte B, de Souza Aranha Vieira DA, Dharan A, Campbell EM, Brandariz-Nunez A, Diaz-Griffero F (2014) MxB binds to the HIV-1 core and prevents the uncoating process of HIV-1. *Retrovirology* 11: 68

Gamble TR, Yoo S, Vajdos FF, von Schwedler UK, Worthylake DK, Wang H, McCutcheon JP, Sundquist WI, Hill CP (1997) Structure of the carboxyl-terminal dimerization domain of the HIV-1 capsid protein. *Science* 278: 849-853

Gaudin R, Alencar BC, Arhel N, Benaroch P (2013) HIV trafficking in host cells: motors wanted! *Trends in cell biology* 23: 652-662

Goff SP (2001) Intracellular trafficking of retroviral genomes during the early phase of infection: viral exploitation of cellular pathways. *The journal of gene medicine* 3: 517-528

Guth CA, Sodroski J (2014) Contribution of PDZD8 to Stabilization of the Human Immunodeficiency Virus (HIV-1) Capsid. *Journal of virology* 88: 4612-4623

He J, Chen Y, Farzan M, Choe H, Ohagen A, Gartner S, Busciglio J, Yang X, Hofmann W, Newman W, Mackay CR, Sodroski J, Gabuzda D (1997) CCR3 and CCR5 are co-receptors for HIV-1 infection of microglia. *Nature* 385: 645-649

Hulme AE, Perez O, Hope TJ (2011) Complementary assays reveal a relationship between HIV-1 uncoating and reverse transcription. *Proceedings of the National Academy of Sciences of the United States of America* 108: 9975-9980

Kim SY, Byrn R, Groopman J, Baltimore D (1989) Temporal aspects of DNA and RNA synthesis during human immunodeficiency virus infection: evidence for differential gene expression. *Journal of virology* 63: 3708-3713

Lakadamyali M, Rust MJ, Zhuang X (2006) Ligands for clathrin-mediated endocytosis are differentially sorted into distinct populations of early endosomes. *Cell* 124: 997-1009

Lehmann M, Milev MP, Abrahamyan L, Yao XJ, Pante N, Mouland AJ (2009) Intracellular transport of human immunodeficiency virus type 1 genomic RNA and viral production are dependent on dynein motor function and late endosome positioning. *The Journal of biological chemistry* 284: 14572-14585

Li Y, Kar AK, Sodroski J (2009a) Target Cell Type-Dependent Modulation of Human Immunodeficiency Virus (HIV-1) Capsid Disassembly by Cyclophilin A. *Journal of virology* 83: 10951-10962

Li Y, Kar AK, Sodroski J (2009b) Target cell type-dependent modulation of human immunodeficiency virus type 1 capsid disassembly by cyclophilin A. *Journal of virology* 83: 10951-10962

Lukic Z, Dharan A, Fricke T, Diaz-Griffero F, Campbell EM (2014) HIV-1 Uncoating is Facilitated by Dynein and Kinesin-1. *Journal of virology* 88: 8911-23

McDonald D, Vodicka MA, Lucero G, Svitkina TM, Borisy GG, Emerman M, Hope TJ (2002) Visualization of the intracellular behavior of HIV in living cells. *The Journal of cell biology* 159: 441-452

Melkonian KA, Maier KC, Godfrey JE, Rodgers M, Schroer TA (2007) Mechanism of dynamitin-mediated disruption of dynactin. *The Journal of biological chemistry* 282: 19355-19364

Naviaux RK, Costanzi E, Haas M, Verma IM (1996) The pCL vector system: rapid production of helper-free, high-titer, recombinant retroviruses. *Journal of virology* 70: 5701-5705

Nepveu-Traversy ME, Berube J, Berthoux L (2009) TRIM5alpha and TRIMCyp form apparent hexamers and their multimeric state is not affected by exposure to restriction-sensitive viruses or by treatment with pharmacological inhibitors. *Retrovirology* 6: 100

Pauza CD, Trivedi P, McKechnie TS, Richman DD, Graziano FM (1994) 2-LTR circular viral DNA as a marker for human immunodeficiency virus type 1 infection in vivo. *Virology* 205: 470-478

Pawlica P, Le Sage V, Poccardi N, Tremblay MJ, Mouland AJ, Berthoux L (2014) Functional evidence for the involvement of microtubules and dynein motor complexes in TRIM5alpha-mediated restriction of retroviruses. *Journal of virology* 88: 5661-5676

Perron MJ, Stremlau M, Song B, Ulm W, Mulligan RC, Sodroski J (2004) TRIM5alpha mediates the postentry block to N-tropic murine leukemia viruses in human cells. *Proceedings of the National Academy of Sciences of the United States of America* 101: 11827-11832

Pornillos O, Ganser-Pornillos BK, Kelly BN, Hua Y, Whitby FG, Stout CD, Sundquist WI, Hill CP, Yeager M (2009) X-ray structures of the hexameric building block of the HIV capsid. *Cell* 137: 1282-1292

Pornillos O, Ganser-Pornillos BK, Yeager M (2011) Atomic-level modelling of the HIV capsid. *Nature* 469: 424-427

Rasaiyaah J, Tan CP, Fletcher AJ, Price AJ, Blondeau C, Hilditch L, Jacques DA, Selwood DL, James LC, Noursadeghi M, Towers GJ (2013) HIV-1 evades innate immune recognition through specific cofactor recruitment. *Nature* 503: 402-405

Roa A, Hayashi F, Yang Y, Lienlaf M, Zhou J, Shi J, Watanabe S, Kigawa T, Yokoyama S, Aiken C, Diaz-Griffero F (2012) RING domain mutations uncouple TRIM5alpha restriction of HIV-1 from inhibition of reverse transcription and acceleration of uncoating. *Journal of virology* 86: 1717-1727

Sabo Y, Walsh D, Barry DS, Tinaztepe S, de Los Santos K, Goff SP, Gundersen GG, Naghavi MH (2013) HIV-1 induces the formation of stable microtubules to enhance early infection. *Cell host & microbe* 14: 535-546

Sayah DM, Sokolskaja E, Berthoux L, Luban J (2004) Cyclophilin A retrotransposition into TRIM5 explains owl monkey resistance to HIV-1. *Nature* 430: 569-573

Schaller T, Ocwieja KE, Rasaiyaah J, Price AJ, Brady TL, Roth SL, Hue S, Fletcher AJ, Lee K, KewalRamani VN, Noursadeghi M, Jenner RG, James LC, Bushman FD, Towers GJ (2011) HIV-1 capsid-cyclophilin interactions determine nuclear import pathway, integration targeting and replication efficiency. *PLoS Pathogens* 7: e1002439

Schrader M, King SJ, Stroh TA, Schroer TA (2000) Real time imaging reveals a peroxisomal reticulum in living cells. *Journal of cell science* 113 (Pt 20): 3663-3671

Shah VB, Shi J, Hout DR, Oztop I, Krishnan L, Ahn J, Shotwell MS, Engelman A, Aiken C (2013) The host proteins transportin SR2/TNPO3 and cyclophilin A exert opposing effects on HIV-1 uncoating. *Journal of Virology* 87: 422-432

Shi J, Zhou J, Shah VB, Aiken C, Whitby K (2011) Small-molecule inhibition of human immunodeficiency virus type 1 infection by virus capsid destabilization. *Journal of virology* 85: 542-549

Slonska A, Polowy R, Golke A, Cymerys J (2012) Role of cytoskeletal motor proteins in viral infection. *Postępy Higieny i Medycyny Doświadczalnej (Online)* 66: 810-817

Spitzer M, Wildenhain J, Rappsilber J, Tyers M (2014) BoxPlotR: a web tool for generation of box plots. *Nature methods* 11: 121-122

Stremlau M, Owens CM, Perron MJ, Kiessling M, Autissier P, Sodroski J (2004) The cytoplasmic body component TRIM5alpha restricts HIV-1 infection in Old World monkeys. *Nature* 427: 848-853

Stremlau M, Perron M, Lee M, Li Y, Song B, Javanbakht H, Diaz-Griffero F, Anderson DJ, Sundquist WI, Sodroski J (2006) Specific recognition and accelerated uncoating of retroviral capsids by the TRIM5alpha restriction factor. *Proceedings of the National Academy of Sciences of the United States of America* 103: 5514-5519

Sun X, Yau VK, Briggs BJ, Whittaker GR (2005) Role of clathrin-mediated endocytosis during vesicular stomatitis virus entry into host cells. *Virology* 338: 53-60

Veillette M, Bichel K, Pawlica P, Freund SM, Plourde MB, Pham QT, Reyes-Moreno C, James LC, Berthoux L (2013) The V86M mutation in HIV-1 capsid confers resistance to TRIM5alpha by abrogation of cyclophilin A-dependent restriction and enhancement of viral nuclear import. *Retrovirology* 10: 25

Vodicka MA, Goh WC, Wu LI, Rogel ME, Bartz SR, Schweickart VL, Raport CJ, Emerman M (1997) Indicator cell lines for detection of primary strains of human and simian immunodeficiency viruses. *Virology* 233: 193-198

Yang Y, Fricke T, Diaz-Griffero F (2013) Inhibition of reverse transcriptase activity increases stability of the HIV-1 core. *Journal of virology* 87: 683-687

Yoder A, Guo J, Yu D, Cui Z, Zhang XE, Wu Y (2011) Effects of microtubule modulators on HIV-1 infection of transformed and resting CD4 T cells. *Journal of virology* 85: 3020-3024

Zennou V, Petit C, Guetard D, Nerhbass U, Montagnier L, Charneau P (2000) HIV-1 genome nuclear import is mediated by a central DNA flap. *Cell* 101: 173-185

Zhang H, Dornadula G, Orenstein J, Pomerantz RJ (2000) Morphologic changes in human immunodeficiency virus type 1 virions secondary to intravirion reverse transcription: evidence indicating that reverse transcription may not take place within the intact viral core. *Journal of human virology* 3: 165-172

Zhang H, Dornadula G, Pomerantz RJ (1998) Natural endogenous reverse transcription of HIV-1. *Journal of reproductive immunology* 41: 255-260

Zhou L, Sokolskaja E, Jolly C, James W, Cowley SA, Fassati A (2011) Transportin 3 promotes a nuclear maturation step required for efficient HIV-1 integration. *PLoS Pathogens* 7: e1002194

Zufferey R, Nagy D, Mandel RJ, Naldini L, Trono D (1997) Multiply attenuated lentiviral vector achieves efficient gene delivery in vivo. *Nature Biotechnology* 15: 871-875

The following study, published in Journal of general virology, demonstrates that the involvement of microtubules and dynein motor complexes in the restriction mediated by owl monkey TRIMCyp is cellular context-specific.

ANNEX B

INHIBITION OF MICROTUBULES AND DYNEIN RESCUES HIV-1 FROM OWL MONKEY TRIMCYP-MEDIATED RESTRICTION IN A CELLULAR CONTEXT-SPECIFIC FASHION

PAULINA PAWLICA, CAROLINE DUFOUR, LIONEL BERTHOUX

Published on 25th of November 2014 in *Journal of General Virology*

B.1 Contributions

L.B. and P.P. designed the study and interpreted the results. P.P. performed 80% of the experiments. L.B. prepared the manuscript.

B.2 Summary

Interferon-induced restriction factors can significantly affect the replicative capacity of retroviruses in mammals. Tripartite motif protein 5, isoform α (TRIM5α) is a restriction factor that acts at early stages of the virus life cycle by intercepting and destabilizing incoming retroviral cores. Sensitivity to TRIM5α maps to the N-terminal domain of the retroviral capsid (CA) proteins. In several New World and Old World monkey species, independent events of retrotransposon-mediated insertion of the cyclophilin A (CypA) coding sequence in the trim5 gene have given rise to TRIMCyp (also called TRIM5-CypA), a hybrid protein that is active against some lentiviruses in a species-specific fashion. In particular, TRIMCyp from the owl monkey (omkTRIMCyp) very efficiently inhibits HIV-1. Previously, we showed that disrupting the integrity of microtubules (MTs) and of cytoplasmic dynein complexes partially rescued replication of retroviruses, including HIV-1, from restriction mediated by TRIM5α. Here we show

that efficient restriction of HIV-1 by omkTRIMCyp is similarly dependent on the MT network and on dynein complexes, but in a context-dependent fashion. When omkTRIMCyp was expressed in human HeLa cells, restriction was partially counteracted by pharmacological agents targeting MTs or by siRNA-mediated inhibition of dynein. The same drugs (nocodazole and paclitaxel) also rescued HIV-1 from restriction in cat CRFK cells, although to a lesser extent. Strikingly, neither nocodazole, paclitaxel nor depletion of the dynein heavy chain (DHC) had a significant effect on the restriction of HIV-1 in an owl monkey cell line. These results suggest the existence of cell-specific functional interactions between MTs/dynein and TRIMCyp.

B.3 Introduction

The replication of retroviruses and retrotransposons is inhibited by a diverse family of type I interferon (IFN) stimulated gene products commonly called restriction factors (Harris *et al*, 2012; Malim & Bieniasz, 2012; Zheng *et al*, 2012). The replication of human immunodeficiency virus type 1 (HIV-1) is reduced by IFN treatment of cells in vitro (Ho *et al*, 1985; Yamamoto *et al*, 1986) and in vivo (Skillman *et al*, 1996). At least some of the restriction factors that mediate the IFN-induced restriction of HIV-1 have been uncovered. For instance, the interferon-induced transmembrane proteins 2 and 3 (IFITM2 and IFITM3) can affect entry or immediate post-entry steps of HIV-1 replication (Lu *et al*, 2011). If the virus reaches the cytoplasm, it can then be inhibited by myxovirus resistance protein 2 (Mx2, also called MxB) (Goujon *et al*, 2013; Kane *et al*, 2013). Mx2 binds CA proteins that are part of the 'intact' (not-yet-disassembled) HIV-1 core, and interferes with core disassembly (uncoating) (Fricke *et al*, 2014; Liu *et al*, 2013). TRIM5α is another IFN-inducible factor that intercepts incoming retroviruses in the cytoplasm of infected cells (Stremlau *et al*, 2004). Restriction is host- and virus-specific, and HIV-1 is generally insensitive to human TRIM5α, as its CA is not recognized by the human version of the protein (Hatziioannou *et al*, 2004; Keckesova *et al*, 2004; Sebastian & Luban, 2005; Stremlau *et al*, 2004; Stremlau *et al*, 2006; Yap *et al*, 2004). However, HIV-1 is efficiently inhibited by TRIM5α expressed in several monkey species (up to ~100-fold in single-cycle assays), including macaques and the

African green monkey (Hatziioannou *et al*, 2003). TRIM5α belongs to the tripartite motif (TRIM) family of proteins, a very large family (close to 100 members) of ubiquitin ligases that function in various pathways including antiviral defense (Han *et al*, 2011; Reymond *et al*, 2001). TRIM proteins contain, starting at the N-terminal domain, a RING domain, one or two B-boxes, and a Coiled-Coil domain. Most of them also have an additional functional domain at the C-terminus (Sardiello *et al*, 2008); in the case of TRIM5α, this additional domain is a PRYSPRY motif, also called SPRY or B30.2 (Song *et al*, 2005). The PRYSPRY domain is responsible for the specificity of restriction, by mediating direct interactions with surface patches present in the N-terminal region of retroviral CA proteins (Biris *et al*, 2013; Sebastian & Luban, 2005; Yang *et al*, 2014). In several independent instances, retrotransposition events have led to the insertion of the CypA coding sequence into the trim5 locus of New World or Old World primate species, leading to the expression of various TRIMCyp hybrid proteins. TRIMCyp expressed in the owl monkey (Aotus trivirgatus) very efficiently decreases HIV-1 infectivity (~100- to 500-fold in single cycle assays) (Nisole *et al*, 2004; Sayah *et al*, 2004). Among the other TRIMCyp hybrid proteins discovered, those expressed in pig-tailed macaques (Macaca nemestrina) and in some rhesus macaques (Macaca mulatta) do not restrict HIV-1, but target other lentiviruses like HIV-2 (Brennan *et al*, 2008; Newman *et al*, 2008; Virgen *et al*, 2008; Wilson *et al*, 2008).

Restriction of HIV-1 by omkTRIMCyp seems to occur by a mechanism similar to that of TRIM5α and is initiated by the direct binding of the CypA domain of TRIMCyp to CA proteins that are part of incoming cores (Black & Aiken, 2010; Price *et al*, 2009; Shi *et al*, 2013). This interaction occurs relatively quickly, within an hour following virus entry into the cytoplasm (Hulme *et al*, 2011) and results in the destabilization of the retroviral core, a process sometimes referred to as premature decapsidation (Bérubé *et al*, 2007; Diaz-Griffero *et al*, 2007; Diaz-Griffero *et al*, 2006b). Over-expression of omkTRIMCyp in human cells results in an HIV-1 inhibition as potent as what is observed in owl monkey cell lines such as OMK cells, showing that the HIV-1 restriction-null endogenous human TRIM5α does not interfere with restriction in this context (Berthoux *et al*, 2005a). Interestingly, TRIM5 proteins are expressed at very

low levels endogenously in the absence of IFN (Carthagena *et al*, 2008), as illustrated by the difficulty to detect them by immunoblotting or immunofluorescence microscopy. Moreover, restriction by TRIM5α or TRIMCyp involves their aggregation or multimerization on the targeted retroviral core, as seen in various imaging studies (Campbell *et al*, 2008; Ganser-Pornillos *et al*, 2011; Zhao *et al*, 2011). Taken together, these observations raise an intriguing question: how can a sparsely expressed restriction factor quickly and efficiently intercept incoming retroviral cores in a process that may require hundreds or thousands of TRIM5 molecules? To address this question, we have hypothesized that TRIM5 proteins associate with cytoskeleton components used by retroviruses for their transport toward the nucleus, which would dramatically enhance the probability of successful interception. omkTRIMCyp, like TRIM5α, forms cytoplasmic bodies (CBs) whose sizes are dependent on expression levels (Perez-Caballero *et al*, 2005). TRIM5α CBs co-localize with ubiquitin (Campbell *et al*, 2008) and proteasomal subunits (Danielson *et al*, 2012; Lukic *et al*, 2011), which supports a functional role for CBs since the proteasome is involved in TRIM5α-mediated restriction (Anderson *et al*, 2006). On the other hand, CBs and proteasome were found to be dispensable for HIV-1 restriction by omkTRIMCyp (Perez-Caballero *et al*, 2005), pointing to the possibility of differences between the precise mechanisms of action for these two restriction factors. TRIM5α CBs associate with MTs and their movements along these filaments have been reported (Campbell *et al*, 2007). HIV-1 and other viruses are thought to recruit dynein motor complexes translocating on MTs for their retrograde transport (toward the nucleus) [reviewed in (Dodding & Way, 2011; Hsieh *et al*, 2010; Mouland & Milev, 2012)]. In a previous report, we showed that restriction of HIV-1 and N-tropic murine leukemia virus (N-MLV) by TRIM5α could be significantly attenuated by pharmacological treatments that affect the integrity and dynamics of MTs (Pawlica *et al*, 2014). TRIM5α-mediated restriction was also inhibited by pharmacological or RNAi-mediated disruption of dynein complexes (Pawlica *et al*, 2014). Because of the reported differences between TRIM5α and omkTRIMCyp in restricting HIV-1, we investigated whether the MT network and dynein complexes were relevant to omkTRIMCyp-mediated restriction.

B.4 Results

The size and localization of TRIMCyp CBs are modulated by MTs and cytoplasmic dynein. Previously, we showed that treatment of HeLa cells with nocodazole, a drug that inhibits MT polymerization (Luduena & Roach, 1991), increased the size of TRIM5α CBs and caused them to localize closer to the nucleus, on average (Pawlica *et al*, 2014). Depleting DHC also caused TRIM5α CBs to be larger, and they were found to localize closer to the plasma membrane, on average (Pawlica *et al*, 2014). We used the same approach to analyze the effect of these two interventions on omkTRIMCyp CBs. HeLa cells stably expressing omkTRIMCyp or transduced with the empty vector where stained with a monoclonal anti-FLAG antibody. Cells were treated with nocodazole at a concentration (2 μM) previously determined to result in efficient MTs disassembly (Pawlica *et al*, 2014), or left untreated (Fig. 1a). Alternatively, cells were transfected with a DHC siRNA under conditions leading to a ~85% decrease in DHC protein expression levels (Pawlica *et al*, 2014), or were transfected with a control (luciferase-targeting) siRNA (Fig. 1b). No staining was detected in the empty vector-transduced cells under the conditions used (Fig. 1a,b). The size of omkTRIMCyp CBs, as represented by the area on the two-dimensional images recorded, was calculated, along with their relative localization as previously described (Pawlica *et al*, 2014). In the absence of drug and in the cells transfected with the luciferase-targeting siRNA, omkTRIMCyp CBs had a median area of ~0.12 μm^2, while the mean area was of ~0.13 μm^2 (Fig. 1c). Treatment with nocodazole increased the median and mean size of CBs by 16.7% and 20.3%, respectively (Fig. 1c, left panel). DHC depletion increased the median size of omkTRIMCyp by 16.7% but had a bigger effect on their mean size, compared with the control siRNA (a 67.0% increase, indicating that the effect was much more pronounced on a minority of CBs). The effect was significant in both experiments ($P = 0.01$ and $P = 0.002$, respectively) and showed that the dynamics of TRIMCyp bodies are affected by treatments that disrupt MTs or interfere with cytoplasmic dynein function, similar to TRIM5α (Diaz-Griffero *et al*, 2006a; Pawlica *et al*, 2014).

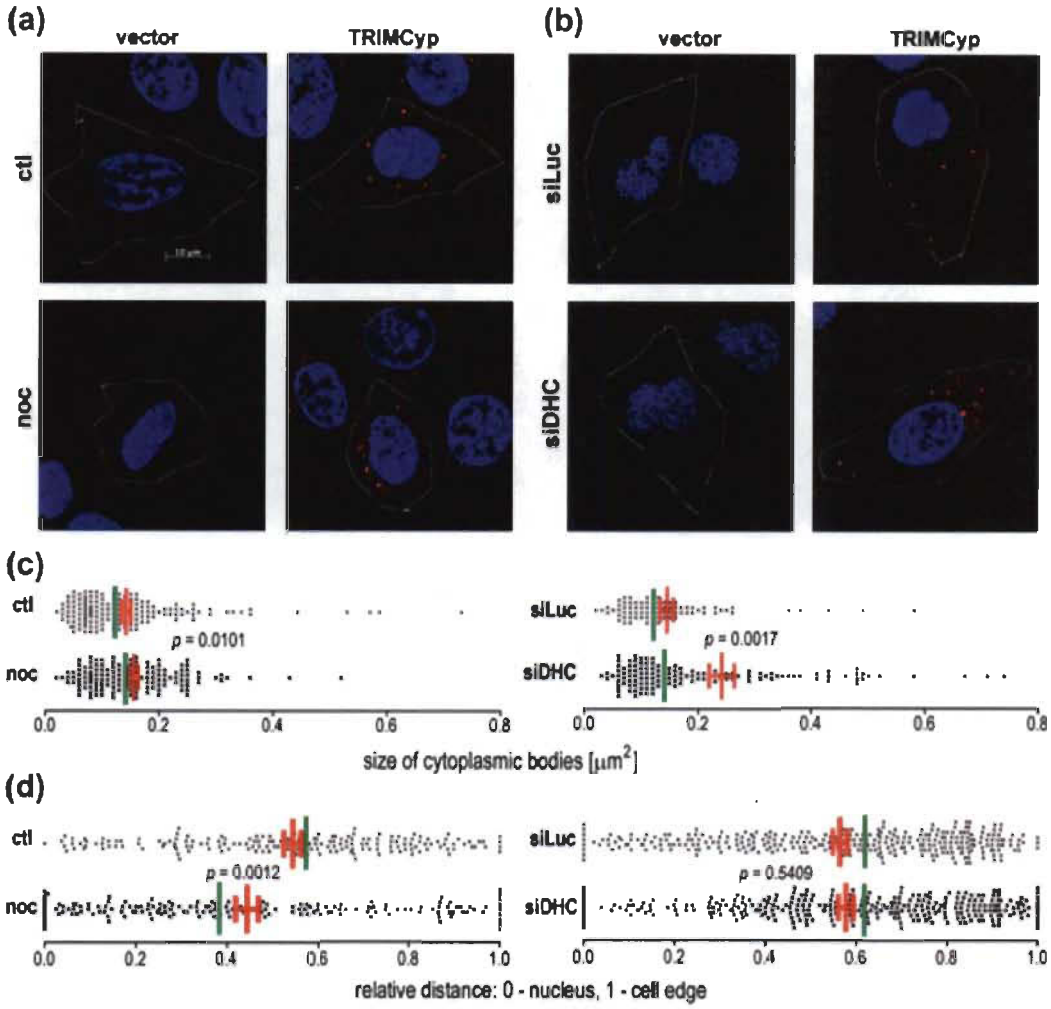

Figure 1. **Dynein heavy chain (DHC) depletion and MTs perturbation alter the size and/or distribution of omkTRIMCyp CBs.**
(a, b) immunofluorescence microscopy. HeLa cells transduced with FLAG-tagged omkTRIMCyp and control cells transduced with the empty vector were (a) seeded on glass coverslips and 24 hours later treated or not with 2 μM of nocodazole (noc) for 6 h, or (b) transfected with 40 nM of siRNAs targeting DHC or luciferase and 48 hours later seeded on glass coverslips and incubated for an additional 24 h. Cells were fixed and immunostained for FLAG (red). DNA was stained with Hoechst33342 (blue). Representative images are shown with outlined cell edges. (c) Sizes of CBs. All CBs were outlined in cells from a minimum of 5 randomly chosen fields and their area was calculated using image analysis software (AxioVision). Red bars show the means with SEM and green bars show the medians. *P* values were calculated using Student *t*-test analysis. (d) The relative localization of all TRIMCyp CBs from a minimum of 5 randomly chosen cells was calculated using the formula x/(x+y), where x is the shortest distance to the nucleus and y is the shortest distance to the cell's edge. Red bars show the mean with SEM and green bars, the median.

The relative intracytoplasmic position of omkTRIMCyp CBs was determined according to their closest distance to the nuclear membrane and the cytoplasmic membrane (Pawlica *et al*, 2014). Treatment with nocodazole caused omkTRIMCyp CBs to localize closer to the nucleus, relative to the untreated control (Fig. 1d, left panel). This effect was highly significant ($P = 0.001$) and mirrored our previous observations with TRIM5α (Pawlica *et al*, 2014). In contrast, DHC depletion had no significant effect on omkTRIMCyp relative localization (Fig. 1c, right panel). This stands in contrast to what was observed with TRIM5α CBs, which were found to be closer to the cell's edge upon DHC depletion (Pawlica *et al*, 2014). Altogether, results in Fig. 1 show that the dynamics of omkTRIMCyp are sensitive to perturbation of MTs and cytoplasmic dynein, but the specific effects are different from what is observed with TRIM5α, hinting at differences in their interactions with the cytoskeleton.

Nocodazole and paclitaxel partially rescue HIV-1 from restriction by omkTRIMCyp in HeLa cells. The fact that nocodazole treatment altered the dynamics of omkTRIMCyp CBs prompted us to analyze whether disrupting MTs would affect restriction. In addition to nocodazole, we also tested the effect of paclitaxel, a drug that prevents the disassembly of MTs (Jordan *et al*, 1992; Schiff *et al*, 1979). HeLa cells stably expressing omkTRIMCyp or transduced with the parental construct were treated with two different concentrations of nocodazole (Fig. 2a) or paclitaxel (Fig. 2b) and then infected with increasing amounts of an HIV-1 vector, HIV-$1_{CMV\text{-}GFP}$. We previously showed that nocodazole and paclitaxel at these concentrations had the expected effects on the MT network in HeLa cells and were not strongly cytotoxic (Pawlica *et al*, 2014). In the absence of drug, HIV-$1_{CMV\text{-}GFP}$ was restricted 300- to 400-fold by omkTRIMCyp (Fig. 2a, 2b), which is comparable to previous observations (Bérubé *et al*, 2007). Nocodazole increased infectivity of HIV-$1_{CMV\text{-}GFP}$ in HeLa cells expressing omkTRIMCyp by ~50-fold, while only slightly increasing infectivity in the permissive cells transduced with the empty vector (Fig. 2a). Thus, nocodazole counteracted omkTRIMCyp-mediated restriction, and this effect was seen at all virus doses tested and at both drug concentrations. Likewise, paclitaxel increased HIV-$1_{CMV\text{-}GFP}$ infectivity by ~30-fold in HeLa cells expressing omkTRIMCyp, while slightly decreasing infectivity

in the empty vector-transduced control cells (Fig. 2b). In the reciprocal experiment, we infected the same cell lines with HIV-$1_{CMV\text{-}GFP}$ in the presence of increasing nocodazole concentrations and using fixed virus doses. Nocodazole increased infectivity in HeLa-omkTRIMCyp cells by up to ~80-fold, compared with the untreated control, and this effect was observed at a wide range of nocodazole concentrations (Fig. 2c; see non-normalized data in Fig. S1a,b). Like before, nocodazole slightly increased HIV-$1_{CMV\text{-}GFP}$ infectivity in the control cells, by up to ~2-fold at 1 μM (Fig. 2c). We did a similar experiment with increasing concentrations of paclitaxel and fixed virus doses. Paclitaxel treatment increased HIV-$1_{CMV\text{-}GFP}$ infectivity in omkTRIMCyp-expressing cells by up to 15-fold compared to the untreated control (Fig. 2d; see non-normalized data in Fig. S1d). The magnitude of this effect was identical at all the drug concentrations tested. In contrast, paclitaxel decreased HIV-$1_{CMV\text{-}GFP}$ infectivity in the empty vector-transduced control cells by up to 2.5-fold (Fig. 2d; see non-normalized data in Fig. S1c). If the effect of nocodazole and paclitaxel was calculated relatively to the effect seen in control vector-transduced cells treated, rather than relatively to the untreated control, then both drugs were found to stimulate infectivity by roughly the same magnitude, ~50-fold. This observation mirrors previously published findings that nocodazole and paclitaxel both rescue N-MLV and HIV-1 from restriction by endogenous human TRIM5α and exogenous rhesus TRIM5α, respectively, in HeLa cells, and the effects of the two drugs were also of similar magnitude (Pawlica *et al*, 2014).

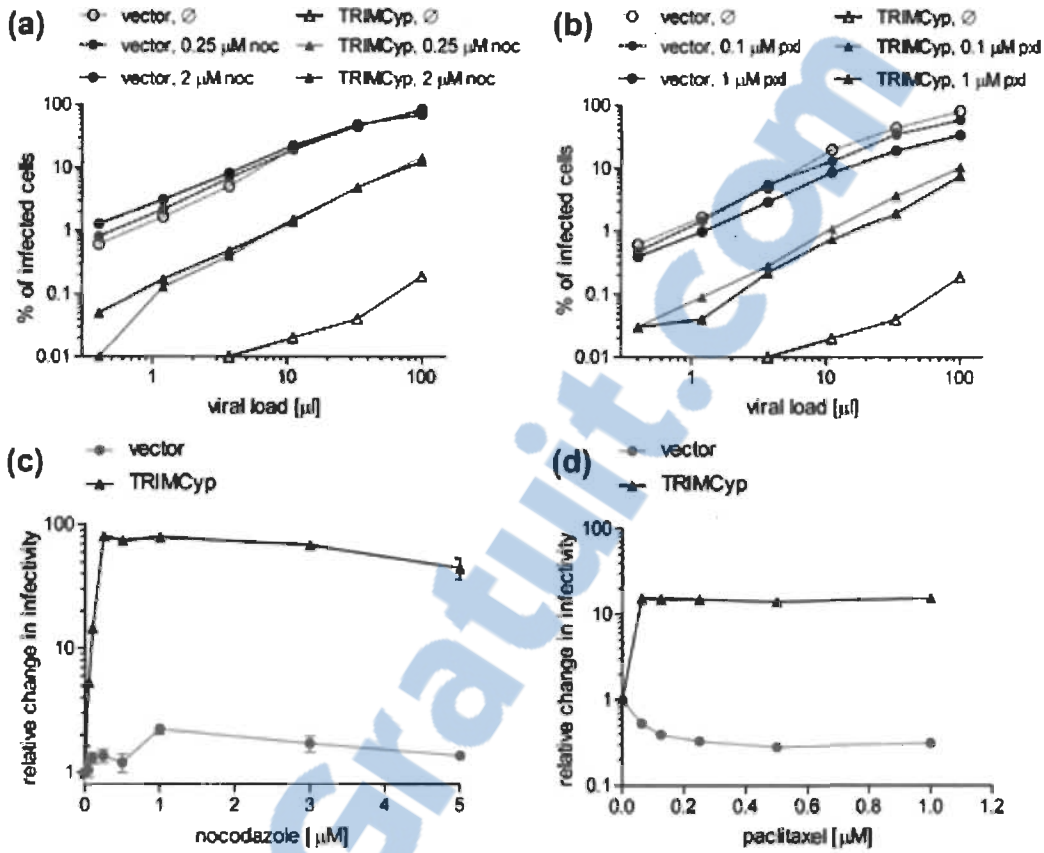

Figure 2. **Pharmacological perturbation of MTs partially counteracts HIV-1 restriction by omkTRIMCyp in HeLa cells.**

(a, b) Effect of nocodazole (noc) and paclitaxel (pxl) on restriction. HeLa cells transduced with FLAG-tagged omkTRIMCyp or the empty vector were infected with multiples doses of HIV-$1_{CMV\text{-}GFP}$ in the presence or absence of indicated concentrations of either nocodazole (a) or paclitaxel (b). Infections were performed for 16 hours. Infected (GFP-expressing) cells were detected by flow cytometry at 2 days post-infection. (c, d) Dose-dependent effect of nocodazole or paclitaxel on restriction. Human HeLa cells transduced with FLAG-tagged omkTRIMCyp or the empty vector were infected for 16 hours with a single dose of HIV-$1_{CMV\text{-}GFP}$ in the presence of increasing concentrations of either nocodazole (c) or paclitaxel (d). The percentages of infected cells were determined by flow cytometry 2 days postinfection, and the results are presented as the fold changes in infectivity relative to the relevant untreated controls. Higher amounts of input virus were used in omkTRIMCyp-expressing cells than in the control cells, so that all values fall within the dynamic range for this assay. The ratio of infected cells in the absence of drug were 0.06% (TRIMCyp, panel c), 0.16% (TRIMCyp, panel d), 2.15% (empty vector, panel c) or 7.93% (empty vector, panel d).

Depletion of DHC partially rescues HIV-1 from omkTRIMCyp-mediated restriction in HeLa cells. Previously, we found that DHC depletion partially suppressed the restriction of HIV-1 by rhesus TRIM5α expressed in HeLa cells (Pawlica *et al*, 2014). On the other hand, DHC depletion had a milder effect on the size and position of omkTRIMCyp CBs, compared to rhesus TRIM5α CBs (Fig. 1). To investigate whether the presence of DHC would be important to restriction mediated by TRIMCyp, we used a siRNA to suppress its expression in HeLa cells that were transduced with omkTRIMCyp or the empty vector. DHC knockdown was efficient (>90%), as shown in Fig. 3a. Then, cells were challenged with HIV-$1_{CMV\text{-}GFP}$ using virus doses leading to ~0.49% infected cells (empty vector-transduced) and 0.17% infected cells (omkTRIMCyp-transduced). When cells were transfected with the DHC-targeting siRNA, infectivity in omkTRIMCyp-expressing cells increased by 34.8-fold ± 1.3 compared to cells transfected with a control siRNA against luciferase (Fig. 3b; see non-normalized data in Fig. S2a). In contrast, the DHC-targeting siRNA had no effect in control cells transduced with the empty vector. Thus, DHC depletion counteracted omkTRIMCyp-mediated restriction, and the magnitude seen was comparable to what was observed with nocodazole and paclitaxel (Fig. 2). To determine whether the pharmacological disruption of MTs (using nocodazole or paclitaxel) and the siRNA-mediated disruption of cytoplasmic dynein counteracted omkTRIMCyp through the same mechanism or by acting independently, HeLa cells expressing omkTRIMCyp were infected with HIV-$1_{CMV\text{-}GFP}$ in the presence of an siRNA targeting DHC or luciferase, and in presence or not of nocodazole or paclitaxel (Fig. 3c; see non-normalized data in Fig. S2b). Like before, paclitaxel (alone or in combination with DHC knockdown) slightly decreased HIV-$1_{CMV\text{-}GFP}$ infectivity (~1.5-fold), while nocodazole and DHC depletion had no significant effect (Fig. 3c). Compared to the untreated control, treatment with nocodazole and paclitaxel increased infectivity in omkTRIMCyp-expressing cells by 27.0-fold (± 2.4) and 59.2-fold (± 3.7), respectively. DHC depletion alone increased infectivity by 16.9-fold (± 0.7) in omkTRIMCyp-expressing cells. Combining DHC depletion with nocodazole and paclitaxel increased infectivity by 32.3-fold (± 6.9) and 53.9-fold (± 4.98), respectively (Fig. 3c). Thus, the effects are almost identical to those obtained with the drugs alone, strongly suggesting that DHC

depletion and MTs perturbation rescued HIV-1 from omkTRIMCyp by interfering with the same pathway. Of note, in this experiment, only 0.14% omkTRIMCyp-expressing cells were infected in the absence of drug, which implies that we would have been able to observe 100-fold increases (or more) in infectivity if they had occurred. Thus, the absence of an additive effect in Fig. 3c is not due to saturated infection.

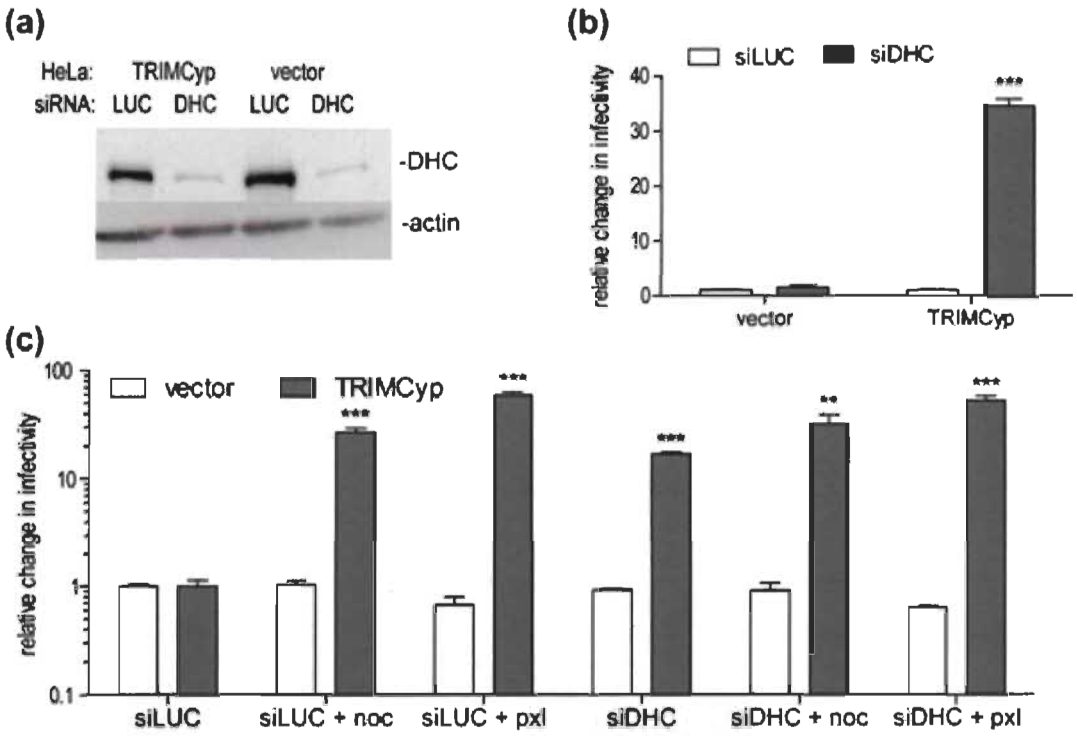

Figure 3. DHC depletion partially counteracts HIV-1 restriction by omkTRIMCyp in HeLa cells.

(a) Western blot analysis of DHC expression in HeLa cells 48 hours after transfection of the siRNAs against DHC (siDHC) or against luciferase (siLuc) as a control. Actin was analyzed as a loading control. (b) HeLa cells transduced with omkTRIMCyp or the empty vector were transfected with the indicated siRNAs and infected 72 hours later in triplicates with single doses of HIV-$1_{CMV\text{-}GFP}$ for 16 h. Infected cells were detected by flow cytometry 2 days postinfection and results are presented as -fold changes relative to the relevant untreated controls (relative change in infectivity). Higher amounts of input virus were used in omkTRIMCyp-expressing cells than in the control cells, so that all values fall within the dynamic range for this assay. The ratio of infected cells in the absence of drug were 0.17% (TRIMCyp) and 0.49% (empty vector). ***, $P \leq 0.0001$ (Student *t*-test). (c) Effect of combining DHC depletion and microtubule perturbation on TRIMCyp-mediated HIV-1 restriction. HeLa cells transduced with omkTRIMCyp or the empty vector were transfected with

40 nM of siRNA against DHC or Luc, then treated or not with either 0.2 μM of nocodazole or 0.1 μM of paclitaxel and infected with HIV-$1_{CMV\text{-}GFP}$. Infection yields were analyzed as above. The ratio of infected cells in the absence of drug were 0.14% (TRIMCyp) and 5.77% (empty vector). ** and *** indicate respectively $P \leq 0.005$ and $P \leq 0.0001$ compared with the untreated omkTRIMCyp-transduced cells, as calculated using the Student *t*-test.

Over-expression of p50/dynamitin partially counteracts omkTRIMCyp-mediated restriction. As an alternative approach to analyze the importance of dynein-mediated transport in omkTRIMCyp-mediated restriction, we over-expressed p50/dynamitin in control and omkTRIMCyp-expressing HeLa cells (Fig. 4a). p50 is a subunit of the dynactin complex that is responsible for binding cargos to the dynein complex. Its over-expression results in the disassembly of dynactin complexes, thereby disrupting cargo binding to dynein (Burkhardt *et al*, 1997; Melkonian *et al*, 2007). Over-expression of p50 increased HIV-$1_{CMV\text{-}GFP}$ infectivity in TRIMCyp-expressing cells by 2.3-fold (± 0.35), while replication in the control permissive cells was not affected (Fig. 4b; see non-normalized data in Fig. S2c). Altogether, the data in Fig. 3 and Fig. 4 strongly suggest that functional dynein complexes are important, but not absolutely necessary, to omkTRIMCyp-mediated restriction.

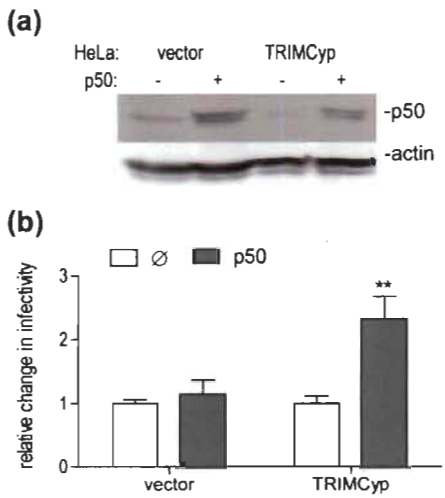

Figure 4. Over-expression of p50/dynamitin decreases omkTRIMCyp-mediated restriction of HIV-1 in HeLa cells.
(a, b) HeLa cells transduced with omkTRIMCyp or the empty vector were transfected with p50/dynamitin-HA or an irrelevant control plasmid.

(a) Detection of p50 in the transfected cells by Western blotting. (b) 48 hours after transfection, cells were infected in triplicates with HIV-$1_{CMV\text{-}GFP}$. Infected cells were counted by flow cytometry 2 days post infection and results are presented as -fold changes in infectivity relative to the relevant mock-transfected control. Higher amounts of input virus were used in omkTRIMCyp-expressing cells than in the control cells, so that all values fall within the dynamic range for this assay. The ratio of infected cells in the mock-transfected cells were 0.25% (for TRIMCyp) and 0.42% (for the empty vector). ** indicates $P \leq 0.005$ in a Student *t*-test.

Nocodazole and paclitaxel partially rescue HIV-1 from omkTRIMCyp-mediated restriction in cat cells. The experiments in Figs 1-4 were all performed in HeLa cells. To analyze whether nocodazole and paclitaxel could also interfere with omkTRIMCyp function in another cell line, we used CRFK cat cells stably expressing omkTRIMCyp, or transduced with the empty vector as a control. Cats, like other feline species, apparently do not have a TRIM5α or TRIMCyp ortholog (McEwan *et al*, 2009), and thus, using this cell line also insured that endogenous TRIM5α did not play a role in the effects seen in HeLa cells. First, CRFK cells were transfected with a construct expressing GFP-α-tubulin and then treated with nocodazole or paclitaxel before being processed for immunofluorescence microscopy. In the absence of drug, individual MTs were clearly visible (Fig. 5a, left panel). Nocodazole prevents polymerization of MTs (Luduena & Roach, 1991) and consequently, MTs appeared shortened and/or disassociated; most of the signal was diffuse and distributed throughout the cytoplasm (Fig. 5a). Paclitaxel, on the other hand, binds to MT polymers to prevent their disassembly (Jordan & Wilson, 2004), resulting in the formation of abnormal MT bundles (Hornick *et al*, 2008), a phenotype that was observed as expected in CRFK cells (Fig. 5a). Next, we analyzed the effect of these pharmacological treatments on HIV-1 infectivity under restriction by omkTRIMCyp. In the absence of treatment, HIV-$1_{CMV\text{-}GFP}$ infectivity in CRFK cells expressing omkTRIMCyp was reduced by ~100-fold compared to the control cells (Fig. 5b-c), which is smaller than what was seen in HeLa cells transduced with the same omkTRIMCyp-expressing construct (Fig. 2a-b). Treatment with nocodazole (Fig. 5b) and paclitaxel (Fig. 5c) increased HIV-$1_{CMV\text{-}GFP}$ infectivity by ~6-fold while having no effect in control permissive cells. Thus, perturbing MTs partially inhibits omkTRIMCyp function in CRFK cells, similar to what

was observed in HeLa cells, although the effect is smaller in CRFK cells. Moreover, the magnitudes of the effects of the two drugs in CRFK cells were similar, as was the case in HeLa cells.

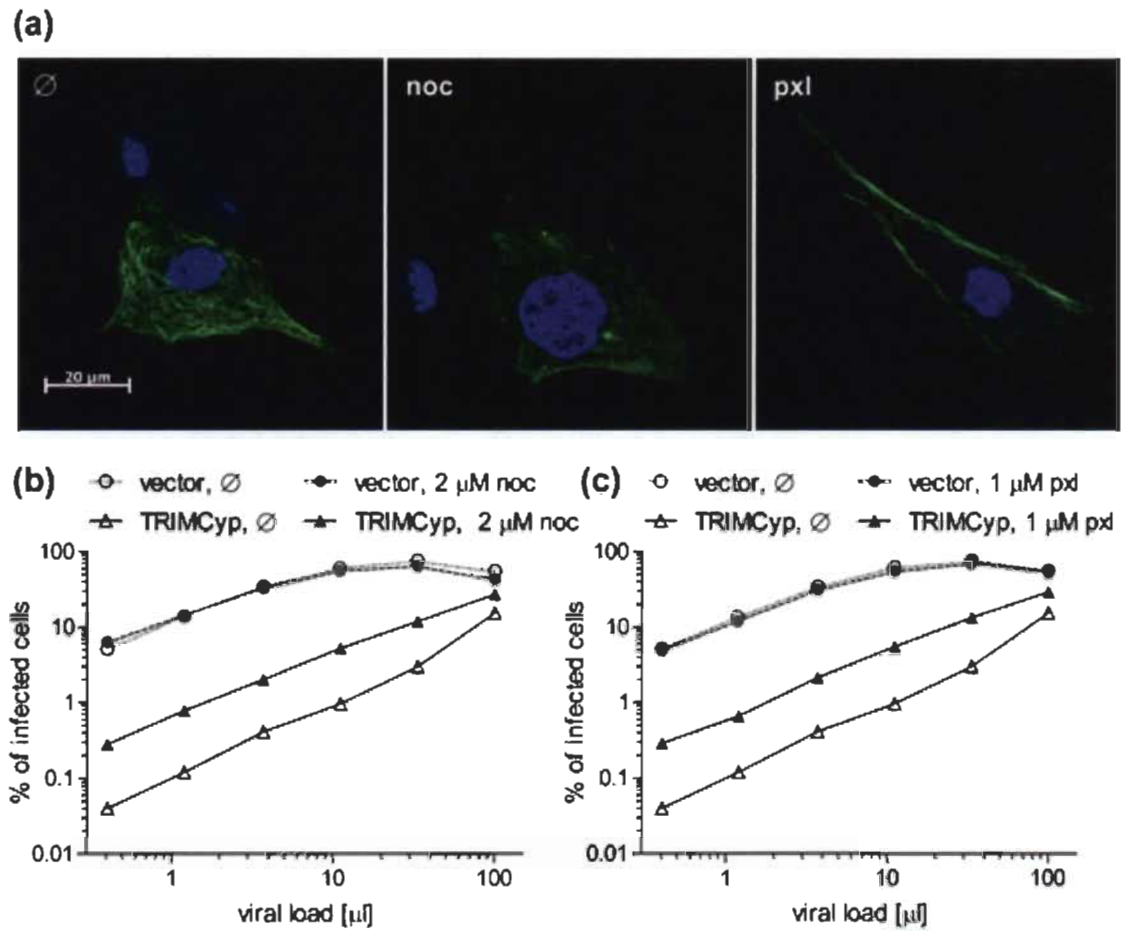

Figure 5. Pharmacological perturbation of MTs partially counteracts HIV-1 restriction by omkTRIMCyp in CRFK cells.

(a) Immunofluorescence microscopy analysis of microtubules. CRFK cells were transfected with GFP-α-tubulin and 2 days later were left untreated or subjected to 2-hour treatments using either 2 µM nocodazole (noc) or 1 µM paclitaxel (pxl) and then fixed. GFP fluorescence was observed by immunofluorescence microscopy, along with DNA which was stained using Hoechst33342 (blue). A representative image from each condition is presented. (B, C) Effect of nocodazole (noc) and paclitaxel (pxl) on restriction. CRFK cells transduced with omkTRIMCyp or with the empty vector were infected with multiples doses of HIV-$1_{CMV\text{-}GFP}$ in the presence or absence of 2 µM nocodazole (b) or 1 µM paclitaxel (c). Infections were performed for 16 hours and infected cells were detected by flow cytometry 2 days later.

Disrupting MTs dynamics or dynein function does not counteract restriction of HIV-1 in owl monkey OMK cells. Finally, we tested whether MTs and cytoplasmic dynein were important to omkTRIMCyp function when expressed endogenously in owl monkey cells. For this, we used OMK cells, which are kidney epithelial cells known to be very poorly permissive to HIV-1 (Sayah *et al*, 2004; Towers *et al*, 2003). GFP-α-tubulin transfection allowed us to analyze the effect of nocodazole and paclitaxel on the MT network in this cell line (Fig. 6a). Similar to what was seen in CRFK cells, treatment with 2 μM nocodazole resulted in GFP-α-tubulin to be more diffuse in the cytoplasm of cells (Fig. 6a), consistent with inhibition of MT polymerization by this drug. Conversely, treatment with 1 μM paclitaxel caused the formation of abnormal MT bundles that were found close to the cell's edge (Fig. 6a). OMK cells were then infected with HIV-$1_{NL43\text{-}GFP}$, a VSV G-pseudotyped HIV-1 vector devoid of an HIV-1 envelope and expressing GFP in place of Nef (He *et al*, 1997). As a non-restricted control, we used $SIV_{mac\text{-}GFP}$, a similarly constructed vector derived from the omkTRIMCyp-insensitive SIV strain mac239 (Berthoux *et al*, 2005b). OMK cells were infected with multiple doses of HIV-$1_{NL43\text{-}GFP}$ and $SIV_{mac\text{-}GFP}$, in absence of drug or in presence of nocodazole (Fig. 6b) or paclitaxel (Fig. 6c). After normalization of the virus amounts used according to their titers in the non-restrictive CRFK cells, we found that as expected, HIV-$1_{NL43\text{-}GFP}$ infectivity was ~500-fold smaller than that of $SIV_{mac\text{-}GFP}$ in these cells (Fig. 6b-c). Addition of nocodazole at 0.1 or 1 μM slightly increased HIV-$1_{NL43\text{-}GFP}$ infectivity, but this drug also had a small positive effect on SIVmac-GFP infectivity (Fig. 6b). Likewise, treatment with paclitaxel slightly increased infectivity of $SIV_{mac\text{-}GFP}$ and also that of HIV-$1_{NL43\text{-}GFP}$, at least at some virus doses (Fig. 6c). Thus, HIV-$1_{NL43\text{-}GFP}$ is not rescued from TRIMCyp-mediated restriction in OMK cells by nocodazole or paclitaxel treatment. The discrepancy between this result and what was observed in HeLa and CRFK cells could possibly be due to differences in restriction sensitivity between the vectors used, HIV-$1_{CMV\text{-}GFP}$ and HIV-$1_{NL43\text{-}GFP}$. To exclude that possibility, we infected OMK cells with several doses of HIV-$1_{CMV\text{-}GFP}$ in absence or presence of nocodazole or paclitaxel. As shown Fig. 6d, neither drug could rescue this vector from restriction by TRIMCyp in OMK cells. As additional evidence that TRIMCyp was expressed and functional in these cells, we tested whether inhibition of

its interaction with HIV-1 capsid would rescue HIV-1 infectivity (Sayah *et al*, 2004). Treatment with 5 μM cyclosporine A during infection and introducing the G89V mutation in HIV-1 capsid both increased HIV-1 infectivity by ~200-fold in OMK cells (Fig. 6e), thus completely disrupting restriction.

It is conceivable, albeit unlikely (since dynein complexes translocate on MTs), that cytoplasmic dynein could have a role in TRIMCyp function in OMK cells even if the MT network does not. To test this possibility, we depleted DHC in OMK cells using the same siRNA that was used in human cells. We found that DHC knockdown by this siRNA was as efficient in OMK cells as in human cells (>90%; Fig. 6f). DHC depletion had no significant effect on HIV-$1_{NL43\text{-}GFP}$, even decreasing infectivity at one of the virus doses compared to the cells transfected with the control (luciferase-targeting) siRNA (Fig. 6g). $SIV_{mac\text{-}GFP}$ infectivity was similarly not significantly affected by DHC depletion (Fig. 6g). Thus, HIV-1 infectivity in OMK cells is not rescued by interfering with the integrity of the MT network or by targeting DHC, suggesting the existence of cell context specificity for the involvement of MTs and cytoplasmic dynein in the restriction process.

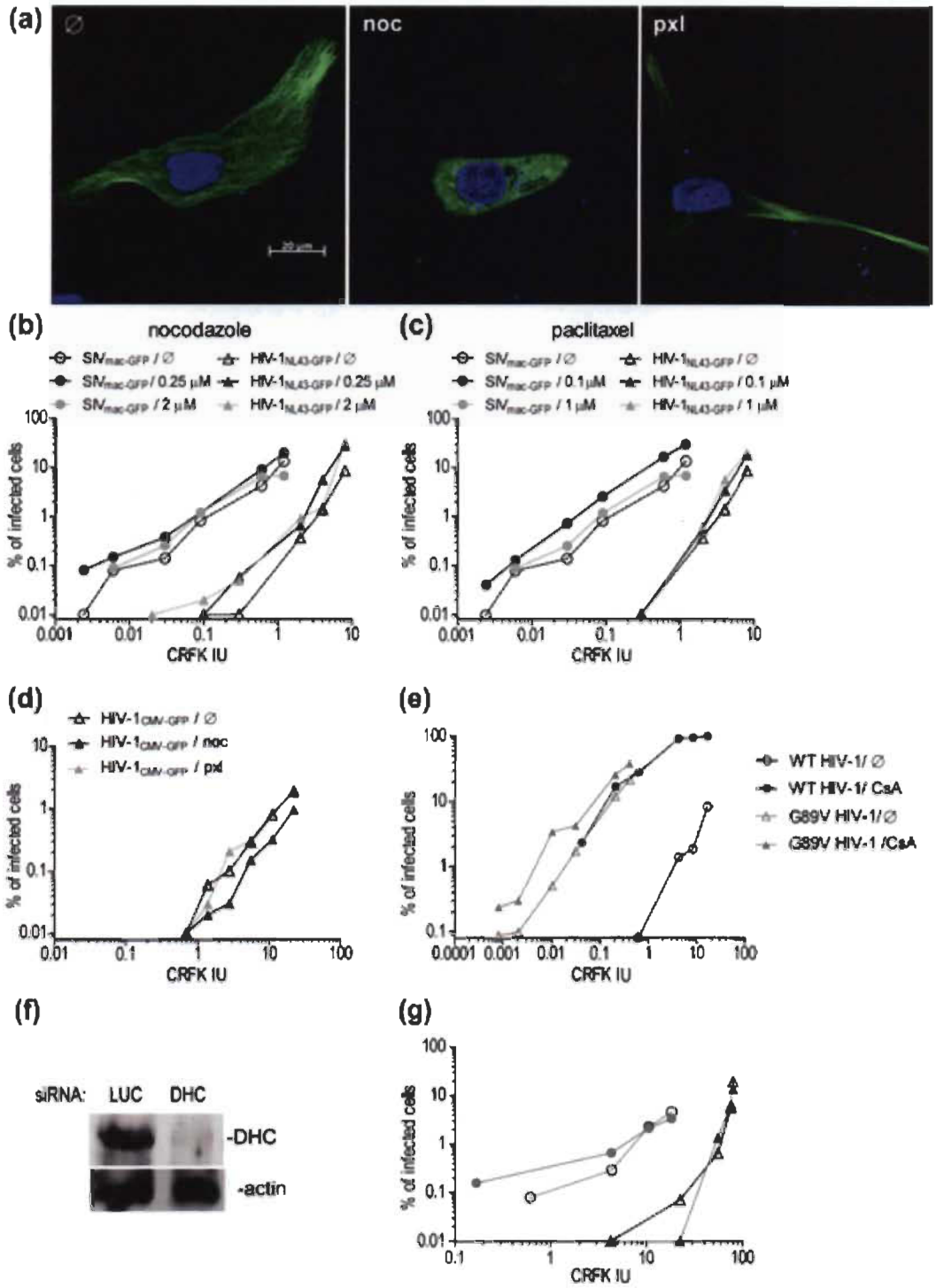

Figure 6. **Pharmacological perturbation of MTs and DHC depletion do not rescue HIV-1 from TRIMCyp-mediated restriction in OMK cells.** (a-d) Effect of nocodazole (noc) and paclitaxel (pxl) on restriction. (a) Immunofluorescence microscopy analysis of microtubules. OMK cells were transfected with GFP-α-tubulin and 2 days later were left untreated or subjected to 2-hours treatments using either 2 µM nocodazole or 1 µM

paclitaxel and then fixed. GFP fluorescence was observed by immunofluorescence microscopy, along with DNA which was stained using Hoechst33342 (blue). A representative image from each condition is presented. (b-d) OMK cells were infected with multiples doses of HIV-$1_{NL43\text{-}GFP}$ (b, c), $SIV_{mac\text{-}GFP}$ (b, c) or HIV-$1_{CMV\text{-}GFP}$ (d) in the presence or absence of nocodazole (b, d) or paclitaxel (c, d) at the indicated concentrations. Infections were performed for 16 hours and infected cells were detected by flow cytometry 2 days later. (e) Abrogation of restriction by CsA treatement or CA mutation. OMK cells were infected with increasing amounts of wild-type (WT) HIV-$1_{CMV\text{-}GFP}$ or the G89V CA mutant and in presence or absence of CsA (5 μM). The x-axis shows the amounts of virus used for both G89V and WT virus as determined by their titers in CRFK cells in the absence of drug. The % of GFP-positive cells were determined by flow cytometry 2 days post-infection. (f) Western blot analysis of DHC expression in OMK cells 48 hours after transfection of the siRNAs targeting DHC (siDHC) or, as a control, luciferase (siLuc). Actin was analyzed as a loading control. (g) OMK cells were transfected with the indicated siRNAs and infected 72 hours later infected with muliple doses of either HIV-$1_{NL43\text{-}GFP}$ or $SIV_{mac\text{-}GFP}$ for 16 h. Infected cells were detected by flow cytometry 2 days postinfection.

B.5 Discussion

Previously, we showed that full restriction by TRIM5α required the presence of a functional MT network, as well as functional dynein complexes (Pawlica *et al*, 2014). This was true whether TRIM5α was expressed endogenously or over-expressed by retroviral transduction. Moreover, the phenotype was observed in human cells and in rhesus macaque cells, and whether the restricted virus was a lentivirus (HIV-1) or an oncoretrovirus (N-MLV). Here, we show that the antiretroviral function of TRIMCyp, a TRIM5 protein bearing a CypA domain instead of a PRYSPRY domain, can be similarly sensitive to inhibition of MTs or dynein complexes. All viruses used in this study were VSV G-pseudotyped, and we cannot totally exclude that such pseudotyping modulates the involvement of microtubules or dynein in omkTRIMCyp-mediated restriction. However, this seems unlikely considering that the mode of virus entry was previously shown to be irrelevant for the involvement of microtubules in TRIM5α-mediated restriction of HIV-1 (Pawlica *et al*, 2014). Interestingly, the MT/dynein dependency of omkTRIMCyp varied between the cell lines used, being high in HeLa cells, relatively less so in CRFK cells, and absent in OMK cells. Endogenous TRIMCyp in OMK cells is

expressed at much lower levels compared to over-expression in HeLa or CRFK cells, but this is unlikely to explain the differences seen here, considering that (i) the magnitude of omkTRIMCyp-mediated HIV-1 restriction is similar in OMK and in TRIM5α-transduced HeLa cells (100-fold or more) and (ii) microtubules and dynein were shown to be important for restriction mediated by both endogenous and over-expressed TRIM5α (Pawlica *et al*, 2014). However, we cannot totally exclude this possibility. Of note, none of the experimental approaches used here had a significant effect on omkTRIMCyp expression levels in HeLa cells (not shown), ruling out such a putative unspecific effect as the cause for the loss of restriction. Because cytoplasmic dynein complexes translocate on MTs (Hook & Vallee, 2006), it appears likely that paclitaxel and nocodazole inhibit TRIM5α and TRIMCyp indirectly, by preventing dynein-mediated transport. In support of this conclusion is the observation that combining DHC depletion with paclitaxel or nocodazole treatment has no additional effect on restriction in cells, and this has been shown for rhesus TRIM5α (Pawlica *et al*, 2014) and now for omkTRIMCyp as well. The fact that neither TRIM5α or TRIMCyp are completely dependent on the presence of an intact MT network or functional dynein, regardless of the cellular context, leads us to conclude that dynein complexes have a function in TRIM5α/TRIMCyp-mediated restriction that is not absolutely required or, possibly, this function can be accomplished by another transporter complex that does not translocate on MTs. This hypothesis helps make sense of the fact that neither DHC depletion nor pharmacological disruption of MTs could rescue HIV-1 infection of owl monkey OMK cells. We speculate that the endogenous omkTRIMCyp expressed in these cells does not require MTs or dynein to make initial contact with the incoming virus capsid core, and elucidating the molecular basis for this behavior will require additional investigations. Alternatively, the discrepancy of results between the cell lines used in this study could stem from different effects of inhibiting MTs and dynein on virus uncoating in these cell lines. Targeting MTs and dynein may delay uncoating, as has been shown recently by us (Pawlica & Berthoux, 2014; Pawlica *et al*, 2014) and by others (Lukic *et al*, 2014), and perhaps this has a greater impact on restriction in some cell lines than in others. Interestingly, Lukic *et al* also included data showing that nocodazole treatment did not rescue HIV-1 from restriction by rhesus TRIM5α or

omkTRIMCyp expressed in HeLa cells, apparently conflicting with our previous report (Pawlica *et al*, 2014) and the present one. However, HeLa cells have been shown to be a highly heterogeneous cell line (Carson & Pirruccello, 2013) including clones with various permissiveness toward HIV-1 infection (De Iaco & Luban, 2014) and it is also known that the magnitude of restriction by TRIM5α and TRIMCyp proteins can vary widely between cell lines (Bérubé *et al*, 2007; Gong *et al*, 2011). Altogether, it appears likely that a cellular context effect explains the different results obtained by Lukic *et al*. In conclusion, the MT network and dynein complexes can potentiate the antiretroviral activity of not only TRIM5α but also TRIMCyp, but is not strictly required.

B.6 Methods

Cells, pharmaceuticals and antibodies. Human embryonic kidney 293T (HEK293T) cells, human epithelial carcinoma HeLa cells, feline renal CRFK cells, owl monkey kidney (OMK) cells were maintained in Dulbecco's modified Eagle's medium (DMEM) with high glucose, supplemented with 10% fetal bovine serum (FBS) and antibiotics at 37°C, 5% CO2. All cell culture reagents were from HyClone (Thermo Scientific, Logan, UT). Nocodazole, paclitaxel and cyclosporine A were from Sigma (St Louis, MI). HeLa and CRFK cells retrovirally transduced to stably express omkTRIMCyp were described before (Bérubé *et al*, 2007; Nepveu-Traversy *et al*, 2009). Rabbit polyclonal antibodies against dynein heavy chain and p50/dynamitin were from Santa Cruz (Dallas, TX) and Millipore (Billerica, MA), respectively. The FLAG epitope was detected using the M2 mouse monoclonal antibody (Sigma). The HRP-conjugated mouse anti-actin antibody was from Sigma. HRP-conjugated goat anti-rabbit and goat anti-mouse antibodies used as secondary antibodies in Western blots were from Santa Cruz.

Plasmid DNAs and retrovirus production. p50/dynamitin-HA was a gift from Tina Schroer (Schrader *et al*, 2000). To produce viral vectors, 10-cm culture dishes of sub-confluent HEK293T cells were co-transfected using polyethylenimine (MW 25,000; Polyscience, Niles, IL) with the appropriate plasmids, as follows: for the viral vector

HIV-$1_{CMV-GFP}$, TRIP-CMV-GFP (10 μg), pΔR8.9 (WT or G89V; 10 μg) and pMD-G (5 μg); for HIV-$1_{NL43-GFP}$, pNL-GFP (10 μg) and pMD-G (5 μg); for $SIV_{mac-GFP}$, $pSIV_{mac-GFP}$ (10 μg) and pMD-G (5 μg) (Berthoux *et al*, 2003; He *et al*, 1997; Zufferey *et al*, 1997). Media were changed 16 hours post transfection and virus-containing supernatants were collected after an additional 1.5 days of culture. Viral stocks were clarified by centrifugation for 5 min at 400 x *g*.

Viral challenges. Cells were seeded in 24-well plates at 10^5 cells/well (CRFK and HeLa cells) or 5 x 10^4 cells/well (OMK cells) and challenged the next day with the appropriate GFP-expressing viral vectors. When applicable, cells were pre-treated for 15 min with nocodazole, paclitaxel or cyclosporine A, and supernatants were replaced with fresh medium 16 hours post infection (p.i.). Cells were trypsinized 48 hours p.i. and fixed in 2% formaldehyde (Fisher Scientific, Waltham, MA). The percentages of GFP-positive cells were then determined by analyzing 10^4 to 10^5 cells on a FC500 MPL cytometer (Beckman Coulter, Brea, CA) using the CXP Software (Beckman Coulter).

siRNA and plasmid transfections. For the siRNA treatments, 10^6 cells were seeded in a 10 cm dish in Opti-MEM (Gibco, Carlsbad, CA) and transfected the next day with 40 nM of siRNA using DharmaFECT 1 (Dharmacon, Lafayette, CO). The siRNA targeting the sequence 5'GATCAAACATGACGGAATT of the dynein heavy chain (DHC), has been described before (Lehmann *et al*, 2009; Pawlica *et al*, 2014) and was purchased from Qiagen (Venlo, Netherlands). A control siRNA (5'CGTACGCGGAATACTTCGATT) targeting the luciferase mRNA (Pawlica *et al*, 2014) was purchased from Dharmacon. 48 hours post transfection, cells were seeded in 24-well plates and infected the next day with HIV-1 vectors as described above. For p50 over-expression, 10^6 cells seeded in a 10-cm dish were polyethyleneimine-transfected with 5 μg of p50/dynamitin-HA or an irrelevant plasmid (pMIP). Cells were seeded in 24-well plates 24 hours later and challenged with viral vectors the next day.

Immunofluorescence (IF) microscopy. For siRNA treatments, HeLa cells in 3.5-cm wells were transfected 48 hours prior to seeding as described above. For the cells

expressing GFP-tubulin, 2 μg of the plasmid were transfected per well using polyethyleneimine 24 hours prior to seeding on coverslips. 2 x 105 cells were seeded on glass coverslips placed in 3.5-cm wells. 24 hours later, the cells were treated or not with nocodazole for 2 hours and then fixed and processed for IF staining. Fixation was done for 10 min in 4% formaldehyde-DMEM in 37°C, followed by three washes with ice-cold PBS. Cells were then permeabilized by treatment with 0.1% Triton X-100, 0.1 mM sodium citrate for 1-2 min on ice. Cells were then washed again three times with PBS and treated with 10% normal goat serum (Sigma, St Louis, MI) containing 0.3 M glycine (Sigma) for 30 min at RT. This was followed by a 4-hours incubation with a murine antibody against the FLAG epitope diluted 1:400 in PBS containing 10% normal goat serum. Cells were washed five times and fluorescently stained with the Alexa594-conjugated goat anti-mouse antibody (Molecular Probes) at a 1:200 dilution. Cells were washed five times in PBS before mounting in Vectashield (Vector Laboratories, Burlington, Ontario). Hoechst33342 (0.8 μg/ml; Molecular Probes) was added along with the penultimate PBS wash to reveal DNA. Z-stacks were acquired on the AxioObserver Microscope (Carl Zeiss, Jena, Germany) equipped with the Apotome module and median Z-stacks were retained for analysis. For the analysis of TRIM5α CB sizes, FLAG foci in a given cell were manually outlined in the AxioVision software for calculation of the surface. A minimum of 80 and up to 180 CBs from 10 randomly chosen cells were included in the analysis. For the analysis of TRIM5α CB localization, the cell's edge was outlined and for each FLAG foci in a given cell, we measured the closest distance to the nuclear membrane and the closest distance to the plasma membrane, using Axiovision. A minimum of 170 and up to 320 CBs from a minimum of 5 randomly chosen cells were included in the analysis.

Statistical analysis. All statistical analyses were done in Graph Prism 5 (GraphPad Software, Inc., La Jolla, CA, USA).

B.7 Acknowledgements

We thank Maximilian Webers and Marie Leclerc for providing technical help. We acknowledge Tina Schroer (Johns Hopkins University) and Ali Saib for sharing plasmid DNA. This work was funded by Canadian Institutes of Health Research operating grant MOP-102712.

B.8 References

Anderson JL, Campbell EM, Wu X, Vandegraaff N, Engelman A, Hope TJ (2006) Proteasome inhibition reveals that a functional preintegration complex intermediate can be generated during restriction by diverse TRIM5 proteins. *Journal of virology* 80: 9754-9760

Berthoux L, Sebastian S, Sayah DM, Luban J (2005a) Disruption of human TRIM5alpha antiviral activity by nonhuman primate orthologues. *Journal of virology* 79: 7883-7888

Berthoux L, Sebastian S, Sokolskaja E, Luban J (2005b) Cyclophilin A is required for TRIM5alpha-mediated resistance to HIV-1 in Old World monkey cells. *Proceedings of the National Academy of Sciences of the United States of America* 102: 14849-14853

Berthoux L, Towers GJ, Gurer C, Salomoni P, Pandolfi PP, Luban J (2003) As(2)O(3) enhances retroviral reverse transcription and counteracts Ref1 antiviral activity. *Journal of virology* 77: 3167-3180

Bérubé J, Bouchard A, Berthoux L (2007) Both TRIM5alpha and TRIMCyp have only weak antiviral activity in canine D17 cells. *Retrovirology* 4: 68

Biris N, Tomashevski A, Bhattacharya A, Diaz-Griffero F, Ivanov DN (2013) Rhesus monkey TRIM5alpha SPRY domain recognizes multiple epitopes that span several capsid monomers on the surface of the HIV-1 mature viral core. Journal *of molecular biology* 425: 5032-5044

Black LR, Aiken C (2010) TRIM5alpha disrupts the structure of assembled HIV-1 capsid complexes in vitro. *Journal of virology* 84: 6564-6569

Brennan G, Kozyrev Y, Hu SL (2008) TRIMCyp expression in Old World primates Macaca nemestrina and Macaca fascicularis. *Proceedings of the National Academy of Sciences of the United States of America* 105: 3569-3574

Burkhardt JK, Echeverri CJ, Nilsson T, Vallee RB (1997) Overexpression of the dynamitin (p50) subunit of the dynactin complex disrupts dynein-dependent maintenance of membrane organelle distribution. *The Journal of cell biology* 139: 469-484

Campbell EM, Dodding MP, Yap MW, Wu X, Gallois-Montbrun S, Malim MH, Stoye JP, Hope TJ (2007) TRIM5 alpha cytoplasmic bodies are highly dynamic structures. *Molecular biology of the cell* 18: 2102-2111

Campbell EM, Perez O, Anderson JL, Hope TJ (2008) Visualization of a proteasome-independent intermediate during restriction of HIV-1 by rhesus TRIM5alpha. *The Journal of cell biology* 180: 549-561

Carson SD, Pirruccello SJ (2013) HeLa cell heterogeneity and coxsackievirus B3 cytopathic effect: implications for inter-laboratory reproducibility of results. *Journal of medical virology* 85: 677-683

Carthagena L, Parise MC, Ringeard M, Chelbi-Alix MK, Hazan U, Nisole S (2008) Implication of TRIM alpha and TRIMCyp in interferon-induced anti-retroviral restriction activities. *Retrovirology* 5: 59

Danielson CM, Cianci GC, Hope TJ (2012) Recruitment and dynamics of proteasome association with rhTRIM5alpha cytoplasmic complexes during HIV-1 infection. *Traffic* 13: 1206-1217

De Iaco A, Luban J (2014) Cyclophilin A promotes HIV-1 reverse transcription but its effect on transduction correlates best with its effect on nuclear entry of viral cDNA. *Retrovirology* 11: 11

Diaz-Griffero F, Kar A, Lee M, Stremlau M, Poeschla E, Sodroski J (2007) Comparative requirements for the restriction of retrovirus infection by TRIM5alpha and TRIMCyp. *Virology* 369: 400-410

Diaz-Griffero F, Li X, Javanbakht H, Song B, Welikala S, Stremlau M, Sodroski J (2006a) Rapid turnover and polyubiquitylation of the retroviral restriction factor TRIM5. *Virology* 349: 300-315

Diaz-Griffero F, Vandegraaff N, Li Y, McGee-Estrada K, Stremlau M, Welikala S, Si Z, Engelman A, Sodroski J (2006b) Requirements for capsid-binding and an effector function in TRIMCyp-mediated restriction of HIV-1. *Virology* 351: 404-419

Dodding MP, Way M (2011) Coupling viruses to dynein and kinesin-1. *The European Molecular Biology Organization journal* 30: 3527-3539

Fricke T, White TE, Schulte B, de Souza Aranha Vieira DA, Dharan A, Campbell EM, Brandariz-Nunez A, Diaz-Griffero F (2014) MxB binds to the HIV-1 core and prevents the uncoating process of HIV-1. *Retrovirology* 11: 68

Ganser-Pornillos BK, Chandrasekaran V, Pornillos O, Sodroski JG, Sundquist WI, Yeager M (2011) Hexagonal assembly of a restricting TRIM5alpha protein. *Proceedings of the National Academy of Sciences of the United States of* America 108: 534-539

Gong J, Shen XH, Qiu H, Chen C, Yang RG (2011) Rhesus monkey TRIM5alpha has distinct HIV-1 restriction activity among different mammalian cell lines. *Current microbiology* 63: 531-537

Goujon C, Moncorge O, Bauby H, Doyle T, Ward CC, Schaller T, Hue S, Barclay WS, Schulz R, Malim MH (2013) Human MX2 is an interferon-induced post-entry inhibitor of HIV-1 infection. *Nature* 502: 559-562

Han K, Lou DI, Sawyer SL (2011) Identification of a genomic reservoir for new TRIM genes in primate genomes. *PLoS genetics* 7: e1002388

Harris RS, Hultquist JF, Evans DT (2012) The restriction factors of human immunodeficiency virus. *The Journal of biological chemistry* 287: 40875-40883

Hatziioannou T, Cowan S, Goff SP, Bieniasz PD, Towers GJ (2003) Restriction of multiple divergent retroviruses by Lv1 and Ref1. *The European Molecular Biology Organization journal* 22: 385-394

Hatziioannou T, Perez-Caballero D, Yang A, Cowan S, Bieniasz PD (2004) Retrovirus resistance factors Ref1 and Lv1 are species-specific variants of TRIM5alpha. *Proceedings of the National Academy of Sciences of the United States of America* 101: 10774-10779

He J, Chen Y, Farzan M, Choe H, Ohagen A, Gartner S, Busciglio J, Yang X, Hofmann W, Newman W, Mackay CR, Sodroski J, Gabuzda D (1997) CCR3 and CCR5 are co-receptors for HIV-1 infection of microglia. *Nature* 385: 645-649

Ho DD, Hartshorn KL, Rota TR, Andrews CA, Kaplan JC, Schooley RT, Hirsch MS (1985) Recombinant human interferon alfa-A suppresses HTLV-III replication in vitro. *Lancet* 1: 602-604

Hook P, Vallee RB (2006) The dynein family at a glance. *Journal of cell science* 119: 4369-4371

Hornick JE, Bader JR, Tribble EK, Trimble K, Breunig JS, Halpin ES, Vaughan KT, Hinchcliffe EH (2008) Live-cell analysis of mitotic spindle formation in taxol-treated cells. *Cell motility and the cytoskeleton* 65: 595-613

Hsieh MJ, White PJ, Pouton CW (2010) Interaction of viruses with host cell molecular motors. *Current opinion in biotechnology* 21: 633-639

Hulme AE, Perez O, Hope TJ (2011) Complementary assays reveal a relationship between HIV-1 uncoating and reverse transcription. *Proceedings of the National Academy of Sciences of the United States of America* 108: 9975-9980

Jordan MA, Thrower D, Wilson L (1992) Effects of vinblastine, podophyllotoxin and nocodazole on mitotic spindles. Implications for the role of microtubule dynamics in mitosis. *Journal of cell science* 102: 401-416

Jordan MA, Wilson L (2004) Microtubules as a target for anticancer drugs. Nature reviews *Cancer* 4: 253-265

Kane M, Yadav SS, Bitzegeio J, Kutluay SB, Zang T, Wilson SJ, Schoggins JW, Rice CM, Yamashita M, Hatziioannou T, Bieniasz PD (2013) MX2 is an interferon-induced inhibitor of HIV-1 infection. *Nature* 502: 563-566

Keckesova Z, Ylinen LM, Towers GJ (2004) The human and African green monkey TRIM5alpha genes encode Ref1 and Lv1 retroviral restriction factor activities. *Proceedings of the National Academy of Sciences of the United States of America* 101: 10780-10785

Lehmann M, Milev MP, Abrahamyan L, Yao XJ, Pante N, Mouland AJ (2009) Intracellular transport of human immunodeficiency virus type 1 genomic RNA and viral production are dependent on dynein motor function and late endosome positioning. *The Journal of biological chemistry* 284: 14572-14585

Liu Z, Pan Q, Ding S, Qian J, Xu F, Zhou J, Cen S, Guo F, Liang C (2013) The interferon-inducible MxB protein inhibits HIV-1 infection. *Cell host & microbe* 14: 398-410

Lu J, Pan Q, Rong L, He W, Liu SL, Liang C (2011) The IFITM proteins inhibit HIV-1 infection. *Journal of virology* 85: 2126-2137

Luduena RF, Roach MC (1991) Tubulin sulfhydryl groups as probes and targets for antimitotic and antimicrotubule agents. *Pharmacology & therapeutics* 49: 133-152

Lukic Z, Dharan A, Fricke T, Diaz-Griffero F, Campbell EM (2014) HIV-1 Uncoating is Facilitated by Dynein and Kinesin-1. *Journal of virology* 88: 13613-25

Lukic Z, Hausmann S, Sebastian S, Rucci J, Sastri J, Robia SL, Luban J, Campbell EM (2011) TRIM5alpha associates with proteasomal subunits in cells while in complex with HIV-1 virions. *Retrovirology* 8: 93

Malim MH, Bieniasz PD (2012) HIV Restriction Factors and Mechanisms of Evasion. *Cold Spring Harbor perspectives in medicine* 2: a006940

McEwan WA, Schaller T, Ylinen LM, Hosie MJ, Towers GJ, Willett BJ (2009) Truncation of TRIM5 in the Feliformia explains the absence of retroviral restriction in cells of the domestic cat. *Journal of virology* 83: 8270-8275

Melkonian KA, Maier KC, Godfrey JE, Rodgers M, Schroer TA (2007) Mechanism of dynamitin-mediated disruption of dynactin. *The Journal of biological chemistry* 282: 19355-19364

Mouland AJ, Milev MP (2012) Role of Dynein in Viral Pathogenesis. In Dyneins: structure, biology and disease, *King SM (ed),* 561-583, pp 561-583. Elsevier

Nepveu-Traversy ME, Berube J, Berthoux L (2009) TRIM5alpha and TRIMCyp form apparent hexamers and their multimeric state is not affected by exposure to restriction-sensitive viruses or by treatment with pharmacological inhibitors. *Retrovirology* 6: 100

Newman RM, Hall L, Kirmaier A, Pozzi LA, Pery E, Farzan M, O'Neil SP, Johnson W (2008) Evolution of a TRIM5-CypA splice isoform in old world monkeys. *PLoS Pathogens* 4: e1000003

Nisole S, Lynch C, Stoye JP, Yap MW (2004) A Trim5-cyclophilin A fusion protein found in owl monkey kidney cells can restrict HIV-1. *Proceedings of the National Academy of Sciences of the United States of America* 101: 13324-13328

Pawlica P, Berthoux L (2014) Cytoplasmic Dynein Promotes HIV-1 Uncoating. *Viruses* 6: 4195-4211

Pawlica P, Le Sage V, Poccardi N, Tremblay MJ, Mouland AJ, Berthoux L (2014) Functional evidence for the involvement of microtubules and dynein motor complexes in TRIM5alpha-mediated restriction of retroviruses. *Journal of virology* 88: 5661-5676

Perez-Caballero D, Hatziioannou T, Zhang F, Cowan S, Bieniasz PD (2005) Restriction of human immunodeficiency virus type 1 by TRIM-CypA occurs with rapid kinetics and independently of cytoplasmic bodies, ubiquitin, and proteasome activity. *Journal of virology* 79: 15567-15572

Price AJ, Marzetta F, Lammers M, Ylinen LM, Schaller T, Wilson SJ, Towers GJ, James LC (2009) Active site remodeling switches HIV specificity of antiretroviral TRIMCyp. *Nature Structural & Molecular Biology* 16: 1036-1042

Reymond A, Meroni G, Fantozzi A, Merla G, Cairo S, Luzi L, Riganelli D, Zanaria E, Messali S, Cainarca S, Guffanti A, Minucci S, Pelicci PG, Ballabio A (2001) The tripartite motif family identifies cell compartments. *The European Molecular Biology Organization journal* 20: 2140-2151

Sardiello M, Cairo S, Fontanella B, Ballabio A, Meroni G (2008) Genomic analysis of the TRIM family reveals two groups of genes with distinct evolutionary properties. *BioMed Central evolutionary biology* 8: 225

Sayah DM, Sokolskaja E, Berthoux L, Luban J (2004) Cyclophilin A retrotransposition into TRIM5 explains owl monkey resistance to HIV-1. *Nature* 430: 569-573

Schiff PB, Fant J, Horwitz SB (1979) Promotion of microtubule assembly in vitro by taxol. *Nature* 277: 665-667

Schrader M, King SJ, Stroh TA, Schroer TA (2000) Real time imaging reveals a peroxisomal reticulum in living cells. *Journal of cell science* 113: 3663-3671

Sebastian S, Luban J (2005) TRIM5alpha selectively binds a restriction-sensitive retroviral capsid. *Retrovirology* 2: 40

Shi J, Friedman DB, Aiken C (2013) Retrovirus restriction by TRIM5 proteins requires recognition of only a small fraction of viral capsid subunits. *Journal of virology* 87: 9271-9278

Skillman DR, Malone JL, Decker CF, Wagner KF, Mapou RL, Liao MJ, Testa D, Meltzer MS (1996) Phase I trial of interferon alfa-n3 in early-stage human immunodeficiency virus type 1 disease: evidence for drug safety, tolerance, and antiviral activity. *The Journal of infectious diseases* 173: 1107-1114

Song B, Gold B, O'Huigin C, Javanbakht H, Li X, Stremlau M, Winkler C, Dean M, Sodroski J (2005) The B30.2(SPRY) domain of the retroviral restriction factor TRIM5alpha exhibits lineage-specific length and sequence variation in primates. *Journal of virology* 79: 6111-6121

Stremlau M, Owens CM, Perron MJ, Kiessling M, Autissier P, Sodroski J (2004) The cytoplasmic body component TRIM5alpha restricts HIV-1 infection in Old World monkeys. *Nature* 427: 848-853

Stremlau M, Perron M, Lee M, Li Y, Song B, Javanbakht H, Diaz-Griffero F, Anderson DJ, Sundquist WI, Sodroski J (2006) Specific recognition and accelerated uncoating of retroviral capsids by the TRIM5alpha restriction factor. *Proceedings of the National Academy of Sciences of the United States of America* 103: 5514-5519

Towers GJ, Hatziioannou T, Cowan S, Goff SP, Luban J, Bieniasz PD (2003) Cyclophilin A modulates the sensitivity of HIV-1 to host restriction factors. *Nature Medicine* 9: 1138-1143

Virgen CA, Kratovac Z, Bieniasz PD, Hatziioannou T (2008) Independent genesis of chimeric TRIM5-cyclophilin proteins in two primate species. *Proceedings of the National Academy of Sciences of the United States of America* 105: 3563-3568

Wilson SJ, Webb BL, Ylinen LM, Verschoor E, Heeney JL, Towers GJ (2008) Independent evolution of an antiviral TRIMCyp in rhesus macaques. *Proceedings of the National Academy of Sciences of the United States of America* 105: 3557--3562

Yamamoto JK, Barre-Sinoussi F, Bolton V, Pedersen NC, Gardner MB (1986) Human alpha- and beta-interferon but not gamma- suppress the in vitro replication of LAV, HTLV-III, and ARV-2. *Journal of interferon research* 6: 143-152

Yang Y, Brandariz-Nunez A, Fricke T, Ivanov DN, Sarnak Z, Diaz-Griffero F (2014) Binding of the rhesus TRIM5alpha PRYSPRY domain to capsid is necessary but not sufficient for HIV-1 restriction. *Virology* 448: 217-228

Yap MW, Nisole S, Lynch C, Stoye JP (2004) Trim5alpha protein restricts both HIV-1 and murine leukemia virus. *Proceedings of the National Academy of Sciences of the United States of America* 101: 10786-10791

Zhao G, Ke D, Vu T, Ahn J, Shah VB, Yang R, Aiken C, Charlton LM, Gronenborn AM, Zhang P (2011) Rhesus TRIM5alpha disrupts the HIV-1 capsid at the inter-hexamer interfaces. *PLoS Pathogens* 7: e1002009

Zheng YH, Jeang KT, Tokunaga K (2012) Host restriction factors in retroviral infection: promises in virus-host interaction. *Retrovirology* 9: 112

Zufferey R, Nagy D, Mandel RJ, Naldini L, Trono D (1997) Multiply attenuated lentiviral vector achieves efficient gene delivery in vivo. *Nature Biotechnology* 15: 871-875

B.9 Supplementary Figures

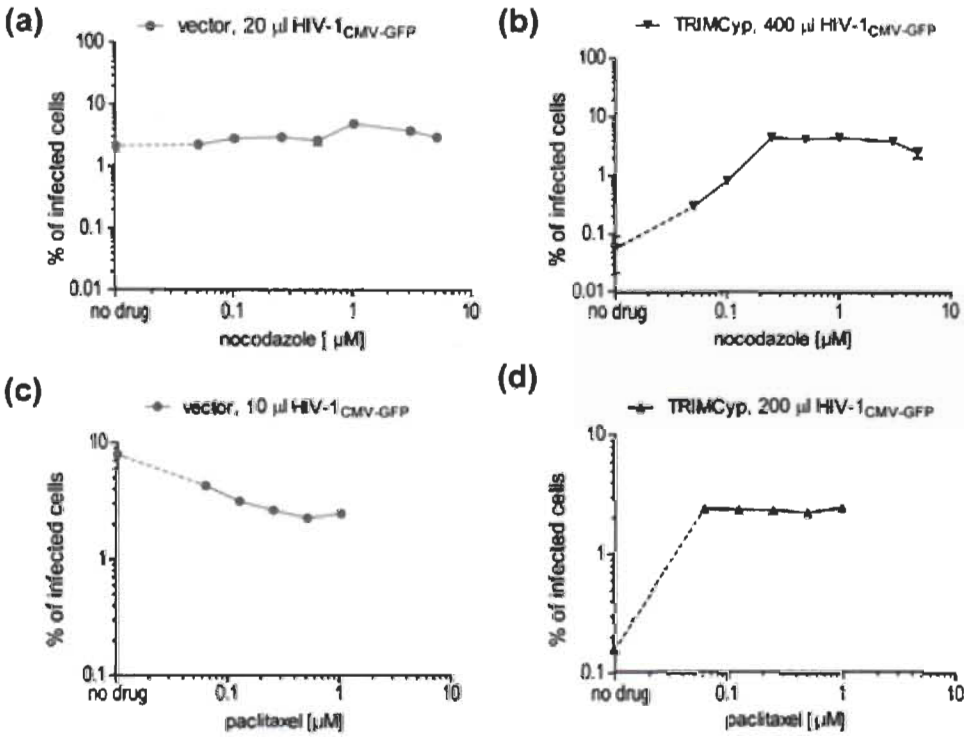

Figure S1. Non-normalized infectivity data. (a, b) Raw infectivity results for the experiment shown in Fig. 2(c). (c, d) Raw infectivity results for the experiment shown in Fig. 2(d). Figure S1. Non-normalized infectivity data. (a, b) Raw infectivity results for the experiment shown in Fig. 2(c). (c, d) Raw infectivity results for the experiment shown in Fig. 2(d).

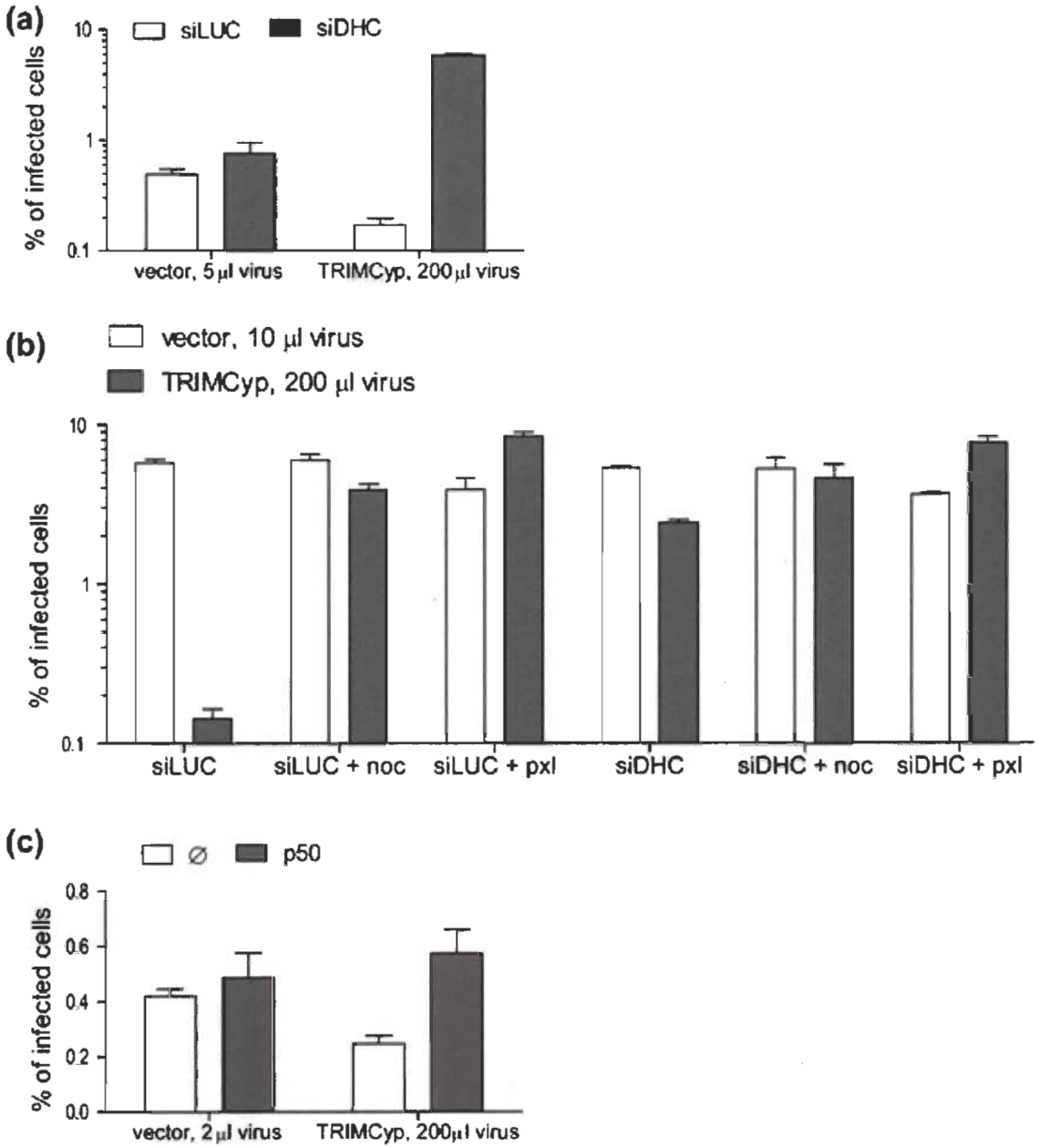

Figure S2. Non-normalized infectivity data. (a) Raw infectivity results for the experiment shown in Fig. 3(b). (b) Raw infectivity results for the experiment shown in Fig. 3(c). (c) Raw infectivity results for the experiment shown in Fig. 4(b).